GEOLOGICAL SURVEY OF WESTERN AUSTRALIA

REPORT 39

GOLD MINERALIZATION IN THE MENZIES–KAMBALDA REGION, EASTERN GOLDFIELDS, WESTERN AUSTRALIA

by
W. K. Witt

DEPARTMENT OF MINERALS AND ENERGY

GEOLOGICAL SURVEY OF WESTERN AUSTRALIA

REPORT 39

GOLD MINERALIZATION IN THE MENZIES–KAMBALDA REGION, EASTERN GOLDFIELDS, WESTERN AUSTRALIA

by
W. K. Witt

Perth 1993

12854—1

Copy editor: J. F. Johnston

National Library of Australia
Cataloguing-in-publication entry

Witt, W. K.
Gold mineralization in the Menzies–Kambalda region, Eastern Goldfields, Western Australia.

Bibliography.
ISBN 0 7309 4483 2.

1. Gold — Western Australia — Kalgoorlie Region.
2. Greenstone belts — Western Australia — Kalgoorlie Region.
I. Geological Survey of Western Australia.
II. Title. (Series: Report (Geological Survey of Western Australia); 39).

553.41099416

ISSN 0508–4741

Copies available from:
Director
Geological Survey of Western Australia
100 Plain Street
EAST PERTH Western Australia 6004
Telephone (09) 222 3222

Contents

Chapter 4 Structural controls on gold mineralization

Chapter 5 Alteration associated with gold mineralization

Chapter 6 Alteration geochemistry

Chapter 7 Fluid composition and the transport and deposition of gold

Chapter 8 Timing relationships between deformation, metamorphism, and mineralization

Chapter 9 Origin of the hydrothermal fluids and a model for the genesis of epigenetic gold mineralization

Plates (in separate wallet)

Figures

Tables

Photographic plates

Acknowledgements

The author acknowledges the assistance and encouragement of the many mining companies (especially Julia Mines N.L., West Coast Holdings Ltd, and the Mount Pleasant group of companies) who provided access to operating mines, drillcore and other data.

Gold mineralization in the Menzies–Kambalda region, Eastern Goldfields, Western Australia

Abstract

The Menzies–Kambalda region forms part of the Norseman–Wiluna belt, in the Eastern Goldfields Province of the Archaean Yilgarn Craton. This roughly 6000 km^2 area has produced 1700 tonnes of gold — from the giant deposits at Kalgoorlie, several other important mining centres, and numerous smaller mines. Although gold has been mined from most rock types, mafic rocks — especially Fe-rich basalt and differentiates of fractionated sills — account for most production. Mineralization occurs in diverse structural settings, in structures which are related to the latest stages of regional deformation (D_3–D_4), or in accommodation structures generated by emplacement of contemporaneous granitoid intrusions. Microtextural and microstructural evidence indicates that these structures were active during gold-related hydrothermal activity.

Peak regional metamorphism occurred during D_3, and regional metamorphic temperatures were enhanced, and subsequently maintained for relatively long periods, in thermal aureoles around syn-D_3 granitoid plutons. A regional carbonation event, involving large volumes of an H_2O–CO_2 fluid and containing mantle-derived carbon, was broadly contemporaneous with regional metamorphism.

Alteration zoning around auriferous structures was controlled, at least partly, by increasing X_{CO_2} towards the centre of the structure. Assemblages in the outer zone of alteration are indistinguishable from those produced by regional carbonation. Inner alteration assemblages vary, on a regional scale, with metamorphic grade (to upper amphibolite facies) and host-rock composition. Alteration of mafic rocks involved introduction of K, CO_2, S, and SiO_2. Potassic alteration of mafic rocks is reflected in the development of muscovite, biotite, and microcline at progressively higher metamorphic grades. Although carbonation of ultramafic rocks is intense, potassic alteration is generally less well-developed. Alteration in granitic rocks is relatively subtle but involves qualitatively similar changes. Regional carbonation assemblages and potassic alteration assemblages in greenschist-facies host rock are apparently retrograde with respect to the metamorphic assemblage. Contrastingly, these same alteration styles display evidence of metamorphic recrystallization in the broad thermal aureoles of syn-D_3 plutons.

Fluid inclusion and thermodynamic studies consistently indicate that gold was deposited from a near-neutral, low-salinity H_2O–CO_2 hydrothermal fluid. There is some textural and geochemical evidence to suggest that, although closely related, potassic alteration post-dated, or occurred during the final stages of, the regional carbonation event. The spatial and temporal relationships among regional metamorphism, potassic alteration assemblages, and metamorphic recrystallization suggest broad contemporaneity between gold mineralization and regional metamorphism.

It is concluded that mineralization was related to a greenstone belt-scale hydrothermal system, centred on syn-D_3 plutons which acted as centres of heat and fluid flux. Hydrothermal fluids derived from the mantle or the lower crust (but possibly including magmatic and/or metamorphic components) were driven through large-scale convection cells causing regional carbonation in shear zones and other active structures. Over time, the fluids equilibrated with regionally abundant granitic rocks. Evolved, potassic fluids deposited gold in active structures during the later stages of the hydrothermal event. The source of the gold is not known but may have been leached from a variety of rocks by carbonating fluids during earlier stages of the hydrothermal event.

Keywords: gold mineralization; greenstone belts; lithological, structural and metamorphic controls; hydrothermal alteration; Yilgarn Craton; Menzies–Kambalda region.

Chapter 1

Introduction

Gold was Western Australia's most important mineral resource until the mid 1960s, and is now ranked second in terms of annual value, after iron ore (Figs 1, 2). Western Australia's gold production in 1988 was approximately 110 tonnes (Fig. 3), with about 135 t production achieved in 1989. Maitland (1919) described the gold deposits of Western Australia known at that time but there has been no more recent summary by the Geological Survey of Western Australia (GSWA). Many reports and bulletins of the Geological Survey describe gold mineralization at individual mines and mining centres, but the scale and widespread geographical distribution of gold deposits have inhibited the production of a comprehensive account covering the whole State.

Instead, the GSWA has embarked upon a program to produce individual reports on a number of regions which together will document gold mineralization throughout the State. The first of these — covering the Southern Cross region — was published in 1991 (Keats, 1991). This report, the second in the series, describes gold mineralization in the Menzies–Kambalda region, in the Eastern Goldfields of the Archaean Yilgarn Craton (Fig. 4).

Gold was discovered at numerous localities throughout the Menzies–Kambalda region in the rush that followed the initial discovery at Kalgoorlie in 1893. Western Australian gold production has been dominated until

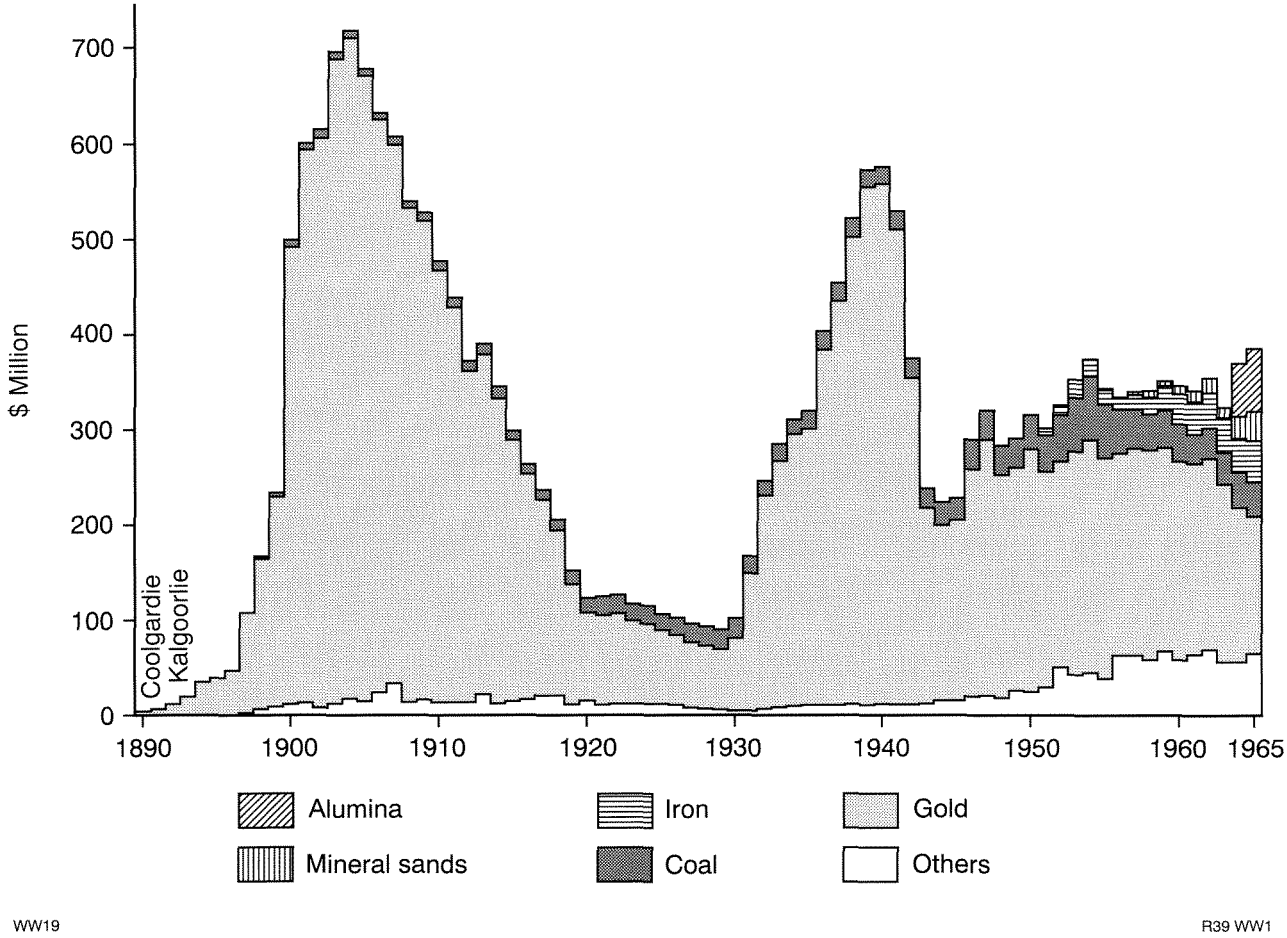

Figure 1. Value of mineral production in Western Australia, 1890–1965, adjusted to 1985 dollars

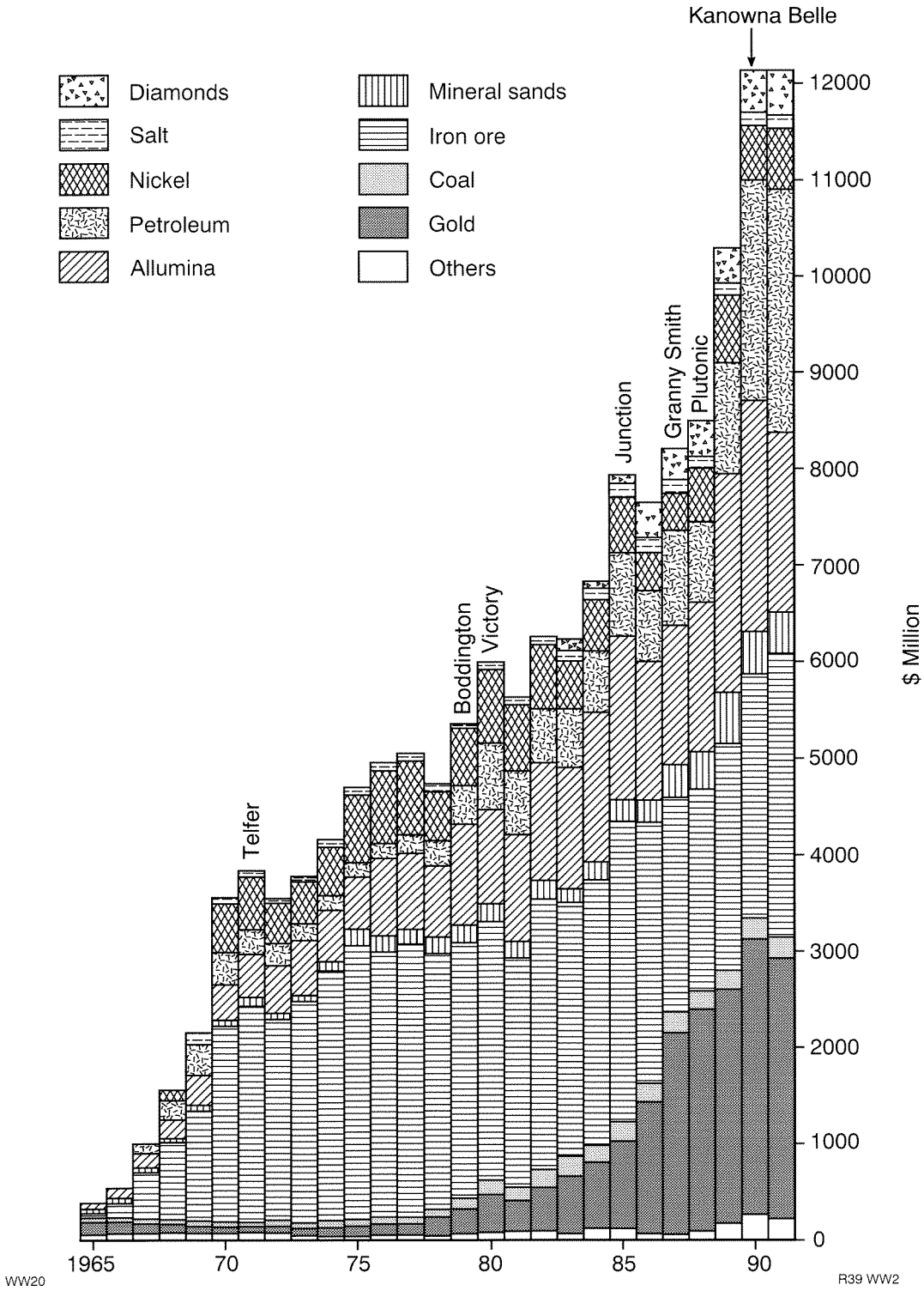

Figure 2. Value of mineral production in Western Australia, 1965–1992, adjusted to 1991 dollars; and principal turning points in the gold industry

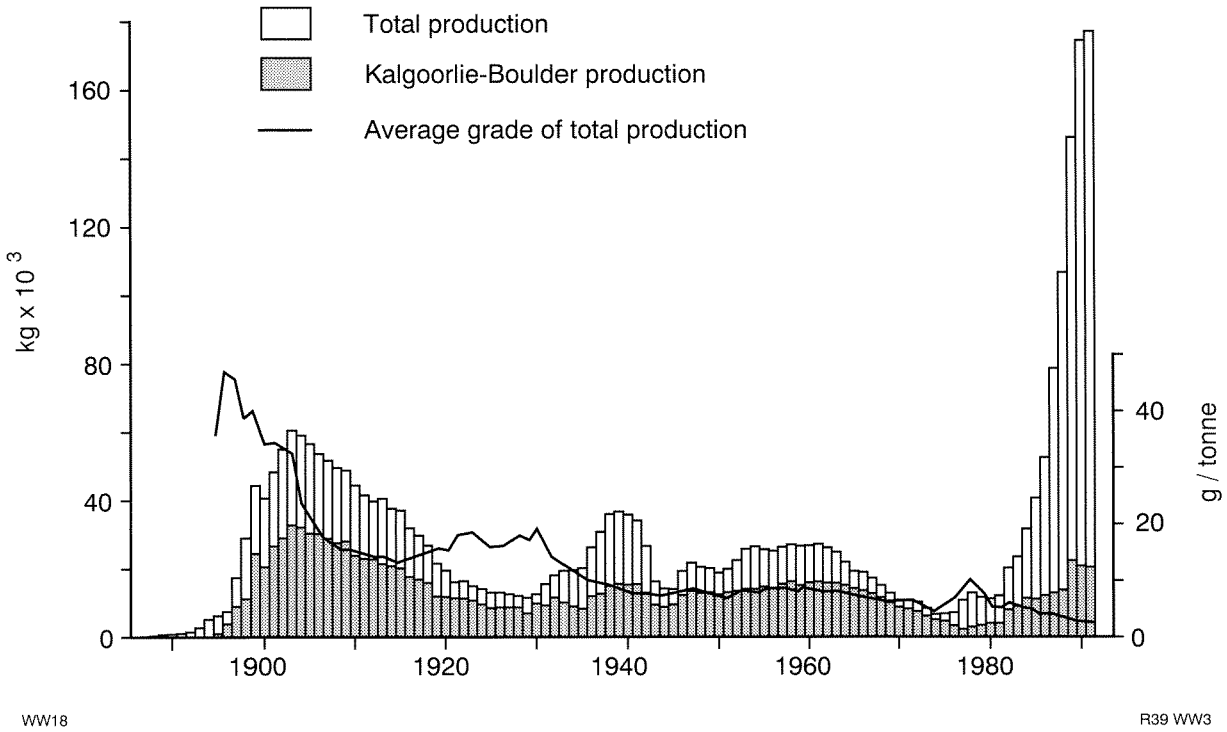

Figure 3. Gold production in Western Australia

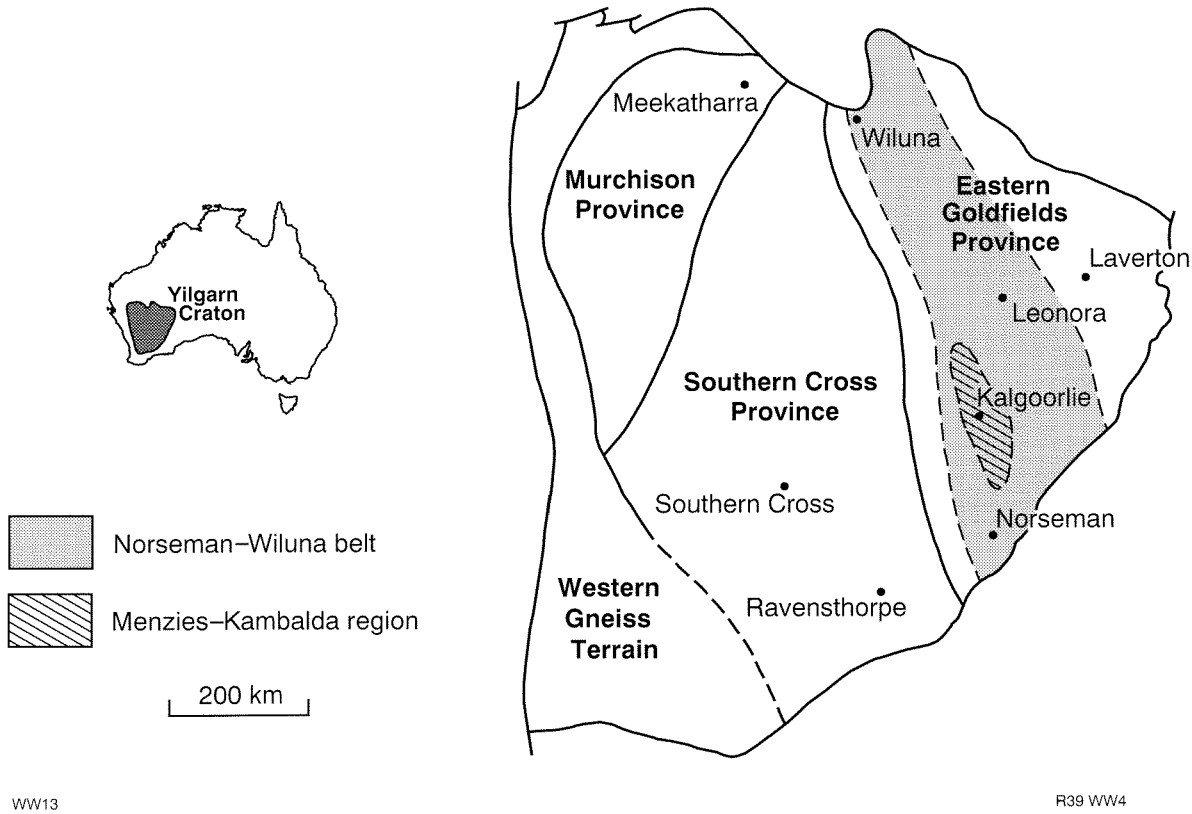

Figure 4. Location of the Menzies–Kambalda region and subdivisions of the Yilgarn Craton

recently by the Golden Mile deposits in the Kalgoorlie–Boulder district (Fig. 3). Production increased rapidly through the 1890s and peaked in 1903 when the Kalgoorlie–Boulder district yielded more than 30 t of gold. Production then declined during the following decades but staged minor recoveries in the 1930s and 1950s. Higher gold prices in the mid- to late-1970s were responsible for renewed interest in gold exploration, and a fourth period of increasing production continues to the present day. The present period of exploration and mining activity has been aided by a weak Australian dollar, and recent technological advances assisting the recovery of gold from low-grade deposits (e.g. the carbon-in-pulp method, heap leaching). A further factor which has helped the industry is the deep weathering profile in the Eastern Goldfields which has facilitated low-cost, openpit-mining methods.

The relative importance of the Menzies–Kambalda region to Western Australia's gold mining industry, and the dominating influence of the Golden Mile deposits, is illustrated in Figure 5. Although important new discoveries (e.g. Telfer and Boddington) have been made outside the Menzies–Kambalda region in recent years, Figure 6 shows the continued importance of the area covered by this report. At the time of writing (December, 1989), gold is treated at 13 centres within the Menzies–Kambalda region. Of 33 Western Australian gold mines commissioned in 1988, six were in the Menzies–Kambalda region. A further ten gold mines commenced operations in 1989*.

Most published descriptions of gold mineralization in the Menzies–Kambalda region are dated, while more recent descriptions have been biased towards the larger deposits. Apart from the summary descriptions of Maitland (1919), the GSWA has published bulletins containing more complete descriptions of mining

* This Report was written and finalized in December 1989. Thus, technical data and production figures are those available at that date.

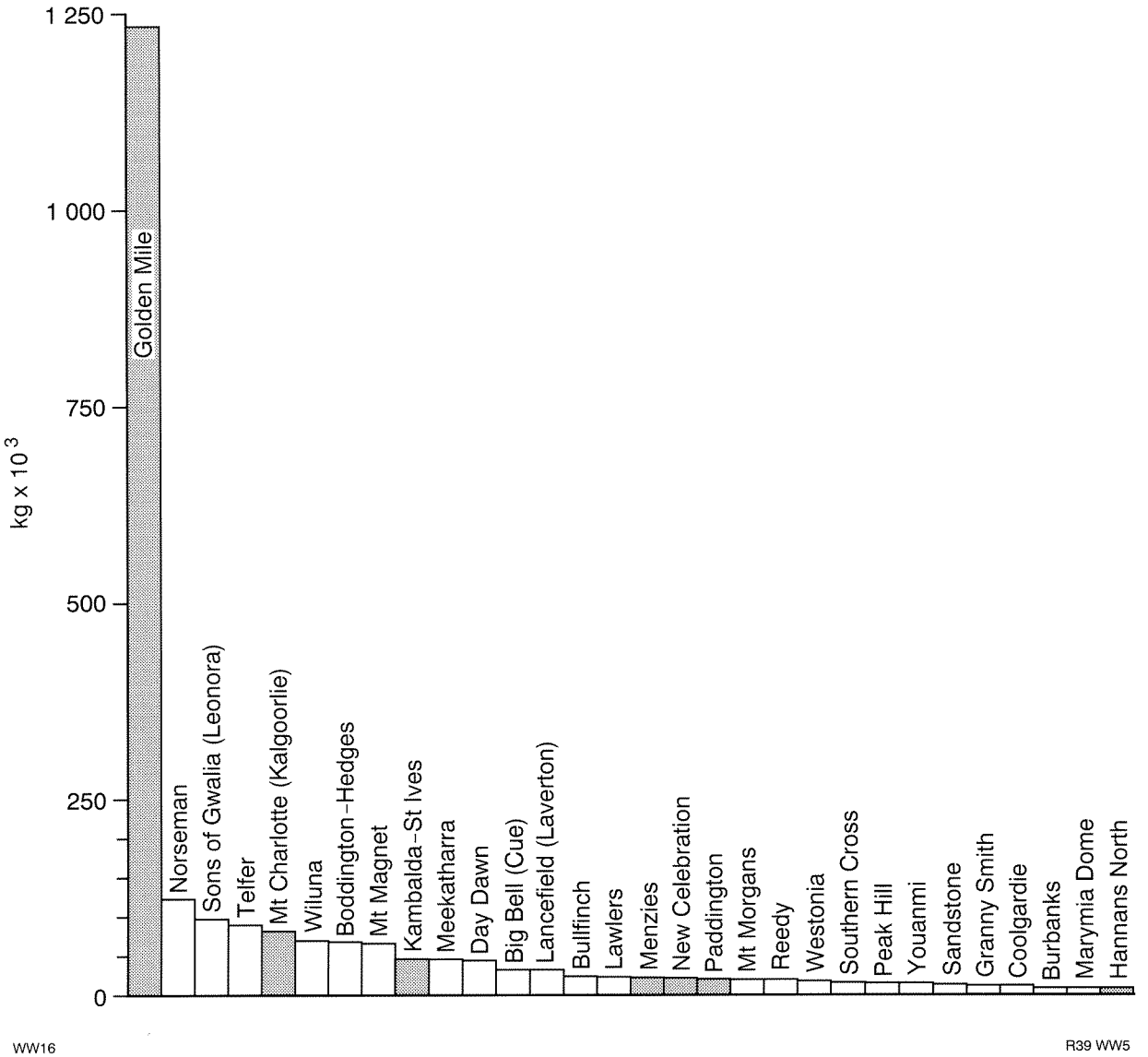

Figure 5. Total gold production from individual Western Australian mines, to 1991. Mines within the Menzies–Kambalda region are indicated by heavy shading

centres at Menzies (Woodward, 1906), Comet Vale and Goongarrie (Jutson, 1921), Ora Banda (Jutson, 1914), and Kalgoorlie–Boulder (see Witt (1993c) for sources). In addition, there have been many shorter descriptions of selected mines and mining centres within the Menzies–Kambalda region which are referenced in the three GSWA Records written in conjunction with this Report (Witt, 1993a,b,c). Recent GSWA publications include descriptions of the geology and mineralization of the Kalgoorlie–Boulder district (Keats, 1987; Swager, 1989). The recent interest in gold in Western Australia has prompted much research on the part of universities, government institutions, and exploration geologists. Results of many of these investigations, including several pertaining to deposits in the Menzies–Kambalda region, were reported to the Gold 88 Conference in Melbourne, in May, 1988 (Goode and Bosma, 1988; Goode et al., 1988). The accumulated data have been used as a basis to constrain genetic models which are still being debated (Groves et al., 1987, 1989; Colvine et al., 1984, 1988; Kerrich, 1986a,b).

This report and three accompanying GSWA Records (Witt, 1993a,b,c) seek to fill a gap in the literature by systematically documenting all gold mines in a densely mineralized portion of a very large greenstone belt, and attempting to relate these gold occurrences to regional structural, metamorphic, and lithostratigraphic observations. The regional observations comprise an important intermediate step which has been lacking in many recent genetic models. Integrated observations at mine and regional scales have been assisted by the current 1:25 000- and 1:50 000-scale mapping for the GSWA 1:100 000 geological map series. The Menzies–Kambalda region comprises the whole, or portions, of RIVERINA** (Swager, 1991), MELITA (Witt, 1993d), MENZIES (Swager, 1991), BARDOC (Witt, 1990), DAVYHURST (Wyche and Witt, 1992), KALGOORLIE (Hunter, 1993),

** Names of 1:250 000 and 1:100 000 scale mapsheets are printed in CAPITAL LETTERS. If necessary for clarity, the appropriate scale is added in parentheses

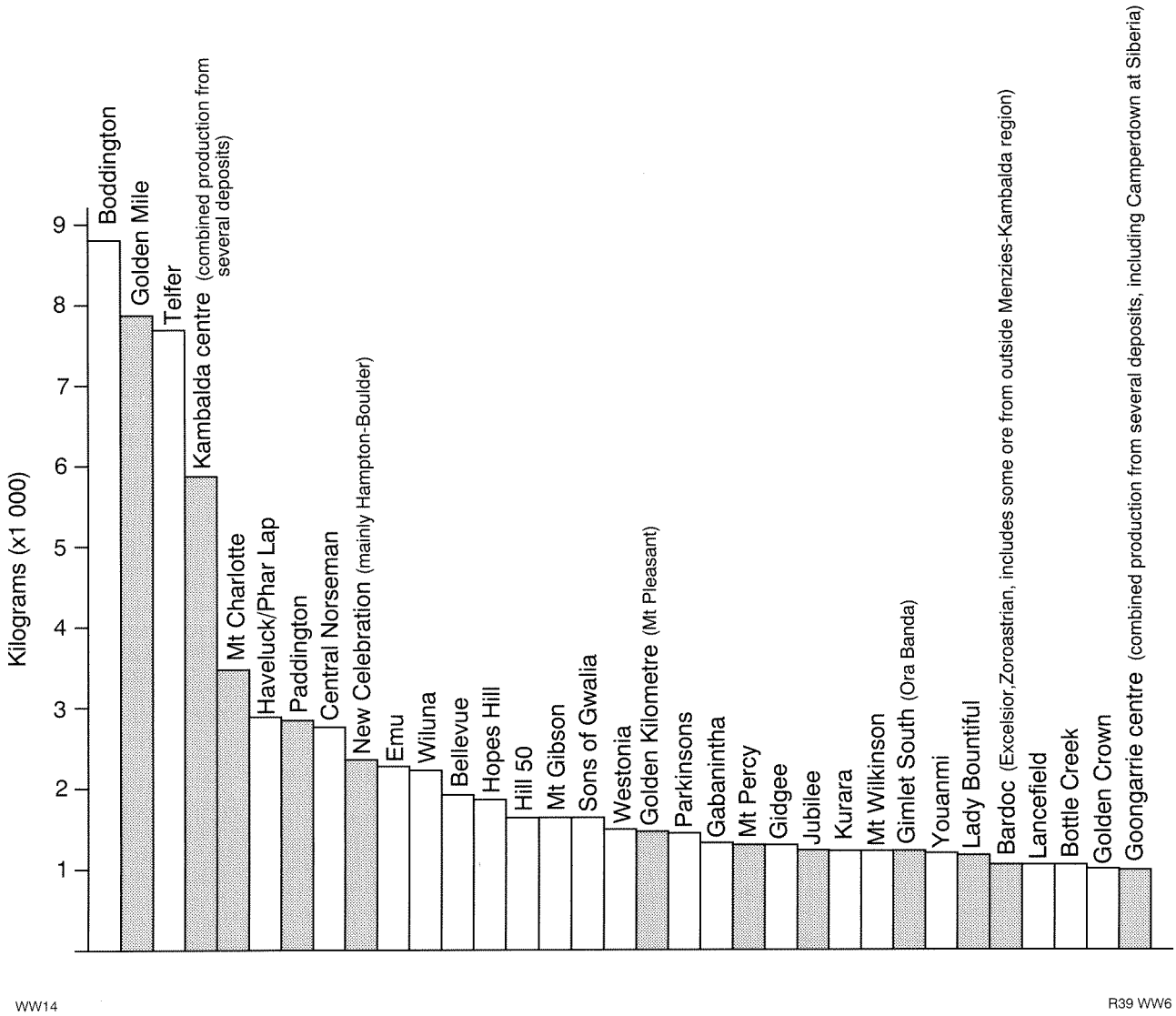

Figure 6. Production from major gold mines for 1988 — at the height of the resurgence in gold mining in the 1980s. Mines within the Menzies–Kambalda region are indicated by heavy shading

KANOWNA (Ahmat, in prep.), YILMIA (Hunter, 1993), LAKE LEFROY and COWAN (Griffin, 1990b) 1:100 000 sheets (Fig. 7). Geological maps and reports covering each of these sheets have been prepared for separate publication, and are referenced above.

An attempt has been made to visit each of the 215 mines in the Menzies–Kambalda region that has produced more than 5 kg of gold, and to record host rocks, structural controls, and alteration styles. Although many mines have been abandoned for up to about 80 years, meaningful data were obtained from most localities. Field work has been biased towards documenting smaller mines and mining areas which have not been described in the past. In many cases, a small suite of samples was collected from exposed workings or mine dumps for petrographic investigation of alteration assemblages, and textural and fabric relationships. More extensive investigations have been carried out at a number of selected deposits where there was ready access to mine exposures and drillcore. Larger mining centres, such as Kalgoorlie–Boulder and Kambalda, have been the subject of much recent research, and no attempt has been made to duplicate this work. Instead, the published results of the investigations have been summarized and referenced.

For this study the Menzies–Kambalda region has been subdivided into seventeen mining areas or groups of mines (Fig. 8). The mining areas are based on distinctive geological characteristics, particularly structural style, and do not necessarily conform to the administrative mining districts and mining centres created by the Department of Minerals and Energy (DOME).

The second part of this regional study has resulted in three GSWA Records which contain a summary of the geology and the main characteristics of gold mineralization in each of the seventeen mining areas, followed by systematic descriptions of each of the mines within that mining area. As much as possible of this information is summarized in Plates 1A, 1B, and 2, herein. The Records are 'Gold deposits of the Menzies and Broad Arrow areas, Western Australia' (Witt, 1993a); 'Gold deposits of the Mount Pleasant – Ora Banda areas, Western Australia' (Witt, 1993b); and 'Gold deposits of the Kalgoorlie – Kambalda – St Ives areas, Western Australia' (Witt, 1993c).

Gold mineralization and the regolith

Many of the openpit gold mines developed in the 1980s, as well as many 'historical' underground mines, were located in the regolith, where levels of gold have been enriched with respect to the unweathered lodes. The regolith is the product of a long and complex history of weathering under a variety of conditions (Butt, 1987). In this current study, investigations have been directed towards mineralization in unweathered rocks (the 'primary zone'). However, the importance of the regolith is recognized, and its development and its significance to gold mineralization are briefly reviewed here. Recent regolith studies have been carried out by geoscientists at the Commonwealth Scientific and Industrial Research Organisation (CSIRO) in Perth, and the following description summarizes the results of their work (see especially Butt, 1987, 1988). For a fuller discussion, the reader is referred to Smith and Keele (1984), Mann (1984), Webster and Mann (1984), and Butt (1989).

Much of the Yilgarn Craton has been exposed to subaerial conditions since the mid-Proterozoic, although Permian glaciation removed much of the earlier topography and surficial material. Subsidence in the southern part of the Yilgarn Craton — including areas to the south of Kalgoorlie — during the Eocene, caused sedimentation in river valleys. Climatic conditions (summarized in Table 1) influenced development of the regolith and the behaviour of gold within it. Two episodes were of particular importance:

(a) Warm, humid conditions in the Cretaceous to mid-Miocene gave rise to lateritic profiles, commonly more than 40 m thick; and

(b) A drier climate since the Miocene, coupled with minor uplift of continental margins coincided with a lowering of the water table and slower erosion and chemical reactions. Subsequent erosion has caused partial truncation of the weathering profile.

Two main types of gold deposits are located within the regolith (Fig. 9).

(a) The first of these, lateritic deposits, are more or less flat-lying zones of fine-grained gold, of extreme fineness, within the ferruginous zone and underlying mottled zone of the weathering profile. Important lateritic deposits (e.g. Boddington, Mt Gibson) have been mined in the western Yilgarn Craton in recent years, but comparable deposits have not been located in the Eastern Goldfields. Only two small deposits in the study area (Enterprise, and BHP's Dark Horse) are located in the ferruginous zone of the laterite profile.

During lateritization, enrichment and lateral dispersion of gold in the ferruginous and mottled zones are due partly to residual concentration and surface wash during reduction of the land surface, and partly to solution as humic acid complexes derived from

Table 1. Periods of exposure to sub-aerial weathering in Western Australia (from Butt, 1988)

Period	*Age (my)*	*Climate*
Late Proterozoic		Glaciation
Early Permian	280 – 270	Glaciation
Mesozoic	230 – 65	Temperate to warm; humid
Palaeocene to Mid-Miocene	65 – 15	Sub-tropical to tropical; humid: probably seasonal (savanna)
Mid-Miocene to Pliocene	15 – 1.8	Sub-tropical; aridity increasing: cooler after 2.5 my
Quaternary	1.8 – 0	Temperate to warm; semi-arid to arid
	(25 000–13 000 yr peak aridity, glacial maximum)	

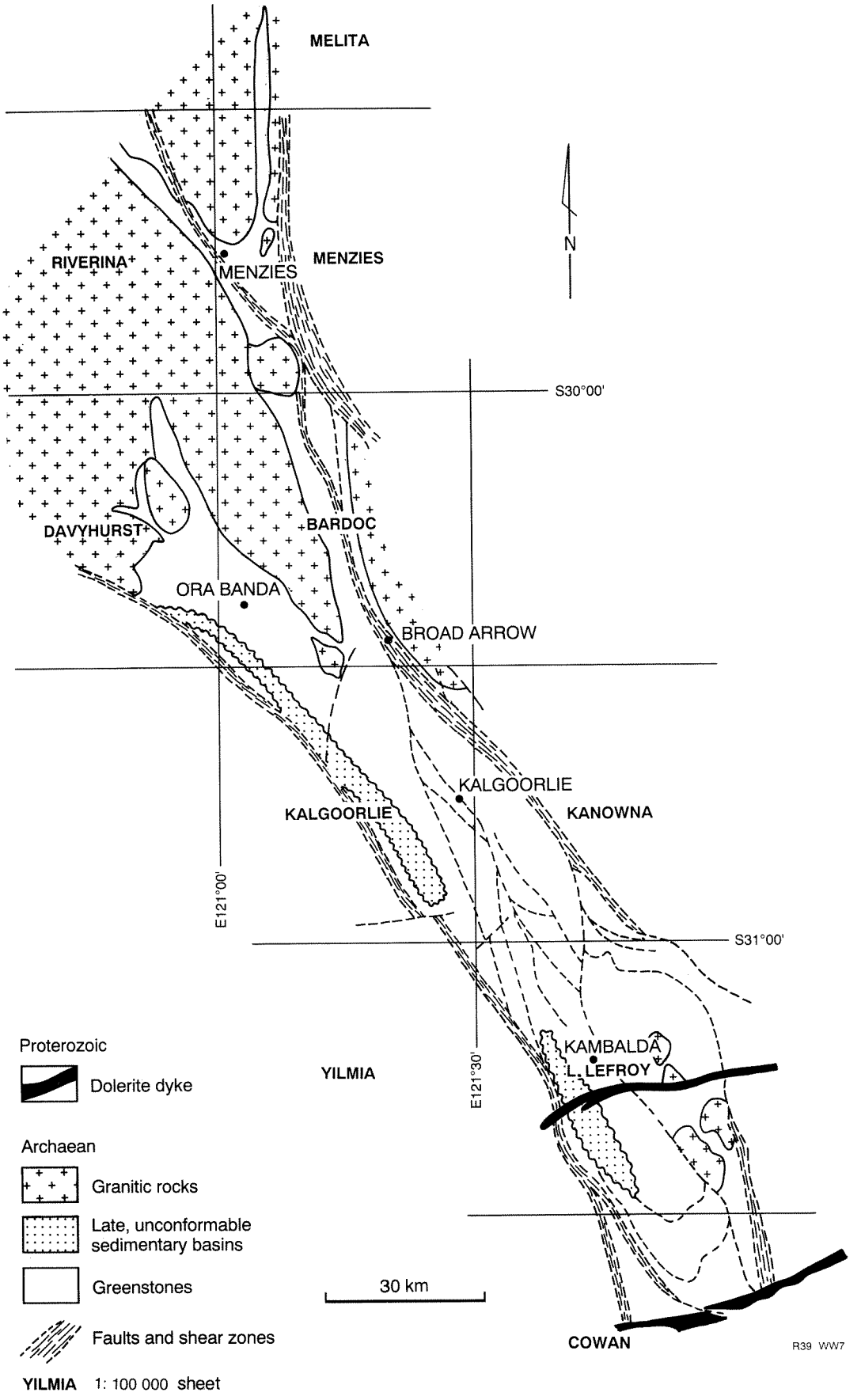

Figure 7. The Menzies–Kambalda region, showing the 1:100 000 sheets

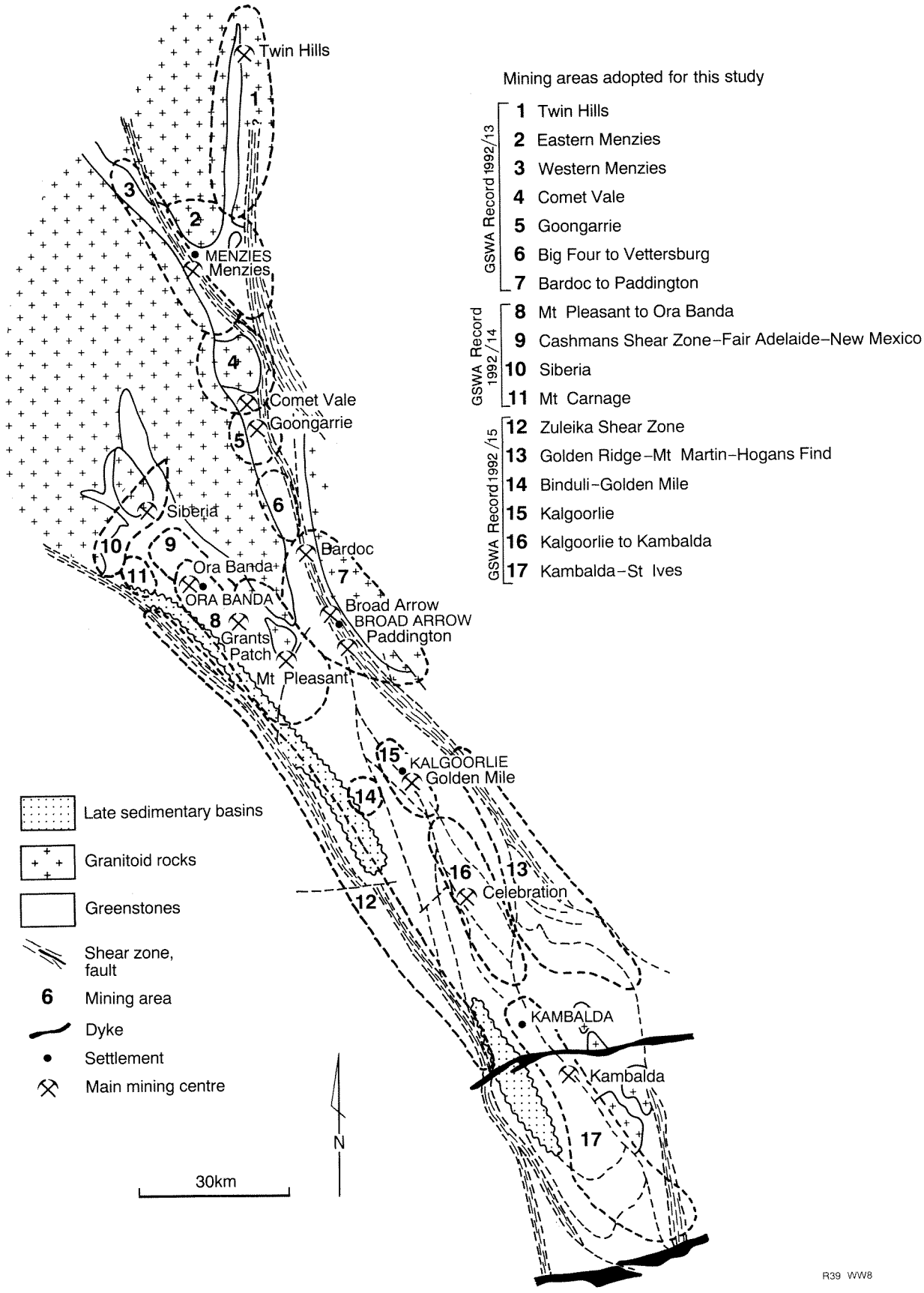

Figure 8. Location of mining areas adopted for this report. Geological symbols as for Figure 7

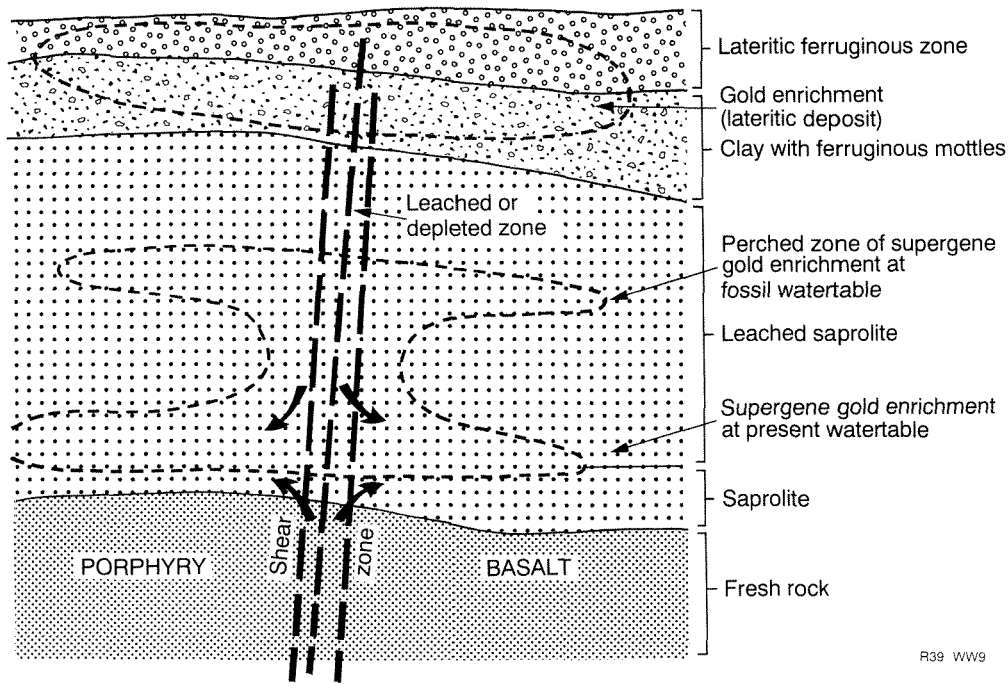

Figure 9. Zones of gold enrichment in the regolith (from Butt, 1988)

organic matter in soil. Reduction of the complexes by ferrous iron results in the incorporation of gold in iron oxide fragments and nodules in these zones.

(b) The second type, supergene deposits, are enrichments within the saprolite, and may be confined to the lode system or laterally dispersed into the weathered wallrocks. The concentrations are located at the present watertable level. These deposits are much more common in the study area than the lateritic deposits.

During more arid climatic conditions, evaporation caused groundwater salinity to increase, favouring the formation of soluble gold chloride complexes, e.g.

$$4Au^{o} + 16Cl^{-} + 3O_2 + 12H^{+} \longrightarrow 4AuCl_4^{-} + 6H_2O$$

Repeated strong leaching of the upper saprolite results in the marked depletion of gold. Gold is reprecipitated at the watertable by reduction of ferrous iron e.g.

$$AuCl_4^{-} + 3Fe^{2+} + 6H_2O \longrightarrow Au^{o} + 3FeOOH + 4Cl^{-} + 9H^{+}$$

The two horizons which are favourable for gold concentration are separated by a 5–15 m-thick barren or depleted zone which has been leached during lowering of the watertable since the Miocene.

A third type of regolith-hosted gold deposit may be represented by the auriferous quartz-rich sands developed over the Liberty Granodiorite in the Lady Bountiful area. The origin of these deposits is not yet clear but they probably represent alluvial concentrations in buried river deposits, residual concentrations developed over weathered vein deposits, or a combination of the two. The deposits occur at the base of a truncated laterite profile and must have developed prior to Tertiary lateritization. Similar 'deep leads' were mined historically in the Paddington and Mount Pleasant areas of the Menzies–Kambalda region.

Chapter 2

Geology of the Menzies–Kambalda region

Regional geology

The Menzies–Kambalda region lies within the Norseman–Wiluna belt (Gee et al., 1981) of the Eastern Goldfields Province in the Archaean Yilgarn Craton (Fig. 10). The geology of the Yilgarn Craton is described by Gee et al. (1981) and Gee (1979), and descriptions of Eastern Goldfields geology are given by Archibald et al. (1981), Hallberg (1986), Barley and Groves (1988), Griffin (1990a), and Swager et al. (1990).

The Norseman–Wiluna belt is characterized by widespread komatiitic volcanism and an absence of banded iron-formations, which distinguish it from adjacent greenstone belts of the northeast Eastern Goldfields Province and the Southern Cross Province. Although the boundaries of the Norseman–Wiluna belt are rather imprecisely defined, the belt is commonly interpreted to be a fault-bound, graben-like structure within an extensive and more stable, shallow basin (Williams, 1974; Gee et al., 1981). Supracrustal rocks in the 'graben' and adjoining areas have been referred to as rift-phase greenstones, and platform-phase greenstones, respectively (Groves and Batt, 1984).

The area shown in Figure 11 comprises most of the Kalgoorlie Terrane, as defined by Swager et al. (1990). The Menzies–Kambalda region, which includes the important mining centres of Menzies, Ora Banda, Broad Arrow, Kalgoorlie, and Kambalda, is bound to the west by the Zuleika Shear, and to the east by the Moriaty Shear, the Menzies–Boorara–Lefroy Shear system and granitic rocks of the Scotia–Kanowna dome. The area is delimited by granitic rocks to the north and by the Proterozoic Binneringie dyke to the south.

There are limited reliable isotopic age data for the Eastern Goldfields Province, with a strong bias towards the southern part of the Norseman–Wiluna belt. U/Pb zircon ages of 2690–2700 Ma have been recorded for the deposition of mafic/ultramafic volcanics at Kambalda (Compston et al., 1986; Browning et al., 1987; Claoué-Long et al., 1988; Campbell and Hill, 1988). Pidgeon (1986) reported a similar U/Pb age (2704 ± 8 Ma) for felsic volcanic rocks which overlie mafic/ultramafic rocks at Ora Banda. Chauvel et al. (1985) reported a rather imprecise Sm–Nd mineral age (2763 ± 32 Ma) for the unmetamorphosed Ora Banda Sill which occurs at a similar stratigraphic level to the felsic volcanic rocks. No ages older than these have been recorded in the Menzies–Kambalda region but older sequences of greenstones have been dated at Norseman (2900 Ma, Campbell and Hill, 1988), and Duketon (2800–2860 Ma in syngenetic galena, Browning et al., 1987), and the Southern Cross and Murchison Provinces (c. 2950 Ma, Pidgeon, 1986; Watkins and Hickman, 1990).

There are no reliable isotopic dates for greenstones west of the Zuleika Shear, but a post-tectonic pegmatite near Coolgardie has yielded a Rb–Sr age of 2643 Ma (Turek and Compston, 1971). Available age data from the Bulong area, east of the Boorara Shear Zone, suggest that the greenstones may be slightly older than those at Kambalda and Ora Banda (2720 ± 10 Ma, reported in Barley and Groves, 1989).

Broadly comparable deformation histories have been documented at several localities within the Norseman–Wiluna belt (Platt et al., 1978; Archibald et al., 1981; Gresham and Loftus-Hills, 1981; Spray, 1985; Swager, 1989; Williams et al., 1989; Witt, 1990). Deformation commenced with an early phase of subhorizontal thrusting and recumbent folding, and was followed by upright folding and strike-slip faulting. This deformation has imparted a strong north-northwest trending tectonic fabric to the Norseman–Wiluna belt that is defined by fold axes, granitic domes, and regional shear zones. Anastomosing regional shear zones divide the Norseman–Wiluna belt into elongate domains, and structural complexity hinders correlation of greenstones across the larger shear zones.

The age of the tectonothermal event is constrained by the U–Pb zircon isotopic ages of late- to post-tectonic granitoids such as the Mungari Granite (2610 Ma, Hill and Compston, 1987) between Kalgoorlie and Coolgardie, and the Liberty Granodiorite (2593 ± 10 Ma, Hill and Campbell, 1989). Thus, in the Menzies–Kambalda region deposition of supracrustal rocks, deformation, metamorphism, and emplacement of granitoids all occurred within a period of about 100 Ma.

Rock types

Recognition of igneous and sedimentary rock types is possible because primary textures and structures are widely preserved in low-strain domains, and in metamorphic rocks up to the greenschist/amphibolite transition (see Figs 12 and 13). The prefix 'meta' is therefore omitted when referring to these rocks. In higher grade, high-strain domains amphibolite, tremolite schist, and felsic schist predominate.

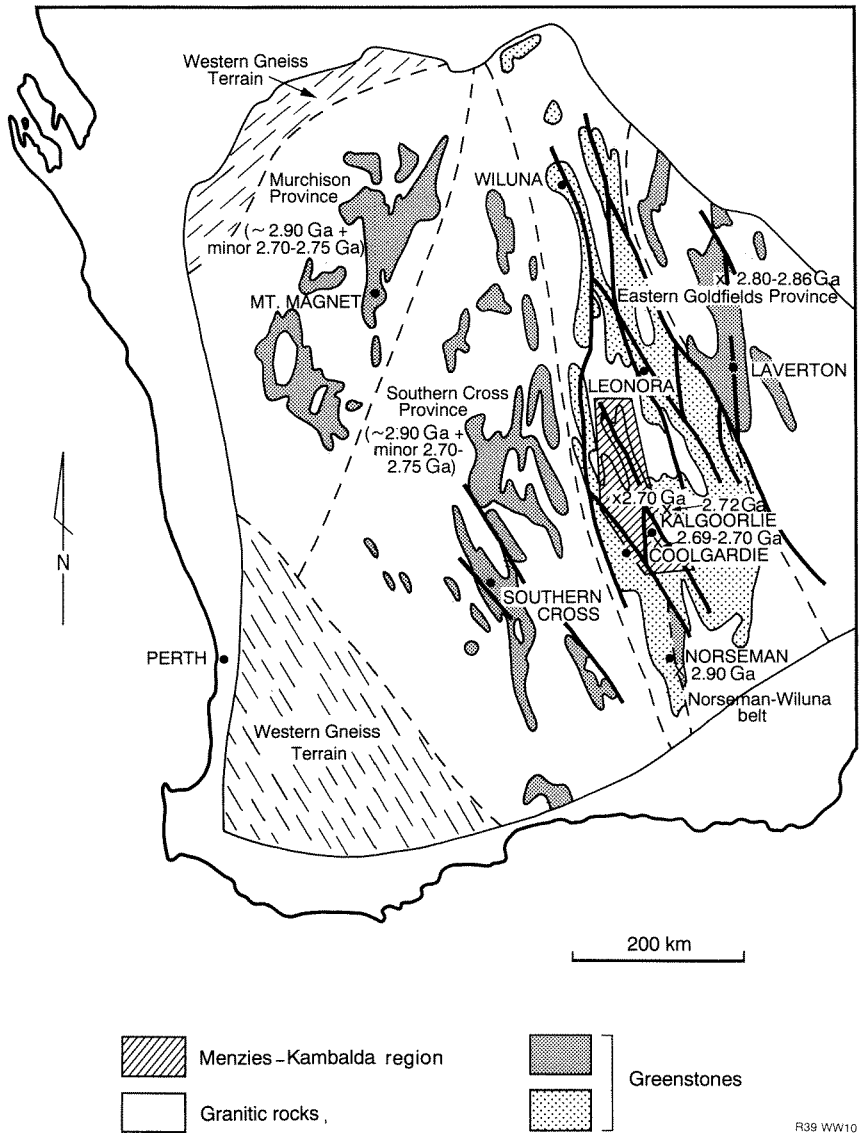

Figure 10. Depositional ages in the Yilgarn Craton, Western Australia. Major divisions of the Craton are modified from Williams (1974). Age data are as follows: Murchison and Southern Cross Provinces — c. 2.90 Ga and minor 2.70–2.75 Ga (U–Pb zircon, Pidgeon, 1986, and other references quoted in Barley and Groves, 1989); northeast Eastern Goldfields Province — 2.80–2.86 Ga (Pb–Pb syngenetic galena, Browning et al., 1987); Norseman — c. 2.90 Ga (U–Pb zircon, Campbell and Hill, 1988); Kambalda — 2.69–2.70 Ga (U–Pb zircon, Claoué-Long et al., 1988; Campbell and Hill, 1988); Ora Banda — 2.70 Ga (U–Pb zircon, Pidgeon, 1986); Bulong — 2.72 Ga (U–Pb zircon, cited in Barley and Groves, 1989)

Komatiites

Komatiites are volcanic peridotites with >18% MgO (Arndt and Nisbet, 1982), although Donaldson et al. (1986) argued, with some justification, for a lower limit of 16% MgO. Platy olivine spinifex texture is diagnostic, but typical komatiite flows consist of a lower orthocumulate zone and an upper spinifex-textured zone (Arndt et al., 1979). Massive komatiite, lacking spinifex texture is also common in the Ora Banda area. Thick, strongly differentiated flows with pyroxene spinifex-textured and gabbroic zones, such as those documented by Arndt (1977) have not been recognized with certainty but may occur in the Ora Banda area (Witt and Harrison, 1989). Discontinuous, sulfide-rich, albitic and carbonaceous interflow sediments occur at Kambalda, but are less common at Ora Banda.

Primary minerals are rarely preserved. Low-grade metamorphic assemblages consist of serpentine, talc, chlorite, and carbonate for more magnesian rocks; and tremolite and chlorite for less magnesian rocks. At higher metamorphic grades, komatiites occur as tremolite–chlorite(–talc) schist.

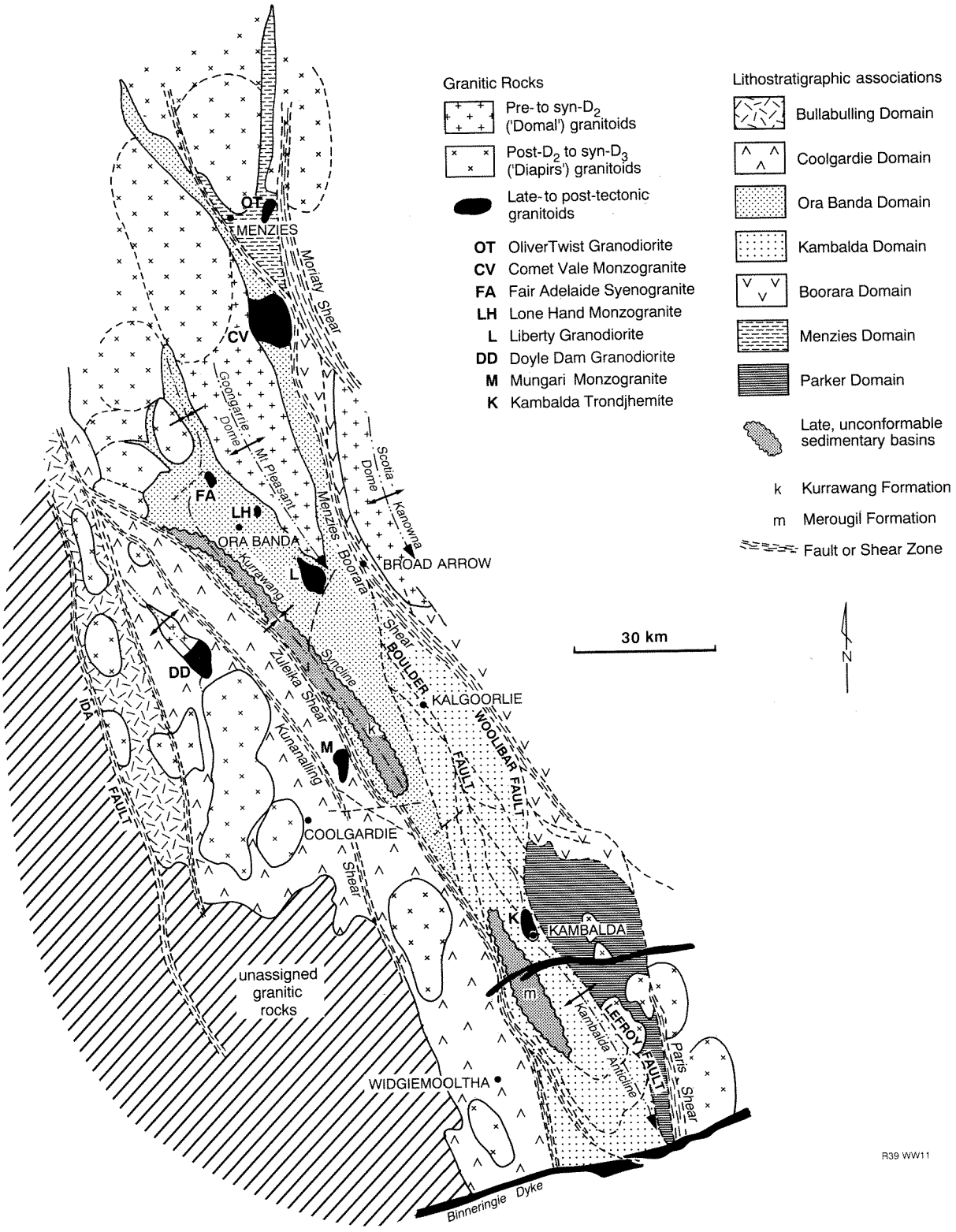

Figure 11. Geology of the Menzies–Kambalda region, and adjoining area to the west, showing major lithostratigraphic associations and division of granitic rocks. Sources: Swager and Witt (1990); Witt and Swager (1989a); Wyche and Witt (1992); Hunter (1988a,b); Griffin (1988a,b); Keats (1987); Ahmat (in prep.) See also Swager et al. (1990)

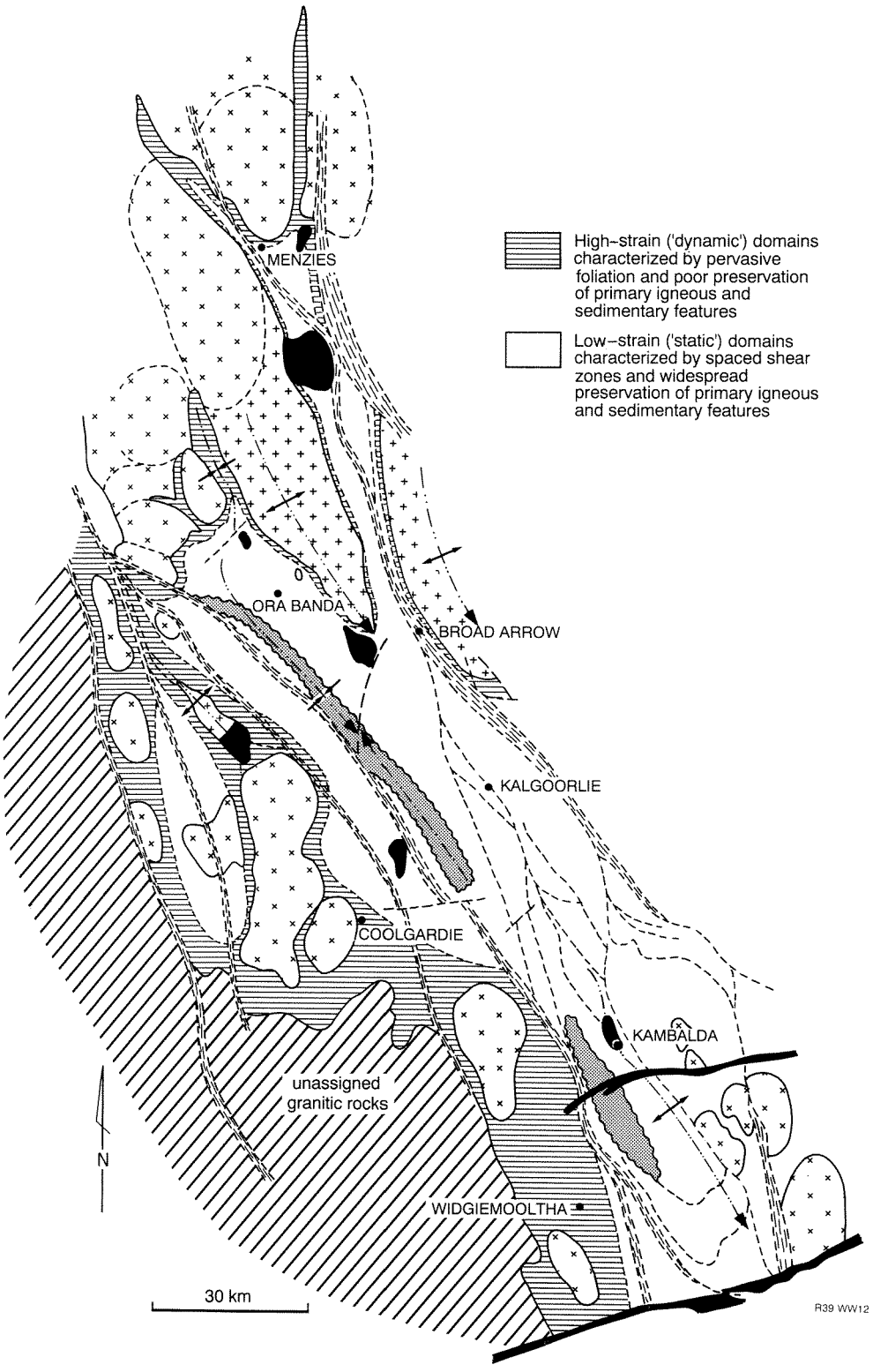

Figure 12. Distribution of high-strain and low-strain domains in the Menzies–Kambalda region, and adjoining area to the west. See Figure 11 for other geological symbols

More detailed descriptions of komatiites in the Menzies–Kambalda region are given by Stolz and Nesbitt (1981); Gresham and Loftus-Hills (1981); Groves and Lesher (1982); Donaldson et al. (1986); Hill et al. (1987) and Morris (in press). The komatiitic rocks are generally regarded as having formed by partial melting of a large percentage of a depleted, deep (>400 km) mantle source (Nesbitt and Sun, 1976; Sun and Nesbitt, 1978; Nesbitt et al., 1979; Takahashi and Scarfe, 1985).

Komatiitic volcanics host nickel-sulfide mineralization in the major nickel mining centre of Kambalda (Groves

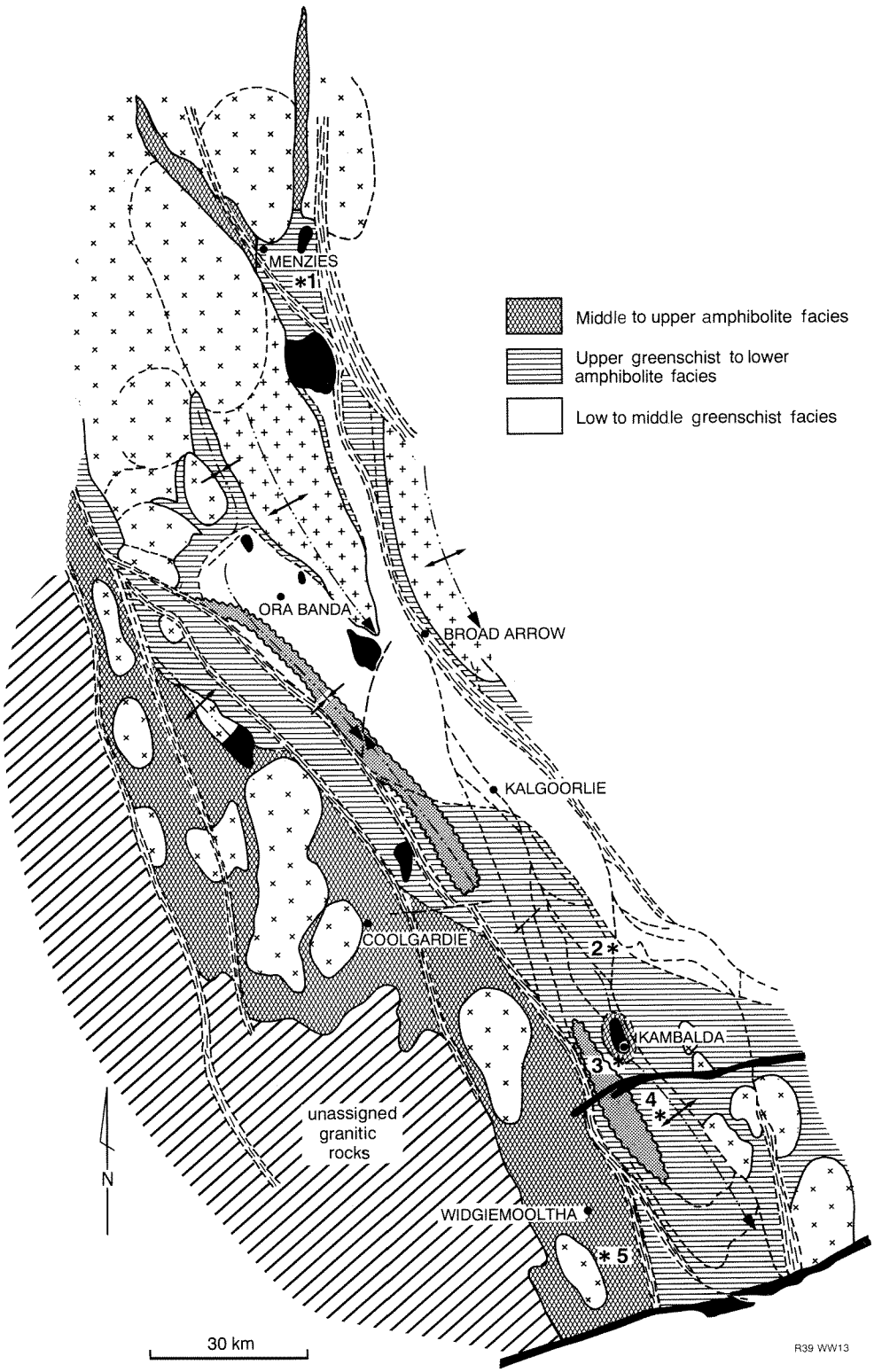

Figure 13. Regional distribution of metamorphic facies in the Menzies–Kambalda region, and adjoining area to the west. Localities marked * have assemblages indicating the following metamorphic conditions:

1. **400–525°C, < 3.8 kb (Ashley and Martyn, 1987);**
2. **500°C, 4 kb (Purvis, 1984);**
3. **575°C, 2.5 kb (Wong, 1986);**
4. **520°C, 2.5 kb (Bavington, 1979);**
5. **500–600°C, 3-5 kb (McQueen, 1981).**

See Figure 11 for geological symbols

and Lesher, 1982; Marston, 1984). Several nickel deposits have been documented in the Widgiemooltha area (McQueen, 1981), and a smaller deposit occurs at Scotia (Christie, 1975; Page and Schmulian, 1981; Stolz and Nesbitt, 1981).

The Walter Williams Formation (equivalent to the Walter Williams unit of Hill et al., 1987) is a thick sequence, up to 250 m, of olivine cumulates which underlies komatiitic volcanic rocks in the Ora Banda Domain. The Walter Williams Formation is poorly exposed, appearing mostly as a silica-rich caprock. Internal structure can be distinguished from relic textures in the caprock, in core and chips from exploration drilling, and in limited unsilicified outcrops. Coarse-grained (2–10 mm) olivine adcumulate is the dominant rock type. A relatively narrow zone of olivine orthocumulate occurs at the base of the formation. Adcumulate rocks are separated from overlying olivine orthocumulate by a thin layer of coarse-grained harrisitic olivine. The transition between the upper olivine orthocumulate zone and overlying spinifex-textured flow units is a complex layered zone of variable thickness, consisting of pyroxenite, gabbro, and Mg-rich leucogabbro (Witt and Harrison, 1989). The Walter Williams Formation appears to be an extensive, sheet-like unit which can be traced almost continuously from Siberia (northwest of Ora Banda) to Ghost Rocks, northwest of Menzies (Hill et al., 1987). Similar rocks at Agnew and Mt Keith in the northern part of the Norseman–Wiluna belt, and at Forrestania in the Southern Cross Province, have been interpreted as intrusive ultramafic rocks (Groves and Lesher, 1982; Marston, 1984). However, recent work on the Walter Williams Formation and other similar occurrences has led Hill et al. (1987) to propose a volcanic origin. These authors suggest that olivine nucleated at the base of massive outpourings of komatiitic lava and that the various olivine textures reflect differing degrees of supercooling and nucleation rates.

Basalt

Table 2 summarizes the range of basalt types found in the Eastern Goldfields Province and their main characteristics. The distinction between different basalt types requires comprehensive geochemical data, and is replaced in this report by a simpler three-fold classification based on textural features which can be observed in the field or in thin section. The high-Mg series/low-Mg series classification of Redman and Keayes (1985) is supplemented by a third group consisting of coarsely plagioclase-phyric basalt. The term komatiitic basalt in particular has genetic connotations (Arndt and Nisbet, 1982) and is avoided in this report. Both pillowed and massive basalts are widespread, and vesicles have been identified in some areas, indicating subaqueous, probably submarine, deposition. Narrow interflow sediments are common. Basaltic rocks are commonly associated with layer-parallel zones of doleritic to gabbroic material, up to 50 m thick. Drilling at Ora Banda and other localities indicates that some of these coarser grained units are more slowly cooled portions of basaltic flows while others appear to be comagmatic sills (Shaw, 1988; Harrison et al., 1990; P. Morris, pers. comm., 1989).

High-Mg series basalt

Redman and Keayes (1985) identified high-Mg series basalt based on the presence of skeletal pyroxene forms. Skeletal pyroxene may be subequant to elongate to acicular, and may form coarse, randomly oriented needles or radiating sheafs of needles ('stringy beef' texture) up to several centimetres in length. Interstitial fan- and/or arborescent-shaped, spherulitic and dendritic pyroxene forms are also common. Early descriptions of these textures in high-Mg series basalt from the Mt Monger area, northeast of Carnilya Hill, were given by Williams (1972). Other high-Mg series basalts are characterized by rounded, pale green to white ocelli or varioles up to about 5 mm across.

High-Mg series basalt may form by fractionation of komatiitic parent melts (Arndt et al., 1977) but Western Australian high-Mg series basalt is more commonly ascribed to primary partial melting of a mantle source (Sun and Nesbitt, 1978; Redman and Keayes, 1985).

Siliceous high-Mg series basalt has been recognized in the Kambalda and Kalgoorlie areas where it overlies komatiitic volcanic rocks and is distinguished from normal high-Mg series basalt by high SiO_2 (>52%), low Ti/Zr, and enrichment of incompatible elements (Redman and Keayes, 1985; Barley and Groves, 1988). Siliceous high-Mg series basalt has been attributed to partial melting of an enriched mantle source (Redman and Keayes, 1985) or crustal contamination of mantle-derived melts (Barley, 1986; Arndt and Jenner, 1986; Sun et al., 1989).

Low-Mg series basalt

Low-Mg series basalt is characterized by intergranular to subophitic textures. Small plagioclase phenocrysts up to about 2 mm occur in some low-Mg series basalt samples. This rock type is widespread in the Eastern Goldfields and has been characterized as low-K tholeiite by Hallberg (1972). There is some chemical overlap between low-Mg series basalt and fractionated (low-Mg) members of the high-Mg series basalt suite, but the latter are still distinguished by the presence of skeletal pyroxene forms (Redman and Keayes, 1985).

Low-Mg series basalt is generally considered to form by smaller amounts of partial melting of a similarly depleted mantle source to that which yielded komatiite and high-Mg series basalt, followed by variable amounts of crystal fractionation (Redman and Keayes, 1985; Nesbitt and Sun, 1976; Morris, in press). Crustally contaminated low-Mg series basalt has been recognized in the Leonora–Laverton area (Jolly and Hallberg, 1990) but to date has not been recognized in the Menzies–Kambalda region.

Plagioclase-phyric basalt

Low-Mg series basalt containing coarse plagioclase phenocrysts up to approximately 3 cm occurs in the Ora Banda area, and outcrops sporadically between Broad Arrow and Menzies. The basalt was characterized as high-Fe tholeiite by Redman and Keayes (1985) and probably has a similar origin to other low-Mg series basalts but has

Table 2. A summary of petrographic, chemical, and petrological features of ultramafic–mafic volcanism in the Eastern Goldfields Province, Western Australia (from Barley and Groves, 1988)

Differentiation series	*Lithology*	*Petrography*	*Chemistry*	*Petrogenesis*
1. Komatiite	(a) Komatiite (>18 wt% MgO)	(a) Olivine-dominated spinifex textures and cumulate zones	Close to chondritic ratios for most trace elements, generally depleted in the more incompatible elements (e.g. Rb, Ba, Th, K, and light REE). CaO/Al_2O_3 generally close to 1 N.B. Enrichment in incompatible elements and SiO_2 may occur locally as in 3	1, 2, and 3 derived from depleted mantle source. Chemical variation between series is the result of (a) degree of partial melting (1 and 2); and (b) crustal contamination (most pronounced in 3). Members within series related by crystal fractionation and magma mixing (1 and 2) and combined assimilation and crystal fractionation (most pronounced in 3)
	(b) Komatiitic basalt (9–15 wt% MgO)	(b) Elongate, subequant to skeletal olivine; acicular, elongate to skeletal pyroxene; interstitial dendritic and/or spherulitic pyroxene, minor plagioclase		
	(c) Komatiitic basalt (5–9 wt% MgO)	(c) Skeletal and/or spherulitic pyroxene, interstitial plagioclase		
2. High-magnesian series basalts	(a) High-Mg basalt (9–15 wt% MgO)	(a) As 1(b)		
	(b) Basalt (5–9 wt% MgO)	(b) As 1(c). Skeletal pyroxene or pyroxene-phyric basalts	As 1(b) and 1(c)	
3. Siliceous high-magnesian series basalts	(a) Siliceous high-Mg Basalt (9–15 wt% MgO) (b) Basalt (variolitic) (5–9 wt% MgO)	(a) & (b) Similar to 1(b) and 1 (c), but with higher modal plagioclase and common prominent development of felsic varioles	>52 wt% SiO_2 and variable enrichment in incompatible elements (e.g. Rb, Ba, Th, K, and light REE). CaO/Al_2O_3 generally less than 1	Derived from 1 or 2 by crustal assimilation and crystal fractionation. Alternative origin from enriched mantle source
4. Low-magnesian series basalts	(a) Tholeiite (<9 wt% MgO)	(a) Intergranular to subophitic textures with plagioclase laths and interstitial stubby or bladed pyroxene	Most MgO-rich lavas depleted in incompatible elements, local enrichment in more evolved members. Fe and Ti enrichment in some suites and intrusions	Parent magmas to 4(a) derived from depleted mantle by lower degrees of partial melting than 1 and 2. Members within series related by crystal fractionation. Pre-eruption plagioclase fractionation important in 4(b)
	(b) Plagioclase megacrystic basalt	(b) Similar to 4(a), but with plagioclase megacrysts (>1 cm)		

undergone some high-level fractionation involving plagioclase.

In high-strain, high-grade metamorphic domains, the three classes of basalt are converted to amphibolite and become very difficult to distinguish without detailed chemical data. However, some idea of relative MgO contents can be ascertained from the metamorphic mineralogy — with higher MgO amphibolites containing more tremolite and less plagioclase than lower MgO amphibolites.

Layered and differentiated mafic/ultramafic sills

Layered and differentiated mafic/ultramafic sills up to about 2 km thick are common in the Menzies–Kambalda region. Emplacement is generally localized at interflow sediment horizons within predominantly basaltic sequences. Based on regular geochemical trends, and reasonable agreement between fine-grained margins and calculated bulk composition, the sills are generally regarded as single pulse intrusions which differentiated in situ. Bulk composition of the sills varies from high-Mg series basalt to tholeiitic (Williams and Hallberg, 1973; Clark, 1980; Witt et al., 1991). Table 3 summarizes the main characteristics of several of the more important sills in the Menzies–Kambalda region. Although an extrusive origin has been proposed for some of these bodies (Tomich, 1974; Golding, 1985), an intrusive origin is more generally accepted. Evidence for an intrusive origin of some bodies includes their broadly transgressive nature (Ora Banda Sill, Witt and Swager, 1989a); intrusive contacts (Golden Mile Dolerite, Clark, 1980); and melting of roof rocks to incorporate xenocrysts or alkali elements (Ora Banda Sill, Mt Pleasant Sill, Witt, 1987; Witt et al., 1991). Furthermore, spinifex-textured upper zones comparable to those in thick layered flows (Arndt, 1977) have not been recognized in layered complexes with high-Mg bulk compositions (e.g. Mt Pleasant Sill).

A number of these sills have been studied in some detail, and cross sections documenting zoning in individual sills have been shown in the relevant sections of this study (Witt, 1993b,c). Their role as host rocks to gold mineralization is discussed in chapter 3.

Felsic volcanics and volcaniclastic rocks

Intermediate to felsic volcaniclastic sedimentary rocks are widespread, though poorly exposed, in the Menzies–Kambalda region. Best exposures are found on the margins of salt-lake systems such as Lake Lefroy and Lake Goongarrie. A wide range of rock types includes coarse-grained granite-pebble conglomerate, polymictic conglomerate, greywacke, sandy and silty sedimentary rocks, including plagioclase-rich crystal tuffs or reworked tuffs, and grey and black shale. The epiclastic or pyroclastic origin of these rocks is commonly difficult to determine. However, widespread graded bedding and local cross-bedding in finer grained sedimentary rocks suggest subaqueous deposition of detritus derived from a predominantly volcanic source. The finer grained rocks may represent distal turbiditic sediments while coarser fragmental rocks are probably proximal mass-flow and related deposits.

Although epiclastic sediments are dominant, true pyroclastic deposits and lavas have been recognized at several localities (e.g. Gibson–Honman Rock, Griffin et al., 1983). Roberts and Elias (1990) described the Newtown Felsic Volcanics in the Kambalda – St Ives area as comprising massive porphyritic rhyolite, lapilli tuff, volcanic conglomerate, and laminated tuffs. Near White Flag Lake and Ora Banda, autobrecciated andesite flows have been described by Hunter (1993) and Witt (1990). At Binduli, coarse fragmental rocks containing angular dacite clasts are interpreted as agglomerate. The volcanic rocks are commonly interpreted as representing emergent centres of subaerial volcanism from which the subaqueous epiclastic deposits were derived (e.g. Groves and Lesher, 1982).

Few chemical data are available but K-feldspar is subordinate to plagioclase in most of the felsic to intermediate volcanic and related volcaniclastic rocks, suggesting dacitic to rhyodacitic compositions predominate. Hallberg and Giles (1986) recognized two types of felsic volcanic centres in the Leonora–Laverton area, north of the Menzies–Kambalda region. These are:

(a) andesite-dominated calc-alkaline complexes derived by shallow hydrous melting of large ion lithophile (LIL)-enriched mantle; and

(b) a bimodal association of tholeiitic basalt with mildly peralkaline rhyolite, the latter probably derived from crustal melting. A more substantial geochemical data base is required before the applicability of this two-fold classification to the intermediate to felsic volcanic and volcaniclastic rocks of the Menzies–Kambalda region can be assessed.

Sedimentary rocks

Quartz-rich, cross-bedded sandstone and conglomerate occur in late, tectonically controlled basins. Polymictic conglomerate contains rounded pebbles and cobbles of granitoid, porphyry, chert, sandstone, banded iron-formation, and less abundant mafic volcanics. Palaeocurrent directions suggest derivation from a source area to the west and predominantly longitudinal current flow along north-northwest-trending elongate basins (Barley and Groves, 1988). Witt and Swager (1989b) interpreted the Kurrawang Formation to have been deposited in a partly synclinal basin, confined to the west by a regional shear zone (the Zuleika Shear). Sediments were derived from an uplifted block to the west of the shear zone during transpressional deformation.

Stratigraphy

Early regional stratigraphic correlations suggested by Gemuts and Theron (1975) and Williams (1969) lacked adequate structural control and now require revision.

Table 3. Summary of characteristics of the main layered and differentiated sills in the Menzies–Kambalda area

	Mt Ellis Sill	*Mt Pleasant Sill*	*Williamstown/Mt Hunt/ Pernatty Dolerite*	*Defiance Dolerite*	*Ora Banda Sill*	*Golden Mile Dolerite/ Triumph Gabbro*	*Junction Dolerite*
Occurrence	Grants Patch Mt Ellis Windanya	New Mexico Ora Banda Mt Pleasant Windanya Goongarrie	Golden Mile Celebration	Victory–Defiance (Kambalda)	Mt Carnage New Mexico Ora Banda Grants Patch	Golden Mile Celebration	St Ives
Thickness	Up to ~600 m	Up to ~600 m	Up to ~400 m	~300 m	~2000 m	Up to 800 m, more commonly ~400 m	400–500 m
Number of zones	4	12	4	10	6–8	10	?5
Petrography	Fe-rich gabbro and granophyre ↑ Olivine gabbro	Fe-rich granophyre ↑ Peridotite	Gabbro ↑ Pyroxenite	Fe-rich granophyre ↑ Pyroxenite	Ferro-gabbro (felsic granophyre below roof) ↑ Peridotite	Fe- rich granophyre ↑ Pyroxenite	Fe-rich granophyre ↑ Pyroxenite
Bulk MgO content (calculated)	7.6%	~11%	18.7%	9.1%	16–18%	5.4%	?
References	Witt (1987, 1990)	Witt (1987, 1990) Witt et al. (1991)	Travis et al. (1971) Williams and Hallberg (1973)	Clark et al. (1986) Roberts (1988) Roberts and Elias (1990)	Williams and Hallberg (1973) Witt (1987, 1990)	Travis et al. (1971) Clark (1980) Phillips (1986)	Roberts and Elias (1990)

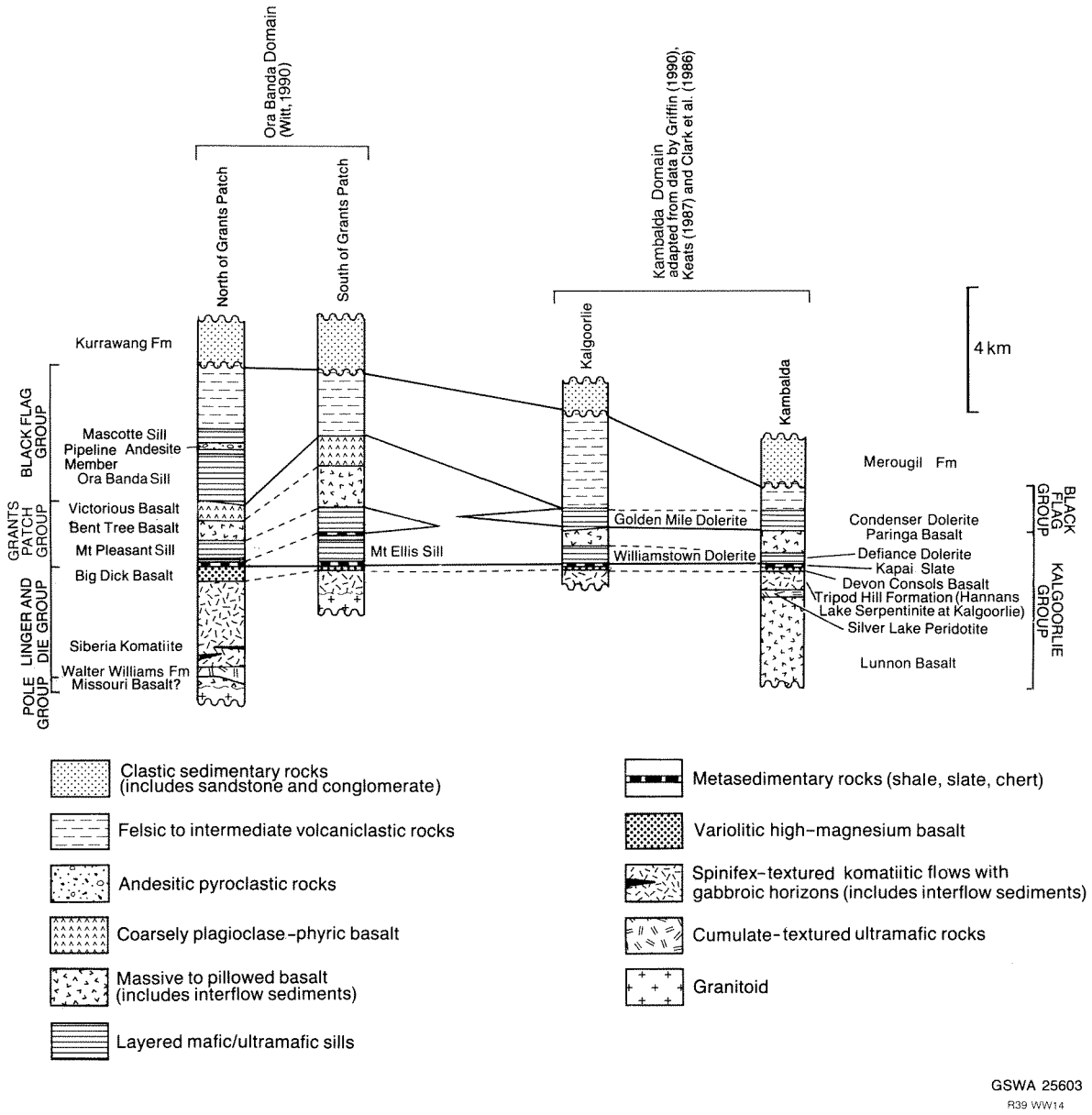

Figure 14. Possible correlations between greenstone sequences at Ora Banda, Kalgoorlie, and Kambalda

Swager et al. (1990) proposed a revised structural–stratigraphic interpretation, based on 1:100 000 mapping by the GSWA and several published local stratigraphic successions (Table 4). Travis et al. (1971) published a stratigraphy for the Kalgoorlie area, based on extensive exploration drilling and underground development. Mapping by Western Mining Corporation around Kambalda has established a similar greenstone succession (Roberts, 1988), and this is generally correlated with the Kalgoorlie greenstones (Clark et al., 1986; Griffin, 1990b; Roberts and Elias, 1990). The portion of the Kalgoorlie Terrane occupied by the Kalgoorlie–Kambalda greenstone succession (or lithostratigraphic association) has been termed the Kambalda Domain by Swager et al. (1990). Recent mapping by the GSWA, north of Kalgoorlie, has led to the recognition of another greenstone succession similar to that at Kalgoorlie and Kambalda (Witt and Harrison, 1989; Witt, 1990). The area underlain by this lithostratigraphic association has been termed the Ora Banda Domain (Swager et al., 1990). Possible correlations between the Ora Banda and the Kalgoorlie–Kambalda successions are shown in Figure 14. At the present erosion level, a broad expanse of felsic volcaniclastic-dominated rocks (Black Flag Group) separates the mafic/ultramafic sequences at Ora Banda and Kalgoorlie. It is not clear if the lower mafic/ultramafic parts of the two sequences are continuous beneath the Black Flag Group or if they were deposited in separate basins and subsequently overlain by a more extensive sequence of felsic volcaniclastic rocks. The areal extent of the Ora Banda and Kambalda Domains is shown in Figure 11.

Christie (1975), Page and Schmulian (1981), and Stolz and Nesbitt (1981) described a slightly different succession at Scotia which has subsequently been shown to extend from east of Goongarrie to south of Paddington

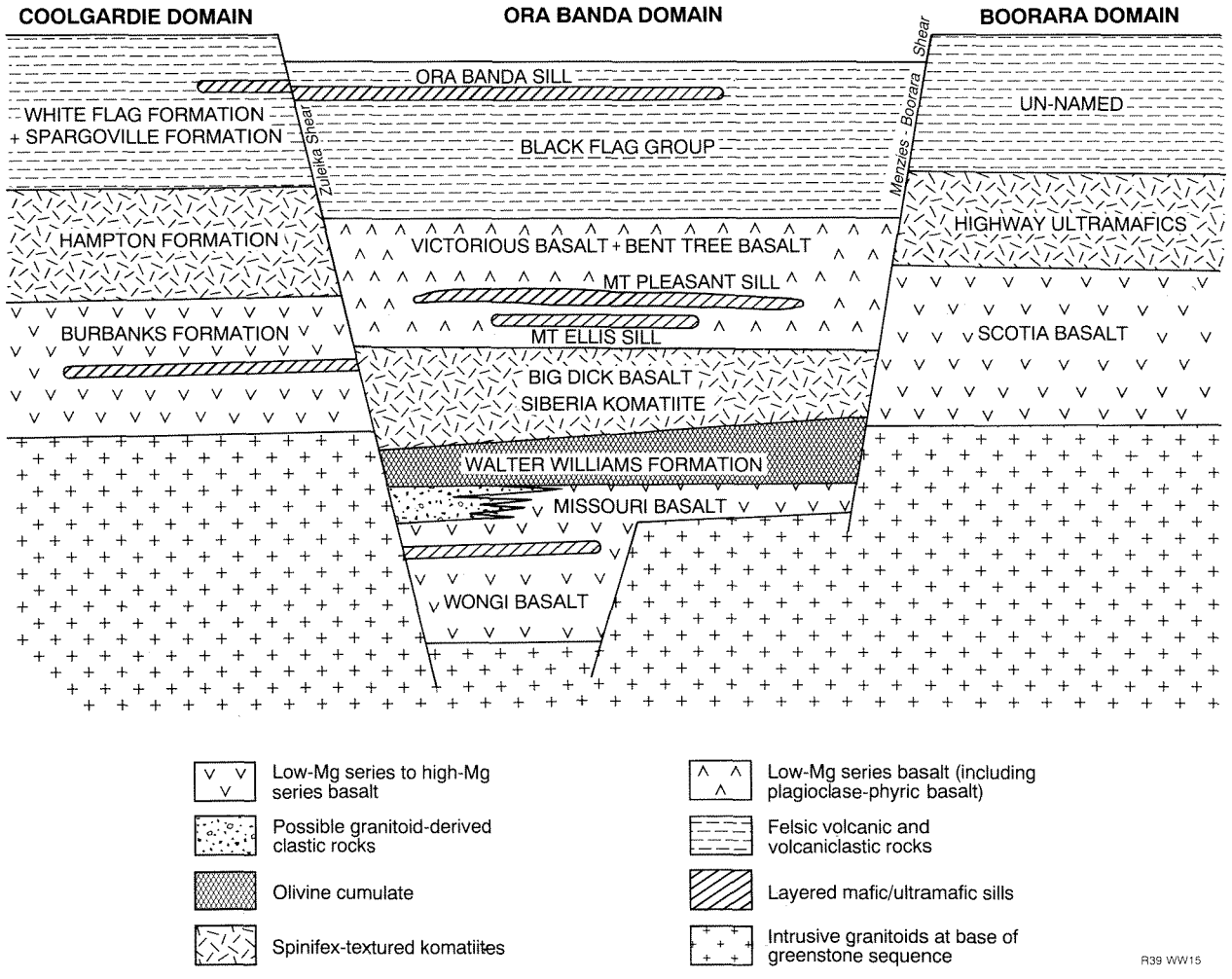

Figure 15. Interpreted pre-compressional deformation east–west section (schematic) through the central portion of the Menzies–Kambalda region

(Witt and Swager, 1989a). This association is interpreted as extending southwards to the strongly deformed Golden Ridge belt and Carnilya Hill. This sequence defines the Boorara Domain (Swager et al., 1990) and differs from those in the Ora Banda and Kambalda Domains, primarily in the absence or weak development of the upper basalt unit and associated sills (Table 4). Hunter (1993) recognized a similar stratigraphic succession to that at Scotia, in the Coolgardie area. The areal extent of the Boorara and Coolgardie Domains is shown in Figure 11.

A fourth lithostratigraphic association recognized around Menzies is shown in Figure 11. Although rock types are broadly similar to those found in the Boorara and Coolgardie Domains, structural complexity prevents recognition of a coherent stratigraphic sequence (Swager, 1991). The Bullabulling Domain is a strongly deformed sequence of alternating basalt and felsic schists (Swager et al., 1990).

The Coolgardie, Ora Banda, Kambalda, and Boorara Domains are separated by regional shear zones which have accommodated significant but unquantified strike-slip and subvertical movements. Correlations across these regional shear zones must be viewed with caution. However, the similar stratigraphic successions and rock types invite interpretation of the regional shear zones, such as the Zuleika Shear and the Boorara Shear, as long-lived features which were initiated as growth faults. Deposition of the Walter Williams Formation and the upper mafic sequence was restricted to the Ora Banda and Kambalda Domains, which were bound by the two shears (Fig. 15).

While most published stratigraphic columns emphasize a lower mafic/ultramafic sequence overlain by an upper felsic volcanic and volcaniclastic sequence, recent observations indicate the presence, at some localities, of probable felsic volcanic- and/or granitoid-derived sediments in the lower part of the greenstone succession. At Mt Shea, coarse-grained dacitic/andesitic fragmental rocks are interbedded with Hannans Lake Serpentinite. North and west of Siberia, felsic schists are found within the Wongi and Missouri Basalts. Most notably at Black Rabbit Dam, a thick unit of plagioclase-rich felsic schist interfingers with Missouri Basalt, and both upper and lower contacts of the felsic schist are stratigraphically controlled. Interleaving of felsic schists and volcaniclastic rocks with mafic and ultramafic volcanics appears to increase east (Kanowna, Bulong) and west (Chadwins Dam) of the Menzies–Kambalda region.

Table 4. Stratigraphic correlations for the Ora Banda, Kambalda, Coolgardie, and Boorara Domains of the Kalgoorlie Terrane

Stratigraphic succession	*Characteristic lithologies*	*Ora Banda Domain*	*Kambalda Domain*	*Coolgardie Domain*	*Boorara Domain*
Polymictic conglomerate unit	Polymictic conglomerate; immature sandstone; coarse trough cross beds, graded beds	Kurrawang Formation	Merougil Conglomerate	Absent	Absent
Felsic volcanic and sedimentary unit	Felsic volcaniclastic–sedimentary rocks, ranging from coarse clastic sandstone to interbedded sand/siltstone Rhyolite to dacite, locally andesite; lava, tuff, agglomerate	BLACK FLAG GROUP: Pipeline Andesite; Orinda Sill; Ora Banda Sill	BLACK FLAG GROUP: Junction Dolerite; Condenser Dolerite; Golden Mile Dolerite; Triumph Gabbro	BLACK FLAG GROUP: White Flag Formation; Powder Sill; Spargoville Formation	Felsic unit, volcanic and sedimentary rocks
Upper basalt unit	High-Mg and tholeiitic basalt; massive, pillowed and vesicular lavas	GRANTS PATCH GROUP: Victorious Basalt; Bent Tree Basalt; Mt Pleasant Sill; Mt Ellis Sill	KALGOORLIE GROUP: Paringa Basalt; Defiance Dolerite; Williamstown Dolerite; Kapai Slate; Devon Consols Basalt; Kambalda Komatiite	COOLGARDIE GROUP: Absent or thin and discontinuous	Absent or thin and discontinuous
Komatiite unit	Massive olivine adcumulate and/or thick komatiite flows, overlain by thin komatiite flows with minor interflow sedimentary beds; high-Mg basalt at top	LINGER AND DIE GROUP: Big Dick Basalt; Siberia Komatiite; Walter Williams Formation		Hampton Formation	Highway Ultramafics
Lower basalt unit	Tholeiitic and high-Mg basalt flows, subaqueous	POLE GROUP: Missouri Basalt; Wongi Basalt	Lunnon Basalt	Golden Bar Sill; Burbanks Formation; Three Mile Sill	Big Blow Chert; Scotia Basalt
References		Witt (1987, 1990)	Roberts (1988) Woodall (1965) Langsford (1989)	Hunter (1993)	Christie (1975) Witt (1990)

Structure

The earliest phase of deformation in the Norseman–Wiluna belt involved some form of rifting which formed depositional basins for the greenstone sequences. This section describes the subsequent phase of compressional deformation in the Menzies–Kambalda region which appears to be consistent with the deformation history throughout the Kalgoorlie Terrane.

Archibald et al. (1978) presented one of the earliest structural studies in the Eastern Goldfields, based on mapping around Widgiemooltha, west of Kambalda (Fig. 11). Subsequent studies south of Kambalda (Gresham and Loftus-Hills, 1981; Griffin, 1990b) recognized many of the structural elements recorded by Archibald and his coworkers, though they differed in some details. Swager (1989) described the structural history of the Kalgoorlie greenstones and correlated events in that area with those recorded in the Widgiemooltha and Kambalda areas. Witt (1990) described a similar deformational history for greenstones in the Ora Banda and Boorara Domains. The following history of deformation for the Menzies–Kambalda region, used in this report and summarized in Table 5, is modified only slightly from those of Swager (1989) and Witt (1990). The east-trending folding event recorded by Gresham and Loftus-Hills (1981) and Griffin (1990b) is omitted from this report. There is no evidence of an easterly trending axial planar fabric, and domal structures can be adequately explained by progressive east–west shortening or interference between flat-lying recumbent folds and east–west shortening.

D_1 Subhorizontal thrusting and recumbent folding

Archibald et al. (1978) first recognized early recumbent folding in the Widgiemooltha area, and Spray (1985) proposed an early thrust surface along a granite/greenstone contact exposed on the margins of Lake Dundas, south of Norseman. Early subhorizontal thrust faulting and/or recumbent folding has also been proposed for several localities in the Menzies–Kambalda region.

Gresham and Loftus-Hills (1981) and Griffin (1990b) recognized several D_1 thrust surfaces south of Kambalda. Swager (1989) interpreted the Mt Hunt and Feysville Faults (Fig. 16) as D_1 thrusts, and also proposed a D_1 thrust and recumbent fold in the Golden Mile mining area at Kalgoorlie. Swager and Griffin (1990) recognized two major thrust sheets in the Kambalda Domain (Fig. 16). There are no obvious indications of D_1 deformation in the Ora Banda Domain, although subhorizontal movements along contacts between greenstones and early ('domal') granitoids may have occurred (Witt, 1990). The overturned Carnilya Hill Anticline is considered to be a D_1 recumbent fold which has been pushed over the D_1 Talcum Fault, suggesting transport from the southwest.

D_2 Regional folding

Upright, open to tight folds with north-northwest trending fold axes dominate the structure of the Menzies–Kambalda region (Fig. 11). The regional D_2 event has

Table 5. Structural history of the Menzies–Kambalda region

Event	*Description*	*Localities*	*References*
D_1	Subhorizontal thrusting and recumbent folding	Kalgoorlie to south of Kambalda	1, 2
		Carnilya Anticline	3
		Subhorizontal granite–greenstone contacts	4
D_2	Upright regional folds with NNW-trending axial planes and shallowly plunging fold axes	Kambalda Anticline	1, 2
		Goongarrie–Mt Pleasant Anticline	4
		Scotia–Kanowna Anticline	4
		Kurrawang Syncline	5
D_3	Sinistral strike-slip movement on NNW-trending shear zones, and continued regional shortening; sub-vertical movements on some shear zones during late D_3	Boorara–Menzies Shear	4, 6
		Moriaty Shear	7
		Boulder–Lefroy Fault	8, 9
		Zuleika Shear	6
D_4	Dextral movements on NNW-trending shear zones, and formation of N–S to NNE dextral faults	Kalgoorlie	8, 9
		Paddington	4
		Mt Pleasant (Black Flag Fault?)	4

References: 1. Gresham and Loftus-Hills (1981); 2. Swager and Griffin (1990); 3. Perriam (1985); 4. Witt (1990); 5. Hunter (1993); 6. Swager et al. (1990); 7. Swager (1991); 8. Mueller et al. (1988); 9. Swager (1989)

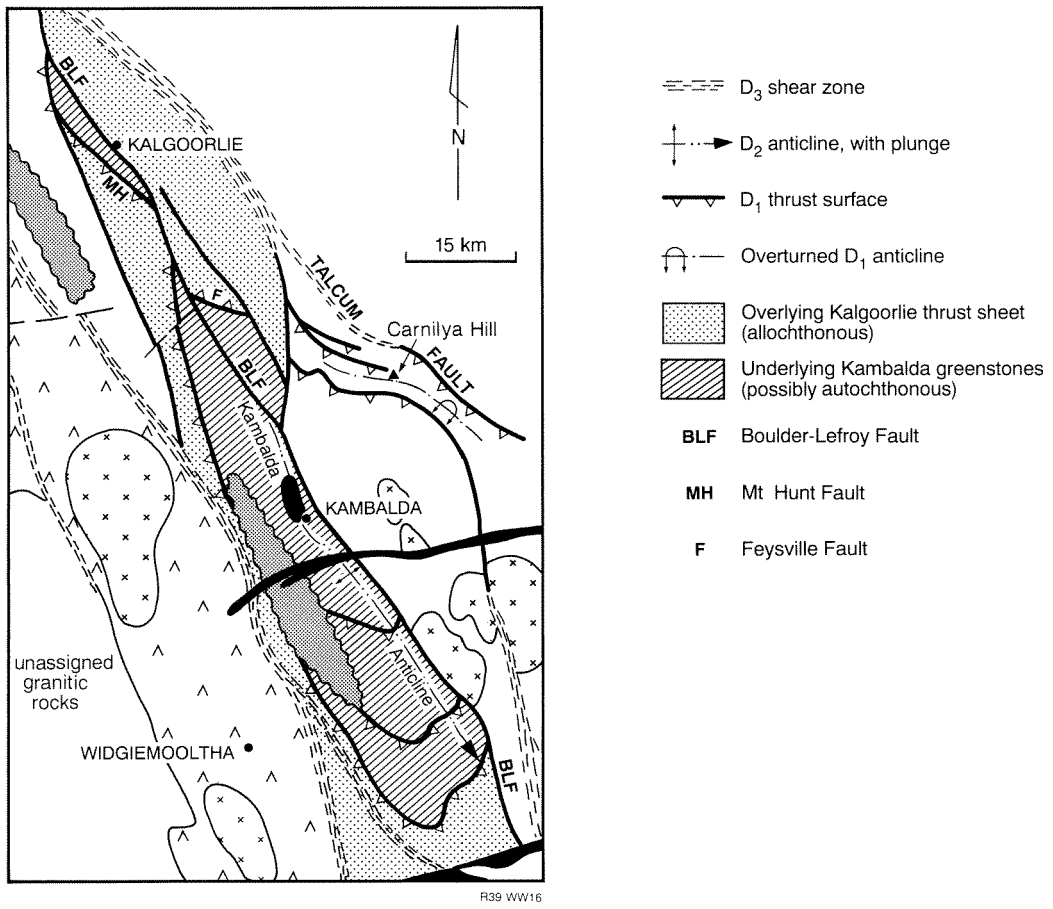

Figure 16. D_1 structures between Kalgoorlie and St Ives (after Swager and Griffin, 1990). Geological symbols as in Figure 11

resulted in the Goongarrie–Mt Pleasant and Scotia–Kanowna Anticlines, which are cored by large granitoid domes. The Kambalda Anticline, and the Kurrawang and Merougil Synclines, are also D_2 folds.

D_1 thrust surfaces south of Kambalda have been folded by the D_2 Kambalda Anticline (Fig. 16). The northern extension of the Kambalda Anticline, between Kambalda and Kalgoorlie, has been sheared out by the Boulder–Lefroy Fault (Swager, 1989). Other regional faults such as the Zuleika Shear, also appear to be partly localized along anticlinal fold axes.

D_3 Sinistral strike-slip faulting

D_2 folds underwent further compression during a major episode of sinistral strike-slip faulting which produced north to north-northwest trending, upright regional shear zones, as well as a number of smaller, subparallel structures. Swager et al. (1990) recognized two classes of regional shear zone.

(a) Fundamental structures which separate domains having contrasting stratigraphic successions (e.g. the Zuleika Shear and the Menzies–Boorara Shear system) form the first class.

They are interpreted as long-lived structures, possibly initiated as growth faults during deposition of the greenstones (see above), but periodically or continuously reactivated during subsequent periods of deformation. A dominant sinistral movement along these structures is indicated by rotated minor D_2 fold axes (e.g. Mt Ellis area), drag folds and s–c fabrics, but the amount of displacement cannot be quantified.

(b) The second group comprises regional shear zones such as the Boulder–Lefroy Fault, across which greenstone successions are readily correlated.

Movement of about 10 km across the Boulder–Lefroy Fault can be measured by the displacement of the Triumph and Pernatty Dolerites (Langsford, 1989). A similar displacement (about 12 km) across the Kunnanalling Shear, in the Coolgardie Domain, is indicated by the offset of komatiitic rocks (Swager, 1989). These 'smaller scale' regional shear zones are commonly associated with F_3 en echelon folds formed during strike-slip movements. Examples of F_3 folds adjacent to the Boulder–Lefroy Fault occur in the Kalgoorlie mining area, e.g. the Boomerang Anticline, and near Celebration mining centre (Witt, 1993c).

Overlap between regional folding and sinistral strike-slip movements is well demonstrated near Mt Ellis, where D_2 fold axes are progressively rotated and then displaced northwards along north to north-northwest trending D_3 sinistral shear zones (Witt, 1990).

Subvertical movements on fault-bound slices within major strike-slip systems are common during wrench faulting (Sylvester, 1988). The widespread preservation of steeply dipping to subvertical stretching lineations and mineral lineations on S_3 shear surfaces, particularly in the narrow Bardoc–Broad Arrow greenstone belt, suggest that significant subvertical movements may have taken place towards the end of D_3.

D_4 Dextral strike-slip movements

D_3 structures are offset by north to north-northeast trending dextral (D_4) faults in the Kalgoorlie mining area and near Paddington. D_4 faults also occur at Mt Pleasant (the Black Flag Fault). The scale of development of these D_4 structures and associated movements is much smaller than the main D_3 sinistral movement.

North-northwest trending lithological contacts and shear zones were continuously reactivated during successive episodes of deformation giving rise to complex deformation histories (e.g. the Bardoc Tectonic Zone, Cashmans Shear Zone, Witt, 1990).

Local deformation

Local deformation related to forceful emplacement of granitic plutons occurs at several localities and locally interacts with regional structures. Examples are found in the Siberia mining area, and around the Liberty Granodiorite, near Mt Pleasant.

Strain resulting from regional deformation has been markedly heterogeneous (Fig. 12). Deformation was concentrated in regional and district-scale shear zones, and largely partitioned around weakly deformed domains such as the Ora Banda – Mt Pleasant area. Narrow to broad zones of pervasive deformation occur as aureoles around post-D_2 to syn-D_3 diapiric granitoids (Fig. 12). This heterogeneous distribution of strain is used as a basis for a structural classification of gold deposits in Chapter 4. Broad zones of pervasive deformation which characterize much of the Coolgardie Domain are not recognized in the Menzies–Kambalda region.

Intrusive rocks

Perring et al. (1988) divided granitic rocks in the Eastern Goldfields into internal and external granitoids, and these have been discussed by Hallberg (1988), and Bettenay (1988), respectively. External granitoids separate large greenstone belts such as the Norseman–Wiluna belt and the Southern Cross greenstone belt, and probably formed by partial melting of granitic gneiss. Internal (I-type) granitoids occur within greenstone belts. They are compositionally varied and formed during deep-seated processes in the lower crust and upper mantle. Granitic rocks in the Menzies–Kambalda region (including both external and internal granites) were emplaced throughout the compressional phase of deformation, and can be divided into three groups, based on their relationships with large-scale structures (Witt and Swager, 1989b). The distribution of the three structural groups of intrusive granitoid in the Menzies–Kambalda region and adjoining areas is shown in Figure 11.

(a) Pre- to syn-D_2 ('domal') granitoids form the first group.

'Domal' granitoids occur in the cores of regional D_2 anticlines and are broadly conformable with the overlying greenstone succession. They are commonly composite plutonic complexes which display strongly deformed, contact-parallel marginal zones and a more pervasive regional foliation. These bodies may be early (syn-D_2) solid state diapirs which have been strained during later deformation, or they may have been emplaced at the base of the greenstone pile prior to regional folding. Examples include the Goongarrie–Mt Pleasant dome and the Scotia–Kanowna dome.

(b) The second group comprises post-D_2 to syn-D_3 granitoids ('diapirs').

This group of granitoids consists of roughly circular to slightly ovoid plutons with internal and external marginal zones of strong contact-parallel deformation. Contacts are commonly associated with down-dip lineations, except where overprinted by D_3 shear zones. These features are consistent with emplacement as magmatic diapirs. They commonly intrude, deflect, or offset D_2 fold axes (e.g. Kurrawang Syncline), whereas deflection of D_3 shear zones is less pronounced. Examples occur northwest of Ora Banda (Siberia), and north of Menzies (the Jorgenson Monzogranite).

(c) The late- to post-tectonic granitoids form the third group.

Late-tectonic granitoids are generally massive, although they may exhibit deformation where cut by strike-parallel shear zones. The granites cut across greenstone contacts and were forcefully emplaced by predominantly brittle deformation of country rocks, or were passively emplaced by stoping. Examples include the forcefully emplaced Liberty Granodiorite, and the passively emplaced Lone Hand Monzogranite.

The granitoids are compositionally diverse, ranging from trondjhemite to syenogranite, with granodiorite and monzogranite dominant. Some preliminary geochemical results indicating the presence of I-type granitoids (Chappell and White, 1974) were presented by Witt and Swager (1989b) but more data are required to fully characterize the range of granite types. There is no simple evolution from early biotite(–hornblende) granodiorite to later more K_2O-rich rocks, as suggested by Williams et al. (1976) and Hallberg (1985) for adjoining areas of the eastern Yilgarn Craton. Granodiorites contain local concentrations of rounded enclaves of F- and LIL-enriched tonalite and quartz diorite. Most of the early (domal) and late-tectonic granitoids appear to be relatively dry, lacking internal pegmatitic segregations or evidence of widespread post-magmatic alteration. However, post-D_2 to syn-D_3 diapirs display a more restricted range of

predominantly monzogranitic compositions and typically contain numerous small irregular pegmatitic segregations. They are equivalent to the synkinematic granitoids of Bettenay (1988) and Archibald et al. (1981), which also contain pegmatitic bodies.

Small, fine-grained porphyritic intrusive bodies, locally known as 'porphyries', are common throughout the Menzies–Kambalda region. Perring (1988) described ten varieties of porphyry from the Kambalda area, but a more restricted, field-based division is adopted in this report. Varieties include quartz–feldspar(–biotite) porphyry, plagioclase porphyry, hornblende–plagioclase porphyry, and lamprophyre. The bodies are commonly emplaced as dykes and sills, up to about 50 m thick, into shear zones and other planes of weakness such as interflow sediment horizons within basaltic or komatiitic volcanic sequences. The porphyries are generally found in association with gold mineralization. They are less commonly mineralized, and are generally cut by ore-bearing structures. Emplacement of many porphyry units appears to have occurred during D_3 but some may have been emplaced during earlier periods of deformation, or even prior to compressional deformation.

Metamorphism

Metamorphism was a complex long-lived event, and peak metamorphism may not have been contemporaneous throughout the whole of the Menzies–Kambalda region. Binns et al. (1976) concluded, from a broad regional study of the Eastern Goldfields Province, that metamorphic grades are related to structural setting. Relatively undeformed areas with widespread preservation of igneous textures and structures ('static domains') range from prehnite–pumpellyite facies to middle amphibolite facies. Barley and Groves (1987) suggested that metamorphic grade in 'static domains' is related to stratigraphic level, and proposed a sea-floor alteration (hydrothermal metamorphism) origin for the observed metamorphic assemblages. More strongly deformed domains with penetrative fabrics ('dynamic domains') are characterized by middle amphibolite- to lower granulite-facies metamorphism. The latter domains occur in linear belts along the margins of the greenstone belts and are commonly intruded by synkinematic diapirs.

The distribution of metamorphic grades and the preservation of relict igneous minerals in low-grade, and high-grade metamorphic domains led Binns et al. (1976) to conclude that regional metamorphism was a single, widespread event related to mobilization of granitic rocks. Rapid differential uplift of a uniform buried terrain, coincident with granitic diapirism, gave rise to linear high-strain and high-grade metamorphic belts (Archibald et al., 1978, 1981). Wong (1986) rejected differential uplift in the low-strain Kambalda area and suggested that high-grade assemblages adjacent to the Kambalda Granodiorite formed a contact aureole which was superimposed on regional metamorphism (cf. Jolly, 1978). Similarly, Bickle and Archibald (1984) interpreted metamorphic assemblages in the high-strain Widgiemooltha area as recording the superimposition of a thermal aureole related to granitic intrusions upon regional metamorphism.

The restricted age span during which volcanism, deformation, and metamorphism occurred prompted Barley and Groves (1987, 1988) to suggest that metamorphism in the Norseman–Wiluna belt was a single, progressive event which began as sea-floor hydrothermal metamorphism, and continued as burial metamorphism in a high heat-flow environment, and culminated in syntectonic dynamothermal metamorphism.

Figure 13 shows the distribution of metamorphic grade in the Menzies–Kambalda region, based on mineral assemblages proposed by Binns et al. (1976) and Ahmat (1986). However, the boundaries must be regarded as approximate, in the absence of detailed mineralogical studies of mafic rocks (except for Kambalda and Widgiemooltha) and the restricted occurrence and poor exposure of pelitic rocks which could yield definitive metamorphic assemblages. The widespread presence of andalusite suggests a low-pressure regional metamorphic event, but it should also be noted that kyanite has been recorded in shear zones at a number of localities (Purvis, 1984; Griffin, 1990b).

Detailed studies have not been carried out in the areas of lower metamorphic grade indicated on Figure 13, but metamorphic conditions at Kambalda have been established by Wong (1986) and Bavington (1979). Lower amphibolite grade temperatures of 520°C ± 20°C increase to about 575°C ± 20°C in a 400 m-wide zone adjacent to the Kambalda Trondjhemite, where serpentinized ultramafic rocks have been metamorphosed to talc–forsterite assemblages (Donaldson, 1983). Metamorphic pressures of 2.5 ± 1 kb are commonly cited for the Kambalda area (Roberts et al., 1989; Roberts and Elias, 1990). In the Widgiemooltha area, peak metamorphic conditions of 500–600°C and 3–5 kb have been recorded in upper amphibolite facies rocks (McQueen, 1981; Bickle and Archibald, 1984). Ashley and Martyn (1987) determined metamorphic conditions of 400–525°C and less that 3.8 kb from quartz–aluminosilicate assemblages near Menzies. Purvis (1984) used similar assemblages at Mt Martin, north of Kambalda, to determine metamorphic conditions of 500°C and 4 kb.

Figure 12 can be compared with Figure 13 to demonstrate a fair correlation between high-grade metamorphic areas and 'dynamic domains', and between low-grade metamorphic areas and 'static domains'. However, upper greenschist- to lower amphibolite-facies rocks occur in both 'dynamic domains' (e.g. northwest of Ora Banda) and 'static domains' (e.g. south of Kambalda). Higher grade areas display a close spatial relationship with post-D_2 to syn-D_3 (synkinematic) diapirs (although aureoles south and west of Kalgoorlie are broader than those in the Menzies and Ora Banda areas). This may reflect an overall tilting of the crust to expose deeper, higher grade rocks to the south and west. Emplacement of diapirs during regional metamorphism raised metamorphic temperatures within thermal aureoles adjacent to the intrusions, but did not generate classic, overprinting contact aureoles. These thermal aureoles would be

broader at deeper crustal levels, where ambient regional metamorphic grade was higher.

Metamorphic amphiboles in high-strain ('dynamic') domains are aligned within the plane of the regional foliation. These dominant metamorphic fabrics, and the broad spatial relationship between metamorphic grade and post-D_2 to syn-D_3 diapirs indicate broad synchroneity between peak metamorphism, granitoid emplacement, and D_3 deformation, a conclusion consistent with that of Archibald et al. (1981). However, unoriented porphyroblasts of amphibole and other minerals are common, and indicate an extended history of deformation and recrystallization. It is therefore concluded that peak metamorphism outlasted deformation, at least within many high-strain domains (Binns et al., 1976).

Pre- to syn-D_2 granitoid domes have much narrower metamorphic aureoles than post-D_2 to syn-D_3 diapirs. Andalusite porphyroblasts overprint the regional metamorphic fabric in narrow contact metamorphic aureoles adjacent to late-tectonic granitoids such as the Mungari Granite and Liberty Granodiorite. The late granitoids are therefore interpreted as post-dating peak metamorphism.

Tectonic setting

The Norseman–Wiluna belt has long been regarded as some form of ensialic rift (Groves et al., 1978; Groves and Batt, 1984), based on radiogenic initial lead isotopic compositions of granites (Oversby, 1975); the remnants of interpreted gneissic basement in some granitic bodies (Archibald and Bettenay, 1977); U-rich zircon xenocrysts in basalts at Kambalda (Compston et al., 1986); and geochemical evidence for contamination of basalt and komatiite at Kambalda by sialic crust (Arndt and Jenner, 1986; Barley, 1986). More recently, Barley and Groves (1987, 1988) compared lithostratigraphic associations in the Norseman–Wiluna belt and the early hydrothermal metamorphic profile in little-deformed ('static') domains with those of marginal basins. The short time span between volcanism, regional deformation, and dynamothermal metamorphism is comparable to that for opening and closing of some younger marginal basins. The compositions of mafic to ultramafic volcanic, and granitic rocks are also compatible with a continental margin environment (Morris, in press; Witt and Swager, 1989b). Closure of a marginal basin due to collision between plates or microplates could explain the transpressional nature of the regional deformation (Barley et al., 1989; Witt et al., 1989).

Although direct comparisons with Phanerozoic plate-tectonic environments may not be warranted, a continental margin setting seems the most likely environment for the geological evolution of the Menzies–Kambalda region (Swager et al., 1990). The original configuration of tectonic elements is complicated by the effects of transpressional deformation. Systematic mapping and detailed studies of adjoining areas are required before the broader tectonic setting of the Eastern Goldfields Province can be interpreted with more confidence.

Chapter 3

Stratigraphic and lithological controls on gold mineralization

Stratigraphic controls on gold mineralization

Well-controlled stratigraphic successions in the Ora Banda and Kambalda Domains (Table 4; Fig. 14) permit an assessment of stratigraphic control on gold mineralization in these areas. Although not strictly regarded as stratigraphic units, large layered and differentiated mafic/ultramafic sills are included in this assessment because they are extensive, and conformable within the stratigraphic successions. Porphyry-hosted mineralization and mineralization hosted by smaller gabbroic bodies are included with the stratigraphic unit into which they have been emplaced. Granitoid-hosted deposits are excluded from this discussion.

Stratigraphic controls in the Ora Banda Domain

The resource figures for each stratigraphic unit of the Ora Banda Domain are shown in Table 6. The Grants Patch Group is clearly the principal mineralized unit, with significant resources in both Bent Tree Basalt and Victorious Basalt. Resources hosted by Victorious Basalt are mainly from the Ora Banda and Grants Patch areas, and the more recently discovered Racetrack deposit at Mt Pleasant. The main deposits within Bent Tree Basalt are at Ora Banda in an as yet undeveloped underground resource, and at Goongarrie. Other significant host rocks are Missouri Basalt and the Mt Pleasant Sill. Mineralization occurs almost exclusively in the uppermost flow(s) of Missouri Basalt, in the Comet Vale and Siberia mining areas (e.g. Sand Queen, Sand King, Camperdown). The significance of the Mt Pleasant Sill is based primarily on recent developments in the Mt Pleasant area (Golden Kilometre, Southern Shoot). The main sources of mineralization within Big Dick Basalt are at Thiel Well, and at BHP's Enterprise deposit, east of Ora Banda.

Figure 17 demonstrates the dominant contribution of the modern bulk-mining phase to the total gold production, and illustrates significant differences between host units for modern and historical production. Historically, the dominance of Victorious Basalt and uppermost Missouri Basalt is evident, but recent exploration has identified resources throughout much of the lower part of the Ora Banda Domain greenstone sequence.

Stratigraphic controls in the Kambalda Domain

Gold resources within the Kambalda Domain (Table 7) are dominated by the Golden Mile deposits, and it is a reflection of the size of these deposits that historical production is the dominant contributor to the total (Fig. 17). The Golden Mile deposits are hosted primarily by the Golden Mile Dolerite, and, to a lesser extent, by upper Paringa Basalt.

Recent discoveries, particularly in the Kambalda–St Ives mining area, have indicated that gold deposits can occur in units throughout the lower part of the stratigraphic succession. Significant deposits are hosted by Defiance Dolerite (Defiance, Revenge); Kapai Slate (Victory, North Orchin); Devon Consols Basalt (Orion, Brittania, Sirius); and equivalent stratigraphic units in the Kalgoorlie mining area (Mt Percy). The main deposits hosted by Kambalda Komatiite are at Mt Percy and the Hampton–Boulder deposit at New Celebration; however, both these orebodies are hosted primarily by porphyry intrusives within the ultramafic rocks (see below).

Summary

Historically, there has been a concentration of gold production from just below, or at, the transition from mafic/ultramafic volcanism to felsic (?calc-alkaline) volcanism and related sedimentation, in those areas where stratigraphic successions can be confidently recognized. Thus, the Golden Mile Dolerite is the dominant host rock in the Kalgoorlie mining area, and Victorious Basalt is important in the Ora Banda Domain. Another horizon — upper Missouri Basalt — just below the base of komatiitic volcanism is important within the Ora Banda Domain. Groves et al. (1987) suggested that hydrothermal fluids were ponded in fractured brittle lithologies, directly beneath relatively ductile units which did not fracture during deformation. The historical concentration of gold mining from basalt and dolerite beneath the relatively

Figures in this chapter do not include a further 25 t Au reserves for the Golden Mile and a further 8.5 t historical Au production from Hannans North (near Mt Charlotte). These extra figures were 'discovered' during a review of the manuscript by the author in June, 1993, and included in Witt (1993c) and Plate 1 of this publication. Their exclusion has minimal impact on the tables, diagrams, and conclusions of this chapter

Table 6. Stratigraphic controls on gold mineralization in the Ora Banda Domain. Three categories: total, recent and historic production

Stratigraphic unit	*Recent production*			*Historical production*			*Total production*		
	No. of mines	*Au (kg)*	*%*	*No. of mines*	*Au (kg)*	*%*	*No. of mines*	*Au (kg)*	*%*
Black Flag Group	0	-	-	5	559	3.1	**5**	**559**	**0.7**
Grants Patch Group	15	26 903	46.4	26	8 358	46.2	**31**	**35 261**	**46.4**
Victorious Basalt	6	14 193	24.5	5	7 296	40.3	**7**	**21 489**	**28.3**
Bent Tree Basalt	9	12 710	21.9	21	1 062	5.9	**24**	**13 772**	**18.1**
Linger and Die Group	2	4 073	7.0	23	2 165	12.0	**25**	**6 238**	**8.2**
Big Dick Basalt	2	4 073	7.0	6	508	2.8	**8**	**4 581**	**6.0**
Siberia Komatiite	0	-	-	13	1 194	6.6	**13**	**1 194**	**1.6**
Walter Williams Fm	0	-	-	4	463	2.6	**4**	**463**	**0.6**
Pole Group	3	10 334	17.8	10	5 971	33.0	**11**	**16 305**	**21.4**
Missouri Basalt	3	10 334	17.8	9	5 942	32.8	**10**	**16 276**	**21.4**
Wongi Basalt	0	-	-	1	29	0.2	**1**	**29**	**-**
Layered Sills	2	16 643	28.7	22	1 040	5.7	**24**	**17 683**	**23.2**
Ora Banda Sill	0	-	-	1	70	0.4	**1**	**70**	**0.1**
Mt Pleasant Sill	2	16 643	28.7	18	928	5.1	**20**	**17 571**	**23.1**
Base	0	-	-	9	89	0.5	**9**	**89**	**0.1**
Granophyre	2	16 643	28.7	5	512	2.8	**7**	**17 155**	**22.6**
Others	0	-	-	4	327	1.8	**4**	**327**	**0.4**
Mt Ellis Sill	0	-	-	3	42	0.2	**3**	**42**	
Total	**22**	**57 953**		**86**	**18 093**		**96**	**76 046**	

Table 7. Stratigraphic controls on gold mineralization in the Kambalda Domain. Three categories: total, recent and historic production

Stratigraphic unit	*Recent production*			*Historical production*			*Total production*		
	No. of mines	*Au (kg)*	*%*	*No. of mines*	*Au (kg)*	*%*	*No. of mines*	*Au (kg)*	*%*
Black Flag Group	1	1 356	0.4	3	14	-	**3**	**1 370**	**0.1**
Kalgoorlie Group	15	84 147	24.7	13	173 666	15.1	**23**	**257 813**	**17.3**
Paringa Basalt	2	21 492	6.3	3	171 974	15.0	**5**	**193 466**	**13.0**
Kapai Slate	3	17 525	5.1	1	21	-	**3**	**17 546**	**1.2**
Devon Consols Basalt	6	14 223	4.2	3	81	-	**7**	**14 304**	**1.0**
Kambalda Komatiite	3	25 907	7.6	5	1 582	0.1	**6**	**27 489**	**1.8**
Lunnon Basalt	1	5 000	1.5	1	8	-	**2**	**5 008**	**0.3**
Layered Sills	12	255 534	74.9	6	974 390	84.9	**15**	**1 229 924**	**82.6**
Williamstown/Defiance	6	40 276	11.8	3	385	-	**6**	**40 661**	**2.7**
Golden Mile/Junction	6	215 258	63.1	3	974 005	84.8	**9**	**1 189 263**	**79.9**
Total	**28**	**341 037**		**22**	**1 148 070**		**41**	**1 489 107**	

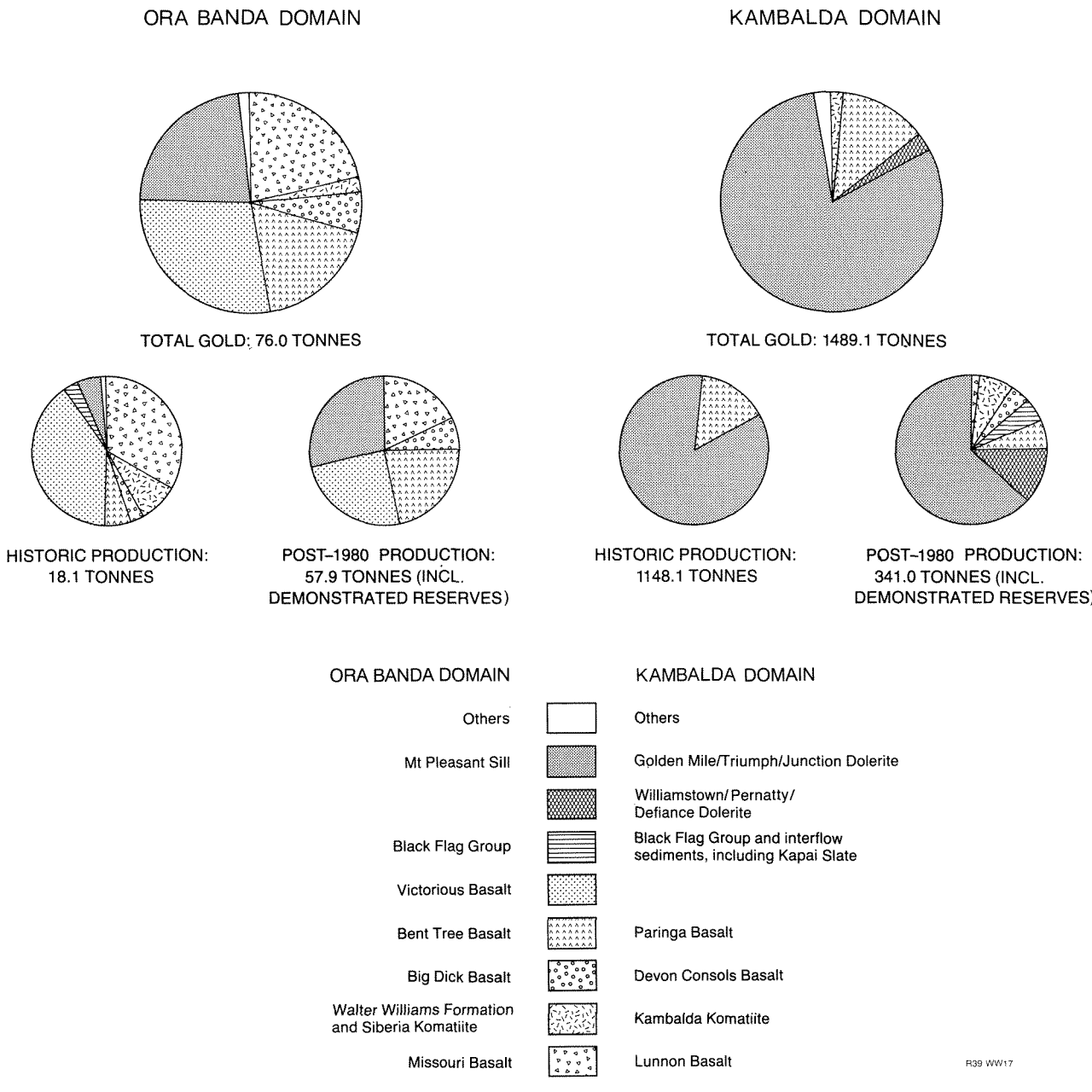

Figure 17. Stratigraphic controls of gold mineralization in the Menzies–Kambalda region

ductile Black Flag Group sedimentary rocks and beneath the ultramafic Walter Williams Formation, is consistent with this suggestion. However, the occurrence of numerous small historical deposits throughout both stratigraphic successions; and the more widespread distribution of gold mineralization indicated by more recent mining, particularly at Kambalda, suggest stratigraphic controls are less specific than initially supposed. A mechanism similar to that proposed by Groves et al. (1987) may operate on a local scale, based on the ductility contrast between volcanic rocks and interflow sediments, but gross stratigraphic controls on gold mineralization are not readily apparent.

Lithological controls on gold mineralization

Lithological controls on gold mineralization in the Menzies–Kambalda region are summarized in Tables 8–13, and Figure 18. Mafic rocks are clearly the predominant host rock. Within this category, the iron-rich, granophyric-textured, quartz-bearing zones (granophyre) of layered and differentiated mafic/ultramafic sills have yielded more gold than any other type of host rock. Low-Mg series basalt also hosts significant amounts of gold mineralization, but high-Mg series basalt is no more

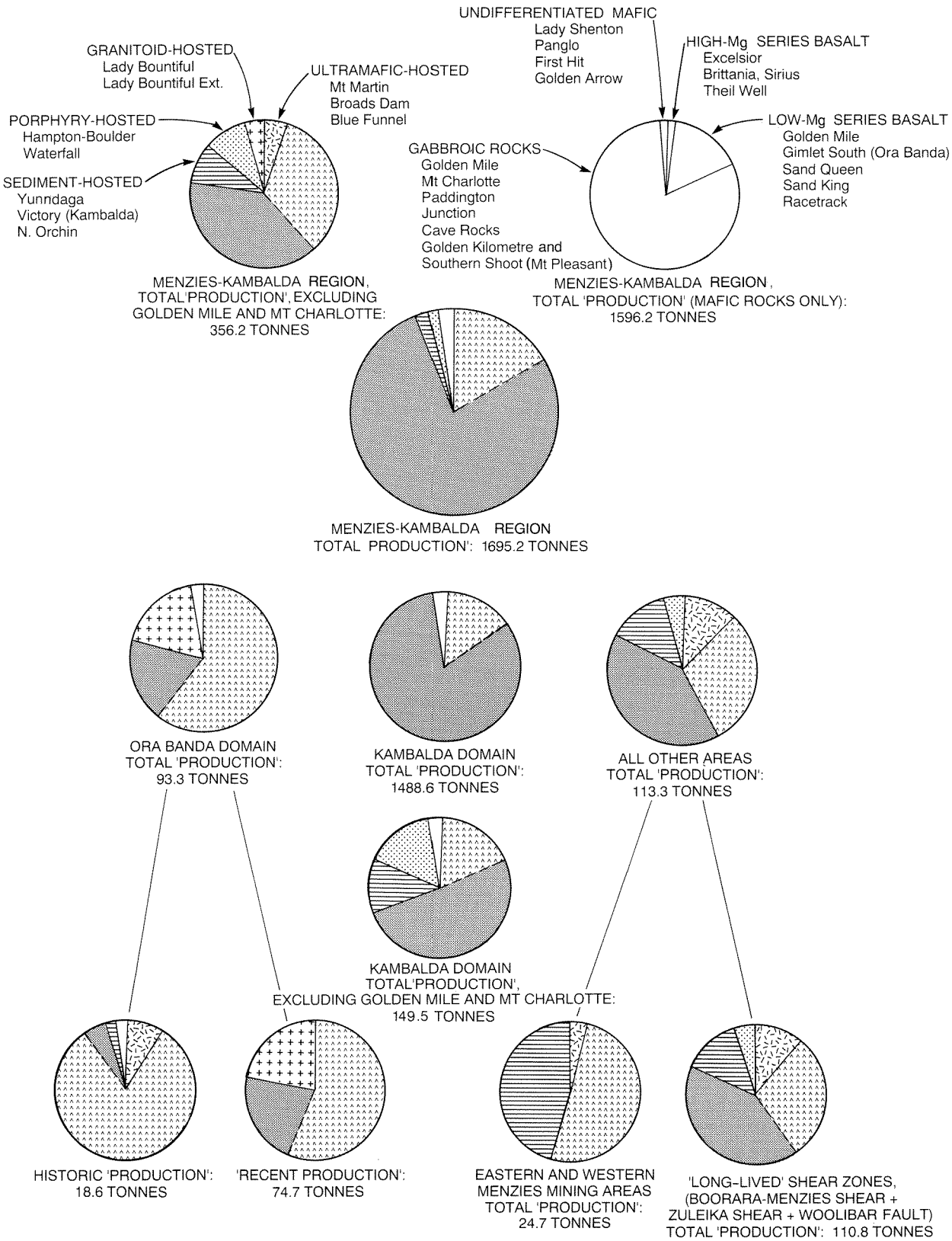
GRANITOID-HOSTED
Lady Bountiful
Lady Bountiful Ext.
ULTRAMAFIC-HOSTED
Mt Martin
Broads Dam
Blue Funnel
PORPHYRY-HOSTED
Hampton-Boulder
Waterfall
SEDIMENT-HOSTED
Yunndaga
Victory (Kambalda)
N. Orchin
MENZIES-KAMBALDA REGION,
TOTAL 'PRODUCTION', EXCLUDING
GOLDEN MILE AND MT CHARLOTTE:
356.2 TONNES
UNDIFFERENTIATED MAFIC
Lady Shenton
Panglo
First Hit
Golden Arrow
HIGH-Mg SERIES BASALT
Excelsior
Brittania, Sirius
Theil Well
LOW-Mg SERIES BASALT
Golden Mile
Gimlet South (Ora Banda)
Sand Queen
Sand King
Racetrack
GABBROIC ROCKS
Golden Mile
Mt Charlotte
Paddington
Junction
Cave Rocks
Golden Kilometre and
Southern Shoot (Mt Pleasant)
MENZIES-KAMBALDA REGION,
TOTAL 'PRODUCTION' (MAFIC ROCKS ONLY):
1596.2 TONNES
MENZIES-KAMBALDA REGION
TOTAL PRODUCTION': 1695.2 TONNES
ORA BANDA DOMAIN
TOTAL 'PRODUCTION':
93.3 TONNES
KAMBALDA DOMAIN
TOTAL 'PRODUCTION':
1488.6 TONNES
ALL OTHER AREAS
TOTAL 'PRODUCTION':
113.3 TONNES
KAMBALDA DOMAIN
TOTAL 'PRODUCTION',
EXCLUDING GOLDEN MILE AND MT CHARLOTTE:
149.5 TONNES
HISTORIC 'PRODUCTION':
18.6 TONNES
'RECENT PRODUCTION':
74.7 TONNES
EASTERN AND WESTERN
MENZIES MINING AREAS
TOTAL 'PRODUCTION':
24.7 TONNES
'LONG-LIVED' SHEAR ZONES,
(BOORARA-MENZIES SHEAR +
ZULEIKA SHEAR + WOOLIBAR FAULT)
TOTAL 'PRODUCTION': 110.8 TONNES
Ultramafic rocks
(including basal sections of mafic/ultramafic sills)
Mafic rocks
(including high – Mg series and low – Mg series basalt)
Mafic rocks (gabbroic and doleritic sections of mafic/ultramafic sills)
Sedimentary rocks, volcaniclastic rocks, felsic volcanics
(including interflow sediments, eg. Kapai Slate)
Porphyry
Granite
Others
R39 WW18

Table 8. Lithological controls on gold mineralization in the Menzies–Kambalda region

Rock type	*No. of mines*	*Au production (kg)*	*(%)*
Ultramafic rocks	50	18 506	1.1
Mafic Rocks	151	1 596 206	94.1
High-Mg series basalt	20	27 373	1.6
Low-Mg series basalt	51	251 952	14.9
Gabbroic sections of mafic/ultramafic sills	42	1 294 179	76.3
Undifferentiated mafics	38	22 702	1.3
Felsic volcanics and volcaniclastic sediments	30	34 216	2.0
Porphyry	18	29 757	1.8
Granite	12	16 554	1.0
Total	**261**	**1 695 239**	

Table 9. Lithological controls of gold mineralization in the Ora Banda Domain of the Menzies–Kambalda region

Rock type	*Recent production*			*Historical production*			*Total production*		
	No. of mines	*Au (kg)*	*%*	*No. of mines*	*Au (kg)*	*%*	*No. of mines*	*Au (kg)*	*%*
Ultramafic rocks	0	-	-	26	1 621	8.7	**26**	**1 621**	**1.7**
Mafic rocks	22	58 318	78.0	57	16 058	86.5	**66**	**74 376**	**79.7**
High-Mg series basalt	2	4 073	5.4	7	537	2.9	**9**	**4 610**	**4.9**
Low-Mg series basalt	18	37 602	50.3	36	14 380	77.4	**41**	**51 982**	**55.7**
Gabbroic sections of mafic/ultramafic sills	2	16 643	22.3	14	1 141	6.1	**16**	**17 784**	**19.1**
Felsic volcanics and volcaniclastic sediments	0	-	-	3	408	2.2	**3**	**408**	**0.4**
Porphyry	1	156	0.2	7	252	1.4	**5**	**408**	**0.4**
Granite	6	16 263	21.8	5	228	1.2	**10**	**16 491**	**17.7**
Total	**29**	**74 737**		**98**	**18 567**		**110**	**93 304**	

Table 10. Lithological controls of gold mineralization in the Kambalda Domain of the Menzies–Kambalda region

Rock type	*Recent production*			*Historical production*			*Total production*		
	No. of mines	*Au (kg)*	*%*	*No. of mines*	*Au (kg)*	*%*	*No. of mines*	*Au (kg)*	*%*
Ultramafic rocks	0	2 520	0.7	2	1 100	0.1	**2**	**3 620**	**0.2**
Mafic rocks	23	295 778	86.9	12	1 146 414	99.9	**27**	**1 442 190**	**96.9**
High-Mg series basalt	7	13 302	3.9	3	45	-	**8**	**13 347**	**0.9**
Low-Mg series basalt	3	26 492	7.8	3	171 979	15.0	**5**	**198 469**	**13.3**
Gabbroic sections of mafic/ultramafic sills	13	255 984	75.1	6	974 390	84.9	**14**	**1 230 374**	**82.6**
Felsic volcanics and volcaniclastic sediments	3	18 553	5.4	3	43	-	**6**	**18 598**	**1.2**
Porphyry	5	23 678	6.9	5	494	-	**7**	**24 172**	**1.6**
Granite	0	-	-	1	15	-	**1**	**15**	**-**
Total	**31**	**340 529**		**23**	**1 148 066**		**43**	**1 488 595**	

Figure 18. Lithological controls of gold mineralization in the Menzies–Kambalda region

Table 11. Lithological controls on gold mineralization in the Menzies district (Twin Hills, eastern Menzies, and western Menzies mining areas)

Rock type	*No. of mines*	*Au production (kg)*	*(%)*
Ultramafic rocks	9	986	4.0
Mafic rocks (undifferentiated)	33	12 455	50.3
Felsic volcanics and sedimentary rocks	17	11 294	45.7
Porphyry	0	-	-
Granite	0	-	-
Total	**59**	**24,735**	

Table 12. Lithological controls on gold production from major ('long-lived') shear zones (Zuleika Shear, Boorara–Menzies Shear system, Woolibar Fault, and Paris Shear)

Rock type	*No. of mines*	*Au production (kg)*	*(%)*
Ultramafic rocks	16	13 101	11.8
Mafic rocks	42	77 625	70.0
High-Mg series basalt	3	9 416	8.5
Low-Mg series basalt	0	-	-
Gabbroic sections of mafic/ultramafic sills	9	46 021	41.5
Undifferentiated mafics	30	22 188	20.0
Felsic volcanics and volcaniclastic rocks	22	14 948	13.5
Porphyry	3	5 149	4.6
Granite	0	-	-
Total	**83**	**110 823**	

Table 13. Lithological controls on gold mineralization in all areas outside the Ora Banda and Kambalda Domains (includes the Menzies Domain, the Boorara Domain and 'long-lived' shear zones)

Rock type	*No. of mines*	*Au production (kg)*	*(%)*
Ultramafic rocks	22	13 265	11.7
Mafic rocks	55	79 638	70.3
High-Mg series basalt	3	9 416	8.3
Low-Mg series basalt	5	1 501	1.3
Gabbroic sections of mafic/ultramafic sills	9	46 021	40.6
Undifferentiated mafics	38	22 700	20.0
Felsic volcanics and volcaniclastic sediments	21	15 213	13.4
Pophyry	6	5 177	4.6
Granite	1	48	-
Total	**105**	**113 341**	

favourable a host rock than non-mafic rock types. These conclusions remain valid, even after the dominating influence of the Golden Mile Dolerite at Kalgoorlie is removed. Although gabbroic and doleritic host rocks dominate the total resource figures, it is emphasized that other rock types may be important, and indeed the dominant host rock, within individual mining centres.

While the Kalgoorlie mining area is dominated by the quartz dolerite-hosted Golden Mile and Mt Charlotte deposits, recent discoveries at Mt Percy are hosted by a diverse range of rock types, including porphyry, high-Mg series basalt, and pyroxenitic rocks of the Williamstown Dolerite. The situation at Kambalda is similar. Resources are contained mainly in quartz dolerite or quartz gabbro of the Defiance Dolerite and Junction Dolerite. However, high-Mg series (Devon Consols) basalt and an interflow sediment (Kapai Slate) are locally important host rocks, and the Hunt mine is hosted by low-Mg series (Lunnon) basalt. At the New Celebration mining centre, porphyry intrusives are the dominant host rock.

Although important at Mt Pleasant, quartz gabbro is a less dominant host rock in the Ora Banda Domain than in the Kambalda Domain. The major host rock in the Ora Banda Domain is iron-rich, low-Mg series basalt, commonly with small to large plagioclase phenocrysts (Victorious Basalt, uppermost Missouri Basalt). Granite is a third important host rock with several significant deposits in, or overlying, the Liberty Granodiorite in the Lady Bountiful area.

Quartz gabbro and quartz dolerite host rocks account for about 40% of resources from all remaining areas (Table 13). Most deposits outside the Kambalda and Ora Banda Domains occur within 'long-lived' regional shear zones (e.g. the Menzies–Boorara Shear system, and the Zuleika Shear). Ultramafic rocks, sedimentary rocks, and porphyries appear to be more important in this environment (Table 12) than in the less-deformed domains in which stratigraphic sequences can be recognized. Granodiorite-derived sedimentary rocks are particularly important in the Menzies district (Table 11; e.g. Yunndaga, Goodenough).

Discussion

The proportion of gold hosted by quartz gabbro and quartz dolerite in particular, and by mafic rocks in general, is much greater than the estimated proportion of the Menzies–Kambalda greenstone belt underlain by these rocks. Most other rock types, possibly excepting porphyry, are under represented as host rocks, compared to their estimated abundance. The different host rocks are discussed in turn in the following sections.

Layered and differentiated mafic/ultramafic sills

Quartz gabbro and quartz dolerite

Iron-rich, granophyric-textured, quartz gabbro or quartz dolerite (granophyre) host major gold deposits at

Table 14. The main layered and differentiated mafic/ultramafic sills in the Menzies–Kambalda region, and their associated granophyric quartz gabbro- and quartz dolerite-hosted gold deposits. Compositional data refers to the Fe-enriched quartz dolerite zone of each sill, unless otherwise specified

Sill	*Mines*	*Mining locality*	*Contained gold (t)*
Mt Pleasant	*Golden Kilometre*		
	Southern Shoot	Mt Pleasant	16.6
$FeO+Fe_2O_3$ = 17.2%	Lady Evelyn	Ora Banda	0.3
$(FeO+Fe_2O_3)/MgO$	King Edward	Lady Bountiful	<0.1
= 11.03	Lady Bountiful (a)	Lady Bountiful	<0.1
	Great Ora Banda	Ora Banda	<0.1
	Golden Buckle	Mt Pleasant	<0.1
			17.1
Golden Mile (Triumph) Dolerite	Golden Mile (a)	Kalgoorlie	1 050.4
	Mt Charlotte	Kalgoorlie	103.3
	Location 48 Inc	Celebration	1.1
$FeO+Fe_2O_3$ = 15.2%	Wildcatters	Celebration	0.7
$(FeO+Fe_2O_3)/MgO$	Argo, Triumph,		
= 11.7	Merrock	Celebration	<0.1
			1,155.6
Williamstown Dolerite (c)	Pernatty	Celebration	7.6
	White Hope	Celebration	1.2
Fe Total = 7.75%			
Fe Total/MgO			
= 0.79			
			8.8
Defiance Dolerite	Defiance (b)	Kambalda	22.0
	Revenge (b)	Kambalda	8.0
$FeO+Fe_2O_3$ = 10.0%	North Orchin (b)	Kambalda	1.5
$(FeO+Fe_2O_3)/MgO$			
= 2.32			
			31.5
Junction Dolerite	Junction (b)	Kambalda	32.0
Unassigned dolerite	Paddington	Paddington	22.9
(Boorara–Menzies Shear Zone)	Boorara	Golden Ridge	1.7
	Zoroastrian	Bardoc	1.4
	South Duke	Broad Arrow	0.4
	Jennys Reward	Goongarrie	0.1
FeO Total = 9.6%	Bardoc GMs	Bardoc	<0.1
FeO Total/MgO	Nerrin Nerrin	Bardoc	<0.1
= 1.81			
			26.6
Unassigned dolerite (Zuleika Shear)	Cave Rocks	Siberia	**18.0**

(a) Estimate of the proportion of total production hosted by quartz dolerite; some (generally subordinate) gold hosted by other lithologies.

(b) Accurate production and reserve figures not available; estimate only, based on scale of workings and limited information.

(c) Compositional data refer to the mafic section of the sill, not necessarily the most Fe-enriched section.

Compositional data are taken from Witt et al., 1991 (Mt Pleasant Sill); Clark, 1980 (Golden Mile Dolerite); L. Y. Golding, 1978 (Williamstown Dolerite); Western Mining Corporation, unpublished data (Defiance Dolerite); and Bloch, 1988 (unassigned dolerite at Paddington).

the Golden Mile (1236 t Au), Mt Charlotte (103 t Au), Junction (32 t Au), Paddington (27 t Au), Defiance (22 t Au), Cave Rocks (18 t Au), and Mt Pleasant (17 t Au). In areas of relatively low-strain, such as Mt Pleasant, Kalgoorlie, and Kambalda, the host rocks occur within layered or differentiated mafic/ultramafic sills. It seems probable that similar host rocks within major shear zones, such as occur at Paddington and Cave Rocks, are tectonically disrupted slices of larger sills. For example, Bloch (1988) has shown that the western contact of the dolerite at Paddington transgresses geochemical zoning within the body. The main doleritic and gabbroic host rocks in the Menzies–Kambalda region and their associated gold deposits are listed in Table 14. Although the great bulk of mineralization in these deposits is hosted by quartz dolerite or quartz gabbro, adjacent zones of the sills also contain relatively minor gold.

Table 3 indicates a diverse range of bulk compositions for mafic/ultramafic sills in the Menzies–Kambalda region. Williams and Hallberg (1973) divided such sills into layered high-Mg sills, and differentiated tholeiitic sills, based on the presence or absence of well-developed phase layering and cumulate textures. Witt et al., (1988, 1991) noted that presently available data indicate that iron-rich granophyre formed in both layered and differentiated sills and that a break at about 14–16% MgO separates those which developed granophyre from more magnesian sills which did not.

The Golden Mile Dolerite (GMD) displays a distinct tholeiitic fractionation trend, and the GMD granophyre formed from in situ fractionation of a single pulse of a moderately iron-rich magma (Table 14; Clark, 1980). More extreme in situ fractionation, including the development of a prominent olivine cumulate basal zone, was required to produce a similar iron-rich granophyre in the relatively magnesian Mt Pleasant Sill (Fig. 19). Fractionation may have been promoted by hydrous contamination from unconsolidated sedimentary country rocks (Witt et al., 1991). Mineralized sills have bulk compositions which tend to promote the early crystallization of olivine or pyroxene. Sills (such as the Mt Ellis Sill) in which plagioclase crystallized early fractionate toward a quartz dolerite with similar $FeO + Fe_2O_3$ but lower $(FeO + Fe_2O_3)/MgO$ than other granophyres (Table 14, Fig. 19), and these are not favourable host rocks.

Other zones within mafic/ultramafic sills

Apart from granophyre, and to a lesser extent adjacent zones, layered and differentiated mafic/ultramafic sills in the Menzies–Kambalda region have not yielded much gold. Glenrock (70 kg Au) is the largest of several historical gold mines hosted by the upper gabbroic section of the Ora Banda Sill in the Mt Carnage mining area. The lower pyroxenitic section of the Williamstown Dolerite is a minor host rock at Mt Percy in the Kalgoorlie mining area. The lower ultramafic section of the Mt Pleasant Sill hosts numerous small mines north and east of Ora Banda. These mines, located in and adjacent to a prominent shear zone at the base of the sill, have yielded a total of <70 kg Au.

Basaltic rocks

Basaltic rocks comprise the second most productive host rock for gold in the Menzies–Kambalda region. As with mafic/ultramafic sills, basaltic rocks span a wide range of compositions — divided into three groups as described in Chapter 2. The most important group is the low-Mg series basalt, including those with prominent phenocrysts of plagioclase. Low-Mg series basalt is a minor host rock for the Golden Mile deposits, Kalgoorlie, but because of their size, the Golden Mile deposits contribute a significant proportion of the total low-Mg series basalt-hosted production in the Menzies–Kambalda region. Low-Mg series basalt is the most important host rock in the Ora Banda Domain. Plagioclase-phyric Missouri Basalt, and more coarsely plagioclase-phyric Victorious Basalt, have always been the more important host rocks, and in more recent times several deposits have been located in aphyric Bent Tree Basalt. The more important orebodies in these units are listed in Table 15.

The relative importance of low-Mg series basalt as a host rock to gold mineralization in the Menzies–Kambalda region may lie in its relatively iron-rich composition. Low-Mg series basalt has higher $(FeO + Fe_2O_3)/(FeO + Fe_2O_3 + MgO)$, and in some cases higher absolute $FeO + Fe_2O_3$ than high-Mg series basalt. In this context it is interesting to note that only the uppermost, plagioclase-phyric flow(s) of Missouri Basalt are mineralized. Limited data show this section to be the most iron-rich (approximately 14% $FeO + Fe_2O_3$) in a thick sequence of basalt comprising high-Mg series Wongi Basalt and overlying low-Mg series Missouri Basalt (Morris and Witt, unpublished data).

High-Mg series basalt is a far less important host rock, although some significant deposits have recently been identified. These include Brittania and Sirius (total production approximately 8 t Au) at Kambalda; Mt Percy at Kalgoorlie (approximately 1.5 t Au in Devon Consols Basalt); Excelsior (approximately 3 t Au) at Bardoc; and Thiel Well (3 t Au) in the Mt Carnage mining area. Historically, the only deposit of any significance hosted by high-Mg series basalt was New Mexico (430 kg Au), between Ora Banda and Siberia.

Lady Shenton was the largest of several mines which yielded a total of >12 t Au from probable orthoamphibolitic rocks in the western Menzies mining area. The presence of strongly pleochroic, dark green hornblende suggests these rocks are mostly metamorphosed low-Mg series basalt, but geochemical data are required to confirm these observations.

Ultramafic rocks (of komatiitic origin)

Ultramafic rocks are, generally speaking, minor host rocks to gold mineralization in the Menzies–Kambalda region. However, several significant deposits have recently been identified in komatiitic rocks within regional shear zones. Examples include Broads Dam (2.3 t Au) and Blue Funnel (1.5 t Au) in the Zuleika Shear, Mt Martin (>7 t Au) in the Woolibar Fault, and Victory/Talbot (1.5 t Au) in the Menzies–Boorara Shear system. Outside regional

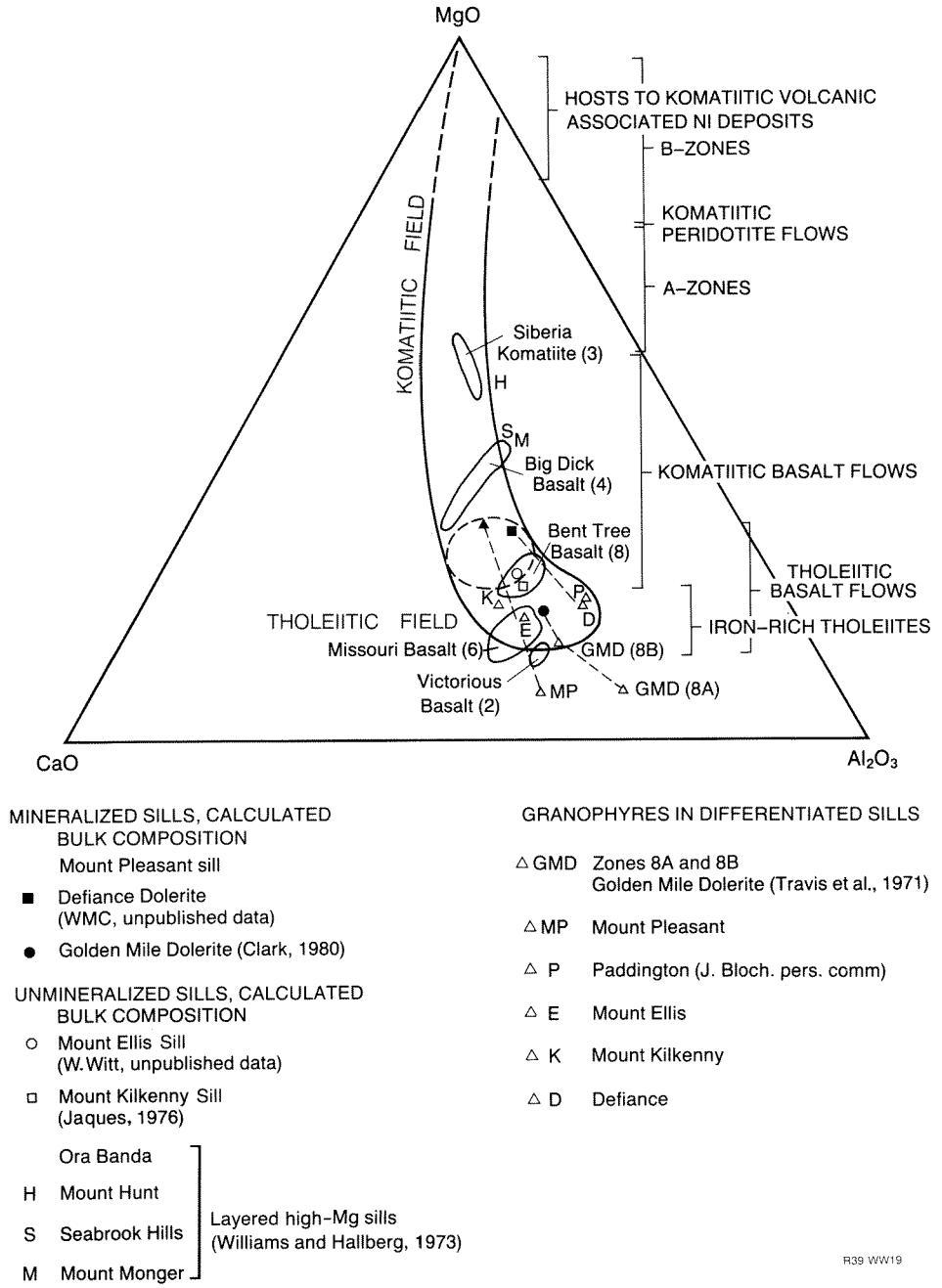

Figure 19. MgO–Al_2O_3–CaO diagram (after Groves and Lesher, 1982), showing bulk composition of several mineralized and unmineralized Archaean mafic/ultramafic sills, and some volcanic rocks from the Ora Banda Domain (Witt, unpublished data). Figures in brackets are the number of samples which define the compositional field of the volcanic unit

shear zones, however, little gold has been won from ultramafic rocks. The most significant examples, none of which are considered mineable under present economic conditions (1989), are Red Hill (983 kg Au) at Kambalda; Vettersburg (656 kg Au) north of Bardoc; Happy Jack (221 kg Au) at Comet Vale; and Dixie (204 kg Au) near Mt Pleasant.

Komatiitic rocks are also important as host rocks to mineralized porphyry at several centres, including Mt Percy and New Celebration in the Menzies–Kambalda region, and also in the Coolgardie area, west of Kalgoorlie.

Felsic volcanic and sedimentary rocks

Felsic volcanic rocks host little or no gold mineralization in the Menzies–Kambalda region. Sedimentary rocks are minor host rocks, but are locally important.

Table 15. Important gold deposits hosted by low-Mg series basalt in the Ora Banda Domain

Basalt unit	*Mine*	*Mining locality*	*Contained gold (t)*
Victorious Basalt	Gimlet South etc	Ora Banda	10.9
	Racetrack	Mt Pleasant	5.8
$FeO+Fe_2O_3$ = 9.2%	Coronation		3.6
$(FeO+Fe_2O_3)/MgO$	Prince of Wales	Grants Patch	
= 2.28	Woolshed (a)	Mt Pleasant	0.5
			20.8
Bent Tree Basalt	New Boddington,		
	Franks Dam, etc	Goongarrie	5.9
$FeO+Fe_2O_3$ = 11.3%	Gimlet South		
$(FeO+Fe_2O_3)/MgO$	(underground)	Ora Banda	5.3
= 1.60	Eureka	Bardoc	1.9
	Bent Tree	Grants Patch	0.8
	Woolshed (a)	Mt Pleasant	0.5
			14.4
Missouri Basalt	Sand King	Siberia	8.6
	Sand Queen	Comet Vale	5.6
$FeO+Fe_2O_3$ = 13.6%	Missouri	Siberia	0.9
$(FeO+Fe_2O_3)/MgO$	Camperdown	Siberia	0.8
= 3.13			
			15.9

(a) Estimate of the proportion of total production hosted by respective basalt units at Woolshed

All compositional data from Witt (unpublished data). Victorious Basalt,(average of two analyses); Bent Tree Basalt (average of 8 analyses); Missouri Basalt (average of 6 analyses).

Granodiorite- or tonalite-derived, arkosic siltstone, grit, and conglomerate (PLATE VIII,B*), and minor shale, are important host rocks in the Menzies district, hosting several of the largest historic mines, including Yunndaga (10 t Au), Goodenough (263 kg Au) and probably a sizeable proportion of the Menzies Alpha mineralization (557 kg Au). Recent developments at Kambalda have identified an interflow sediment (Kapai Slate) as an important host rock which contains mineralization at Victory (10 t Au) and North Orchin (6.5 t Au). Kapai Slate is also one of the more important host rocks at Mt Percy, in the Kalgoorlie mining area. Regionally, the Kapai Slate is a sulfidic black shale, but is locally albitic, and contains magnetite in the Kambalda area.

Sedimentary rocks of the Black Flag Group are poorly mineralized. Historically the largest producing mine in the Black Flag Group was the Star of W.A. (324 kg Au) near Paddington. More recently a resource of 1.75 t Au at Binduli, west of Kalgoorlie, has been identified. However, Binduli may be more appropriately viewed as a porphyry-hosted deposit within the Black Flag Group sedimentary rocks.

* PLATES I–XIV (referred to in small capital letters and roman numerals) are photographic plates located at the end of the text.

Porphyry

Although porphyry is a minor host rock in the Menzies–Kambalda region, it is locally important, hosting some very significant mines, most of which are within or adjacent to regional shear zones. With the exception of Waterfall (4.5 t Au) in the Menzies–Boorara Shear system, most mineralized porphyries occur within komatiitic rocks. The main porphyry-hosted deposits, apart from Waterfall, are associated with the Boulder–Lefroy Fault in the New Celebration area, where the largest resource occurs at the Hampton–Boulder deposit (>25 t Au). Smaller deposits in similar porphyry/komatiite associations occur at Mt Percy (approximately 2.5 t Au), and at Hawkins Find (0.5 t Au). A variety of porphyries occurs in the mineralized environment, including leucocratic quartz–feldspar porphyry, intermediate biotite- and hornblende-bearing porphyries, and albite-rich porphyry.

Granitoids

Granitic rocks are not significant host rocks in the Menzies–Kambalda region in terms of total production, but are locally important. At Lady Bountiful, the Liberty Granodiorite contains a resource of almost 7 t Au. A further resource of approximately 8.7 t Au occurs in surficial quartz-rich sands in channels overlying the granodiorite. Outside the Menzies–Kambalda region other important granitoid-hosted deposits identified in recent years include Granny Smith (23.7 t Au) near Laverton, and Porphyry (8.6 t Au) at Edjudina.

The Liberty Granodiorite is a late-tectonic intrusive. Other more leucocratic late-tectonic granitoids contain minor mineralization (Liberty and Swan in the monzogranitic phase of the Liberty Granodiorite; Fair Adelaide in syenogranite, north of Ora Banda). Earlier diapiric and domal granitoids are generally poorly mineralized although recent drilling at Cawse, east of Ora Banda, has outlined a resource of approximately 590 kg Au in monzogranite of the Goongarrie – Mt Pleasant dome.

The results of this investigation indicate that lithological controls on gold mineralization in the Menzies–Kambalda region are similar to those for the Norseman–Wiluna belt as a whole (Groves, 1988; Groves and Barley, 1988). Host rocks in other provinces of the Yilgarn Craton are more diverse but generally dominated by either mafic lithologies or banded iron-formations (Groves, 1988; Groves et al., 1988a). The Abitibi greenstone belt in the Superior Province of Ontario also displays a greater diversity of host rock types than does the Menzies–Kambalda region, even allowing for the dominance of the Golden Mile deposits in the latter (Colvine et al., 1988). In Ontario, mafic host rocks are less dominant, and granitoids (small felsic intrusions, syenites, and alkalic volcanic rocks) more common. In Zimbabwe, mafic rocks are the dominant host rocks although banded iron-formations are also important, and quartzofeldspathic sedimentary rocks are especially prospective lithologies in the relatively restricted Sebakwian Group (Foster and Wilson, 1984).

Conclusions

1. There appears to be little evidence for gross stratigraphic control of gold mineralization in those parts of the Menzies–Kambalda region where stratigraphic successions can be recognized. Some concentration of gold near transitions from mafic to ultramafic volcanism (Ora Banda Domain) and from mafic/ultramafic to felsic volcanism (Ora Banda and Kambalda Domains) are adequately explained in terms of control by host-rock lithology. A similar lack of stratigraphic control on gold mineralization has been documented for the Abitibi greenstone belt in Ontario, Canada (Kerrich, 1986a).

2. The most important host rock in the Menzies–Kambalda region is quartz dolerite and quartz gabbro, despite the overwhelming dominance of the Golden Mile and Mt Charlotte deposits. The second most important host rock is low-Mg series basalt, particularly basalt with plagioclase phenocrysts. These rock types are characterized by high $\Sigma FeO/(\Sigma FeO + MgO)$, and in many cases high absolute ΣFeO ($\Sigma FeO = FeO + Fe_2O_3$ = up to about 18%). The high iron content of these favourable rock types is consistent with the model of Phillips and Groves (1983) whereby gold sulfide complexes in hydrothermal solutions are destabilized by reaction with iron silicates and iron carbonate in the wallrocks to form sulfide minerals. However, Bohlke (1988) suggested that the whole-rock Fe/(Fe + Mg) ratio may be more important than total Fe in controlling the deposition of sulfides and gold mineralization.

3. Although iron-rich gabbroic and basaltic rocks are the major host rocks in the Menzies–Kambalda region, all rock types host significant historical and modern deposits and locally may be the favourable host rock (e.g. porphyry at New Celebration). Alternative mechanisms must be sought for the deposition of gold in these rock types (see Chapter 7).

4. The Menzies–Kambalda region — and the Norseman–Wiluna belt as a whole — is somewhat unusual in the predominance of mafic host rocks, particularly of quartz-bearing zones within mafic/ultramafic sills. Mafic/ultramafic sills are not major host rocks in other Archaean gold provinces of the Yilgarn Block, nor in Ontario and Zimbabwe. These other gold provinces are generally characterized by a more diverse range of host rocks, and BIFs — notably absent from the Norseman–Wiluna belt — are important.

Chapter 4

Structural controls on gold mineralization

All documented Archaean gold deposits in the Kambalda–Menzies region are structurally controlled, i.e. they occur in specific structural sites such as shear zones, fracture arrays and quartz veins. This chapter discusses the deposits in terms of their structural setting and the type of structure with which they are associated, and attempts to relate these mineralized structures to regional and local deformation events.

Classification of ore-bearing structures

Archaean gold-bearing structures are commonly subdivided according to their brittle, brittle–ductile transition, or ductile character (e.g. Colvine et al., 1984, 1988), following the work of Sibson (1977, 1983; see also Ramsay and Huber, 1987). Figure 20 is a modified presentation of diagrams from Colvine et al. (1988), depicting the main characteristics of each of these types of ore-bearing structure. Brittle deformation produces discrete faults, quartz veins, breccias, fault gouge, and tension gashes. Ductile deformation generates pervasive fabrics without rupture, resulting in a pronounced schistose to gneissic rock but lacking quartz veins. Structures formed in the field of brittle–ductile deformation exhibit both brittle and ductile features.

The limitations of this approach are discussed by R.G. Roberts (1988). In practice, the great majority of gold-bearing structures in the Menzies–Kambalda region fall within the brittle–ductile transition; mineralization associated with entirely brittle structures is comparatively uncommon, and truly ductile structures lacking veins have not been observed. However, the concept of relatively brittle versus relatively ductile failure is a useful one and forms the basis for a classification of ore-bearing structures used in this report (Plates 1A, 1B). Each type of mineralized structure (Fig. 21) is considered briefly here, progressing from relatively brittle to relatively ductile structures.

1. *Simple quartz veins*: Purely brittle quartz veins with little or no ductile fabric in adjacent wallrocks are developed in some granitic rocks (e.g. Lady Bountiful, PLATE I, A).

2. *Quartz vein 'stockworks' bounded by discrete oblique faults*: The best known example of this type of deposit is Mt Charlotte where two sets of intersecting quartz veins, locally referred to as a 'stockwork', are developed between faults which are oblique to local lithological contacts (Clark, 1980; Clout et al., 1988).

3. *Quartz veins with narrow zones of deformed wallrock*: Quartz veins in many rock types, particularly those in mafic rocks and oriented at a high angle to the plane of regional or local flattening (e.g. Boddington and Kermans lodes at Goongarrie; Great Ora Banda), are more commonly associated with a relatively narrow margin of moderately to strongly foliated wallrocks (PLATE I, B). These structures are differentiated from type 5 structures by the relative simplicity of the vein system, and from brittle–ductile shear zones (type 7) by the comparatively restricted development of ductile fabrics relative to the vein or vein system.

4. *Subparallel quartz veins between conformable bounding shears*: These structures form in zones of strong deformation where relatively narrow lenses or horizons of contrasting ductility occur together. Quartz veins form in relatively brittle host lithologies while shearing is focussed along contacts with adjacent, more ductile rocks — examples include Paddington (PLATES I, C and II, A) and Waterfall. Similar structures at the Sigma mine, Quebec have been described in some detail by Robert et al., (1983) and Robert and Brown (1986a).

   A crack-seal mechanism of formation (Ramsay and Huber, 1987) is indicated for quartz veins in structural types 1 to 4, by the laminated nature of the veins in which slivers of wallrock occur in the veins, subparallel to vein margins (e.g. PLATE I, A).

5. *Tabular zones of quartz veining and brecciation*: Mappable structures comprising quartz veins, quartz–carbonate breccias, minor shears, and one or more foliations in highly altered wallrocks, are typified by the Defiance lodes at Kambalda (Clark et al., 1986). Veining and brecciation predominate over ductile features such as shears and a pervasive or closely spaced foliation. Tapered and branching quartz veins, and breccias in which wallrock fragments are commonly not markedly rotated from their original orientation suggest that fluid overpressure and hydraulic fracture are important processes in the development of these systems (PLATES III, E, and VI, D). Mineralized vein/breccia systems are widespread in relatively undeformed (low-strain) structural domains in the Menzies–Kambalda region. Examples include mineralized structures at the Golden Mile, Kalgoorlie; Defiance at Kambalda; the GK Zone at Mt Pleasant;

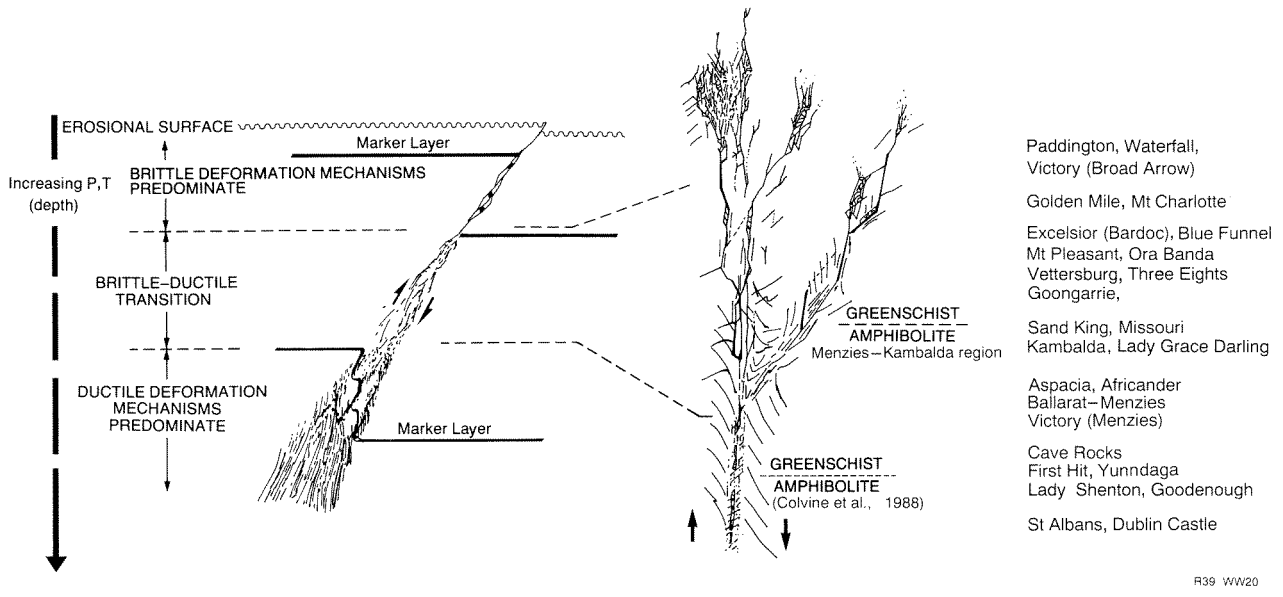

Figure 20. Schematic representation of an ideal ore zone (after diagrams in Colvine et al., 1988), showing the variations in types of structures with depth. Also shown are estimated relative depths of formation of several mines in the Menzies–Kambalda region, based on their type of mineralized structure and geological setting. Note that the greenschist/amphibolite facies transition in the Menzies–Kambalda region (based on estimated metamorphic grade in mine areas) is shown at a shallower level than that indicated on the original figure by Colvine et al. (1988)

Sand King at Siberia (PLATE II, C); and the Gimlet South lode at Ora Banda.

6. *Pipe-like breccia zones*: Most vein/breccia systems have an irregular, tabular shape, but pipe-like breccia systems are represented by the flat lode system (e.g. Oroya shoot) of the Golden Mile. Base metal-rich gold mineralization is associated with a pipe-like breccia system in the Black Flag Fault, at the Black Flag mine, near Mt Pleasant (PLATE VIII, G–H). The breccia is associated with widespread textural evidence for open space growth including delicate colloform quartz (PLATE III, A), features which are otherwise rare in the Menzies–Kambalda region.

7. *Brittle–ductile shears*: Brittle–ductile shears contain elements of both brittle and ductile deformation. They are subdivided into two types according to the relative proportion and timing of quartz veins and other brittle deformation features.

7a. *Veined brittle–ductile shears*: Veined brittle–ductile shears consist of several anastomosing zones of deformation defined by a well-developed shear fabric. These zones of ductile deformation enclose irregular lenses of less deformed rock, or lithons. The proportion of lithons to sheared rock may be relatively high, especially in mafic rocks (commonly 30–50% lithons). An important feature of veined brittle–ductile shears is the presence of associated veining and brecciation. Veins are generally conformable or subconformable with the ductile shear fabric but splays and branching veins are common (PLATES II, A–B; III, B–D). The proportion of veining and brecciation is small compared to the total width of sheared rock, and decreases to a very small proportion in 'ductile' shears (see type 8 below). Although hydraulic fracture probably occurs periodically throughout the development of these structures (e.g. Kerrich and Allison, 1978), veins that cut across the ductile fabric (PLATES III, B–D), and unstretched angular fragments of foliated wallrock in brecciated sections (PLATES VI, B; III, F), indicate that brittle deformation generally outlasts ductile deformation. Veined brittle–ductile shears (subsequently referred to as veined shears for convenience) are commonly oriented at a low angle to the regional north-northwest structural trend of the Menzies–Kambalda region (e.g. Excelsior at Bardoc; Hunt mine, Kambalda). Detailed descriptions of similar mineralized structures in Canada are given by Kerrich and Allison (1978), Guha et al. (1983), and Robert and Brown (1986a).

7b. *Banded brittle–ductile shears*: Banded brittle–ductile shears occur in relatively high-grade metamorphic rocks (e.g. Menzies, Twin Hills) where they are commonly conformable with the north-northwest structural trend of the Menzies–Kambalda region. Lithons are smaller and less abundant than in veined brittle–ductile shears, and the penetrative shear fabric is more regular and systematic (PLATES IV, C–D) as a result of the progressive increase in incremental strain intensity (Ramsay and Graham, 1970). Although Colvine et al. (1984; 1988) regarded similar structures in Canada as ductile, the banded brittle–ductile shears in the Menzies–Kambalda region contain stretched and boudinaged quartz and carbonate veins (PLATE IV, F), indicating a brittle component of deformation. However, in contrast to the veined shears described above, ductile deformation outlasted the main period of vein formation, and brecciated domains are rare or

absent. A well-developed stretching lineation is common, reflecting the orientation of boudins, mineral orientation and/or slickensides. The centres of these structures are zones of intense ductile deformation with a regular, banded (or cherty) appearance in planes normal to the extension direction and parallel to the stretching lineation, but with an irregular or contorted banding in sections normal to the lineation (PLATES IV, D–E). These structures are subsequently referred to as banded shears. Mineralized structures in the Red Lake and Detour Lake areas of Ontario (Andrews et al, 1986; Marmont, 1986) display many of the features of banded shears.

8. *'Ductile' shears*: Truly ductile shears without associated veining probably do not exist in the Menzies–Kambalda region. Some ultramafic-hosted shears (e.g. Happy Jack at Comet Vale, Pride of Erin at Siberia) contain a very few small veins, and are locally devoid of veining. These structures are considered ductile shears for the purposes of this report.

Structural setting of the ore-bearing structures

Regional deformation, described in Chapter 2, resulted in a markedly heterogeneous distribution of strain in the Menzies–Kambalda region. Strain was strongly partitioned into regional shear zones which enclose relatively undeformed domains. The partitioning of strain during regional deformation allows the Menzies–Kambalda region to be divided into four types of structural domain (Fig. 22). The term 'structural domain' is used in this context to distinguish such areas from lithostratigraphic domains described in Chapter 2 (e.g. the Kambalda Domain). The types of structural domains are shown below.

(a) Regional shear zones: Regional shear zones are comparable to the regional-scale deformation zones described by Andrews et al. (1986) and Colvine et al. (1988). They are broad north to north-northwest trending zones of deformation from 500 metres to several kilometres in width, and up to hundreds of kilometres long. Internally, the shear zones consist of a disorganized set of elongate, narrow, fault-bound slices of a variety of rock types. Although local mine successions within regional shear zones have been suggested (e.g. Hancock et al., 1990), these are not consistent for more than a few kilometres along strike (Plate 2A) and cannot be interpreted as original stratigraphy. This relationship contrasts with the relatively consistent stratigraphic successions in less deformed structural domains adjacent to the regional shear zones. Within the regional shear zones, anastomosing zones of intense ductile deformation wrap around relatively undeformed lithons. The proportion of lithons decreases and the width of the high-strain zones increases with metamorphic grade (?depth). Pervasive alteration of all rock types, particularly mafic and ultramafic rocks is characteristic. Carbonation is prevalent at lower metamorphic grades but silicification may be more important at higher metamorphic grades. Economically, the most important regional shear zones in the Menzies–Kambalda region are the Boulder–Lefroy Fault and the 'long-lived' Menzies–Boorara Shear system (which includes the Bardoc Tectonic Zone) and the Zuleika Shear.

(b) Areas of moderate to strong transpression: Structural domains which record moderate to strong transpression are characterized by closely spaced, subparallel, north to north-northwest trending, district-scale shear zones which are separated by relatively wide zones of undeformed or weakly deformed rock. Stratigraphic successions are preserved in these domains but may be tectonically attenuated and displaced by transcurrent movement of several kilometres or more along strike-parallel, district-scale shear zones. District-scale shear zones are several metres to several tens of metres wide and several kilometres to tens of kilometres in strike length. Within the Menzies–Kambalda region, the narrow greenstone belt between the Bardoc Tectonic Zone and the Goongarrie–Mt Pleasant dome, and a narrow belt of greenstones west of the Boulder–Lefroy Fault, are structural domains of moderate to strong regional transpression.

(c) Relatively undeformed domains: Large areas in which primary igneous textures and structures are widely preserved, and characterized by relatively few, widely spaced district-scale shear zones, occur between Ora Banda and Mt Pleasant, and around Kambalda. Compression was the main form of deformation in these structural domains, except in relatively narrow zones adjacent to regional shear zones. Relatively undisturbed stratigraphic successions are preserved, and can be traced, commonly through more strongly deformed structural domains, over strike lengths of more than 100 kilometres.

(d) A fourth structural domain is defined by local deformation related to the forceful emplacement of granitic intrusives, or to the complex interaction between granitoid emplacement and regional deformation. Forceful emplacement of granitoids causes compression of adjacent rocks, and/or generates important accommodation structures (Witt and Swager, 1989b). The most important of these structural domains are around the Siberia and Comet Vale areas.

This four-fold division of the Menzies–Kambalda region into structural domains forms a useful basis for a discussion of the ore-bearing structures, because structures within each domain exhibit some consistent characteristics (Table 16).

Regional shear zones

Regional shear zones in the Menzies–Kambalda region have yielded more than 140 t (including demonstrated reserves) of gold (Table 17). This is over 50% of all gold produced from the Menzies–Kambalda region, excluding that produced from the Golden Mile and Mt Charlotte.

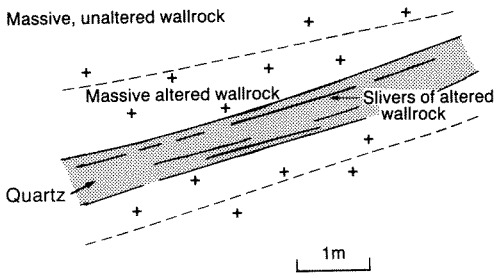

TYPE 1 SIMPLE QUARTZ VEIN

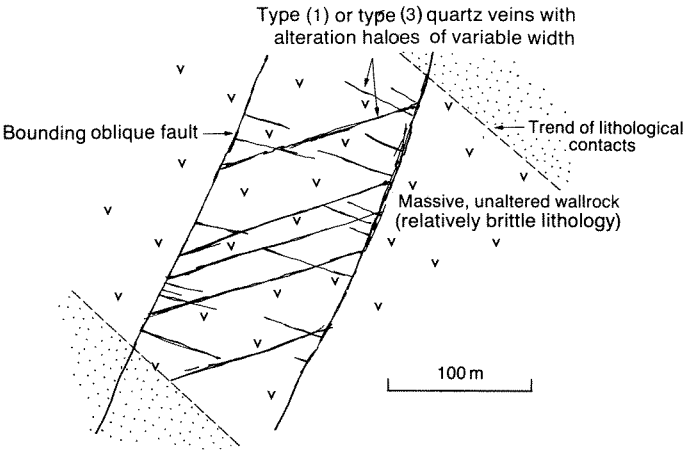

TYPE 2 QUARTZ VEINS BETWEEN BOUNDING OBLIQUE FAULTS

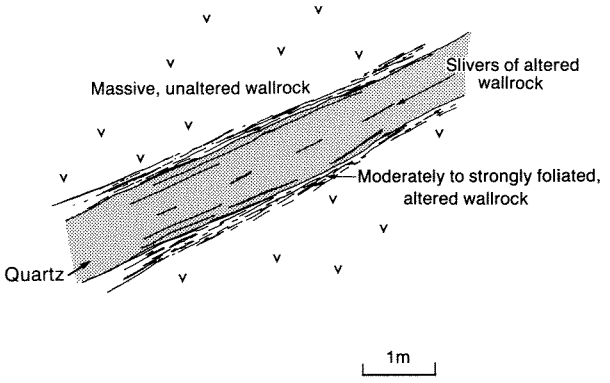

TYPE 3 QUARTZ VEIN WITH NARROW ZONES OF FOLIATED WALLROCK

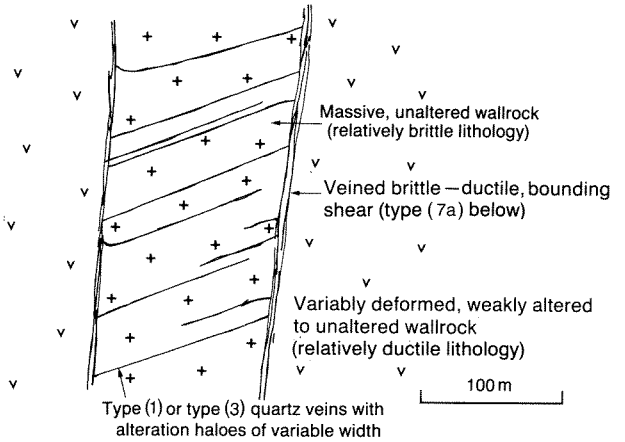

TYPE 4 QUARTZ VEINS BETWEEN CONFORMABLE BOUNDING SHEARS

R39 WW21

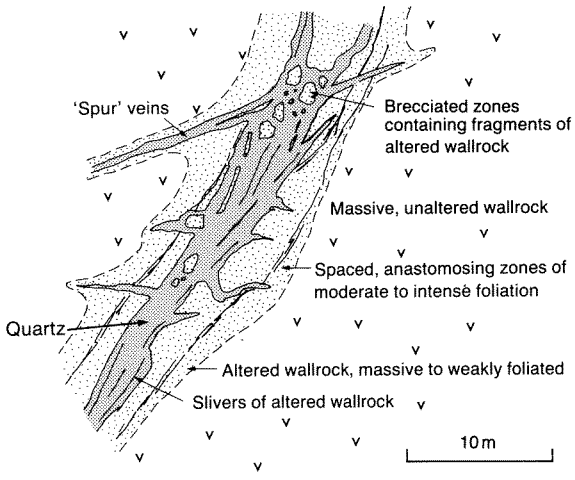

TYPE 5 TABULAR ZONE OF IRREGULAR QUARTZ VEINING AND BRECCIATION

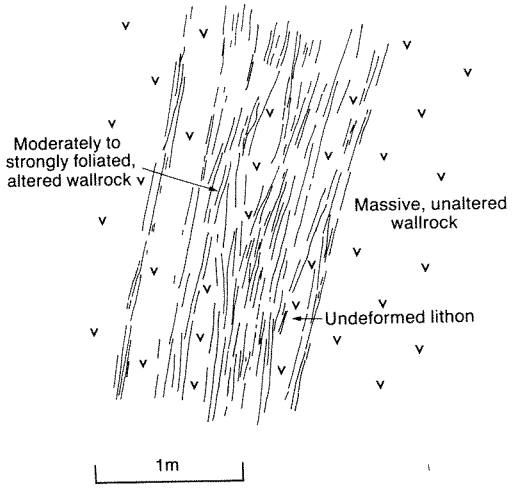

TYPE 8 DUCTILE SHEAR ZONE

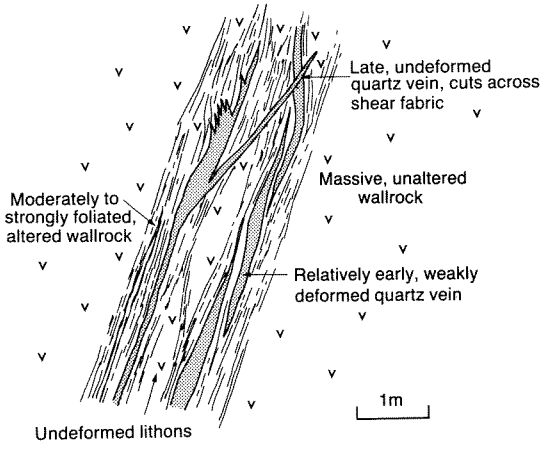

TYPE 7a. VEINED BRITTLE – DUCTILE SHEAR

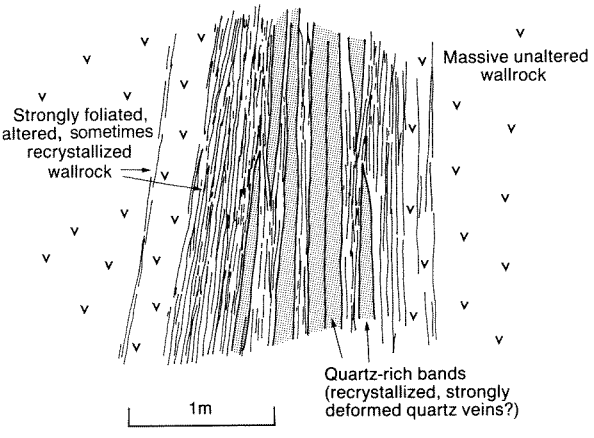

TYPE 7b. BANDED BRITTLE – DUCTILE SHEAR

R39 WW21

Figure 21. Schematic sketches of different types of mineralized structure recognized in the Menzies–Kambalda region. Note that the scale is variable and that the scale bar gives only an order of magnitude for size

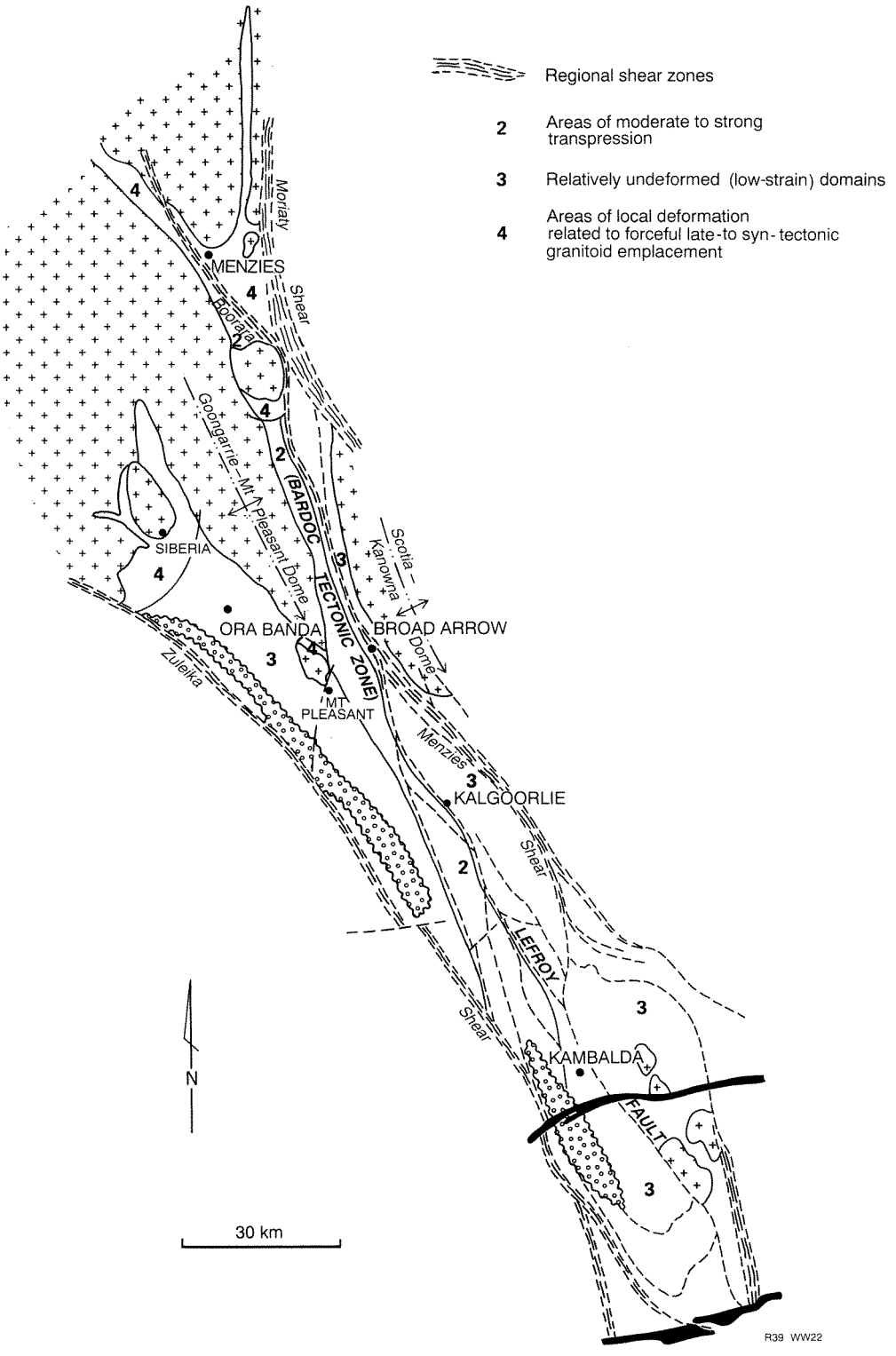

Figure 22. Structural domains within the Menzies–Kambalda region. Geological symbols as for Figure 7

Mineralized structures within these shear zones are diverse, reflecting in part the depth and temperature at which they formed (Fig. 20).

A particularly important structural setting for gold mineralization in regional shear zones consists of subparallel quartz vein sets, developed in relatively brittle host rocks, between strike-parallel bounding shears (type 4 above). In some cases, quartz veining is concentrated in the margins of the brittle host rock, adjacent to the bounding shears, while in other examples, quartz veins extend across the entire width of the host rock unit. Examples within the Menzies–Boorara Shear system include Paddington, where the host rock is mainly quartz

Table 16. Association of different types of mineralized structure with structural domains in the Menzies–Kambalda region

Structural domain / *Mineralized structure*	*1. Regional shear zones*		*2. Areas of moderate to strong transpressional deformation*	*3. Relatively undeformed domains*	*4. Domains of local deformation related to emplacement of granitoids*
	Relatively low-grade metamorphism (shallow?)	*Relatively high-grade metamorphism (deep?)*			
Quartz veins (type 1 and 3)	Minor to absent	Minor to absent	Common	Common	Common
Subparallel quartz vein sets between bounding oblique faults (type 2)	Absent	Absent	?Rare to absent	Minor to common	Rare to absent
Subparallel quartz vein sets between conformable bounding shears (type 4)	Common	Absent	?Rare to minor	Absent	Absent
Tabular quartz vein/breccia systems (type 5)	Absent	Absent	?Rare to minor	Common	Common
Veined brittle–ductile shears (type 7a)	Very common	Common	Common	Common	Common
Banded brittle–ductile shears (type 7b)	Absent	Common	?Minor (?at higher metamorphic grades)	?Absent	?Minor to common (at higher metamorphic grades)
Ductile shear zones (type 8)	Minor	Minor	Minor	Minor to absent	Minor

NOTE: The relative abundance of various structures in areas of moderate to strong transpressional deformation is difficult to assess because of the small number of deposits in these domains. Bracketed numbers refer to types of mineralized structure portrayed in Figure 21 and discussed in text.

dolerite; and Waterfall, where the host rock is quartz–feldspar porphyry. In both cases, quartz-vein sets are subhorizontal to shallowly dipping, suggesting formation during (late D_3) subvertical movements on the bounding shear zones. The subhorizontal quartz veins at Paddington overprint a north-northwest trending, spaced S_2/S_3 foliation and therefore post-date major strike-slip movements.

Other porphyry-hosted mineralization is associated with easterly trending subvertical vein sets between bounding shears. Examples include the Hampton–Boulder deposit on the Boulder–Lefroy Fault, and Hawkins Find on the Zuleika Shear. These quartz veins are oriented subparallel to the regional axis of compression and may have formed as tensional veins during strike-slip movements on bounding shears, or possibly later if compression outlasted transcurrent movements. Subvertical veined shear zones which bound the quartz vein sets are also mineralized, but are less important than the veins.

Planar zones of intense deformation, conformable within regional shear zones, are important structures for mineralization in their own right, even where not associated with quartz-vein sets in relatively brittle lithologies. Steeply dipping, conformable, veined shear zones (type 7a structures) commonly occur within ultramafic rocks (e.g. Blue Funnel, Broads Dam, Pakeha – Mt Corlac, Victory at Broad Arrow). Ultramafic rocks are particularly susceptible to ductile deformation, but additionally are sinks for CO_2 due to their high bivalent metal content (Kerrich, 1986b). Regional shear zones focussed CO_2-bearing fluids. Intense carbonation promoted brittle deformation of the ultramafic rock and the formation of mineralized vein systems. At Victory and Talbot mines, Broad Arrow, subhorizontal veins in ultramafic rocks overprint a strong ductile fabric and subvertical quartz veins, both of which formed during sinistral strike-slip movements. Although the steeply dipping structures which formed during sinistral strike-slip faulting at Victory and Talbot are also mineralized, they appear to be less important to mineralization than the subhorizontal quartz veins (R. Saville, pers. comm., 1987).

Many other mineralized, conformable veined shear zones are localized at lithological contacts. For example, subvertical sediment/ultramafic contacts are important in the Valhalla–Duke area of the Bardoc Tectonic Zone (Plate 2B). Mineralization at Excelsior, Bardoc is located in and adjacent to a sheared ultramafic/basalt contact, but the operation is enhanced by a broad zone of fine-scale quartz veining and brecciation in silicified basalt adjacent to the main shear (PLATE III, H).

Mineralization in most conformable veined shears does not appear to have a distinct plunge, and the mineralized shears may have formed during any of the repeated movements on the regional shear zones. However, much mineralization appears to be related to late quartz veining within the shears suggesting that gold-bearing fluids were introduced during the latest (D_3/D_4) movements. Observations at Victory (Broad Arrow) suggest gold was introduced during D_3 strike-slip deformation, and later movements.

Table 17. Gold production from mines located in regional shear zones

Mine	*Mining locality*	*Contained Au (t)*
BOORARA–MENZIES SHEAR ZONE		**75.6**
Type (4) structures		
Paddington 1 and 2	Paddington	29.3
Waterfall	Golden Ridge	4.5
Type (7) structures		
Excelsior	Bardoc	3.0
Golden Arrow	Broad Arrow	2.7
Boorara	Golden Ridge	1.9
Zoroastrian	Bardoc	1.4
Mount Corlac	Paddington	0.9
Victory	Broad Arrow	0.9
Type (8) structures		
Yunndaga	Menzies	10.0
Lady Shenton	Menzies	5.8
First Hit	Menzies	2.7
Robinson Crusoe	Menzies	1.2
Menzies Alpha	Menzies	0.5
Friday	Menzies	0.4
Florence	Menzies	0.3
Flying Fish	Menzies	0.2
Little Wonder	Menzies	0.2
Dublin Castle	Menzies	0.1
Lady Sherry	Menzies	0.1
Lady Harriet	Menzies	0.1
WOOLIBAR FAULT		**7.1**
Type (8) structures		
Mount Martin	Celebration	7.1
ZULEIKA SHEAR ZONE		**26.9**
Type (4) structures		
Hawkins Find	Zuleika	0.5
Type (7) structures		
Broads Dam	Zuleika	2.3
Blue Funnel	Zuleika	1.5
Type (8) structures		
Cave Rocks	Kambalda	18.0
BOULDER–LEFROY FAULT		**30.6**
Type (4) structures		
Hampton–Boulder/Jubilee	Celebration	25.2
Mutaroo	Celebration	3.2
Type (7) structures		
Golden Hope	Celebration	1.5
All regional shear zones		**140.2**

At Menzies, where the Menzies–Boorara Shear system occurs within relatively high-grade metamorphic (and possibly deeper) rocks, conformable structures dominate the mineralized environments; structures which are oblique to the main tectonic fabric are rare, and subparallel vein sets or 'stockworks' between bounding shears have not been recognized. The main auriferous structures are pipe-like or lenticular ore shoots within banded shears (type 7b structures) which are conformable within the central part of the Menzies–Boorara Shear system (Witt, 1993a, fig. 4a,b). The mineralized banded shears are

interpreted as planes of intense ductile deformation within pervasively foliated rocks of the regional shear zone. Ore shoots plunge uniformly 30–40°S, colinear with the stretching direction as indicated by slickensides and mineral lineations. Similar siliceous pipe-like orebodies within mineralized shear zones and colinear with stretching lineations have been described at the Sons of Gwalia mine at Leonora (Skwarnecki, 1987; Williams et al., 1989) and at several mines in the Red Lake area of Ontario (Andrews et al., 1986). Williams et al. (1989) interpreted the steeply plunging ore bodies at the Sons of Gwalia mine as sheath folds which nucleated at irregularities in the shear zone and propagated parallel to the movement direction. A similar interpretation is possible for the Menzies area but fold structures have not been identified in hand specimens from Menzies. However, hand specimens show clear evidence for boudinaged quartz–carbonate veins (PLATES IV, F, and IX, B). An alternative explanation is that zones of silicification and quartz veining in the centres of mineralized shears were boudinaged during progressive shearing. Although boudins normally form normal to the extension direction, high fluid pressures or complex multiple movements could have caused individual boudins to break up into several pods which were subsequently stretched into their present orientation, subparallel to the direction of extension.

Zones of mineralized, conformable veined shears (type 7a structures) flank the central zone of banded shears but still occur within the Menzies–Boorara Shear system (Plate 1A). The veined shears contain some late quartz veins and rare zones of brecciation, but these features are less common than in similar structures in lower metamorphic grade rocks between Bardoc and Paddington. A similar relationship is observed on a smaller scale in core from the First Hit mine area where a central mineralized zone of intense ductile deformation is flanked by zones of weakly mineralized to barren quartz veining and brecciation (Witt, 1993a, fig. 7). Inclined shafts on some veined shears appear to reflect the same 30–40°S plunge seen in the banded shears. Many of the mineralized veined shears appear to be localized by lithological contacts, a feature which is not readily apparent for the banded shears. Historical documentation suggests that the ore bodies hosted by veined shears were more continuous and less irregular than those hosted by banded shears (Woodward, 1906).

The different styles of deformation (type 7a and 7b structures), in close proximity to one another, may reflect progressive movement in the centres of the regional and mineralized shear zones, after shear zone margins had ceased to be active. Progressively higher temperatures related to syn-D_3 emplacement of the nearby Jorgenson Monzogranite could have caused later D_3 movements to take place under conditions more favourable for ductile deformation than were present during earlier stages of D_3 deformation. Alternatively, the banded shears may have formed earlier and deeper, and the veined shears formed later, at lower pressures, during uplift related to diapiric emplacement of the Jorgenson Monzogranite. The consistent plunge of the orebodies, colinear with stretching lineations within the dominant shear fabric of the regional shear zone, suggests that mineralization occurred during the main oblique strike-slip (sinistral) D_3 movement on the shear zone. The slightly steeper than subhorizontal movement direction, indicated by the 30–40°S stretching fabric is attributed to interaction with syn-D_3 emplacement of the Jorgenson Monzogranite (Witt, 1993a, fig. 2).

Areas of moderate to strong transpression

Areas of moderate to strong transpression have yielded only about 9.4 t of gold (including demonstrated reserves), mainly from the narrow Goongarrie – Mt Ellis belt, west of the Bardoc Tectonic Zone (7.6 t Au). No significant production is recorded from the zone to the west of the Boulder–Lefroy Fault, or north of Comet Vale, but reserves announced at Inclined Shaft, west of Celebration, occur within the former area.

The most important centre within this type of structural domain is Goongarrie where mineralized district-scale shear zones, related P shears, and oblique quartz veins formed (or were active) during regional sinistral D_3 movements (Witt, 1993a, fig. 13). The district-scale shear zones may be splays from the adjacent Bardoc Tectonic Zone but more probably they are simply subparallel structures which formed during major strike-slip movements (D_3) on the regional structure. The mineralized district-scale shears are regarded as veined shears (type 7a structures), but northwest-trending quartz veins are type 3 structures.

North-northwest trending, subvertical veined shears (type 7a structures) are the main mineralized structures south of Goongarrie, but most of the mines located on these structures are small and produced little gold. Many of these mineralized shears are district-scale shear zones (Witt, 1993a, fig. 30), but others appear to be more restricted features localized at interflow-sediment horizons (e.g. Eureka), ultramafic/porphyry contacts (Big Four, Despatch), or within ultramafic rocks (Vettersburg). These north-northwest trending structures probably formed during sinistral strike-slip movements on the Bardoc Tectonic Zone but were most likely reactivated during late-D_3 subvertical movements and later (D_4) dextral movement. Mineralization may have been introduced during any or all of these movements.

District-scale shear zones and related structures may be important in the Wildcatters–Inclined Shaft area, west of Celebration, but little is known about these deposits at the time of writing (December, 1989).

At the Star of W.A. mine flat-lying quartz veins, formed during subvertical D_3 movements, are mineralized.

Relatively undeformed structural domains

Relatively undeformed structural domains have yielded approximately 1600 t Au (including demonstrated reserves), dominated by the Kalgoorlie mining area (1350 t Au). Kambalda (97 t Au) and the Mt Pleasant – Ora Banda mining area (68.5 t Au) have yielded much smaller, but significant, amounts of gold.

Kalgoorlie and Kambalda – St Ives mining areas

The most important structures at Kalgoorlie and Kambalda are second and third order splays adjacent to, and related to, the Boulder–Lefroy Fault. Mueller et al. (1988) and Swager (1989) have shown how mineralized zones of veining and brecciation (type 5 structures), and veined shears (type 7a structures), of the Golden Mile, Kalgoorlie can be related to D_3 sinistral strike-slip movements on the Boulder–Lefroy Fault. Mt Charlotte mineralization, however, is related to quartz-vein sets (type 2 structures) which formed during D_4 dextral movement on oblique faults which splay off the Boulder–Lefroy Fault. Preliminary observations suggest that mineralized structures at Mt Percy may also have formed during D_4.

At Kambalda, mineralized splay structures related to the Boulder–Lefroy Fault include zones of veining and brecciation (type 5 structures), and veined shear zones (type 7a structures). The nature of these structures depends on several factors, including their orientation, and host rock lithology. For example, subvertical north-northwest trending structures localized by narrow sediment horizons at Victory, North Orchin, and Orion are veined shears and mylonites. Intense brittle deformation within a north-northwest trending shear zone has formed a broad zone of brecciation beneath ultramafic rocks at Hunt mine (Witt, 1993c) in response to a buildup of high fluid pressures (Phillips and Groves, 1984). Flatter structures such as those at Defiance, Orchin, and Revenge (also ?Junction) are tabular zones of veining and brecciation. These relatively brittle features are best developed in quartz dolerite whereas ductile fabrics are better developed in the same structures where they cut mafic (?chloritic)-rich zones of zoned dolerite bodies and high-Mg basalt.

Mineralization probably developed initially in north-northwest trending veined shear zones during D_3 strike-slip deformation but later subvertical movements were even more important. This later period of deformation caused reverse movements and extension on gently arched, flat-lying type 5 structures, and at Victory and Orion produced shallow west-dipping quartz veins which overprint veined shear zones.

The Mt Pleasant – Ora Banda mining area and the Cashmans Shear Zone

In the Ora Banda – Mt Pleasant structural domain (Witt, 1993b), relatively brittle structures such as quartz veins (type 1 and 3 structures) and tabular vein/breccia systems (type 5 structures), oriented at a high angle to regional structural trends, host the largest producing mines (Golden Kilometre at Mt Pleasant, Lady Bountiful, Grants Patch and Ora Banda). However, northwest- to north-striking veined shear zones (type 7a structures) also host mineralization. The orientation, the sense of displacement, and the relative importance of ductile versus brittle deformation are the characteristics of mineralized structures in the Ora Banda – Mt Pleasant structural domain compatible with formation within a sinistral wrench system. The structures probably formed as small-scale fractures and shears during large-scale D_3 strike-slip movements on bounding regional shear zones (the Zuleika Shear and the Menzies–Boorara Shear system). Stresses related to D_3 movements on the bounding shear zones may have been transmitted through the intervening low-strain domain, thus controlling the orientation of fractures and shears. From this point of view, the predominance of relatively brittle mineralized structures, at a high angle to the north-northwest regional fabric of the Menzies–Kambalda region, mirrors on a regional scale the same sort of strain partitioning which produced type 4 mineralized structures in regional shear zones (e.g. Paddington). Alternatively, the structures may be related to sinistral shear movement which developed on the western limb of the Goongarrie – Mt Pleasant Anticline during D_2 regional folding. Evidence for late reverse movement on mineralized structures at King Edward, Grants Patch, and Bent Tree suggest northwest to northerly structures may have continued to be active during late D_3 deformation. Mineralized structures continued to form, even during the latest stages of regional deformation. The easterly trending Lady Bountiful structure initially formed in mafic rocks of the Mount Pleasant Sill, was active during emplacement of the late-tectonic Liberty Granodiorite, and finally extended into the granodiorite itself following emplacement and crystallization. The mineralized quartz veins in Liberty Granodiorite at Swan and Liberty are oriented approximately 45° to the regional axis of compression and probably developed as complementary fractures in a relatively isotropic host rock.

Widely spaced, district-scale shear zones in the Ora Banda – Mt Pleasant structural domain are also mineralized. Historically, widespread mining along the Cashmans Shear Zone was concentrated at intervals where the sheared horizon (the metasedimentary rock at the base of the Mt Pleasant Sill) changes strike. Localities where the Cashmans Shear Zone changes to a progressively more westerly strike were zones of extension during sinistral movement. These localities are characterized by widespread quartz veining in the hanging wall and footwall of the shear zone, and the orientation of these veins suggests formation during sinistral strike-slip faulting. Sinistral movement may have occurred during D_2 regional folding and/or D_3. Other data indicate the shear zone was active over an extended period (Witt, 1990). Quartz veins are widespread immediately north and south of the relatively rigid Lone Hand Monzogranite — areas which lie in the pressure shadow of the late-tectonic granitoid during sinistral movements. Mineralization at Lady Evelyn occurs in a splay structure off the Cashmans Shear Zone.

The late ($?D_4$), relatively brittle Black Flag Fault, and a sub-parallel structure, are mineralized at Black Flag and Royal Standard.

Eastern greenstones, Bardoc to Paddington mining area

Brittle mineralized structures at a high angle to regional structural trends are not common in the narrow, relatively undeformed greenstone belt east of the Bardoc

Tectonic Zone. This belt contains several mines (e.g. Wycheproof), and numerous undocumented workings on strike-parallel veined shear zones (type 7a structures) which are commonly localized at interflow-sediment horizons (Witt, 1993a). The strike length of the mineralized shears appears much shorter (< 2 km) than that of the district-shale shear zones west of the Bardoc Tectonic Zone. The sediments commonly accommodated early intrusion of gabbroic or doleritic bodies, and during later deformation, were sites of emplacement of small felsic porphyry intrusives. Therefore, a basalt/dolerite/sedimentary rock/porphyry association is common in this area. Mineral lineations and ore shoots are commonly down-dip on subvertical shear planes, possibly indicating that the orebodies formed during late-D_3 subvertical movement.

Areas of local deformation related to forceful late to syntectonic emplacement of granitoids

Structural domains in which most mineralized structures appear to be related to forceful emplacement of granitoids have yielded almost 18 t Au (including demonstrated reserves). Timing of these structures is interpreted from the timing of emplacement of associated post-D_2 to syn-D_3 and late-tectonic granitoids. In the Siberia mining area (11.3 t Au production), forceful emplacement of diapiric granitoids to the north and west has pushed the greenstones eastwards and upwards along east-northeast-trending dextral shear zones (Witt, 1993b). Such structures are mineralized at Siberia Consols, Cave Hill, and Pride of Erin, where veined and ductile shear zones (type 7a and type 8 structures) occur in ultramafic rocks. Mineralization also occurs in veined shear zones on ultramafic/porphyry contacts that are subparallel to diapir margins, at Black Rabbit, Yellow Belle, Three Eights, and Merry Dance. Granite-up sense of movement across these structures is predicted but could not be demonstrated.

Thiel Well is on another mineralized veined shear zone, which occurs adjacent to an east-northeast accommodation shear, and may be genetically related to granitoid emplacement. Mineralized easterly trending veins (type 1 structures) and vein/breccia systems (type 5 structures) at Fair Adelaide and New Mexico, respectively, may be Riedel shears (Sylvester, 1988) related to the east-northeast accommodation structures, but the extensional nature of the mineralized structures is equally compatible with formation as tensional structures due to east-west compression (cf. Golden Kilometre at Mt Pleasant). Evidence for reverse movement on these south-dipping structures may reflect continuing sinistral movement on the Zuleika Shear during and after emplacement of the Siberia diapirs.

Relatively brittle type 3 and type 5 structures occur in mafic rocks in the eastern part of the Siberia mining area. The Missouri lode is oriented normal to a diapir margin whereas other structures record similar dextral movements to those which took place across the east-northeast-trending accommodation shears. The change in style, from the western to the eastern part of the Siberia mining area, is believed to reflect the geometry of the greenstones with respect to the rigid Goongarrie – Mt Pleasant granitoid dome. Greenstones in the west of the Siberia area were displaced across east-northeast shears but compression in the relatively narrow greenstone belt between Bonnie Doon and Camperdown produced extensional structures. North of Camperdown, the Wongi Hills belt is apparently unmineralized, despite the presence of favourable host rocks (Missouri Basalt), perhaps because very strong compression prevented access to hydrothermal fluids.

Comet Vale is another important area where mineralized structures were generated by forceful granitoid emplacement. The mineralized north-trending quartz vein (a type 3 structure) at Sand Queen is oriented approximately normal to the margin of the late-tectonic Comet Vale Monzogranite, while other veined and ductile shear zones (type 7a and type 8 structures) are oriented approximately parallel to the granitoid contact.

At Dixie, north of Mt Pleasant, compression of ultramafic rocks between the Liberty Granodiorite and the Goongarrie – Mt Pleasant dome generated zones of contact-parallel shearing which are mineralized.

In the eastern Menzies mining area, (D_3) sinistral strike-slip movement on the Menzies–Boorara Shear system during, and possibly after, emplacement of the diapiric Jorgenson Monzogranite to the north caused the greenstones to ride up over the diapir along shallow-dipping curved shear zones (Witt, 1993a). Consistently south-plunging mineral lineations, and deflection of adjacent porphyry intrusives, indicate reverse movement across the mineralized structures. A similar curvilinear mineralized structure (the Sheba Fault) has been described in South Africa by Anhaeusser (1965). Mineralization at Goodenough occurs in one of these shear zones. The structure is a banded shear zone (type 7b structure), reflecting the higher metamorphic grade (?temperature and depth) of the Menzies area. Smaller mines in ultramafic rocks to the south are veined shears (type 7a structures), probably related to the same movements which here would have been predominantly dextral. Other mines (Kensington, Maranoa, Sunday Gift) occur in veined shears, oriented at a high angle to the flat-lying reverse shears, in relatively undeformed units. The relatively brittle nature of these structures reflects their orientation, approximately parallel to the local axis of compression (Witt, 1993a). North-northwest trending veined shears in the southern part of the mining area (Dunlop, Broughtonville, Queens Birthday) are probably related to regional deformation in a manner similar to structures in the greenstones east of the Bardoc Tectonic Zone (e.g. Wycheproof).

Discussion

Although Colvine et al. (1984, 1988) recognized other factors, they emphasized the dependence of brittle versus ductile behaviour on temperature and pressure which in turn they related to depth (Fig. 20). Other factors which may influence the style of deformation are set out below.

The structural setting of deformation: Zones of high strain such as regional shear zones are dominated by conformable brittle–ductile shear zones. Relatively brittle structures such as quartz veins and vein/breccia systems oriented at large angles to the regional structural fabric are common in less deformed structural domains.

Local stress fields, related to forceful granitoid emplacement or interference between regional deformation and granitic rocks, can produce relatively brittle extensional structures oriented within the regional structural fabric of the Menzies–Kambalda region and relatively ductile structures oriented at a high angle to this fabric.

The relative competency of the rock: Relatively isotropic rocks such as granite or dolerite are less likely to accommodate ductile deformation than rocks in which planes of weakness have already developed, such as schists and gneisses. This is reflected, on a regional scale, by the restriction of the more brittle type 1 and 2 structures to late-tectonic granitoids and quartz dolerite; and, locally in the Kambalda – St Ives mining area, by the varying character of the structures such as the Defiance lodes in quartz dolerite and pyroxenitic rocks.

Ultramafic rocks are particularly amenable to ductile shear because the metamorphic assemblage includes a large amount of chlorite. Furthermore, metasomatic effects can influence deformation behaviour. For example, pervasive carbonation of schistose rocks can promote brittle failure under stress, while sericitization of isotropic rocks may promote ductile failure.

Fluid pressure: Phillips (1972), Kerrich and Allison (1978), and Kerrich (1986a) have stressed the importance of high fluid pressure in producing brittle failure (hydraulic fracture and hydraulic brecciation). These processes dominate the formation of mineralized vein/breccia systems such as the Golden Mile lodes and the Golden Kilometre deposit at Mt Pleasant. Fluctuating fluid pressures can cause rapid alternations between ductile and brittle conditions in brittle–ductile shear zones, but are especially important in lower grade metamorphic rocks. For example, high fluid pressures at Hunt mine have produced large, mineralized breccia bodies beneath 'impermeable' ultramafic rocks. Veins and breccias are less common in banded (?deeper) brittle–ductile shears in higher grade metamorphic rocks (e.g. Menzies, Cave Rocks) because higher fluid pressures are required before fracturing is achieved under increased lithostatic load.

Temperature gradients at constant depth: Temperature gradients at constant depth may be caused by granitic intrusions. Variations in temperature with time as well as within space may occur, with higher temperatures promoting ductile behaviour. The banded shears in the western Menzies mining area may be related to relatively deep crustal levels being uplifted by diapiric emplacement of the Jorgenson Monzogranite, but the presence of closely associated veined shears suggests local temperature gradients (time or space) may have been important.

First-order regional shear zones in the Norseman–Wiluna belt are generally considered to be barren of gold mineralization (Eisenlohr, 1987; Cassidy, 1988; Groves et al., 1988a), and the role of subsidiary second and third order splays adjacent to the major structures is commonly emphasized (Groves and Barley, 1988; Mueller et al., 1988). On the other hand, Colvine et al. (1988) stressed the importance of regional shear zones (or 'deformation zones') as hosts to gold-bearing structures in Ontario, Canada. This study has shown that gold occurs in a variety of structural settings — including regional shear zones, splays off regional shear zones, and in large low-strain domains between regional shear zones. Groves et al. (1984) suggested that regional uplift may have been an essential process in the development of Archaean gold deposits between Kalgoorlie and Norseman because major producing centres occurred in anticlinal zones. This concept is hard to sustain if the distribution of metamorphic grade reflects the degree to which deeper levels of the crust have been uplifted by granitic diapirism or regional tilting. The Kalgoorlie mining area is characterized by low to very low metamorphic grades (Binns et al., 1976; Archibald et al., 1978) whereas surrounding areas (Kambalda, Coolgardie, Siberia, and Menzies) are higher grade and presumably represent deeper, uplifted crust. The apparent association of gold mineralization with anticlinal zones probably reflects host-rock controls because mafic rocks predominate in the lower parts of greenstone successions in the Menzies–Kambalda region.

Several authors (Harris, 1987; Mueller et al., 1988; Swager, 1989) have stressed the importance of strike-slip faulting to the formation of mineralized structures in the Menzies–Kambalda region. Sinistral strike-slip faulting (D_3) appears to have been important in generating mineralized structures in relatively low-strain structural domains such as Kalgoorlie (Golden Mile), Goongarrie, and the Mt Pleasant to Ora Banda mining area. Where sinistral strike-slip faulting has been identified as generating mineralized structures, P, D, and R' structures (Sylvester, 1988), and reverse faults, have all been mineralized. Mineralized Riedel (R') shears have been identified at Kalgoorlie (Swager, 1989) but not elsewhere. This is surprising because R' shears not only form early but are by nature extensional and therefore should form favourable sites for mineralization (R. G. Roberts, 1988). Hodgson (quoted in Colvine et al., 1988), in a study of Canadian Archaean gold deposits, also found that P and D shears were most commonly mineralized.

However, a further result of this study stressed the variety of regional and local deformation movements which have generated ore-bearing structures in the Menzies–Kambalda region. The Cashmans Shear Zone, which follows the base of the Mt Pleasant Sill around the nose of the Kurrawang Syncline, may have formed during D_2 regional folding, although later (D_3) movements may have been important in the formation of auriferous vein systems associated with this structure (Witt, 1993b, fig. 17). Many ore-bearing structures at Kambalda, and many of those in regional shear zones (e.g. Paddington), formed during (late D_3) predominantly subvertical movements. Eisenlohr (1987) has drawn attention to the importance of late dip-slip movements on gold-bearing structures elewhere in the Norseman–Wiluna belt. Quartz

Table 18. Possible controls on variable plunges of ore shoots in mineralized shears in the Boorara–Menzies shear system, and adjacent greenstones

Locality	*Plunge of ore shoot*	*Possible controls*
Western Menzies	30–40°S	Stretching lineation
Goongarrie	60°S	Intersection of two mineralized structures
Vettersburg	50–60°N, S	Unknown
Wycheproof	Subvertical	Stretching lineations
Paddington	?No plunge aspect	Subhorizontal veins

veins at Mt Charlotte formed during D_4 dextral faulting. Forceful emplacement of granitic rocks during or after major strike-slip faulting (D_3) has been responsible for the formation of many ore-bearing structures in the Siberia, Comet Vale, and eastern Menzies mining areas. Stott and Smith (1988) have recorded similar granite emplacement-related structures which host gold mineralization in Ontario.

Recognition of the timing of the formation of ore-bearing structures places only a maximum age constraint on the age of gold mineralization because the structures may be continually active during progressive D_2–D_4 deformation. 'Long-lived' regional shear zones may have been continually active since early synvolcanic development as growth faults. Northwest- to north-northwest-trending shear zones, in particular, record evidence for complex multiple movements, up to and including D_4. The orientation of ore shoots within mineralized shears is not diagnostic since they may form either parallel to, or normal to, stretching lineations (R.G. Roberts, 1988). However, in most cases, mineralization in strike-parallel shear zones is associated with late quartz veining which cuts across ductile shear fabrics and displays little evidence for later deformation on a significant scale. This observation suggests that gold was deposited during latest major movements on the shear zones. At Menzies, auriferous quartz veins in mineralized shears at mines such as First Hit, Lady Shenton, and Yunndaga do show evidence of major deformation. Even here though, particularly high gold grades are associated with arsenopyrite adjacent to a few relatively late veins which display evidence of only minor recrystallization. All linear fabrics and ore shoots in the western Menzies mining area plunge consistently south at 30–40° suggesting mineralization was introduced during oblique strike-slip shearing (D_3), and there is little evidence for later subvertical or dextral movements. Despite the similarity of the structural setting and mineralized structures in the western Menzies mining area to those at Sons of Gwalia, at Leonora, there is no evidence to indicate the presence of D_1 mineralization, as suggested by Williams et al. (1989). Alternatively, the range of orientations of colinear fabrics and ore shoots at Leonora may reflect complex multiple movements similar to those recorded for shear zones in the greenstone belt between Menzies and Paddington (Table 18; see also Witt, 1990, for discussion of multiple movements on the Bardoc Tectonic Zone).

Conclusions

1. All Archaean gold deposits in the Menzies–Kambalda region are structurally controlled.
2. Gold-bearing structures occur in a variety of structural domains. Although regional shear zones and their subsidiary splay structures are important, relatively low-strain domains between bounding regional shear zones also contain significant gold deposits.
3. Sinistral strike-slip faulting generated many of the ore-bearing structures (particularly in low-strain domains) but others formed during subvertical movements and dextral faulting. Still other structures formed during syntectonic to late-tectonic, forceful emplacement of granitic rocks.
4. A wide variety of brittle to almost entirely ductile host structures have been recognized. The character of these ore-bearing structures reflects many factors, but the metamorphic grade and structural setting of the host rocks, and the orientations of the structures within regional and local stress fields, are of prime importance.
5. It is concluded that gold in the Menzies–Kambalda region was deposited in active structures during the period D_3 to D_4. D_3–D_4 included major sinistral strike-slip faulting, and less pronounced subvertical movements and dextral faulting, all of which occurred relatively late in the tectonothermal evolution of the granite–greenstone terrain. The late timing for gold mineralization is supported by textural evidence in associated hydrothermal alteration assemblages discussed in Chapter 7.

Chapter 5

Alteration associated with gold mineralization

All mineralized structures in the Menzies–Kambalda region are associated with hydrothermal alteration of their wallrocks. The nature of this alteration is quite varied, reflecting primarily the composition and metamorphic grade of the host rock. The approach taken in this section is to describe typical alteration assemblages for mafic, ultramafic, and granitic rocks in turn, and to document the changes which occur in these rocks with increasing metamorphic grade (Fig. 13). Results are summarized in Tables 19–21.

Alteration in mafic rocks

At low- to mid-greenschist facies metamorphic grades, hydrothermal alteration of mafic rocks is characterized by an outer zone of chlorite–carbonate (calcite) alteration and an inner zone of sericite–pyrite(–ankerite) alteration (e.g. Grants Patch, Ora Banda, Witt, 1993b). This alteration scheme is typical also of mafic-hosted deposits in low-grade metamorphic domains elsewhere in the Eastern Goldfields (Skwarnecki, 1988) and in Ontario, Canada (Colvine et al., 1984, 1988). In very iron-rich rocks such as the granophyric-textured quartz dolerite zones of layered and differentiated sills, ankerite is the dominant species of carbonate in the chlorite–carbonate alteration assemblage, and an intermediate, carbonate-rich (ankerite–siderite) zone is developed between inner and outer zones. Typical alteration assemblages are those displayed by Mt Charlotte (Clark, 1980) and the Golden Mile (Phillips, 1986) at Kalgoorlie, and by the Golden Kilometre deposit at Mt Pleasant (PLATES V, A–D). These alteration assemblages are compared in Table 22.

Outer alteration zones are, in most cases, about the same size or a little wider than inner alteration zones (e.g. at Mt Pleasant the chlorite–carbonate zone is about 10 m wide). However, at Kalgoorlie overlapping alteration haloes related to widespread and closely spaced fracturing has produced a regional carbonation halo measured in kilometres (Phillips, 1986). Within the chlorite–carbonate zone of alteration, metamorphic actinolite and albite are converted to chlorite–calcite, and chlorite–sericite (–calcite), respectively (reactions 1–3, Table 23). In addition, minor pyrrhotite develops at the expense of all iron-bearing minerals. The presence of ankerite instead of calcite in very iron-rich rocks suggests some partitioning of iron and magnesium between carbonate and chlorite. Silicification of mafic rocks (PLATES III, H and IV, A) occurs in some deposits (e.g. Excelsior at Bardoc, Grants Patch and some Golden Mile lodes). The weak development of secondary silica in many other deposits suggests SiO_2 produced by reactions 1–3 is removed by the hydrothermal fluid, though it may be redeposited in quartz veins. Pyrrhotite may form at the expense of Fe-bearing silicates, carbonates, and oxides by reactions such as 9–11 (Table 23).

Characteristic reactions within the inner zone of alteration include conversion of chlorite to ankerite and siderite, and of plagioclase (albite) to sericite, (Table 23, reactions 5–8). Bright-green Cr-rich muscovite (fuchsite) occurs in altered high-Mg basalt at some localities (e.g. Mt Percy, Kalgoorlie; Excelsior, Bardoc). Gold is closely associated with pyrite which forms at the expense of Fe-carbonate and magnetite (reactions 12 and 13).

The intermediate, carbonate-dominated zone of alteration appears to develop preferentially in very iron-rich rocks (e.g Golden Mile, Golden Kilometre) and is poorly developed or absent in many other mafic-hosted gold deposits such as Grants Patch and Ora Banda. Pyrrhotite-forming reactions (9–11) and reaction 8, in addition to 5, 6, and 7, appear to be important in producing this intermediate zone of alteration. At Mt Pleasant, the transition between the outer chlorite–carbonate zone and the intermediate carbonate–sericite zone is marked by anomalous concentrations of secondary albite. Secondary albite presumably formed from Na flushed out during sericitization of metamorphic albite in (inner) zones of more intense alteration. Clark (1980) noted a similar occurrence of secondary albite at Mt Charlotte, and suggested reaction 4 to account for it.

The three deposits considered in Table 22 are hosted by structures dominated by brittle deformation in low-strain structural domains. Igneous textures are preserved in all zones at Mt Charlotte. At the Golden Mile and Golden Kilometre, outer zones of alteration preserve igneous textures (PLATES V, F and X, A). Widely spaced microshears become progressively more closely spaced throughout the intermediate, carbonate-rich zone, developing into weak to moderate pervasive foliation(s) in the inner, sericite–pyrite zone.

More ductile, shear-related structures with similar alteration assemblages are represented by weakly to moderately deformed chloritic zones of alteration, and an intense ductile fabric associated with the inner sericite–pyrite alteration zone (e.g. the north-trending shear at Grants Patch).

North of Mt Pleasant, towards Siberia, mineralization occurs in mafic rocks at progressively higher metamorphic grades. Biotite becomes an increasingly important

Table 19. Metamorphic and metasomatic assemblages associated with mineralization in mafic rocks in the Menzies–Kambalda region

		Inner alteration zone	*Outer alteration zone*	*Metamorphic assemblage*	*Example*	
		MICROCLINE (M or X) DIOPSIDE (M or X) GARNET (M or X)	HORNBLENDE (R, X) CALCIC PLAGIOCLASE (R, M) BIOTITE (M)	Hornblende Calcic plagioclase Ilmenite	Twin Hills St Albans Dublin Castle	
600°C	(D)	Calcic plagioclase (M) Calcite (M) Pyrrhotite (M) Pyrite (M) Arsenopyrite (M)	Calcite (M) Sphene (M) Pyrrhotite (M)			
		QUARTZ (M) BIOTITE (M) CALCIC PLAGIOCLASE (M) Calcite (M)	BIOTITE (M) HORNBLENDE (R, X) CALCIC PLAGIOCLASE (R, M)	Hornblende Calcic plagioclase Ilmenite	First Hit Lady Shenton	Menzies
500°C	(C)	Sphene (M) Pyrrhotite (M) Pyrite (M) Arsenopyrite (M)	Calcite (M) Garnet (X) Ilmenite (R) Pyrrhotite (M) Pyrite (M)		Camperdown Sand King	Siberia
		QUARTZ (M) ANKERITE (M) ALBITE (M)	BIOTITE (M) <—— ——> CHLORITE (M)	Actinolite or hornblende Albite or calcic plagioclase Ilmenite (–Epidote)	Wycheproof Goongarrie Hunt	
400°C	(B)	MUSCOVITE (M) Rutile (M) Pyrite (M)	CALCITE (M) Sphene (M) Epidote (R, M) Pyrrhotite (M) Pyrite (M)		Defiance New Mexico	Kambalda
		MUSCOVITE (M) ANKERITE (M) SIDERITE (M)	CHLORITE (M) CALCITE OR ANKERITE (M) ALBITE (R, M)	Actinolite Albite Ilmenite (–Epidote)	Ora Banda Grants Patch	
300°C	(A)	Pyrite (M) Pyrrhotite (M) Arsenopyrite (M)	Epidote (R, M) Ilmenite (R) Pyrrhotite (M)		GK, Mt Pleasant Golden Mile, Kalgoorlie	
		Approximately 0.2 <—— increasing X_{CO_2} ——> 0				

NOTE: Temperatures (approximate only) are based on data in Figure 23. Settings of example deposits are approximate, based on alteration assemblages and limited fluid inclusion data. Broken arrows in outer alteration zone at 400°C indicate that biotite increases and chlorite decreases towards the centre of the mineralized structure and the inner alteration zone.
Metasomatic minerals in upper case lettering commonly form >10% of the alteration assemblage, but assemblages are varied and one or more of these minerals may be a minor component, or even absent, in some deposits.
Metasomatic minerals in lower case lettering normally form <10% of the alteration assemblage.
(R) Relict metamorphic mineral
(M) Metasomatic mineral, or relict mineral which is so thoroughly recrystallized as to be unrecognizable as a relict mineral
(X) Porphyroblast mineral, formed by recrystallization of metamorphic or metasomatic assemblages.
Bracketed figures (A)–(D) in left of table correspond broadly to metamorphic settings in Figures 33, 34, and 35

alteration mineral in this direction. At Grants Patch, minor biotite occurs with ankerite and idioblastic pyrite in late veins which cut across sericitized basalt (PLATE XIII, D), or as infill in brecciated silicified and sericitized basalt. Minor patchy biotite overprints sericitic alteration at Ora Banda, but displays variable retrograde alteration to chlorite (distinctive anomalous brown interference colours distinguish it from earlier chlorite in the outer zone of alteration). At New Mexico, an inner zone of quartz–sericite alteration is overprinted by schistosity-controlled and veinlet-controlled biotite–carbonate–pyrite (–tourmaline) alteration (PLATE XIII, E). Reactions such as reaction 14 and 15 (Table 23) are probably involved. Carbonate minerals associated with this later phase include ankerite and calcite.

At upper greenschist- to lower amphibolite-facies metamorphic grades (e.g. at Kambalda and Goongarrie), relicts of an earlier sericitic alteration are rarely observed (see, however, Camperdown deposit, Witt, 1993b). Biotite alteration may have developed directly from chloritic or metamorphic assemblages in these rocks. For example, chlorite–calcite–plagioclase–pyrrhotite schist passes into biotite–plagioclase–calcite–pyrite schist in mineralized shears at Goongarrie (PLATES V, G–H). Similar assemblages have been noted at Lady Grace Darling and Wycheproof. The widespread presence of calcite in these higher metamorphic grade rocks probably reflects the instability of ankerite and sericite with respect to biotite and calcite (reaction 14).

Table 20. Metamorphic and metasomatic assemblages associated with gold mineralization in ultramafic rocks in the Menzies–Kambalda area

	Innermost alteration zone	*Inner alteration zone*	*Outer alteration zone*	*Metamorphic assemblage*	*Examples*
500°C	QUARTZ (M) TREMOLITE (X) Pyrrhotite (M) Arsenopyrite (M) Rutile (M)	TREMOLITE (X) BIOTITE (M) Pyrrhotite (M) Rutile (M)	TALC (M) CHLORITE (M, R) Dolomite (M)	Tremolite Chlorite Magnetite	Yunndaga
	QUARTZ (M) DOLOMITE (M)	TALC (M) DOLOMITE (M)	TALC (M) CHLORITE (M, R) DOLOMITE (M)	Tremolite Chlorite Magnetite	Siberia Consols, Vettersburg (Na)
400°C	Pyrrhotite (M) Pyrite (M)	(–Tremolite) (X) Pyrrhotite (M) Pyrite (M)			Hampton–Boulder (Na and K), Last Hope/Golden Mount
(K)					
		Na* K* Albite Biotite (M) (M) Muscovite (M) Fuchsite (M)			Blue Funnel (K), Victory, Broad Arrow (Na and K), Dixie
	~0.2 <———	increasing X_{CO_2} ———		0	

NOTE: Temperatures and settings of mines are approximations only, based on data from nearby mafic-hosted deposits. Values of X_{CO_2} are presumed to be comparable with those for altered mafic rocks (Table 19).
Na* and K* denote additional minerals which characterize sodic and potassic variants of alteration, respectively (see text for explanation). Similarly, (Na) and (K) after the deposit name indicate the nature of alteration at that deposit. See Table 19 for further explanation of symbols for metasomatic minerals

Table 21. Metamorphic and metasomatic assemblages associated with gold mineralization in granitic rocks in the Menzies–Kambalda area

	Inner alteration zone	*Outer alteration zone*	*Metamorphic assemblage*	*Examples*
~500°C	SERICITE (M) QUARTZ (M) Calcite (M) Pyrite (M) Arsenopyrite (M)	SERICITE (M) QUARTZ (M, R) PLAGIOCLASE (R) Calcite (M) Biotite (R, perhaps M) Pyrrhotite (M) Pyrite (M)	Quartz Plagioclase Biotite (–Hornblende)	Yunndaga
				Lady Bountiful
~300°C				Binduli
	~0.2 <———	increasing X_{CO_2} ———	0	

NOTE: Temperatures and settings of mines are approximations only, based on data from nearby mafic-hosted deposits. Values of X_{CO_2} are presumed to be comparable to those for altered mafic rocks (Table 19). See Table 19 for explanation of symbols for metasomatic minerals

Table 22. Alteration assemblages associated with mineralization at Mt Charlotte, the Golden Mile (Kalgoorlie), and Golden Kilometre Shoot (Mt Pleasant)

Locality	*Inner alteration zone*	*Intermediate alteration zone*	*Outer alteration zone*	*Metamorphic assemblage*
Mt Charlotte, Kalgoorlie (Type 1 alteration, 450–1000 m depth, Clark, 1980)	'Bleached zone' SERICITE*, ankerite, albite, quartz, PYRITE*, leucoxene, minor calcite	'Unbleached zone' ankerite, chlorite, ALBITE*, quartz, PYRRHOTITE*, magnetite, ilmenite, leucoxene	'Pervasive alteration' (≡ regional carbonation of Bartram and McCall, 1971) CHLORITE*, ANKERITE*, albite, quartz, magnetite, ilmenite, leucoxene	ACTINOLITE, ALBITE, quartz, ilmenite, magnetite
Golden Mile, Kalgoorlie (Phillips, 1986)	'Pyrite' alteration MUSCOVITE*, ankerite, quartz, PYRITE*, minor albite, siderite, leucoxene	'Carbonate' alteration SIDERITE* and ANKERITE* quartz, albite, MUSCOVITE*, ilmenite, magnetite, PYRITE*, minor tourmaline, paragonite, chalcopyrite	'Chloritic' alteration (≡ regional carbonation of Bartram and McCall, 1971) CHLORITE*, ANKERITE*, albite, quartz, magnetite, ilmenite, minor calcite, siderite	ACTINOLITE, ALBITE, ilmenite, magnetite, quartz, epidote, chlorite
Golden Kilometre, Mt Pleasant (Witt, 1993b)	SERICITE*, ankerite, PYRITE*, quartz, ilmenite, magnetite, minor pyrrhotite, arsenopyrite	ANKERITE*, (+SIDERITE?), SERICITE*, quartz, ilmenite, magnetite, PYRRHOTITE*	CHLORITE*, ANKERITE*, albite, quartz, ilmenite, magnetite, pyrrhotite*, minor sericite, calcite	ACTINOLITE, ALBITE, quartz, ilmenite, minor chlorite

Capitalized minerals are diagnostic, either alone or in combination, of the alteration assemblage
* denotes new mineral or significant additions of mineral to the alteration assemblage

Chlorite–biotite assemblages characteristically form an outer alteration halo around mineralized vein/breccia systems and shear zones at Kambalda (Phillips and Groves, 1984; Clark et al., 1986, 1988; Roberts and Elias, 1990). Typical assemblages in inner and outer alteration zones are shown in Witt (1993c, table 9). Outer zones are generally similar to those at Goongarrie with biotite increasing with respect to chlorite towards the centres of mineralized structures. Chlorite forms at the expense of hornblende in these higher grade metamorphic rocks (reaction 16). Possible biotite-forming reactions 17 and 18 may produce the observed alteration assemblages. Phillips and Groves (1984) suggested reaction 19 to account for an increase in Mg/(Mg + Fe) for chlorite and biotite towards the inner alteration zone.

A well-developed shear fabric is generally present in these assemblages, where they are associated with relatively ductile structures (PLATES V, G–H and VI, C). The shear fabric is recorded in both inner and outer alteration zones, and may even be present in the immediately adjacent unaltered amphibolite (e.g. Wycheproof, Lady Grace Darling). It is defined by subparallel seams of phyllosilicate minerals, but biotite is commonly less well-oriented than chlorite within the seams, suggesting that crystallization of biotite outlasted formation of chlorite, and at least locally outlasted ductile deformation (PLATE IX, G).

Many deposits in the Kambalda – St Ives mining area are characterized by an inner zone of quartz–ankerite–albite(–muscovite)–pyrite alteration which is generally related to late brittle fracturing within the mineralized systems and is superimposed upon earlier chlorite–biotite–calcite assemblages (PLATE IV, B). Reactions 4 and 20 (Table 23) are suggested to account for the presence of albite in these inner alteration zones. Although minor albitization of mafic rocks has been noted elsewhere in the Menzies–Kambalda region, the widespread occurrence and preservation of sodium metasomatism at Kambalda is somewhat unusual.

Alteration assemblages at Siberia and Menzies are representative of those in mid- to upper-amphibolite grade rocks. Foliation-controlled biotitization (with or without minor chloritization) of amphibolite (PLATE IX, D) becomes increasingly intense towards the centres of the mineralized structures. Inner zones of alteration (PLATES IX, E–F) are biotite–calcic plagioclase (–carbonate–quartz)–sulfide assemblages (Table 19). The characteristic carbonate species is calcite; ankerite is generally absent. The amount of calcite tends to increase from the outer alteration zone towards the inner zone, but is generally not as abundant as in deposits in lower grade metamorphic rocks. Calcite is commonly a minor phase in alteration assemblages at Menzies, but tends to be more common in deposits at Siberia. These relationships suggest reactions such as 21–23 (Table 23). Some of these reactions strip Fe from the alteration assemblage which may be redeposited as Fe sulfides. Ilmenite is widespread in outer alteration zones but sphene characterizes inner zones of alteration (reaction 24).

The above reactions (21–23) represent dehydration and decarbonation of earlier lower grade assemblages. These may be appropriate at some localities, but it is more likely that in many deposits the observed alteration assemblages formed directly from amphibolitic metamorphic rocks, according to reactions such as 25 and 26.

Table 23. Possible metasomatic reactions involved in hydrothermal alteration of mafic rocks

1. $6Ca_2(Fe, Mg)_5Si_8O_{22}(OH)_2 + 12CO_2 + 14H_2O \longrightarrow 5(Fe, Mg)_6Si_4O_{10}(OH)_8 + 12CaCO_3 + 28SiO_2$
   actinolite fluid chlorite calcite fluid

2. $3Ca_2(Mg, Fe)_5Si_8O_{22}(OH)_2 + 2Ca_2Al_3Si_3O_{12}(OH) + 10CO_2 + 8H_2O \longrightarrow 3(Mg, Fe)_5Al_2Si_3O_{10}(OH)_8 + 10CaCO_3 + 21SiO_2$
   actinolite epidote fluid chlorite calcite fluid

3. $6Ca_2(Fe, Mg)_5Si_8O_{22}(OH)_2 + 3NaAlSi_3O_8 + 12CO_2 + 14H_2O + K^+ + 2H^+ \longrightarrow 5(Fe, Mg)_6Si_4O_{10}(OH)_8 + 12CaCO_3 + KAl_3Si_3O_{10}(OH)_2 + 34SiO_2 + 3Na^+$
   actinolite albite fluid chlorite calcite muscovite quartz fluid

4. $Fe_5Al_2Si_3O_{10}(OH)_8 + 3SiO_2 + 2Na^+ + 8H^+ \longrightarrow 2NaAlSi_3O_8 + 8H_2O + 5Fe^{2+}$
   Fe-chlorite quartz fluid albite fluid

5. $Fe_6Si_4O_{10}(OH)_8 + 6CaCO_3 + 6CO_2 \longrightarrow 6CaFe(CO_3)_2 + 4SiO_2 + 4H_2O$
   Fe-chlorite calcite ankerite fluid

6. $Fe_6Si_4O_{10}(OH)_8 + 6CO_2 \longrightarrow 6FeCO_3 + 4SiO_2 + 4H_2O$
   Fe-chlorite siderite fluid

7. $3NaAlSi_3O_8 + K^+ + 2H^+ \longrightarrow KAl_3Si_3O_{10}(OH)_2 + 6SiO_2 + 3Na^+$
   albite fluid muscovite fluid

8. $NaAlSi_3O_8 + (Mg, Fe)_5Al_2Si_3O_{10}(OH)_8 + 5CaCO_3 + K^+ + 5CO_2 \longrightarrow KAl_3Si_3O_{10}(OH)_2 + 5Ca(Mg, Fe)(CO_3)_2 + 3SiO_2 + 3H_2O + Na^+$
   albite chlorite calcite fluid muscovite ankerite fluid

9. $FeTiO_3 + H_2S \longrightarrow FeS + TiO_2 + H_2O$
   ilmenite fluid pyrrh. rut. fluid

10. $FeCO_3 + H_2S \longrightarrow FeS + CO_2 + H_2O$
    siderite(a)fluid pyrrh. fluid

11. $Fe_6Si_4O_{10}(OH)_8 + 6H_2S \longrightarrow 6FeS + 4SiO_2 + 10H_2O$
    Fe-chlorite fluid pyrrh. fluid

12. $FeCO_3 + 2H_2S \longrightarrow FeS_2 + CO_2 + H_2O + 2H^+ + 2e^-$
    siderite(a) fluid pyr. fluid

13. $Fe_3O_4 + 6H_2S + O_2 \longrightarrow 3FeS_2 + 6H_2O$
    magnetite fluid pyrite fluid

14. $KAl_3Si_3O_{10}(OH)_2 + 9Ca(Mg, Fe)(CO_3)_2 + 6SiO_2 + 2K^+ + 3H_2O \longrightarrow 3KAl(Mg, Fe)_3Si_3O_{10}(OH)_2 + 9CaCO_3 + 9CO_2 + 2H^+$
    muscovite ankerite quartz fluid biotite calcite fluid

15. $KAl_3Si_3O_{10}(OH)_2 + 3SiO_2 + 8CaMg(CO_3)_2 + 4H_2O \longrightarrow 8CaCO_3 + Mg_5Al_2Si_3O_{10}(OH)_8 + KAlMg_3Si_3O_{10}(OH)_2 + 8CO_2$
    muscovite quartz ankerite fluid calcite chlorite biotite fluid

16. $Ca_2(Fe^{2+})_5AlSi_7O_{22}(OH)_2 + NaAlSi_3O_8 + 2CO_2 + 2H_2O + 2H^+ \longrightarrow (Fe^{2+})_4(Fe^{3+})Al_2Si_3O_{10}(OH)_8 + 2CaCO_3 + 7SiO_2 + Na^+$
    hornblende albite(b) fluid chlorite calcite quartz fluid

17. $3(Fe^{2+})_5Al_2Si_3O_{10}(OH)_8 + 9SiO_2 + (Fe^{2+})_3O_4 + 6K^+ \longrightarrow 6KAl(Fe^{2+})_{2.66}(Fe^{3+})_{0.33}Si_3O_{10}(OH)_2 + 4H_2O + 4H^+$
    chlorite quartz magnetite fluid biotite fluid

18. $4Ca_2(Fe^{2+})_4(Fe^{3+})AlSi_7O_{22}(OH)_2 + Ca_2Al_3Si_3O_8(OH) + 9H_2O + 10CO_2 + 5K^+ \longrightarrow (Fe^{2+})_5Al_2Si_3O_{10}(OH)_8 + 5KAl(Fe^{2+})_3Si_3O_{10}(OH)_2 + 10CaCO_3 + 13SiO_2 + 9H^+$
    hornblende epidote fluid chlorite biotite calcite quartz

19. $2(Mg_2Fe_4)Si_4O_{10}(OH)_8 + 12H_2S \longrightarrow (Mg_4Fe_2)Si_4O_{10}(OH)_8 + 6FeS_2 + 4SiO_2 + 10H_2O + 12H^+$
    Fe-chlorite fluid Mg-chlorite pyrite quartz fluid

20. $6Mg_5Al_2Si_3O_{10}(OH)_8 + 38SiO_2 + 2H_2O + 12Na^+ \longrightarrow 12NaAlSi_3O_8 + 5Mg_6Si_4O_{10}(OH)_8 + 12H^+$
    Mg-Al chlorite quartz fluid albite Mg-chlorite fluid

21. $CaFe(CO_3)_2 + Fe_5Al_2Si_3O_{10}(OH)_8 + 12H^+ \longrightarrow CaAl_2Si_2O_8 + SiO_2 + 6Fe^{2+} + 2CO_2 + 10H_2O$
    ankerite Fe-Al chlorite fluid anorthite(c) quartz fluid

22. $CaFe(CO_3)_2 + 2KAlFe_3Si_3O_{10}(OH)_2 + 16H^+ \longrightarrow CaAl_2Si_2O_8 + 4SiO_2 + 2CO_2 + 2K^+ + 10H_2O + 7Fe^{2+}$
    ankerite biotite fluid anorthite(c) quartz fluid

23. $2NaAlSi_3O_8 + CaCO_3 + 2H^+ \longrightarrow CaAl_2Si_2O_8 + 4SiO_2 + CO_2 + 2Na^+ + H_2O$
    albite calcite fluid anorthite(c) quartz fluid

24. $FeTiO_3 + CaCO_3 + SiO_2 + 4H^+ + 2e^- \longrightarrow CaTi(SiO_4) + CO_2 + Fe^{2+} + 2H_2O$
    ilmenite calcite quartz fluid sphene fluid

25. $Ca_2(Fe^{2+})_5AlSi_7O_{22}(OH)_2 + 2CO_2 + K^+ + 2H_2S \longrightarrow KAl(Fe^{2+})_2(Fe^{3+})Si_3O_{10}(OH)_2 + 2CaCO_3 + 4SiO_2 + 2(Fe^{2+})S + 2H_2O$
    hornblende fluid biotite calcite quartz pyrrh. fluid

26. $3Ca_2Fe_5AlSi_7O_{22}(OH)_2 + FeTiO_3 + K^+ + 4CO_2 + 13H_2S + 4H^+ + 5e^- \longrightarrow CaAl_2Si_2O_8 + KAlFe_3Si_3O_{10}(OH)_2 + 4CaCO_3 + CaTiSiO_4 + 15SiO_2 + 13FeS + 17H_2O$
    hornblende ilmenite fluid anorthite(c) biotite calcite sphene quartz pyrrh. fluid

Table 23. ***(continued)***

27. $CaAl_2Si_2O_8 + KAlFe_3Si_3O_{10}(OH)_2 + 16SiO_2 + 5CaCO_3 + 12FeS + 15H_2O$ ——> $3Ca_2Fe_5AlSi_7O_{22}(OH)_2 + K^+ + 12H_2S + 5CO_2 + 2H^+ + 3e^-$
anorthite(c) biotite quartz calcite pyrrh. fluid hornblende fluid

28. $Mg_5Al_2Si_3O_{10}(OH)_8 + 3CaCO_3 + 7SiO_2$ ——> $Ca_2Mg_5Si_8O_{22}(OH)_2 + CaAl_2Si_2O_8 + 3H_2O + 3CO_2$
chlorite calcite quartz calcic amphibole anorthite(c) fluid

29. $Ca_2(Mg, Fe)_5AlSi_7O_{22}(OH)_2 + CaAl_2Si_2O_8 + NaAlSi_3O_8 + 2SiO_2 + 2CO_2 + 4K^+ + 6H^+ + e^-$——> $Ca(Mg, Fe)Si_2O_6 + 4KAlSi_3O_8 + 2CaCO_3 + 4(Mg, Fe)^{2+} + Na^+ + 4H_2O$
hornblende calcic plagioclase quartz fluid diopside microcline calcite fluid

30. $KAl(Mg, Fe)_3Si_3O_{10}(OH)_2 + 3CaCO_3 + 6SiO_2$ ——> $KAlSi_3O_8 + 3Ca(Mg, Fe)Si_2O_6 + 3CO_2 + H_2O$
biotite calcite quartz microcline diopside fluid

31. $Ca_2(Mg, Fe)_5AlSi_7O_{22}(OH)_2 + 7CaAl_2Si_2O_8 + NaAlSi_3O_8 + 30SiO_2 + 14K^+ + 6H_2O$——> $3Ca(Mg, Fe)Si_2O_6 + Ca_3Al_2Si_3O_{12} + Ca_3(Mg, Fe)_2Si_3O_{12} + 14KAlSi_3O_8 + 14H^+ + Na^+ + e^-$
hornblende calcic plagioclase quartz fluid diopside garnet microcline fluid

NOTES: In most reactions, SiO_2 may be quartz or dissolved silica in the hydrothermal fluid
Oxidation or reduction of iron is required to balance reactions which show electrons
(a) or siderite in ankerite; (b) albite in plagioclase; (c) anorthite in plagioclase
Abbreviations: rut. = rutile; pyrr. = pyrrhotite; pyr. = pyrite

Outer zones of alteration at Siberia and Menzies are commonly characterized by late, unoriented, relatively coarse-grained, subhedral calcic amphibole (hornblende) which is texturally distinct from metamorphic amphibole in amphibolitic wallrocks (PLATES XI, A and B). Locally, monomineralic bands of amphibole occur within the alteration halo, especially adjacent to carbonate-rich bands and veins (PLATE XI, E). The late amphibole porphyroblasts grow across the phyllosilicate fabric and contain inclusion trails of ilmenite, plagioclase, quartz, calcite, and, less commonly, biotite. These inclusion trails preserve the external foliation, generally with little or no rotation (PLATES XI, C and D). These textural relationships and a commonly inverse modal relationship between biotite and amphibole porphyroblasts suggest an origin for the amphibole during late- to post-deformational metamorphic recrystallization according to decarbonation reactions 27 and 28 (Table 23) or the reverse of reaction 25. The composition of the amphibole reflects that of the unaltered host rock. Dark green, pleochroic hornblende is characteristic of most mafic rocks, but tremolitic amphibole occurs in high-Mg basalt (e.g. at New Mexico and Thiel Well). However, the composition of amphibole in many deposits near Menzies becomes less Fe-rich towards more central zones of relatively intense alteration, suggesting they inherit the compositions of biotite and chlorite precursors (cf. Hunt mine, Kambalda; Phillips and Groves, 1984). Less commonly, garnet porphyroblasts occur in the outer zones of alteration. The occurrence of garnet is very irregular, and it is generally a minor phase, except in the mafic sediment-hosted Lady Harriet mine which also contains plagioclase and chloritoid porphyroblasts (PLATES XII, A–C). The development of both garnet and chloritoid are probably influenced partly by bulk rock composition.

Mines closest to the diapiric syn-D_3 Jorgenson Monzogranite, north of Menzies, display high temperature calc-silicate alteration assemblages (PLATES VI, H and XII, E–G). Assemblages such as diopside–microcline and diopside–garnet probably form by reactions such as 29–31 (Table 23). Mueller (1988) and Keats (1991) documented similar assemblages associated with gold mineralization in the Southern Cross Province of the Yilgarn Craton. Mueller (1988) suggested the Southern Cross deposits are skarns related to associated granitic intrusives. However, there are important differences between the calc-silicate-assemblage gold deposits near Menzies and classic skarn deposits (Kwak, 1986; Einaudi et al., 1981). Calc-silicate assemblages at Menzies form the innermost zone of a zoned alteration system, and textural relationships suggest they replaced, or formed simultaneously with, relatively hydrous (amphibole, biotite) assemblages. Skarns typically evolve from relatively anhydrous to relatively hydrous assemblages. In addition, K-feldspar, rarely a significant component of typical skarns, is a common mineral at Menzies (PLATES XII, E–G), reflecting K-metasomatism of the mafic host rocks.

Epidote is a common mineral in the alteration assemblages in mines close to syn-D_3 diapirs (PLATES VI, G and XII, H) but also occurs in similarly located unmineralized mafic rocks. There is no systematic association of epidote with other minerals in alteration zones associated with mineralized structures, and textural evidence suggests the mineral formed throughout the mineralizing deformation/alteration event. The stability of epidote is favoured by oxygen fugacities above the quartz–fayalite–magnetite buffer assemblage (fO_2 > QFM), a condition which may have resulted from an influx of magmatic fluids from the syn-D_3 diapirs, or from convecting formational waters circulating in response to heat generated by the granitic intrusions. Ferry (1976a) attributed growth of epidote in metamorphosed carbonate rocks in Maine to an influx of H_2O-rich fluids, possibly derived from syntectonic granitoids during metamorphism. Epidote may have taken part in some of the reactions which occurred in the alteration zones. However, its role was probably not essential and it is not considered further here.

Variable sericitization of plagioclase and biotite, and irregular development of prehnite–quartz–carbonate–chlorite assemblages in high-grade metamorphic environments are attributed to retrograde alteration, and thus record decreasing temperatures.

Table 24. Possible metasomatic reactions involved in hydrothermal alteration of ultramafic rocks

1. $3Ca_2(Mg, Fe)_5Si_8O_{22}(OH)_2 + 6CO_2 + 2H_2O \longrightarrow 5(Mg,Fe)_3Si_4O_{10}(OH)_2 + 6CaCO_3 + 4SiO_2$
   tremolite fluid talc calcite quartz

2. $Mg_3Si_4O_{10}(OH)_2 + 3CaCO_3 + 3CO_2 \longrightarrow 3CaMg(CO_3)_2 + 4SiO_2 + H_2O$
   talc calcite fluid dolomite quartz fluid

3. $Mg_3Si_4O_{10}(OH)_2 + 3CO_2 \longrightarrow 3MgCO_3 + 4SiO_2 + H_2O$
   talc fluid magnesite quartz fluid

4. $(Mg, Fe)_5Al_2Si_3O_{10}(OH)_8 + 2CO_2 + SiO_2 + 6H^+ \longrightarrow (Mg, Fe)_3Si_4O_{10}(OH)_2 + 2(Mg, Fe)CO_3 + 2Al^{3+} + 6H_2O$
   chlorite fluid talc magnesite fluid

5. $3Mg_5Al_2Si_3O_{10}(OH)_8 + 15CaCO_3 + 15CO_2 + 2K^+ \longrightarrow 15(Ca, Mg)(CO_3)_2 + 2KAl_3Si_3O_{10}(OH)_2 + 3SiO_2 + 9H_2O + 2H^+$
   chlorite calcite fluid dolomite muscovite quartz fluid

6. $2Mg_3Si_4O_{10}(OH)_2 + Mg_5Al_2Si_3O_{10}(OH)_8 + 2K^+ + 5CO_2 \longrightarrow 2KAlMg_3Si_3O_{10}(OH)_2 + 5MgCO_3 + 5SiO_2 + 2H^+ + 3H_2O$
   talc chlorite fluid biotite magnesite quartz fluid

7. $Mg_6(Si_3Al)O_{10}(OH)_8 + 8SiO_2 + Na^+ + e^- \longrightarrow 2Mg_3Si_4O_{10}(OH)_2 + NaAlSi_3O_8 + 2H_2O$
   chlorite quartz fluid talc albite fluid

8. $Mg_3Si_4O_{10}(OH)_2 + Na^+ + Al^{3+} + 3CO_2 + H_2O \longrightarrow NaAlSi_3O_8 + 3MgCO_3 + SiO_2 + 4H^+$
   talc fluid albite magnesite quartz fluid

9. $5CaMg(CO_3)_2 + 8SiO_2 + H_2O \longrightarrow Ca_2Mg_5Si_8O_{22}(OH)_2 + 3CaCO_3 + 7CO_2$
   dolomite quartz fluid tremolite calcite fluid

10. $Ca_2Mg_5Si_8O_{22}(OH)_2 + NaAlSi_3O_8 + 2Na^+ + 2CO_2 \longrightarrow Na_3Mg_4Al(Si_8O_{22})(OH)_2 + 2CaCO_3 + 3SiO_2 + Mg^{2+}$
    tremolite albite fluid magnesio-arfvedsonite calcite quartz fluid

11. $Ca_2Mg_5Si_8O_{22}(OH)_2 + 3Na^+ + Al^{3+} + 2CO_2 + 2H_2O \longrightarrow Na_3Mg_4Al(Si_8O_{22})(OH)_2 + 2CaCO_3 + Mg^{2+} + 4H^+$
    tremolite fluid magnesio-arfvedsonite calcite fluid

NOTE: In most reactions, SiO_2 may be quartz or dissolved silica in the hydrothermal fluid
Oxidation and reduction of iron is required to balance reactions which show electrons

Alteration in ultramafic rocks

Alteration assemblages in ultramafic rocks (Table 20) appear to be less sensitive to metamorphic grade than those in mafic rocks. The usual configuration is one of metamorphic assemblages (dominantly tremolite and chlorite) passing through talc–chlorite–carbonate schist and talc–carbonate, into an innermost quartz–carbonate alteration zone. Inner zones of alteration may contain minor to moderate amounts of K and/or Na aluminosilicate minerals. Kishida and Kerrich (1987) noted that intensity of alteration in ultramafic rocks at the Kerr Adison mine, Ontario, could be monitored by the dominant Al-bearing silicates (chlorite, muscovite, albite). Carbonate minerals are dolomite, or magnesite in extremely magnesian rocks (cf. McNaughton et al., 1988a). The inner zones of alteration are commonly associated with small but variable amounts of sulfide minerals. Generally, the amount of sulfides in altered ultramafic rocks is much less than that associated with altered mafic rocks. The alteration essentially involves progressive carbonation of the metamorphic assemblage according to reactions 1–4 (Table 24). Reactions 1–3 release SiO_2 from the outer zones of alteration but the silica may be redeposited in central zones or as quartz veins. Reaction 4 involves mobility of aluminium which may be redeposited in aluminous minerals in the inner alteration zone (e.g. reaction 8).

The main K and Na aluminosilicate minerals in the Menzies–Kambalda region are biotite, muscovite, and albite, one of which is generally predominant at any one locality. Muscovite and the bright-green Cr-rich muscovite (fuchsite) is present in small amounts at some localities (e.g. Victory, Broad Arrow; PLATES III, G and IX, C). Moderate to small amounts of biotite are present in mineralized ultramafic rocks at Victory (Broad Arrow), Blue Funnel, Broads Dam and in several small mines on the Cashmans Shear Zone (PLATES X, E and XIII, A). Inner zones of alteration at Vettersburg (PLATE VII, A) and Victory, Broad Arrow contain albite.

Thus, two styles of alteration in mineralized ultramafic rocks are recognized. These have been termed reductive potassic-CO_2 enrichment (biotite, muscovite) and reductive sodic-CO_2 enrichment (albite) by Kerrich (1986a).

Both albite and biotite are relatively abundant in altered, mineralized ultramafic rocks at the Hampton–Boulder deposit, New Celebration. Where both biotite and albite occur together, the biotite appears to be later (e.g. Hampton–Boulder; Victory, Broad Arrow; Blue Funnel).

This contrasts with the situation in altered mafic rocks at Kambalda where albite-rich assemblages overprint biotite–chlorite assemblages.

Reactions 5–8 (Table 24) are suggested for the formation of these inner-zone K and Na aluminosilicate minerals. Biotite appears to be more common in higher grade (upper greenschist to upper amphibolite facies) metamorphic environments such as Menzies (e.g. Yunndaga), whereas muscovite and fuchsite appear to be more common in lower temperature environments (e.g. Mt Percy, Excelsior). However, the distinction is not as clear as for mafic rocks since minor biotite also occurs at Victory (Broad Arrow), Blue Funnel, and Broads Dam.

The main effect of increasing metamorphic grade is the initiation of decarbonation reactions. Decarbonation (the reverse of reaction 1, also reaction 9, Table 24) produces late, unoriented tremolitic amphibole which grows across earlier talc and chlorite fabrics (PLATES VII, B and XI, F) and forms masses of radiating to matted, acicular tremolite in the innermost quartz-rich alteration zone (PLATES VII, C and XI, H). The unoriented tremolite is not simply recrystallized metamorphic amphibole since metamorphic tremolite is destroyed in the outer alteration zone (Witt, 1993a, fig. 19, Witt, 1993b, fig. 20). A broad increase in grainsize of the tremolite prisms can be discerned with higher metamorphic grade. At Yunndaga, the recrystallized assemblage consists of coarse biotite interstitial to unoriented tremolite prisms (PLATE XI, G).

At Vettersburg, late, unoriented amphiboles are partially altered to sodic amphibole (magnesio-arfvedsonite or magnesioreibeckite), along grain boundaries and cross-cutting fractures and veinlets. A similar sodic amphibole forms sheeted veinlet swarms which cut the talc–carbonate alteration zone. The formation of sodic amphibole can probably be attributed to reaction of tremolitic amphibole with late, sodium-rich hydrothermal fluids (reactions 10 and 11, Table 24).

Alteration in rocks of granitic composition

From the limited number of granitoid-hosted deposits examined in the Menzies–Kambalda region, rocks of granitic composition display least variation with metamorphic grade. Although Cassidy (1988) recognized several zones of alteration in mineralized granitoids at Lawlers, zoning in granitic rocks is not as well-developed as for mafic and ultramafic deposits in the Menzies–Kambalda region. Deposits at Binduli (hosted by albitic feldspar porphyry), Lady Bountiful (granodiorite-hosted), and Yunndaga (hosted by granodiorite-derived sedimentary rocks) represent alteration of granitic rocks in areas of progressively higher metamorphic grade. Intense pervasive albitization of the host porphyry at Binduli is the most obvious form of alteration. Albitization is overprinted by minor ankerite and pyrite adjacent to cross-cutting auriferous quartz and albite–carbonate (ankerite) veins. At Lady Bountiful, weak pervasive chloritization of mafic minerals gives way to sericitization adjacent to auriferous quartz veins (PLATE VIII, A). Disseminated and veinlet pyrite in the sericitized granodiorite is associated with minor ankerite, quartz, and biotite (PLATE XIII, C). At Yunndaga, mineralized shears are quartz–sericite–pyrite assemblages (PLATE IX, B). The main chlorite- and sericite-forming reactions in altered granitic rocks are suggested in Table 25.

Intense pervasive albitization of some small porphyry intrusives within ultramafic rocks occurs in the Vettersburg, Hawkins Find, and Siberia mining areas (PLATES VIII, C–F). Secondary albite in the pervasively albitized porphyries is variably recrystallized (PLATE XIV, A), and late, euhedrally terminated albite occurs in mineralized quartz veins and interclast positions in brecciated porphyry (PLATE XIV, B). Pervasive albitization may be overprinted by disseminated and veinlet biotite, ankerite, and pyrite (e.g. PLATES VIII, C and E; XIV, F).

At Vettersburg, albitic porphyry margins against ultramafic rocks are cut by irregular chloritic shears and microshears (PLATE XIV, C). Metamorphic recrystallization of chlorite produces neoblastic amphibole (PLATES XIV, D and E). At Siberia, where the metamorphic grade is higher, there is no clear evidence of earlier chlorite, but disseminated and veinlet-controlled tremolitic amphibole is common within the albitized porphyry (PLATES VIII, F and XIV, G). Neoblastic amphibole increases towards the contact with ultramafic rocks (Witt, 1993b, fig. 20) to the extent that hand specimens superficially resemble leucodoleritic rocks. Late tremolitic amphibole at Three Eights mine is partially altered to magnesioreibeckite (PLATE XIV, H).

Alteration zoning on the local scale

Textural relationships between alteration minerals at transitions between zones suggests a temporal sequence in which minerals in the inner zones of alteration replace those in the outer zones. At a larger scale, this temporal sequence is evident as overprinting of chloritic alteration assemblages by sericite–pyrite alteration adjacent to cross-cutting veins (e.g. PLATE V, D). However, alteration zoning about fluid pathways such as veins and central sections of shear zones probably represents increasing intensity of alteration with respect to a single hydrothermal fluid containing CO_2, S, K, and Au. The spatial relationship between inner and outer alteration zones remains consistent, and direct transitions from unaltered metamorphic assemblages to inner zones of alteration have not been observed. Phillips (1986) alluded to the constant K/Rb ratios in each alteration zone at the Golden Mile deposits, and concluded that contrasting assemblages in the inner, intermediate, and outer zones resulted from a single hydrothermal fluid. Zoned alteration assemblages associated with Archaean lode-gold deposits in mafic to intermediate volcanics at Kambalda, and the Sigma mine, Quebec, have been similarly interpreted (Clark et al., 1988; Robert and Brown, 1986b).

Whilst observations made during this study confirm that carbonation (chloritization) and potassic alteration were closely related, and part of the same hydrothermal event, there is some evidence, on both regional and

Table 25. Possible metasomatic reactions involved in hydrothermal alteration of granitic rocks

1. $6Ca_2Mg_5Si_8O_{22}(OH)_2 + 14H_2O + 12CO_2 \longrightarrow 5Mg_6Si_4O_{10}(OH)_8 + 12CaCO_3 + 28SiO_2$
   hornblende fluid chlorite calcite quartz

2. $2K(Mg, Fe)_3AlSi_3O_{10}(OH)_2 + 4H^+ \longrightarrow (Mg, Fe)_5Al_2Si_3O_{10}(OH)_8 + 3SiO_2 + 2K^+ + (Mg,Fe)^{2+}$
   biotite fluid chlorite quartz fluid

3. $3(Mg, Fe)_5Al_2Si_3O_{10}(OH)_8 + 15CO_2 + 2K^+ \longrightarrow 2KAl_3Si_3O_{10}(OH)_2 + 3SiO_2 + 15(Mg,Fe)(CO_3) + 9H_2O + 2H^+$
   chlorite fluid muscovite quartz in ankerite fluid

4. $2NaAlSi_3O_8 + 2KAlSi_3O_8 + 2H^+ \longrightarrow NaAlSi_3O_8 + KAl_3Si_3O_{10}(OH)_2 + 6SiO_2 + Na^+ + K^+$
   alkali feldspar fluid albite muscovite quartz fluid

5. $40(0.9NaAlSi_3O_8 + 0.1CaAl_2Si_2O_8) + 2KAl_2(Mg,Fe)_{2.5}Si_{2.5}O_{10}(OH)_2 + 6H_2O + 4CO_2 + 2K^+ \longrightarrow 34NaAlSi_3O_8 + 4KAl_3Si_3O_{10}(OH)_2 + (Mg, Fe)_5Al_2Si_3O_{10}(OH)_8 + 4CaCO_3 + 4SiO_2 + 2Na^+$
   plagioclase biotite fluid albite muscovite chlorite calcite quartz fluid

6. $3NaAlSi_3O_8 + K^+ + 2H^+ \longrightarrow KAl_3Si_3O_{10}(OH)_2 + 6SiO_2 + 3Na^+$
   albite fluid muscovite quartz fluid

NOTE: In most reactions, SiO_2 may be quartz or dissolved silica in the hydrothermal fluid

deposit scales, that the fluid evolved towards more potassic compositions during the latest stages of a more prolonged hydrothermal carbonation event.

(a) Mafic and ultramafic rocks in regional shear zones such as the Boulder–Lefroy Fault and the Menzies–Boorara Shear system display evidence of intense pervasive carbonation. These craton-scale structures are commonly envisaged to be pathways which focus fluid flow from deeper levels of the crust or the mantle (Groves et al., 1987, 1988a). Potassic alteration and mineralization are only found in a relatively few shear planes within the regional shear zones. Alteration equivalent to the outer alteration zone (chlorite–carbonate alteration) is characteristic, despite the high fluid/rock ratios implied by the intense carbonation.

(b) The evolution of hydrothermal fluids from essentially carbonating fluids to potassic fluids on a deposit scale is suggested by textural features observed, particularly in some ultramafic-hosted deposits. At Lake View (Comet Vale), strongly deformed and recrystallized carbonation assemblages (including talc and albite) are overprinted by irregular masses of unoriented biotite. At Victory (Broad Arrow) and Golden Mount/Last Hope (Cashmans Shear Zone), massive domains within carbonated (including talc and albite) ultramafic rocks are cut by biotite-rich shear planes (PLATE XIII, A). At Victory (Broad Arrow), late sericite porphyroblasts overprint an earlier chloritic shear fabric (PLATE X, C). Furthermore, late introduction of pyrite and arseno-pyrite (and associated gold) is commonly spatially related to quartz veins which cut across earlier chlorite and biotite fabrics (PLATE VI, A). Biotite and chlorite are intimately associated in some mafic-hosted mineralized shears, but whereas strongly oriented chlorite defines a shear fabric, biotite is commonly more randomly oriented (PLATE IX, G). Weakly deformed biotite porphyroblasts occur within strongly deformed chlorite–carbonate assemblages at Goongarrie, Hampton–Boulder (Celebration), and Ives Reward (Kambalda) (PLATE IX, H).

Quantification of temperature and Xco_2

Quantification of temperature and the mole proportion of carbon dioxide (Xco_2) of hydrothermal fluids during gold-related hydrothermal alteration requires fluid inclusion data and/or thermodynamic analysis of accurate mineralogical data, such as has been carried out at Kalgoorlie and Kambalda (Ho, 1987; Neall and Phillips, 1987). However, such data are available for only a few deposits in the region as a whole. Fluid inclusion studies in the Kalgoorlie area, and associated carbonate mineralogy (Phillips and Brown, 1987) indicate P–T conditions of 1.5–2.0 kb and 280–340°C (Phillips and Groves, 1983; Ho, 1987). Similar studies at the Hunt mine gave P–T estimates of 0.8–3.3 kb and 196–325°C (Ho, 1987). Maximum Xco_2 is in the range approximately 0.15–0.25 at both localities.

Alternatively, T–Xco_2 conditions during hydrothermal alteration can be interpreted from the observed alteration assemblages. For example, Clark et al. (1986, 1988) related the alteration assemblages observed at Victory–Defiance, Kambalda to variable Xco_2 in hydrothermal fluids at P = 2–3 kb and T = 400–410°C (Fig. 23). Alteration assemblages at Kalgoorlie and many other mafic-hosted deposits in low-grade metamorphic districts are also consistent with increasing Xco_2 (and addition of K) towards the inner, central zones of alteration (Fig. 25B). The limitations of this approach are recognized. Pressure constraints are uncertain for many localities within the Menzies–Kambalda region, but the presence of andalusite in pelitic rocks near Menzies suggests a maximum pressure of about 3.8 kb (Holdaway, 1971), even where regional metamorphic grades are high. The stability of quartz–chloritoid in alteration assemblages at the Lady Harriet mine, Menzies, implies minimum pressures of about 2.2 kb (Rao and Johannes, 1979). Deviations from ideal mineral compositions cause additional complexities. However, the form and relative spatial relationships between the curves in Figure 23 will

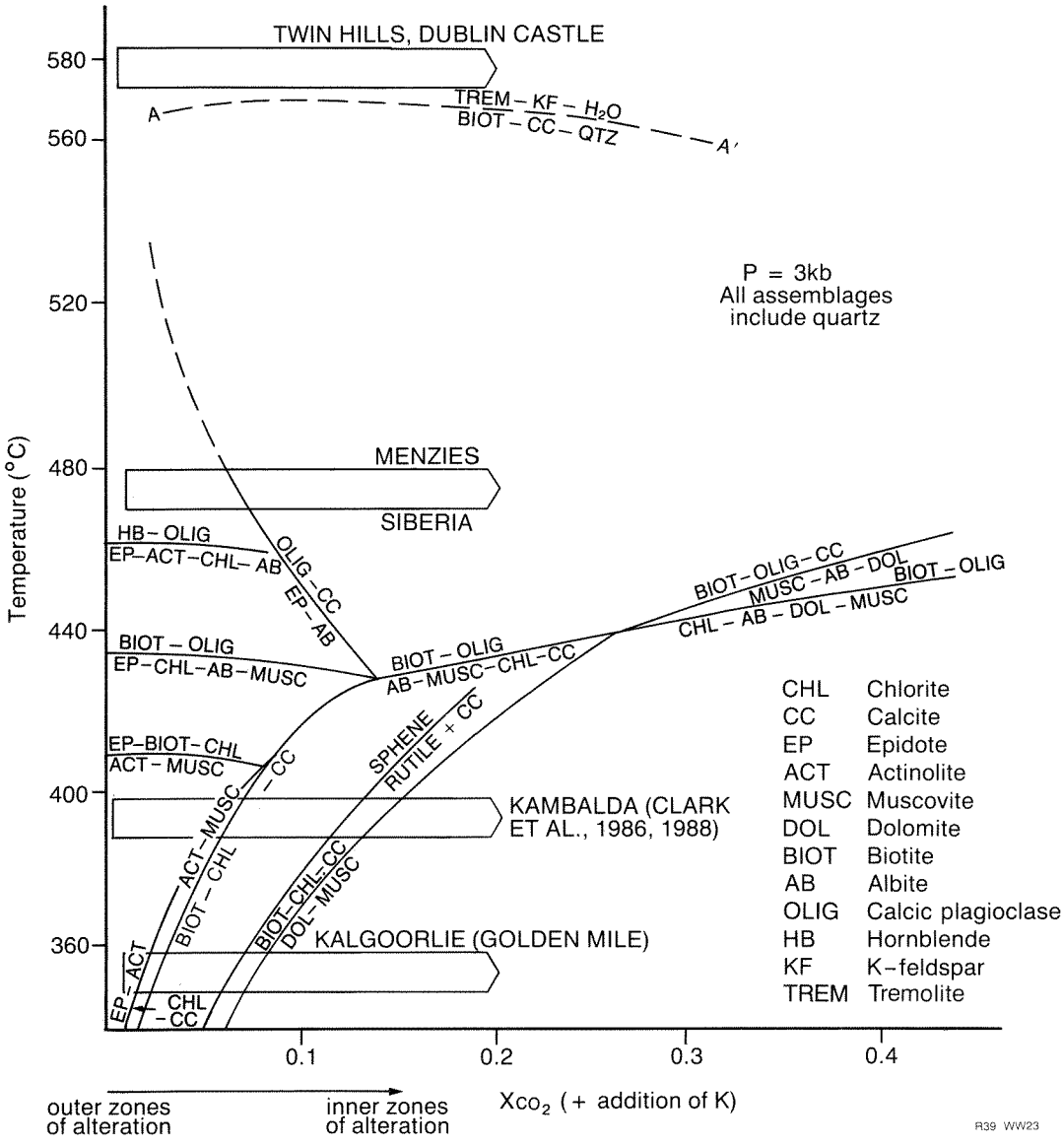

Figure 23. T–Xco_2 diagram for the system K_2O–Na_2O–CaO–MgO–Al_2O_3–SiO_2–H_2O–CO_2 at $P_{total} = Pco_2 + PH_2O$ = 3 kb (after Clark et al., 1986), showing alteration assemblages in some mafic-hosted deposits in the Menzies–Kambalda region. Broken lines represent extrapolation to higher temperatures than those covered by the original diagram. Curve A–A' is from Hoschek (1973). The diagram illustrates the regional temperature control (metamorphism) on the alteration assemblages associated with gold mineralization (indicated by arrow-headed bars). Alteration zoning at individual deposits is controlled by increasing Xco_2 of the hydrothermal fluid, and addition of K towards the centre of the mineralized structure

probably not change markedly within limited excursions from ideal pressure and mineral compositions.

Assemblages such as those at Siberia and Menzies can also be plotted approximately on Figure 23, based on observed alteration assemblages. However, at this stage, the interpretations cannot be compared with data from fluid inclusions and detailed thermodynamic studies. Suggested conditions for metasomatism are 460–550°C at 3 kb, and Xco_2 comparable with those at Kalgoorlie and Kambalda. An upper temperature limit of 550°C in the Menzies district is suggested by the stability of quartz–chloritoid at the Lady Harriet mine (Rao and Johannes, 1979). The stability of tremolite–K-feldspar above 560°C at Xco_2 = 0.2 (Hoschek, 1973) probably defines a lower limit for the diopside–microcline assemblage which occurs at St Albans, Dublin Castle, and in the Twin Hills mining area.

Low temperature (retrograde) assemblages, including combinations of quartz, carbonate, sericite, chlorite, and prehnite, occur as late-stage features in some altered wallrocks at Siberia and Menzies. The upper stability limit of prehnite at PH_2O = 3 kb is about 400°C (Liou, 1971). This stability limit is decreased further in the presence of mixed H_2O–CO_2 fluids (Liou, 1971). The

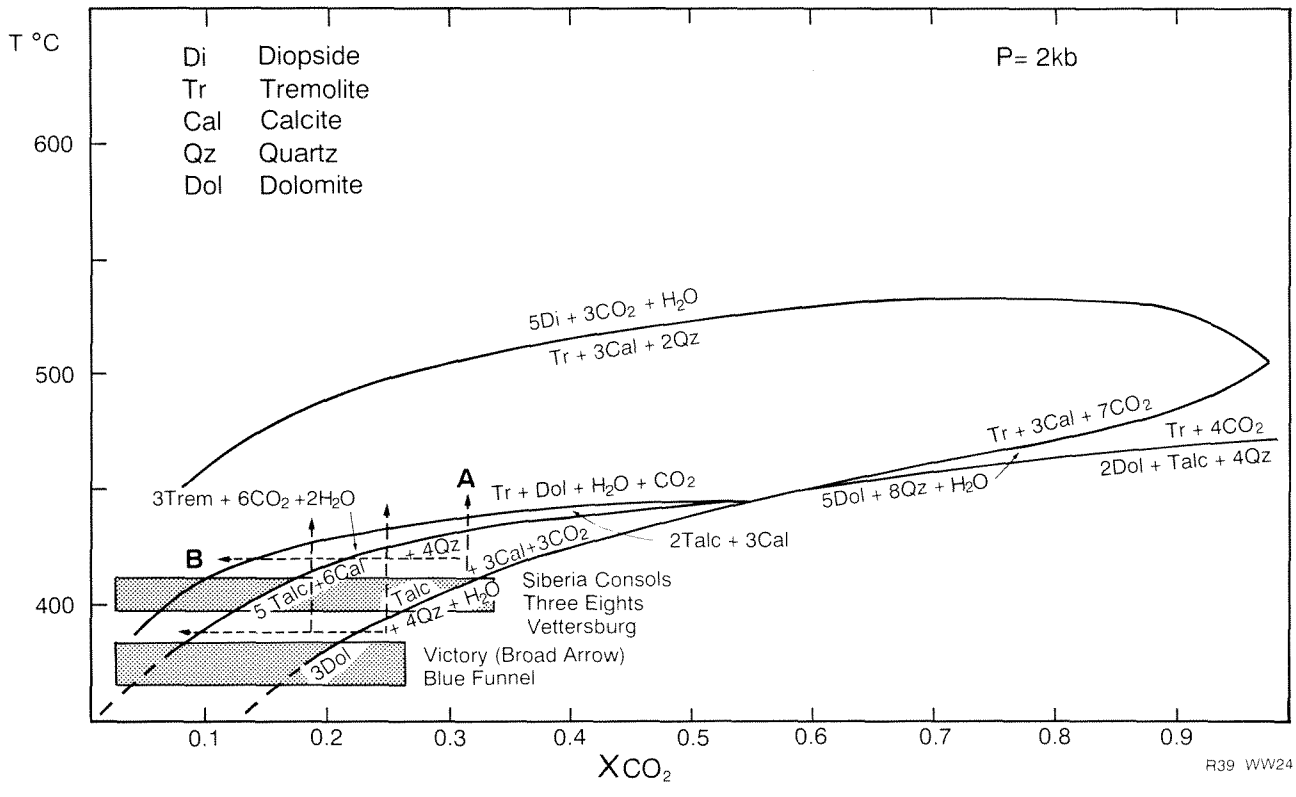

Figure 24. T–Xco_2 diagram at P = 2 kb, showing relative mineral stabilities in the system CaO–MgO–SiO_2–H_2O–CO_2 (after Slaughter et al., 1975), and alteration assemblages in some ultramafic-hosted deposits in the Menzies–Kambalda region. Note that Na_2O, K_2O and Al_2O_3 are not accounted for. Shaded areas represent approximate T–Xco_2 conditions for some mineralized alteration systems in the Menzies–Kambalda region, based on observed mineral assemblages. They illustrate increasing Xco_2 towards the centre of mineralized structures. Siberia Consols and Three Eights are interpreted as lying at higher temperatures than Victory and Blue Funnel, based on regional metamorphic setting and development of decarbonation reactions in assemblages at the former deposits. Note that Siberia Consols probably lies at T > 460°C, based on proximity to mafic-hosted deposits at Siberia (Fig. 23). Plotting Siberia Consols at 460°C requires Xco_2 > 0.7 to stabilize quartz–dolomite assemblages. This seems unreasonably high. However, the same assemblage would be stabilized at lower Xco_2 at P > 2 kb, and curves are also modified in the presence of relatively saline solutions. The broken arrows indicate possible pathways A and B for decarbonation reactions which produce late, unoriented tremolite

stability of sericite with respect to feldspars is also favoured by lower temperatures (Montoya and Hemley, 1975).

Similarly, alteration assemblages in most ultramafic-hosted deposits can be accounted for in terms of increasing Xco_2 towards the inner, central alteration zones (Fig. 24). The instability of metamorphic tremolite and the absence of diopside in altered ultramafic rocks sets a maximum limit to temperatures of alteration. This maximum temperature is approximately 425°C at 2 kb but could be greater than 500°C at higher pressures, assuming Xco_2 < 0.2 approximately (Slaughter et al., 1975). The presence of small amounts of NaCl in the fluid will also raise the temperature of the curves shown in Figure 24 (Bowers and Helgeson, 1983). Bowers and Helgeson (1983) also showed that the position and arrangement of the curves in Figure 24 will be radically modified in the presence of a very saline fluid which may result from phase separation of a more dilute CO_2-bearing hydrothermal fluid. However, it is unlikely that the auriferous fluids were saline enough to undergo phase separation at 2 kb and T > 400°C. The development of muscovite or albite in altered ultramafic rocks is controlled by the relative activities of Na and K in the hydrothermal fluid, though Xco_2 may also exert some influence (Fig. 25A).

Decarbonation reactions produced late, unoriented tremolite porphyroblasts in some ultramafic rocks. These decarbonation reactions appear to require an increase in temperature above that at which the carbonation reactions occurred, although a drop in Pco_2 at constant temperature will promote the same reaction (Fig. 24). Similar parameters probably control the growth of late, unoriented hornblende porphyroblasts in some altered mafic rocks.

Gorman et al. (1981) suggested that massive albitization of porphyries occurred during synvolcanic sea-floor alteration. However, much albite observed in porphyries in the Menzies–Kambalda region is unrecrystallized and undeformed, and appears to have post-dated most deformation. At Hawkins Find and Binduli, albite occurs in late, cross-cutting veins and is clearly present in the auriferous hydrothermal system. Furthermore, conflicting timing relationships between potassic and

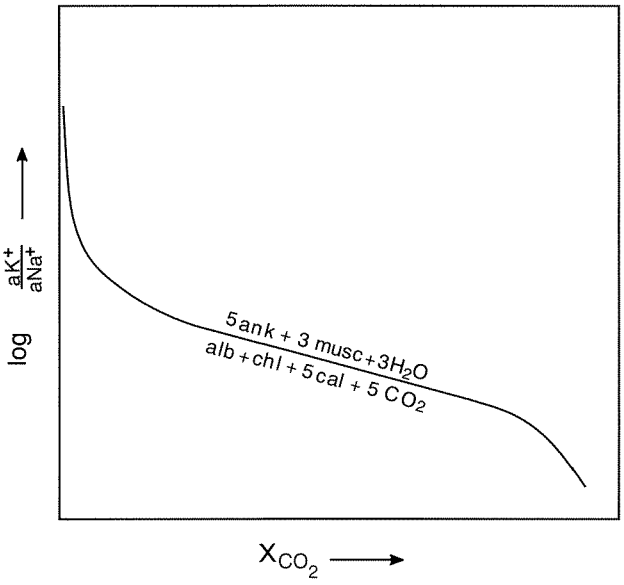

A.

ank = Ankerite
musc = Muscovite
alb = Albite
chl = Chlorite
cal = Calcite
qtz = Quartz

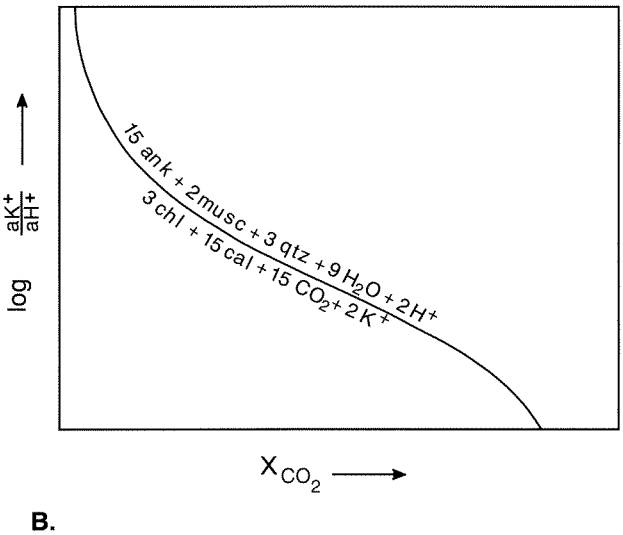

B.

WW15 R39 WW25

Figure 25 A. Schematic, isobaric, isothermal log aK^+/aNa^+ versus Xco_2 diagram for the reaction: albite + chlorite + 5calcite + $5CO_2$ = 5ankerite + 3muscovite + $3H_2O$ (from Kishida and Kerrich, 1987)

B. Schematic, isobaric, isothermal log aK^+/aH^+ versus Xco_2 diagram for the reaction: 3chlorite + 15calcite + $15CO_2$ + $2K^+$ = 15ankerite + 2muscovite + 3quartz + $9H_2O$ + $2H^+$ (from Kishida and Kerrich, 1987)

sodic metasomatism are recognized at Siberia, Hawkins Find, and Kambalda, suggesting overall contemporaneity. These observations favour a late hydrothermal origin for at least some of the albite, controlled by alkali ratios in an evolving fluid. Recent investigations by Bohlke (1988, 1989) have stressed the importance of Al/(Mg + Fe + Cr) in granitic rocks in controlling the relative stabilities of albite and muscovite, in the presence of auriferous hydrothermal fluids. Witt (1992) applied the results given by Bohlke (1988, 1989) to suggest that the same fluids which produced sericitization in mafic rocks in the Menzies–Kambalda region caused albitization of porphyry intrusions.

Timing relationships in alteration assemblages containing biotite and sericite

Figure 23 indicates that alteration assemblages in mafic rocks in the Menzies–Kambalda region are controlled in a regional sense by temperature, but that zoning of alteration assemblages within deposits is controlled by Xco_2 (and addition of K). Where sericite and biotite occur together in alteration assemblages at Lady Bountiful, Grants Patch, and New Mexico, biotite appears to post-date sericitization (PLATES XIII, B–E). This could be interpreted as indicating an increase in temperature during the alteration event, or an evolution towards lower Xco_2 (Fig. 23). Contrastingly, muscovite appears to be later than biotite-dominant assemblages at Goongarrie and Victory (Broad Arrow), suggesting either falling temperature or increasing Xco_2 with time. Falling temperatures are similarly recorded by retrograde assemblages at Siberia and Menzies (see above). Clark et al. (1986) interpreted late muscovite-bearing assemblages at Victory–Defiance (PLATE VI, F) as reflecting increased Xco_2.

Conclusions

1. At individual gold deposits in the Menzies–Kambalda region, alteration assemblages are controlled by increasing Xco_2, and addition of K and S, towards the central structures which acted as fluid pathways. Outer alteration assemblages record carbonation (with or without minor addition of K and S). Inner alteration zones record intense carbonation and significant additions of K and S.

2. Although carbonation and potassic alteration are closely related in time and space, hydrothermal fluids appear to have evolved towards potassic compositions during the latest stages of an extended regional carbonation event.

3. Alteration assemblages are controlled on a regional scale by temperature which in turn correlates broadly with metamorphic grade. Temperature controls the predominant form of K-silicate in the inner alteration zones of mineralized mafic rocks, with muscovite, biotite, and microcline becoming stable at

progressively higher temperatures. Similar regional temperature controls on alteration assemblages in Ontario, Canada, have been documented by Andrews et al. (1986).

4. The presence together of biotite and muscovite in some deposits (e.g. Victory–Defiance at Kambalda) may be explained in terms of Xco_2 gradients within the zoned alteration system. However, in some other deposits, textural and fabric relationships between biotite and muscovite suggest the two minerals are not contemporaneous, and that their formation may have been controlled by changes in temperature or Xco_2 during the mineralization/alteration event.

5. Although potassic alteration is widely associated with gold mineralization, albitization is recorded at many deposits. It is commonly a relatively restricted style of alteration in mafic rocks, but some ultramafic rocks and porphyries record intense albitization. Albitization is a consistently late feature, commonly associated intimately with potassic alteration. Intense albitization of porphyries probably reflects enhanced stability of albite, with respect to muscovite, in rocks with high Al/(Mg + Fe + Cr), when exposed to certain auriferous fluids (Bohlke, 1988, 1989; Witt, 1992).

6. In lower grade metamorphic settings, metasomatic minerals replace metamorphic minerals in the outer zone of alteration, consistent with other evidence that alteration was retrograde with respect to peak metamorphism (Ho, 1987; Clark et al., 1986). However, it should be remembered that apparently retrograde assemblages can be maintained during metamorphism by high Xco_2.

7. Late, unoriented amphibole porphyroblasts overprint a metasomatic shear fabric in altered mafic and ultramafic rocks in many deposits in higher grade metamorphic settings. Less commonly, garnet, andalusite, and chloritoid porphyroblasts have been observed. These observations suggest that alteration assemblages have been metamorphically recrystallized.

Chapter 6

Alteration geochemistry

Eighty-seven samples of altered and unaltered rocks were collected for geochemical analysis. Preferred samples were from underground mining operations and drillcore, but many samples from old, abandoned mines had to be collected from mine dumps where geological controls were less precise. The data are presented in Tables 26–28. Other chemical data on alteration associated with gold mineralization in the Menzies–Kambalda region have been published by Phillips and Groves (1984), Clark et al. (1989), Golding and Wilson (1983), Phillips (1986), Clark (1980), and Barley and Groves (1989).

Gains and losses of major components are shown in Figures 26–28. Enrichment/depletion diagrams for selected deposits are shown in Figures 29–31.

Composition–volume diagrams (e.g. Fig. 32) were used to determine appropriate volume factors for calculating gains and losses of chemical components during alteration (Gresens, 1967). Where composition–volume diagrams yield ambiguous interpretations, Al_2O_3 was considered most likely to be immobile. Choice of volume factor was further influenced by qualitative textural evidence (e.g. preservation of primary textures suggests no significant volume change; brecciation or abundant quartz veining suggests an increase in volume; intense shearing suggests pressure solution, and a decrease in volume). In a few cases where the composition–volume diagram was not definitive, and other evidence contradictory or ambiguous, a volume factor of 1 (no volume change) was assumed.

Unaltered reference material was collected from several mines, but in other cases unaltered host-rock material was not available or could not be positively identified. In these latter cases, published and unpublished whole rock analyses of samples of the appropriate host rock collected from within the Menzies–Kambalda region, but remote from mining operations, were used as reference material (see Witt et al., 1991; Witt, unpublished data; and Morris, in press).

Two points should be kept in mind when assessing the data presented here.

Firstly, samples representing narrow alteration zones, and all samples collected from drillcore, were necessarily small. They were collected to indicate changes in chemical components, not absolute abundances. Furthermore, elements which are concentrated in erratically distributed minerals of low abundance (e.g. Au, Bi, Cu, Mo, Pb, Sb, Zn) may be overestimated or underestimated in individual samples. However, the total data set should provide some indication of the relative enrichments of these elements in the group of deposits as a whole.

Secondly, chemical heterogeneities within unaltered host rocks can give rise to some misleading trends. For example, spinifex-textured komatiite is generally enriched in TiO_2 relative to the lower, cumulate zone of a komatiite flow. Therefore, the apparent TiO_2 depletion in altered ultramafic samples from Yunndaga (for example) may be less significant than it appears if the altered samples are from a cumulate zone of a komatiite flow, since the reference material comprises spinifex-textured komatiite flows.

Metal contents

A comparison of metal contents in altered rocks with equivalent unaltered or 'least altered' lithologies indicates that enrichment factors for gold are much greater than for all other components. Gold enrichment factors greater than 100 are common, and in several deposits an enrichment factor greater than 1000 has been recorded. Base metals (Cu, Pb, Zn) also display significant, though less extreme, enrichment in several of the deposits investigated. Enrichment factors of 2–10 are common, with some deposits recording enrichments of 10–100, particularly for Pb. This separation of gold from base metals is a characteristic feature of Archaean, epigenetic, lode-gold deposits (Fyfe and Kerrich, 1984; Kerrich, 1986b; Perring et al., 1990) and is the basis for the term 'gold only' deposits (Hodgson and McGeehan, 1982).

As, Sb, and W display enrichments up to about 10, less commonly in the range 10–100, in several deposits. Significant enrichments (>2) of Ag and Bi are rare, although other studies of Archaean 'gold only' deposits have noted enrichments of a similar magnitude to those of the base metals (e.g. Kerrich, 1986b).

Granitophile elements (Mo, Nb, Sn) rarely display any significant degree of enrichment in the alteration haloes.

Non-metallic components

The data, including those from Kambalda and the Golden Mile (referenced above) are broadly consistent with other geochemical studies of alteration patterns in Archaean 'gold only' deposits (Kerrich, 1986a; Colvine et al., 1988; Barley and Groves, 1989; Perring et al.,

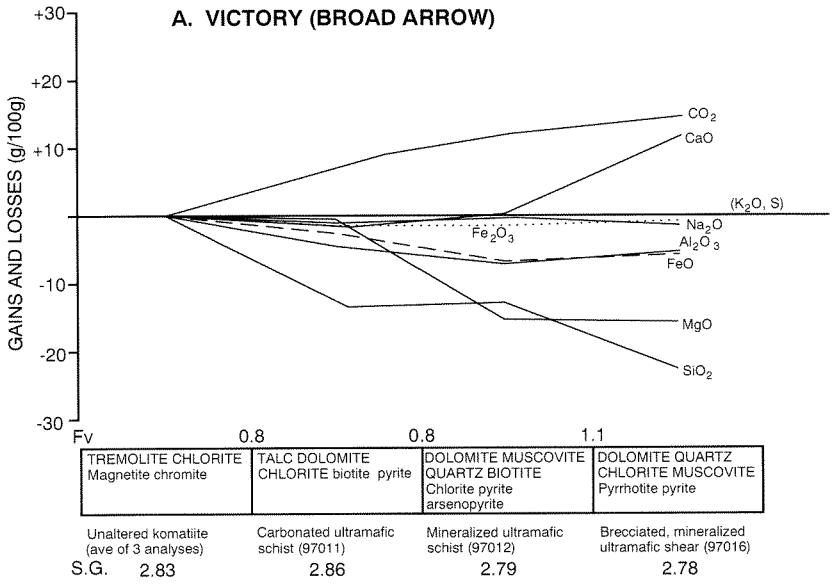
A. VICTORY (BROAD ARROW)
GAINS AND LOSSES (g/100g)
+30
+20
+10
-10
-20
-30
CO2
CaO
(K2O, S)
Na2O
Fe2O3
Al2O3
FeO
MgO
SiO2
Fv
0.8
0.8
1.1
TREMOLITE CHLORITE
Magnetite chromite
TALC DOLOMITE
CHLORITE biotite pyrite
DOLOMITE MUSCOVITE
QUARTZ BIOTITE
Chlorite pyrite
arsenopyrite
DOLOMITE QUARTZ
CHLORITE MUSCOVITE
Pyrrhotite pyrite
Unaltered komatiite
(ave of 3 analyses)
Carbonated ultramafic
schist (97011)
Mineralized ultramafic
schist (97012)
Brecciated, mineralized
ultramafic shear (97016)
S.G. 2.83
2.86
2.79
2.78

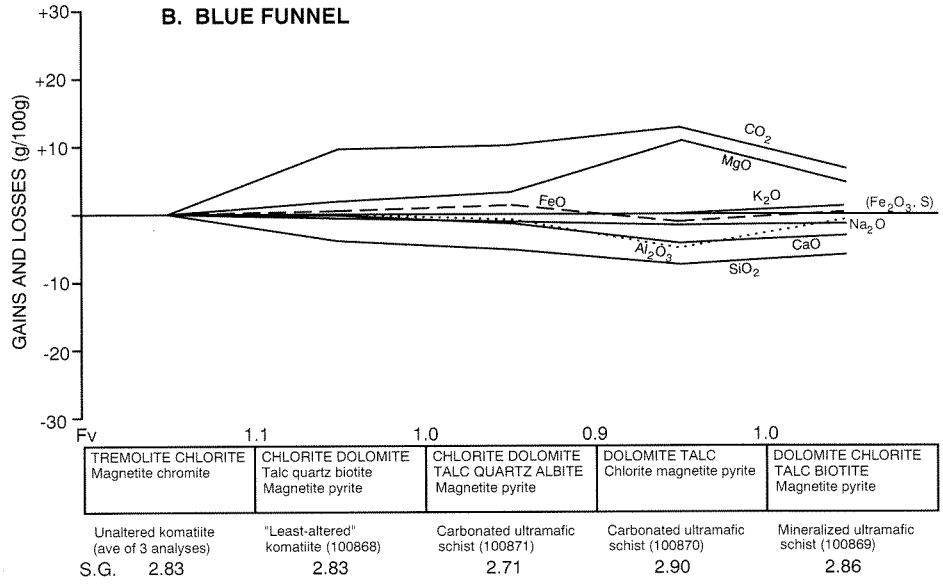
B. BLUE FUNNEL
GAINS AND LOSSES (g/100g)
+30
+20
+10
-10
-20
-30
CO2
MgO
FeO
K2O
(Fe2O3, S)
Na2O
Al2O3
CaO
SiO2
Fv
1.1
1.0
0.9
1.0
TREMOLITE CHLORITE
Magnetite chromite
CHLORITE DOLOMITE
Talc quartz biotite
Magnetite pyrite
CHLORITE DOLOMITE
TALC QUARTZ ALBITE
Magnetite pyrite
DOLOMITE TALC
Chlorite magnetite pyrite
DOLOMITE CHLORITE
TALC BIOTITE
Magnetite pyrite
Unaltered komatiite
(ave of 3 analyses)
"Least-altered"
komatiite (100868)
Carbonated ultramafic
schist (100871)
Carbonated ultramafic
schist (100870)
Mineralized ultramafic
schist (100869)
S.G. 2.83
2.83
2.71
2.90
2.86

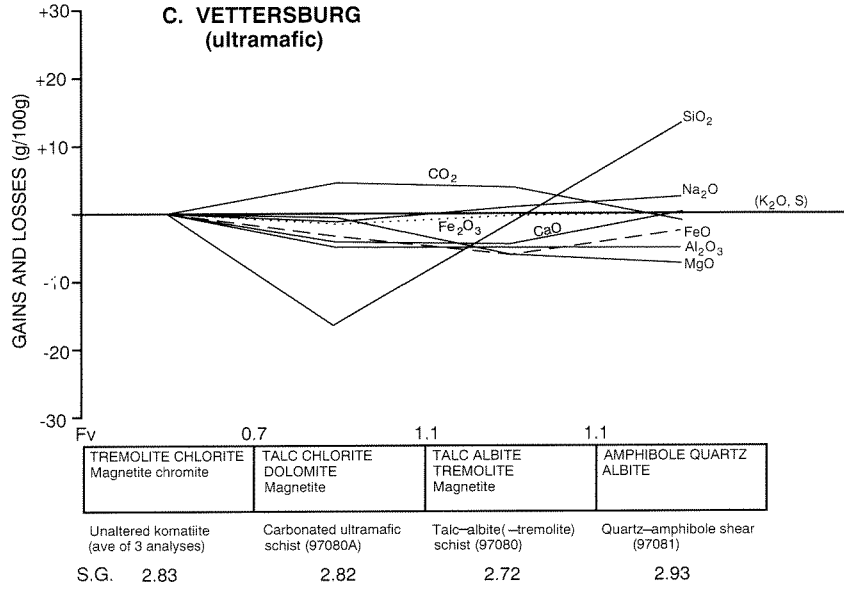
C. VETTERSBURG
(ultramafic)
GAINS AND LOSSES (g/100g)
+30
+20
+10
-10
-20
-30
SiO2
CO2
Na2O
(K2O, S)
Fe2O3
CaO
FeO
Al2O3
MgO
Fv
0.7
1.1
1.1
TREMOLITE CHLORITE
Magnetite chromite
TALC CHLORITE
DOLOMITE
Magnetite
TALC ALBITE
TREMOLITE
Magnetite
AMPHIBOLE QUARTZ
ALBITE
Unaltered komatiite
(ave of 3 analyses)
Carbonated ultramafic
schist (97080A)
Talc–albite(–tremolite)
schist (97080)
Quartz–amphibole shear
(97081)
S.G. 2.83
2.82
2.72
2.93

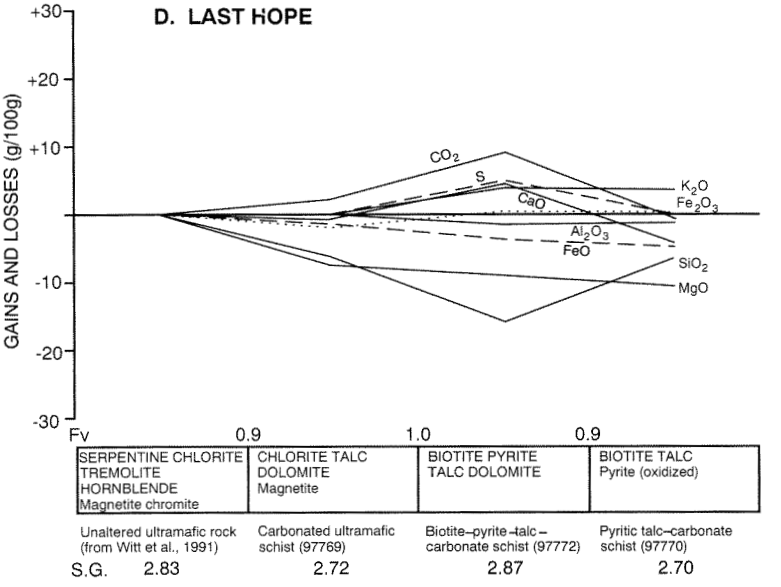
D. LAST HOPE
GAINS AND LOSSES (g/100g)
+30
+20
+10
-10
-20
-30
CO2
S
CaO
K2O
Fe2O3
Al2O3
FeO
SiO2
MgO
Fv
0.9
1.0
0.9
SERPENTINE CHLORITE TREMOLITE HORNBLENDE Magnetite chromite
CHLORITE TALC DOLOMITE Magnetite
BIOTITE PYRITE TALC DOLOMITE
BIOTITE TALC Pyrite (oxidized)
Unaltered ultramafic rock (from Witt et al., 1991)
Carbonated ultramafic schist (97769)
Biotite–pyrite–talc–carbonate schist (97772)
Pyritic talc–carbonate schist (97770)
S.G. 2.83
2.72
2.87
2.70

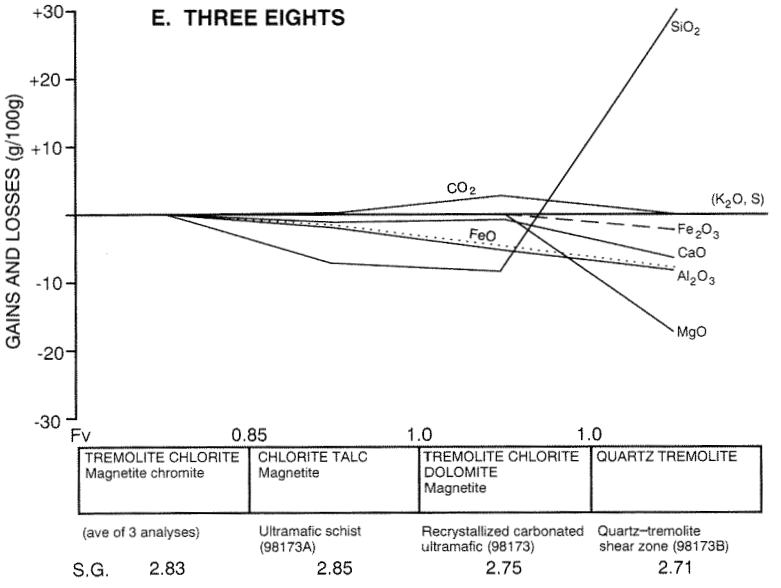
E. THREE EIGHTS
GAINS AND LOSSES (g/100g)
+30
+20
+10
-10
-20
-30
SiO2
CO2
(K2O, S)
Fe2O3
FeO
CaO
Al2O3
MgO
Fv
0.85
1.0
1.0
TREMOLITE CHLORITE Magnetite chromite
CHLORITE TALC Magnetite
TREMOLITE CHLORITE DOLOMITE Magnetite
QUARTZ TREMOLITE
(ave of 3 analyses)
Ultramafic schist (98173A)
Recrystallized carbonated ultramafic (98173)
Quartz–tremolite shear zone (98173B)
S.G. 2.83
2.85
2.75
2.71

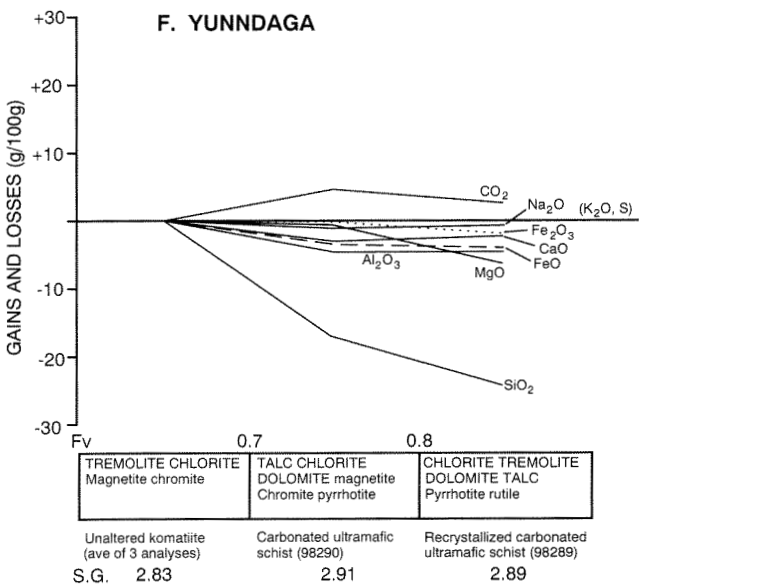
F. YUNNDAGA
GAINS AND LOSSES (g/100g)
+30
+20
+10
-10
-20
-30
CO2
Na2O
(K2O, S)
Fe2O3
CaO
FeO
Al2O3
MgO
SiO2
Fv
0.7
0.8
TREMOLITE CHLORITE Magnetite chromite
TALC CHLORITE DOLOMITE magnetite Chromite pyrrhotite
CHLORITE TREMOLITE DOLOMITE TALC Pyrrhotite rutile
Unaltered komatiite (ave of 3 analyses)
Carbonated ultramafic schist (98290)
Recrystallized carbonated ultramafic schist (98289)
S.G. 2.83
2.91
2.89

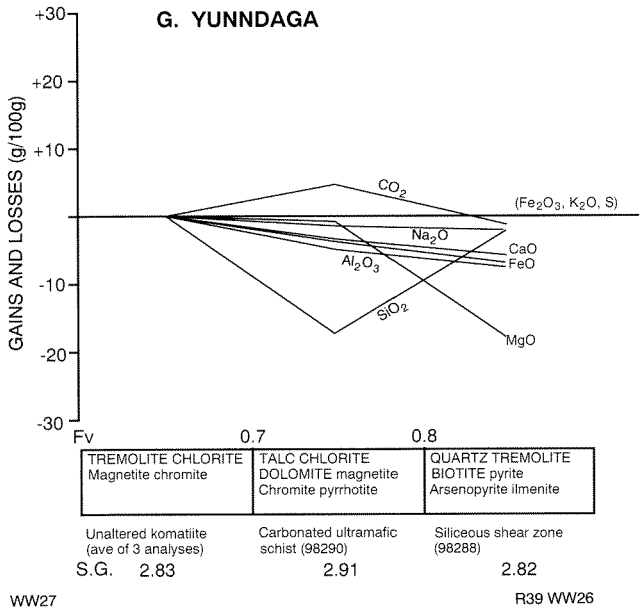

Figure 26. Gain and loss diagrams for altered ultramafic rocks associated with gold mineralization:

A. — Victory (Broad Arrow); B. — Blue Funnel; C. — Vettersburg; D. — Last Hope; E. — Three Eights; F. — Yunndaga; G. — Yunndaga

Notes: (i) Deposits are arranged in approximate order, from low- to high-grade metamorphic setting. (ii) Mineral components of alteration assemblages are listed in approximate order of abundance (left to right, top to bottom); main mineral components are shown in upper case; minor mineral components in lower case. (iii) GSWA sample numbers are shown in brackets below mineral assemblages. (iv) Chemical components in brackets on 0g/100g line are essentially immobile. (v) Fv is volume factor (Gresens, 1967); S.G. is specific gravity

1990). Enrichment factors between 2 and 100 of K_2O, CO_2, and S are recorded at most deposits while most other components are relatively immobile. Potassium enrichment is generally accompanied by a similar degree of enrichment of Ba and Rb, and depletion of Na_2O and Sr. K_2O, as well as CO_2, has been lost where alteration assemblages have been metamorphically recrystallized (e.g. Lady Sherry, Lady Grace Darling).

Most gain-and-loss diagrams indicate increasing mobility of elements towards the innermost zone of alteration (cf. Clark et al., 1989). In many deposits, only CO_2 and H_2O are added in the outer alteration zones, while some or all of SiO_2, Al_2O_3, FeO + Fe_2O_3, MgO, and CaO (in addition to K_2O, CO_2, and S) may display some degree of enrichment or depletion in the inner alteration zones. Examples include the Southern Shoot at Mt Pleasant, Victory at Broad Arrow, and Bellevue near Grants Patch (Figs 26–28). Enrichment and depletion of CaO in mafic rocks is sympathetic to trends in CO_2, suggesting that mobility of CaO is controlled by the composition of the stable carbonate phase (calcite or ferroan dolomite). In relatively restricted zones, such as the siliceous shear at the Golden Kilometre deposit (Mt Pleasant), virtually all elements are mobile, including Al_2O_3, P_2O_5, TiO_2, Zr, and Y (Fig. 30). The trend to increasing mobility of elements is reversed, or otherwise complicated, where metamorphic recrystallization has occurred, as the composition of the altered rock tends to approach that of tremolite or hornblende (e.g. New Mexico, Fig. 27).

The behaviour of F and Li in alteration haloes associated with Archaean lode-gold deposits is not well documented. In the deposits studied in the Menzies–Kambalda region, the behaviour of F and Li is variable, but the two elements normally behave sympathetically, and are commonly enriched by a factor of between 2 and 10. There does not appear to be any greater degree of enrichment of F in deposits from the Mt Pleasant – Lady Bountiful area, where elevated F contents have been documented in the Liberty Granodiorite and the Black Flag Au and base metal deposit (Witt and Swager, 1989b; Bennett, 1989).

One important difference between the results of this study and those of some earlier studies concerns the changes in Fe^{3+}/Fe^{2+} ratio which accompanies alteration. Phillips and Groves (1983), Kerrich (1986b), and Colvine et al. (1988) found that alteration haloes associated with Archaean lode-gold deposits commonly record a decrease in Fe^{3+}/Fe^{2+}, reflecting the reducing nature of the hydrothermal fluid. Fe^{3+} in silicate minerals is reduced to Fe^{2+} in sulfide and carbonate minerals during the alteration process. However, Kerrich (1986b) and Mikucki and Groves (1990) noted several exceptions, where oxidation of wallrocks occurred, especially where

associated with sodic alteration of granitic rocks and porphyry. Data presented in this report display varying trends of oxidation and reduction of wallrocks, but oxidation is more common.

Oxidation (as measured by an increase in Fe^{3+}/Fe^{2+} in alteration assemblages compared to unaltered wallrocks) occurs in ultramafic, mafic, and granitic rocks (e.g. Last Hope, Fig. 29; First Hit, Fig. 30; Lady Bountiful, Fig. 31). Trends do not appear to correlate with metamorphic grade of the host rocks, but enrichment and depletion of Fe_2O_3 are commonly antithetic to trends in FeO, and sympathetic to trends in S (Figs 26–28), suggesting that oxidation of wallrocks is related to formation of sulfides. Where both reduction and oxidation have been recognized within the one deposit, oxidation consistently occurs in the innermost zone(s) of alteration. In some samples, particularly those from higher grade metamorphic settings, (Fe, Mg) silicate minerals (biotite, hornblende, tremolite, diopside, garnet) form part of the oxidized alteration assemblage. However, in other cases, the oxidized alteration assemblages comprise predominantly quartz, sericite, carbonate, and sulfide minerals. Oxidized samples include those collected from drillcore and underground workings, and cannot be attributed to surface weathering. More work is required to determine the origin of the oxidizing fluids, and their relationship to reducing fluids. In particular, it is difficult to reconcile an increase in Fe^{3+}/Fe^{2+} ratios with those samples in which (Fe, Mg) silicate mineral-bearing assemblages have been replaced by sulfides and non-(Fe, Mg) silicate mineral-bearing assemblages.

Perring et al. (1990) noted a trend toward lower K_2O, and higher As and Sb, in alteration associated with mafic-hosted deposits in relatively higher grade metamorphic settings, based on data from ten deposits. Few clear trends for any major or trace elements with metamorphic grade could be discerned for the data presented here. There is a possible trend toward lower maxima of CO_2 enrichment, and degree of carbonation (molar CO_2/CaO, Davies et al., 1990) at higher metamorphic grades (Fig. 33). However, Grants Patch and Lady Grace Darling do not fit this trend, as they exhibit less intense carbonation than predicted for their metamorphic setting. Contrary to the findings of Perring et al. (1990), the data suggest higher degrees of enrichment of As in mafic-hosted deposits in relatively lower grade metamorphic settings. A more substantial data base is required before trends of this nature can be convincingly demonstrated.

Although trends in alteration geochemistry varying with metamorphic grade are difficult to demonstrate, there are some more convincing differences attributable to the composition of the original host rock. Some of these differences have already been described by Clark et al. (1989), for the Kambalda deposits.

The main components added during hydrothermal alteration of mafic rocks are H_2O, CO_2, S, K_2O, Rb, and Ba. Although there are exceptions (e.g. Last Hope), altered ultramafic rocks commonly display relatively minor enrichment of K_2O and S. The low sulfide content in mineralized ultramafic rocks has been attributed to the stability of carbonate minerals over pyrite where auriferous fluids equilibrate with rocks with high Mg/(Mg + Fe) ratios (Bohlke, 1988, 1989). On the other hand, carbonation in many altered ultramafic rocks is more extensive than in altered mafic rocks, reflecting the greater abundance of divalent metals in the former (Kerrich, 1986b). Furthermore, MgO has been lost from, and CaO added to, altered ultramafic rocks in many deposits. These trends have been ascribed by Kishida and Kerrich (1987) to adjustment of the whole-rock chemistry to the composition of dolomite. The mobility of other elements is less consistent. SiO_2 and Al_2O_3 are mobile in some examples, but are not consistently enriched or depleted. Na_2O is concentrated in the inner zones of some mineralized ultramafic-hosted shear zones, especially where there is an association with albite-rich porphyry (e.g. Vettersburg, Fig. 26).

Porphyry intrusions have been intensely albitized, especially where associated with ultramafic rocks. This is evident from the very high Na_2O contents and the abundance of secondary albite observed in thin sections. Albitization is accompanied by increases in Na_2O, Al_2O_3, and SiO_2 (e.g. Three Eights, Fig. 28), although these trends are partly obscured in gain-and-loss figures because unalbitized reference material is rarely available at the mineralized sites. The stability of albite over K-mica during hydrothermal alteration is controlled by the Al/(Fe + Mg + Cr) ratio of the host rock. A fluid which has equilibrated with albite and muscovite in regionally extensive mafic rocks will deposit K-mica in rocks with Al/(Fe + Mg + Cr) < average basalt, and albite in rocks with Al/(Fe + Mg + Cr) > average basalt (Bohlke, 1989; Witt, 1992).

Other rocks with a granitic composition (Lady Bountiful, Bellevue, Yunndaga, Goodenough) are enriched in CO_2 and S during hydrothermal alteration, but display much more limited enrichment of K_2O, Rb, and Ba, or even K_2O depletion. There is little mobility of other elements.

K/Rb and K/Ba ratios

Kerrich (1988, 1989a,b) documented K/Rb and K/Ba ratios in altered wallrocks from several Archaean lode-gold deposits in Canada, and interpreted these in terms of their significance for the source of the hydrothermal fluids. K, Rb, and Ba are coenriched, and linearly correlated over three orders of magnitude. K/Rb ratios from Canadian deposits vary from 200 to 400, increasing at higher Rb values. K/Ba ratios increase from about 10 to about 50. K/Rb and K/Ba data from deposits in the Menzies–Kambalda region are summarized in Figures 34 and 35. The scatter in data at the low end of each figure can be attributed to low analytical precision at these abundances. Trends and ratios are broadly comparable with the data presented by Kerrich (1988, 1989a, b), with some exceptions. As with the data of Kerrich, there is more scatter in the K/Ba diagram than in the K/Rb diagram. Nevertheless, K/Ba ratios for mafic rocks extend to higher values (about 350) than those published by Kerrich. Kerrich has also reported K/Ba ratios of this order for samples from the Macassa mine, in Quebec (unpublished short-course notes). Two biotitized samples

A. GOLDEN KILOMETRE

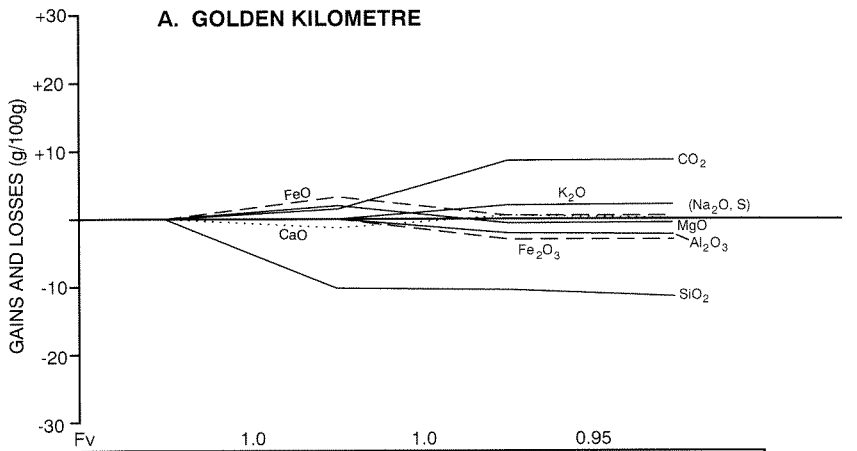

Fv	1.0	1.0	0.95
ACTINOLITE ALBITE QUARTZ Ilmenite magnetite	CHLORITE ALBITE ANKERITE QUARTZ Ilmenite pyrrhotite	CHLORITE ANKERITE SERICITE QUARTZ Ilmenite pyrrhotite	SERICITE ANKERITE QUARTZ chlorite Ilmenite pyrrhotite
Unaltered quartz gabbro (89936)	Chlorite–carbonate alteration (89937)	Transition to carbonate–sericite alteration (89938)	Carbonate–sericite alteration (89939)
S.G. 3.08	3.01	2.88	3.01

A. GOLDEN KILOMETRE (cont.)

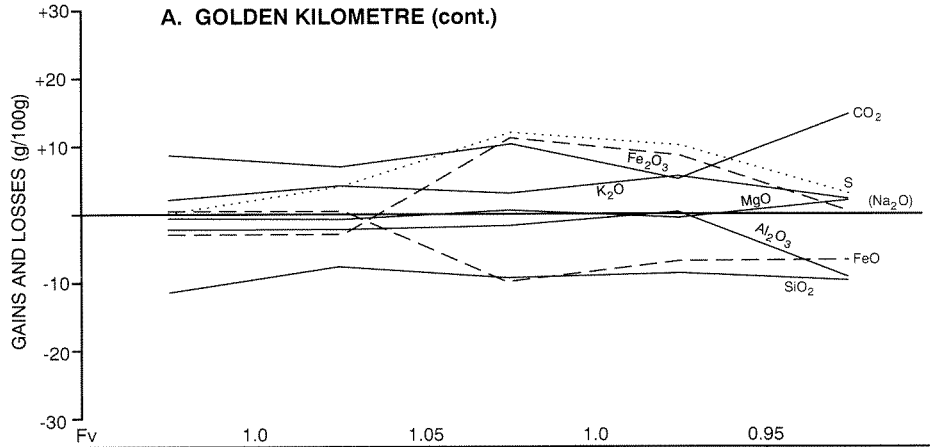

Fv	1.0	1.05	1.0	0.95
SERICITE ANKERITE QUARTZ chlorite Ilmenite pyrrhotite	SERICITE ANKERITE QUARTZ Ilmenite pyrrhotite	SERICITE ANKERITE QUARTZ pyrite Ilmenite pyrrhotite	SERICITE ANKERITE QUARTZ PYRITE	QUARTZ ANKERITE SERICITE pyrite
Carbonate–sericite alteration (89939)	Carbonate–sericite alteration (89942)	Transition to sericite–pyrite alteration (89941)	sericite–pyrite alteration (89943)	Siliceous shear zone (89940)
S.G. 3.01	3.03	3.0	3.16	2.93

B. SOUTHERN SHOOT (Mt Pleasant)

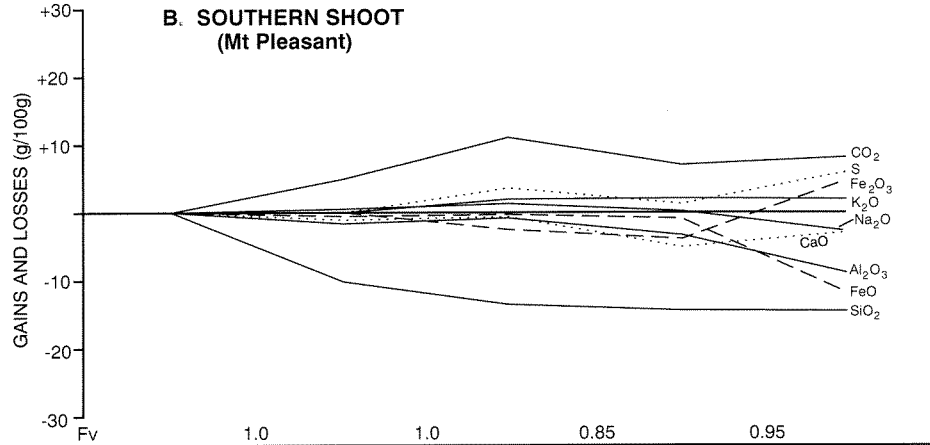

Fv	1.0	1.0	0.85	0.95
ACTINOLITE ALBITE QUARTZ Ilmenite magnetite	CHLORITE ALBITE CARBONATE QUARTZ Pyrrhotite ilmenite	ALBITE CARBONATE QUARTZ SERICITE Pyrrhotite ilmenite	CARBONATE SERICITE QUARTZ ALBITE Pyrrhotite ilmenite	QUARTZ CARBONATE SERICITE pyrite
Unaltered quartz gabbro (89936)	Chlorite–carbonate alteration (89920)	Quartz–carbonate albite alteration (89919)	sericite–carbonate alteration (89924)	Siliceous shear (89923)
S.G. 3.08	2.90	2.95	2.93	2.91

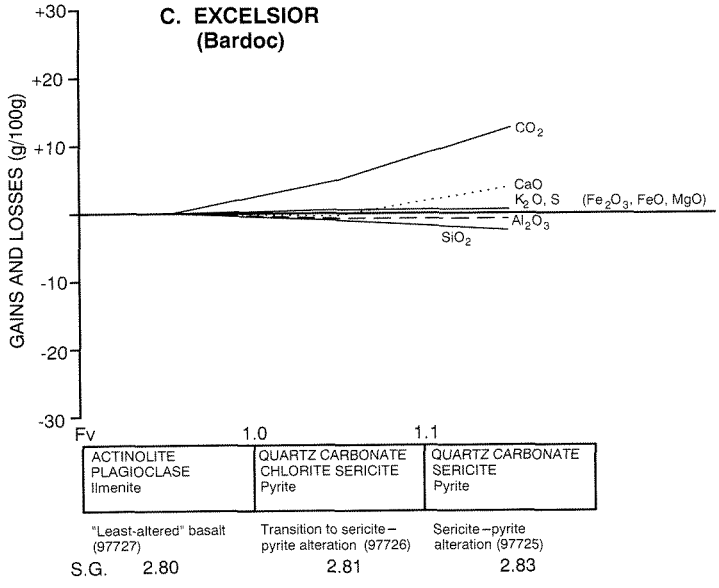
C. EXCELSIOR
(Bardoc)
GAINS AND LOSSES (g/100g)
+30
+20
+10
-10
-20
-30
CO_2
CaO
K_2O, S
(Fe_2O_3, FeO, MgO)
Al_2O_3
SiO_2
Fv
1.0
1.1
ACTINOLITE PLAGIOCLASE Ilmenite
QUARTZ CARBONATE CHLORITE SERICITE Pyrite
QUARTZ CARBONATE SERICITE Pyrite
"Least-altered" basalt (97727)
Transition to sericite–pyrite alteration (97726)
Sericite–pyrite alteration (97725)
S.G. 2.80
2.81
2.83

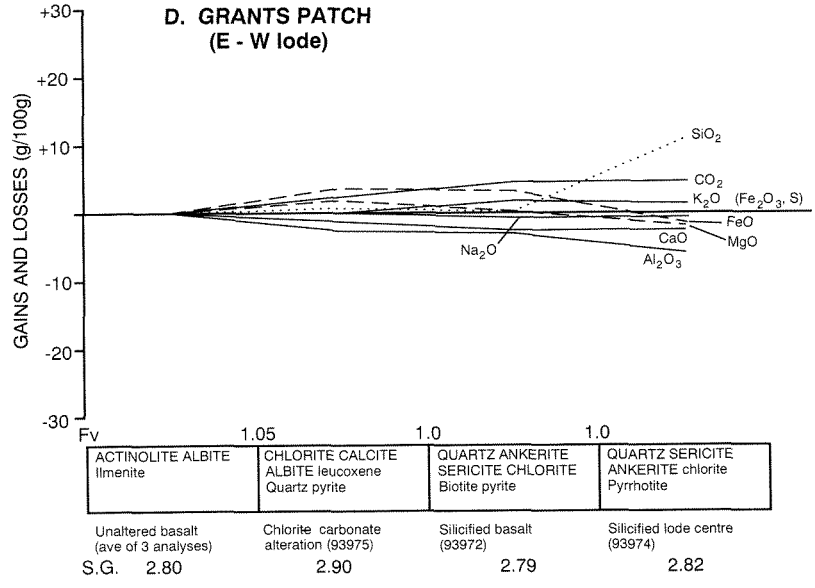
D. GRANTS PATCH
(E - W lode)
GAINS AND LOSSES (g/100g)
+30
+20
+10
-10
-20
-30
SiO_2
CO_2
K_2O
(Fe_2O_3, S)
FeO
MgO
CaO
Na_2O
Al_2O_3
Fv
1.05
1.0
1.0
ACTINOLITE ALBITE Ilmenite
CHLORITE CALCITE ALBITE leucoxene Quartz pyrite
QUARTZ ANKERITE SERICITE CHLORITE Biotite pyrite
QUARTZ SERICITE ANKERITE chlorite Pyrrhotite
Unaltered basalt (ave of 3 analyses)
Chlorite carbonate alteration (93975)
Silicified basalt (93972)
Silicified lode centre (93974)
S.G. 2.80
2.90
2.79
2.82

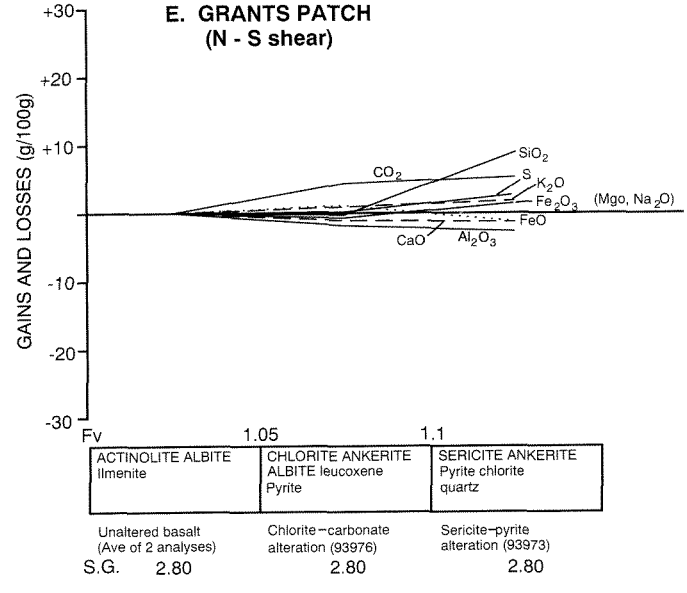
E. GRANTS PATCH
(N - S shear)
GAINS AND LOSSES (g/100g)
+30
+20
+10
-10
-20
-30
SiO_2
CO_2
S
K_2O
Fe_2O_3
(Mgo, Na_2O)
FeO
CaO
Al_2O_3
Fv
1.05
1.1
ACTINOLITE ALBITE Ilmenite
CHLORITE ANKERITE ALBITE leucoxene Pyrite
SERICITE ANKERITE Pyrite chlorite quartz
Unaltered basalt (Ave of 2 analyses)
Chlorite–carbonate alteration (93976)
Sericite–pyrite alteration (93973)
S.G. 2.80
2.80
2.80

F. LADY GRACE DARLING/ LANCASHIRE HERO

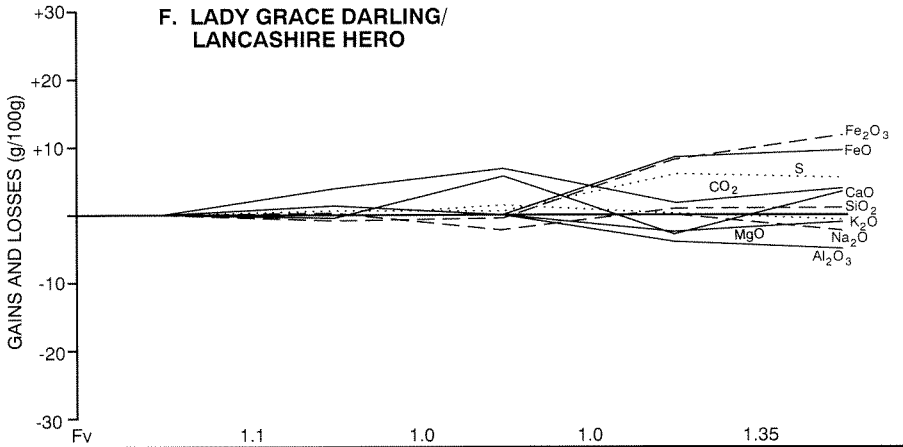

Fv	1.1	1.0	1.0	1.35
ACTINOLITE PLAGIOCLASE QUARTZ Ilmenite	CHLORITE EPIDOTE CARBONATE QUARTZ ACTINOLITE pyrrhotite	BIOTITE CHLORITE CARBONATE pyrite	ACTINOLITE BIOTITE CHLORITE EPIDOTE QUARTZ pyrrhotite Chalcopyrite ilmenite	CHLORITE BIOTITE CARBONATE EPIDOTE DIOPSIDE GARNET Actinolite pyrrhotite ilmenite
"Least-altered" sheared basalt (97710)	Chloritized basalt (97712)	Biotite–chlorite alteration (97086)	Recrystallized biotite–chlorite alteration (97714)	Calc- silicate alteration (97715)
S.G. 2.99	2.93	3.17	3.18	2.67

G. EUREKA

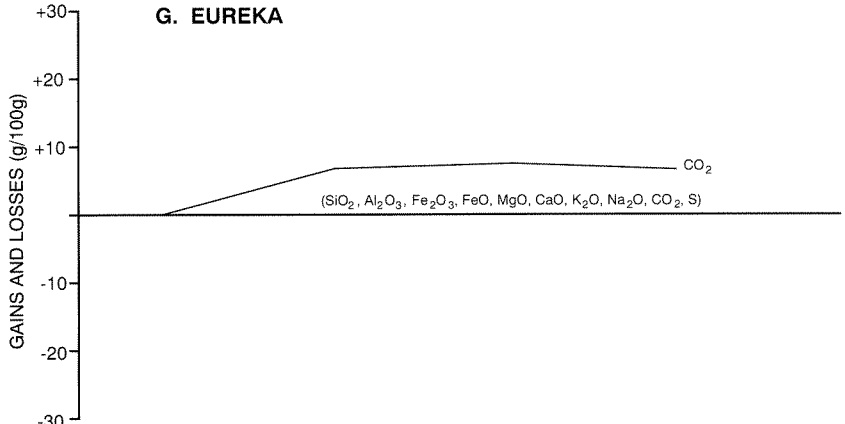

Fv	1.1	1.0	1.0
ACTINOLITE PLAGIOCLASE Ilmenite	CHLORITE CALCITE PLAGIOCLASE QUARTZ Ilmenite sphene pyrrhotite	CHLORITE CARBONATE PLAGIOCLASE Pyrrhotite	CHLORITE CARBONATE PLAGIOCLASE biotite Leucoxene pyrrhotite
Unaltered basalt (ave of 8 analyses)	Chlorite–carbonate alteration (93941)	Chlorite–carbonate alteration with sulfides (93943)	Chlorite–carbonate alteration with biotite (93956)
S.G. 2.80	2.81	2.81	2.79

H. NEW BODDINGTON (GOONGARRIE)

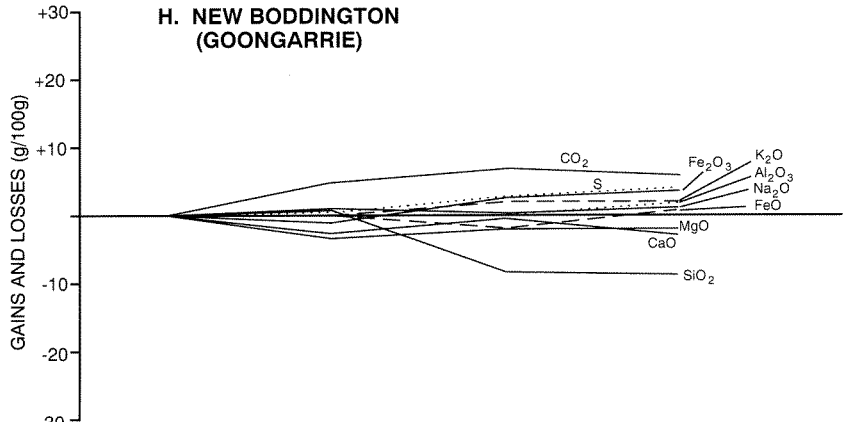

Fv	1.0	1.0	1.05
ACTINOLITE PLAGIOCLASE Ilmenite	CHLORITE CARBONATE PLAGIOCLASE BIOTITE Pyrrhotite	CARBONATE BIOTITE PLAGIOCLASE Pyrite	BIOTITE CARBONATE PLAGIOCLASE CHLORITE MUSCOVITE pyrite
Unaltered basalt (ave of 8 analyses)	Carbonate–chlorite schist (93928)	Carbonate–biotite schist (93922)	Brecciated carbonate–biotite shear (93921)
S.G. 2.80	2.82	2.93	2.87

I. NEW MEXICO

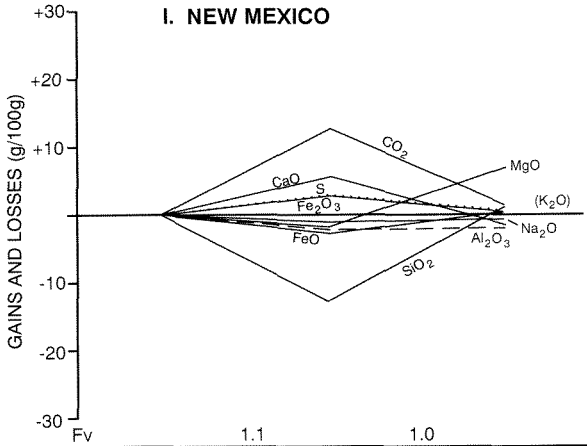

Fv	1.1	1.0
TREMOLITE CHLORITE PLAGIOCLASE Magnetite	QUARTZ CHLORITE CARBONATE BIOTITE Pyrite	CHLORITE TREMOLITE QUARTZ CARBONATE
Unaltered high-Mg basalt (ave of 4 analyses)	Carbonated high-Mg basalt (98140)	Recrystallized, carbonated high-Mg basalt (98141)
S.G. 2.90	2.77	2.90

J. NEW MEXICO

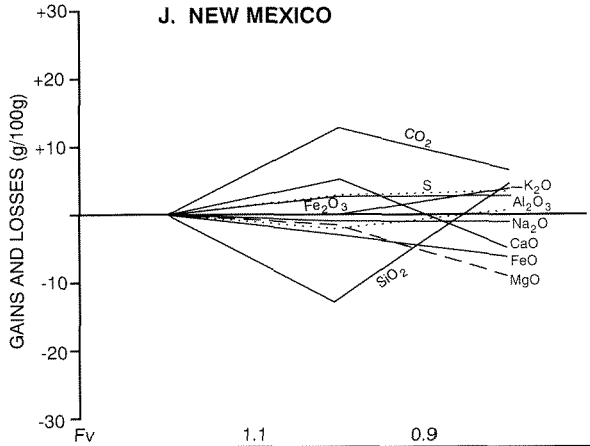

Fv	1.1	0.9
TREMOLITE CHLORITE PLAGIOCLASE Magnetite	QUARTZ CHLORITE CARBONATE BIOTITE Pyrite	MUSCOVITE QUARTZ CARBONATE BIOTITE Pyrite
Unaltered high-Mg basalt (ave of 4 analyses)	Carbonated high-Mg basalt (98140)	Potassic alteration (98143)
S.G. 2.90	2.77	2.85

K. FIRST HIT

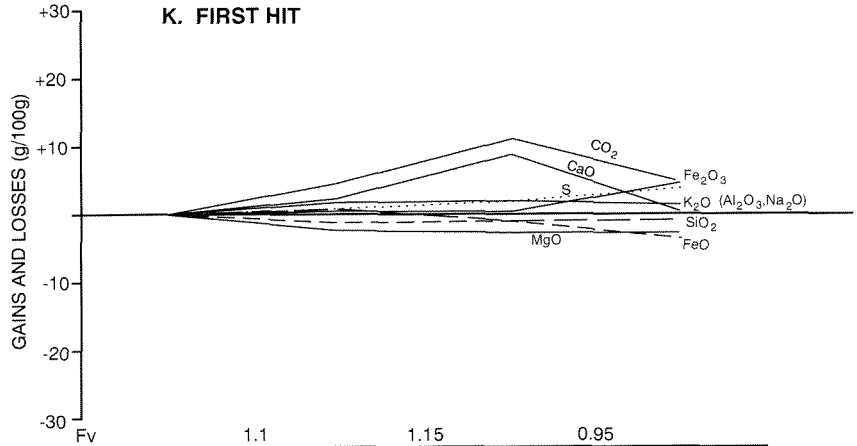

Fv	1.1	1.15	0.95
HORNBLENDE PLAGIOCLASE Ilmenite	PLAGIOCLASE BIOTITE HORNBLENDE CALCITE QUARTZ pyrrhotite Ilmenite	PLAGIOCLASE BIOTITE HORNBLENDE CALCITE QUARTZ pyrrhotite	PLAGIOCLASE BIOTITE QUARTZ PYRITE CALCITE
"Least-altered" amphibolite (98297)	Biotite amphibolite (98295)	Transitional to pyritic shear (98295A/B)	Pyritic shear (98294)
S.G. 3.01	2.89	2.86	2.75

L. SAND KING

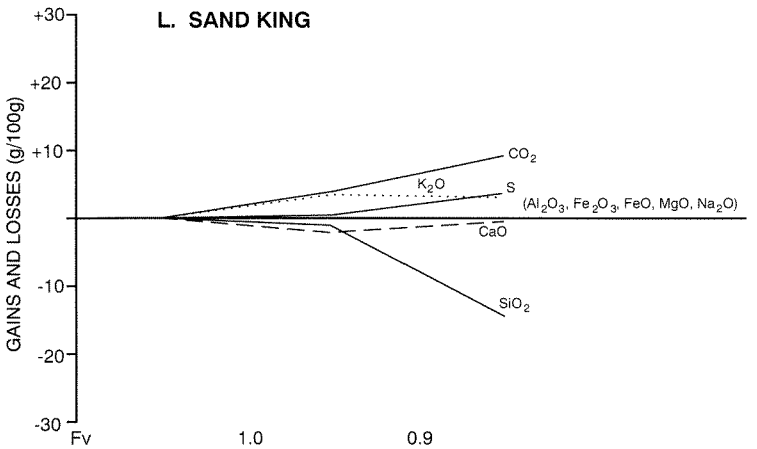

Fv	1.0	0.9
HORNBLENDE PLAGIOCLASE Ilmenite	HORNBLENDE CARBONATE BIOTITE PLAGIOCLASE CHLORITE ilmenite	BIOTITE CARBONATE PLAGIOCLASE Pyrite
Unaltered basalt (Ave of 6 analyses)	Biotite–chlorite alteration (97722)	Biotite–pyrite alteration (97723)
S.G. 2.80	2.90	2.94

M. LADY SHERRY

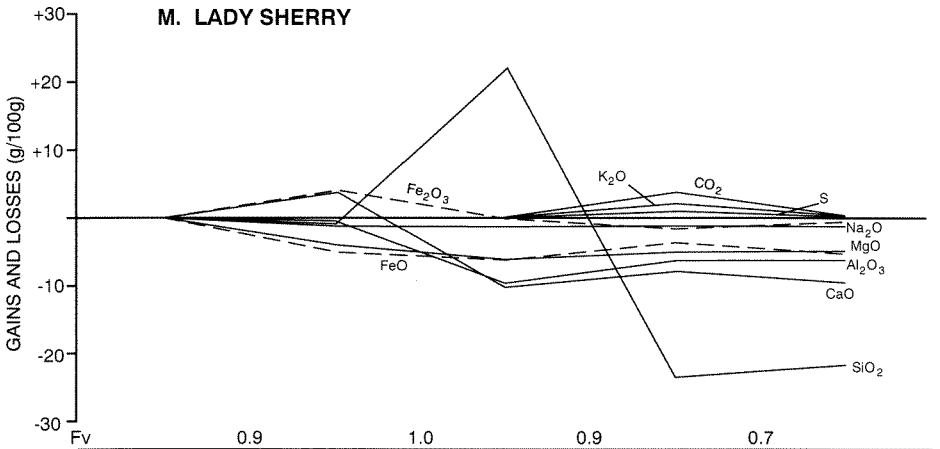

Fv	0.9	1.0	0.9	0.7
HORNBLENDE PLAGIOCLASE Ilmenite	EPIDOTE QUARTZ HORNBLENDE Pyrite	EPIDOTE CHLORITE HORNBLENDE QUARTZ Sphene	PLAGIOCLASE CALCITE BIOTITE pyrrhotite Arsenopyrite sphene	PLAGIOCLASE BIOTITE HORNBLENDE CALCITE Pyrrhotite pyrite Ilmenite magnetite
Unaltered amphibolite (98297)	Quartz–epidote alteration (98230)	Quartz–epidote alteration (98226)	Biotite amphibolite (98228)	Recrystallized biotite amphibolite (98229)
S.G. 3.01	3.15	2.91	2.20	2.93

N. ST ALBANS

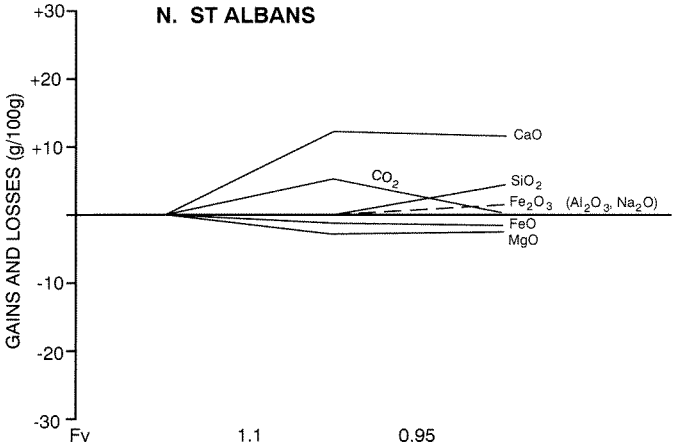

Fv	1.1	0.95
HORNBLENDE PLAGIOCLASE Ilmenite	HORNBLENDE DIOPSIDE BIOTITE ANKERITE Pyrrhotite	DIOPSIDE EPIDOTE CARBONATE GARNET HORNBLENDE PLAGIOCLASE pyrrhotite
Unaltered amphibolite (98297)	Diopsidic amphibolite (98220A)	Garnet–diopside rock (98222)
S.G. 3.01	3.05	3.21

WW32 R39 WW27

from Last Hope display exceptionally low K/Rb and exceptionally high K/Ba.

Kerrich (1989a,b) reported that, although absolute K, Rb, and Ba varied with rock type, there was no apparent host-rock control over K/Rb and K/Ba ratios. His results are essentially duplicated here. K/Rb ratios in ultramafic and mafic rocks are the best indicators of fluid source, since these rocks contain very little K and Rb. Ratios in granitic rocks are influenced by host-rock composition.

Contrary to the conclusions of Perring et al. (1990), there is little evidence for any correlation between metamorphic grade of the host rocks (or the presence of muscovite, biotite, or K-feldspar in alteration assemblages) and K/Rb or K/Ba ratios, from the data presented in Figures 34 and 35. Metamorphic recrystallization of alteration assemblages is accompanied by a decrease in K, Rb, and (in most cases) Ba. However, relative mobilities during recrystallization are variable, resulting in a variety of ratios.

Phillips (1986) interpreted consistent K/Rb ratios in successive alteration zones adjacent to gold lodes on the Golden Mile as indicating that each of three alteration assemblages resulted from the activity of a single hydrothermal fluid. Some deposits (e.g. Golden Kilometre) display consistent K/Rb ratios over several samples. However, other deposits record more variable K/Rb ratios in different alteration zones and assemblages. In fact, taken as a whole, the data suggest a progressive increase in K/Rb and K/Ba ratios from outer alteration zones to inner alteration zones, comparable with the trend towards higher K/Rb at higher Rb documented by Kerrich (1988, 1989a,b). Whilst not inconsistent with the basic conclusions of Phillips (1986), the data from the Menzies–Kambalda region suggest the fluid may have evolved over time or space towards higher K/Rb ratios.

K/Rb ratios for deposits in the Menzies–Kambalda region lie on the 'main trend' of Kerrich (1988, 1989a,b). This has been interpreted as indicating a fluid derived by dehydration of a complex crustal source, and to be inconsistent with a magmatic source. However, these interpretations have been challenged and the subject remains controversial (Burrows and Jemielita, 1989; Kerrich and Fryer, 1989; Perring and Barley, 1990).

Figure 27. Gain and loss diagrams for altered mafic rocks associated with gold mineralization:

A. — Golden Kilometre (Mt Pleasant); B. — Southern Shoot (Mt Pleasant); C. — Excelsior (Bardoc); D. — E–W lode, Grants Patch; E. — N–S shear, Grants Patch; F. — Lady Grace Darling/Lancashire Hero; G. — Eureka; H. — New Boddington (Goongarrie); I. — New Mexico; J. — New Mexico; K. — First Hit; L. — Sand King; M. — Lady Sherry; N. — St Albans

Notes: (i) Deposits are arranged in approximate order, from low- to high-grade metamorphic setting. (ii) Mineral components of alteration assemblages are listed in approximate order of abundance (left to right, top to bottom); main mineral components are shown in upper case; minor mineral components in lower case. (iii) GSWA sample numbers are shown in brackets below mineral assemblages. (iv) Chemical components in brackets on 0g/100g line are essentially immobile. (v) Fv is volume factor (Gresens, 1967); S.G. is specific gravity

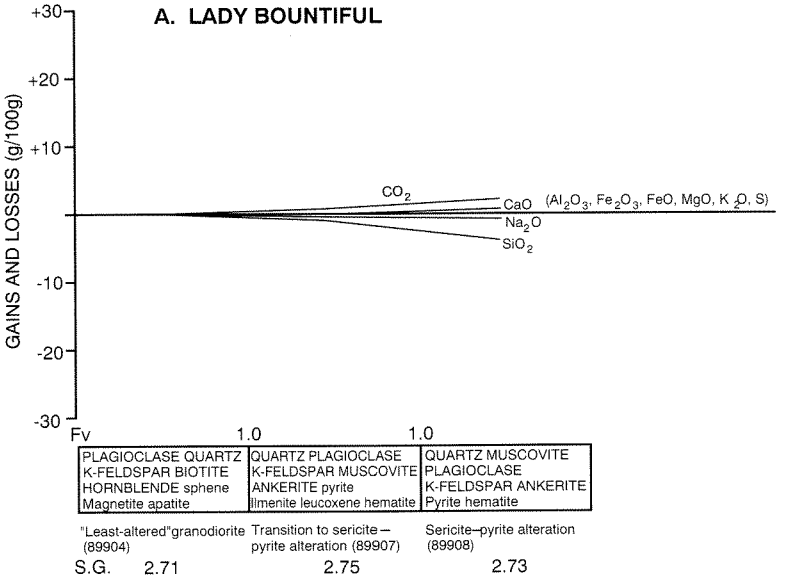

Fv	1.0	1.0
PLAGIOCLASE QUARTZ K-FELDSPAR BIOTITE HORNBLENDE sphene Magnetite apatite	QUARTZ PLAGIOCLASE K-FELDSPAR MUSCOVITE ANKERITE pyrite Ilmenite leucoxene hematite	QUARTZ MUSCOVITE PLAGIOCLASE K-FELDSPAR ANKERITE Pyrite hematite
"Least-altered"granodiorite (89904)	Transition to sericite–pyrite alteration (89907)	Sericite–pyrite alteration (89908)
S.G. 2.71	2.75	2.73

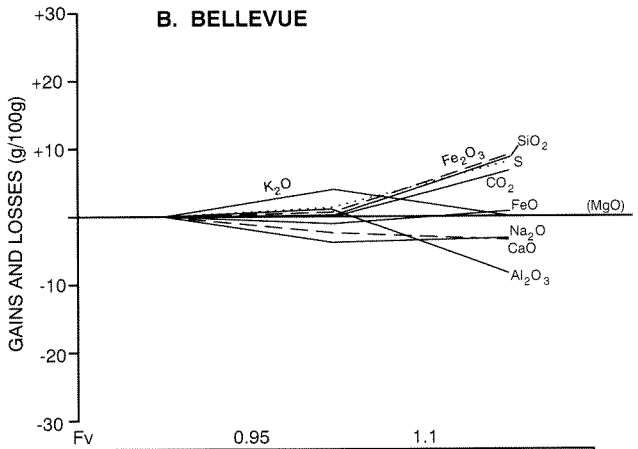

Fv	0.95	1.1
HORNBLENDE QUARTZ PLAGIOCLASE apatite Sphene magnetite	SERICITE QUARTZ Pyrite magnetite	QUARTZ SERICITE Pyrite
"Least-altered" porphyry (97002)	Sericitic alteration (97003)	Silicified brecciated porphyry (97008)
S.G. 2.78	2.86	2.91

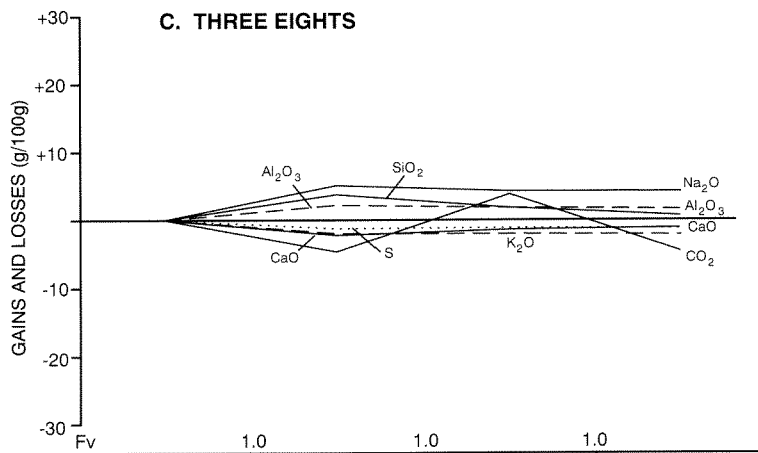

Fv	1.0	1.0	1.0
PLAGIOCLASE (ALBITE) BIOTITE (after HBD) CARBONATE CHLORITE Pyrite sphene	ALBITE AMPHIBOLE Apatite sphene Carbonate magnetite	ALBITE AMPHIBOLE CARBONATE Sphene	ALBITE AMPHIBOLE Apatite carbonate Sphene
"Least-altered" plagioclase hornblende porphyry (1008865)	Albitic porphyry (98176)	Carbonated albitic porphyry (98178)	De-carbonated albitic porphyry (98177)
S.G. 2.65	2.61	2.67	2.65

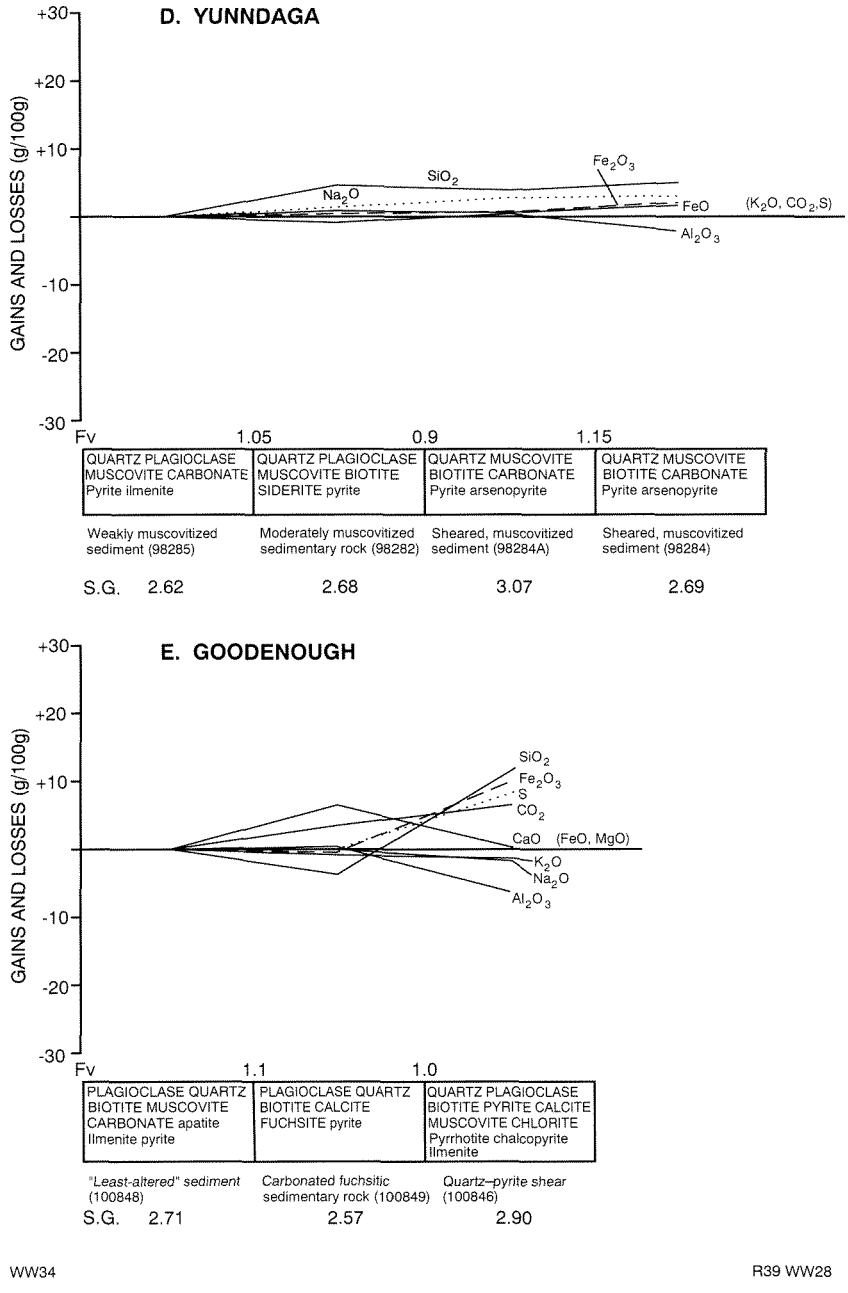

Figure 28. Gain and loss diagrams for altered granitic rocks associated with gold mineralization:

A. — Lady Bountiful; B. — Bellevue; C. — Three Eights (Note: sample 1008865 here is a hypothetical least-altered hornblende–plagioclase porphyry from Mt Percy); D. — Yunndaga; E. — Goodenough

Notes: (i) Deposits are arranged in approximate order, from low- to high-grade metamorphic setting. (ii) Mineral components of alteration assemblages are listed in approximate order of abundance (left to right, top to bottom); main mineral components are shown in upper case; minor mineral components in lower case. (iii) GSWA sample numbers are shown in brackets below mineral assemblages. (iv) Chemical components in brackets on 0g/100g line are essentially immobile. (v) Fv is volume factor (Gresens, 1967); S.G. is specific gravity

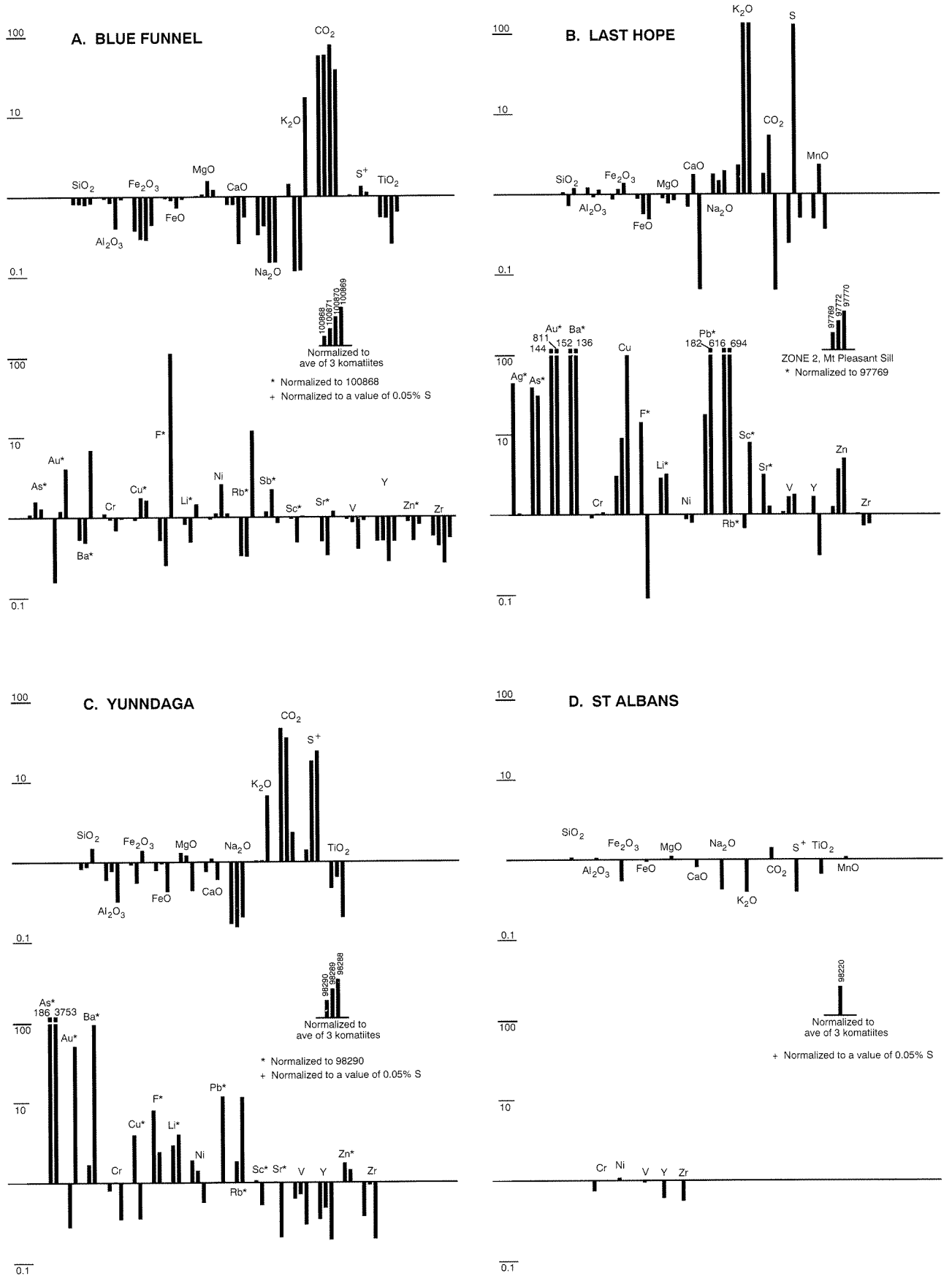

Figure 29. Enrichment/depletion diagrams for altered ultramafic rocks associated with gold mineralization at selected deposits: A. — Blue Funnel; B. — Last Hope; C. — Yunndaga; D. — St Albans
See Figure 26 for spatial relationships between sample numbers and alteration zoning

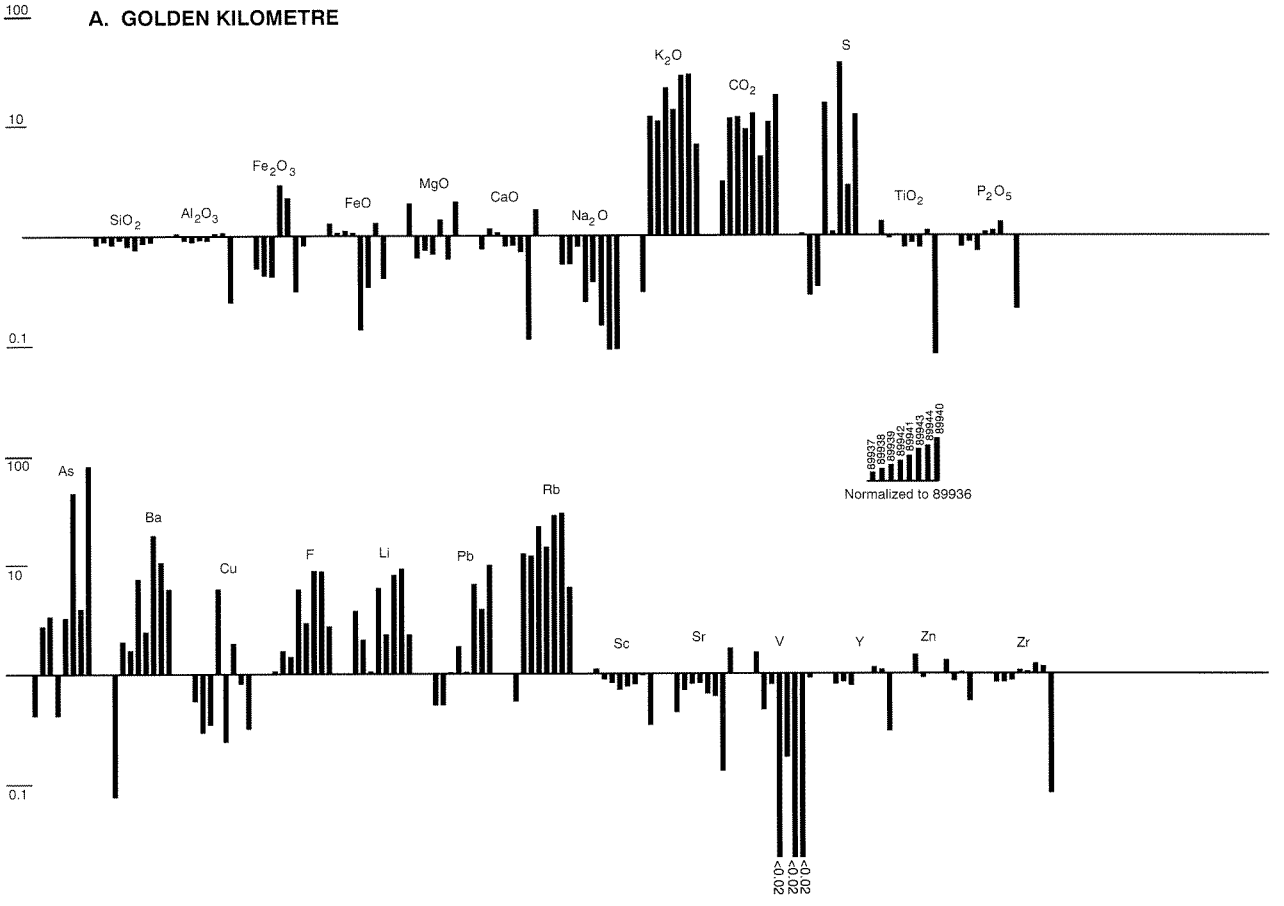
A. GOLDEN KILOMETRE
100
10
0.1
SiO2
Al2O3
Fe2O3
FeO
MgO
CaO
Na2O
K2O
CO2
S
TiO2
P2O5
100
10
0.1
As
Ba
Cu
F
Li
Pb
Rb
Sc
Sr
V
Y
Zn
Zr
<0.02
<0.02
<0.02
89937
89938
89939
89942
89941
89943
89944
89940
Normalized to 89936

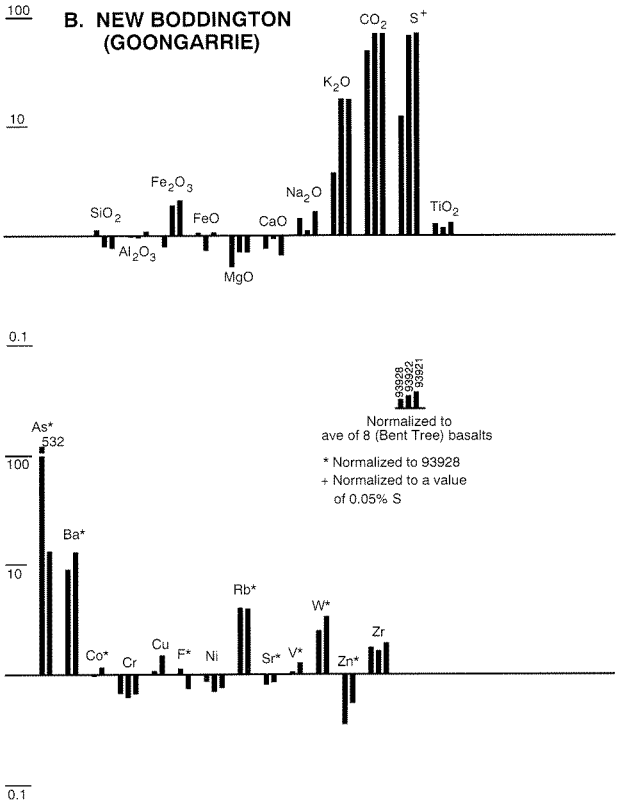
B. NEW BODDINGTON (GOONGARRIE)
100
10
0.1
SiO2
Al2O3
Fe2O3
FeO
MgO
CaO
Na2O
K2O
CO2
S+
TiO2
93928
93922
93921
Normalized to ave of 8 (Bent Tree) basalts
* Normalized to 93928
+ Normalized to a value of 0.05% S
As* 532
100
10
0.1
Ba*
Co*
Cr
Cu
F*
Ni
Rb*
Sr*
V*
W*
Zn*
Zr

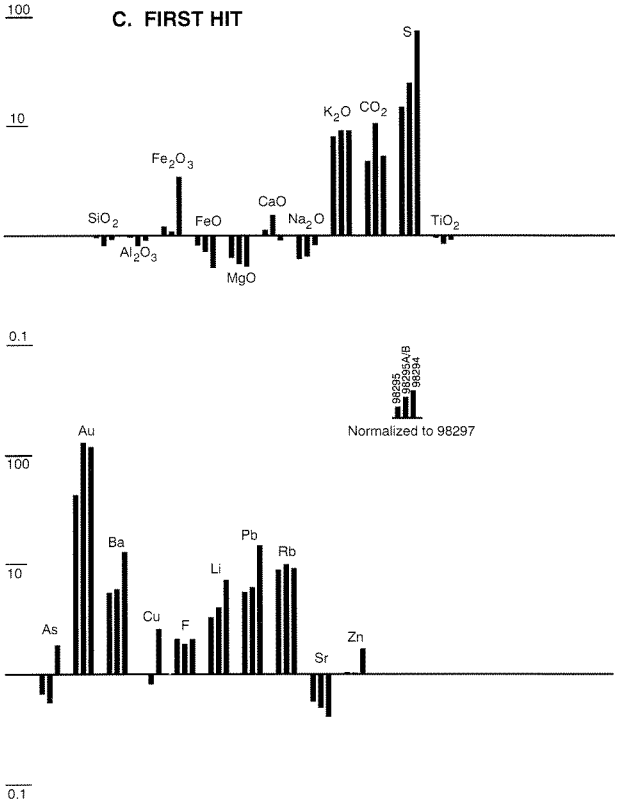
C. FIRST HIT
100
10
0.1
SiO2
Al2O3
Fe2O3
FeO
MgO
CaO
Na2O
K2O
CO2
S
TiO2
98295A/B
98294
Normalized to 98297
100
10
0.1
As
Au
Ba
Cu
F
Li
Pb
Rb
Sr
Zn

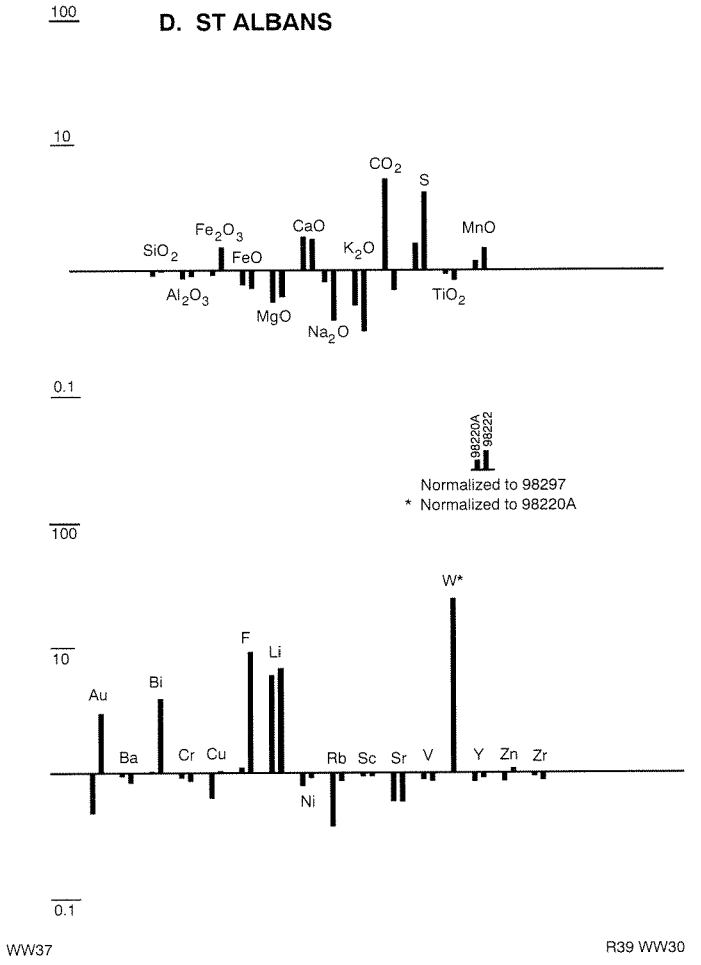

Figure 30. Enrichment/depletion diagrams for altered mafic rocks associated with gold mineralization at selected deposits:

A. — Golden Kilometre (Mt Pleasant);
B. — New Boddington (Goongarrie);
C. — First Hit;
D. — St Albans

See Figure 27 for spatial relationships between sample numbers and alteration zoning

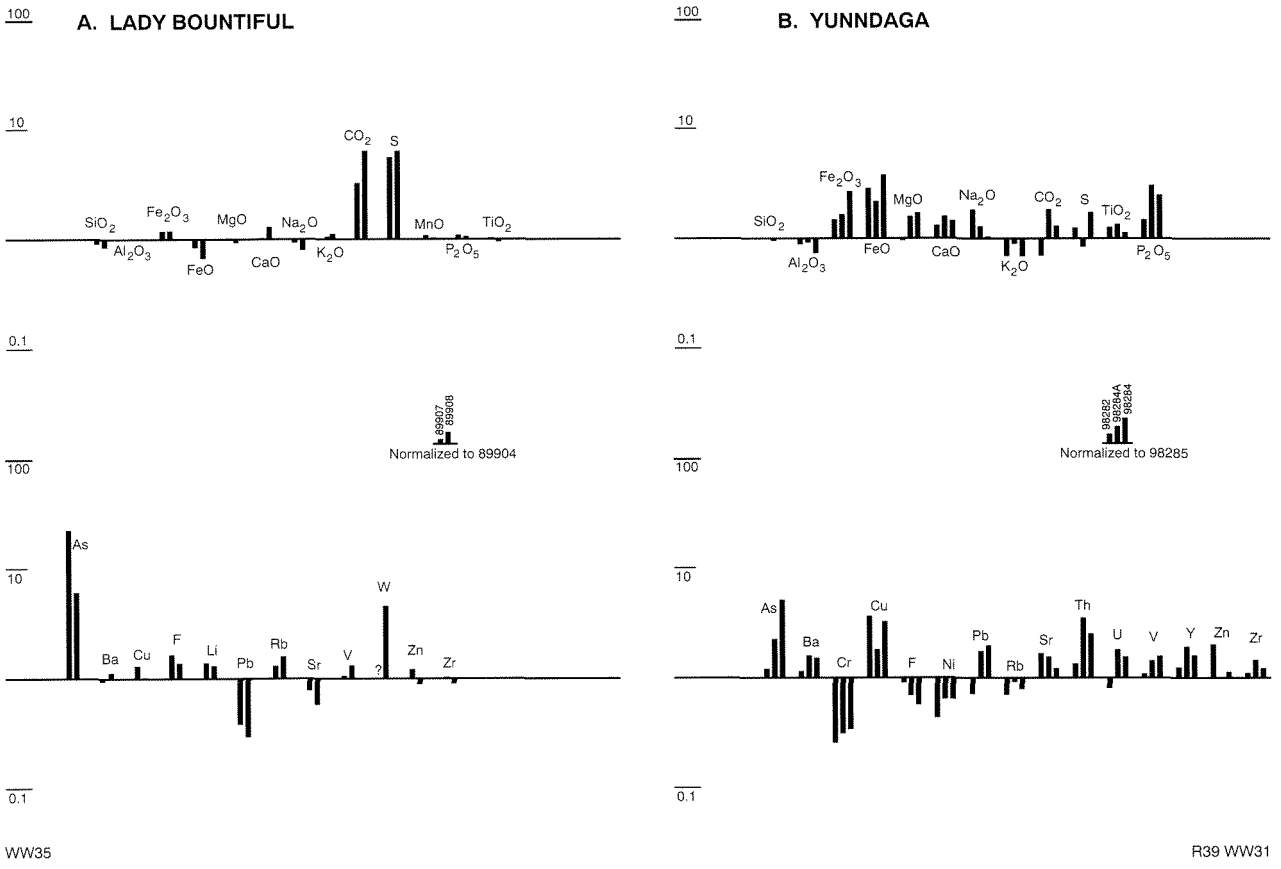

Figure 31. Enrichment/depletion diagrams for altered granitic rocks associated with gold mineralization at selected deposits:

A. — Lady Bountiful;
B. — Yunndaga

See Figure 28 for spatial relationships between sample numbers and alteration zoning

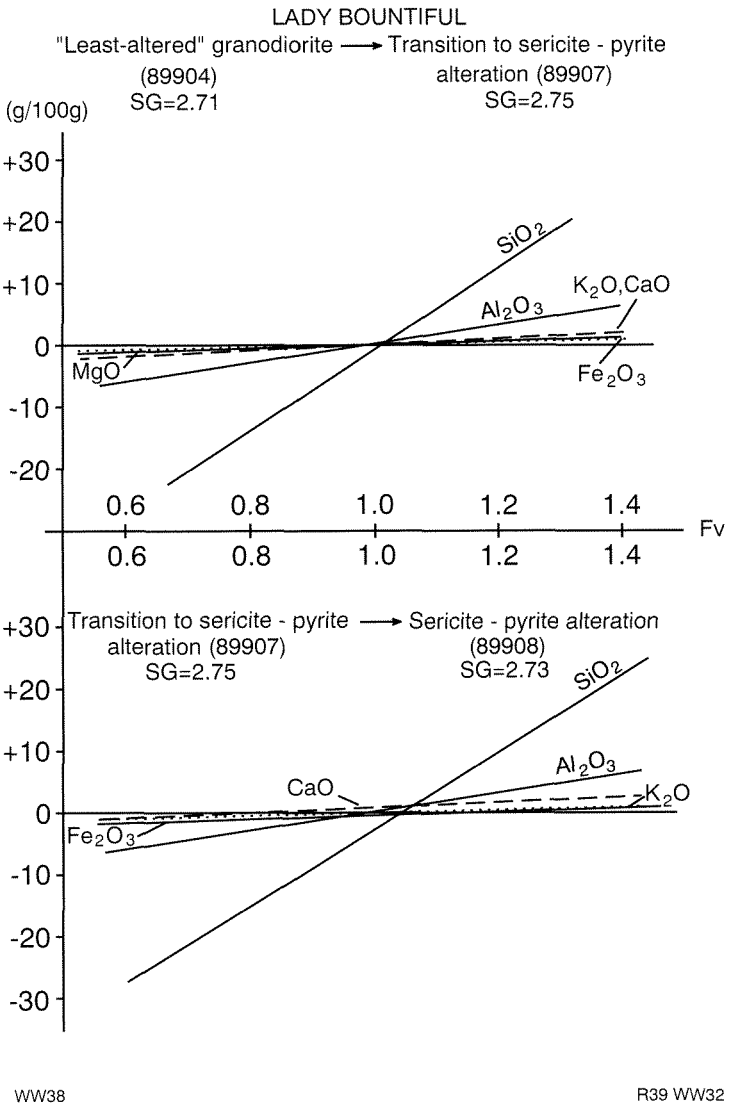

Figure 32. Composition–volume diagram (after Gresens, 1967) for alteration of granitic rocks at Lady Bountiful

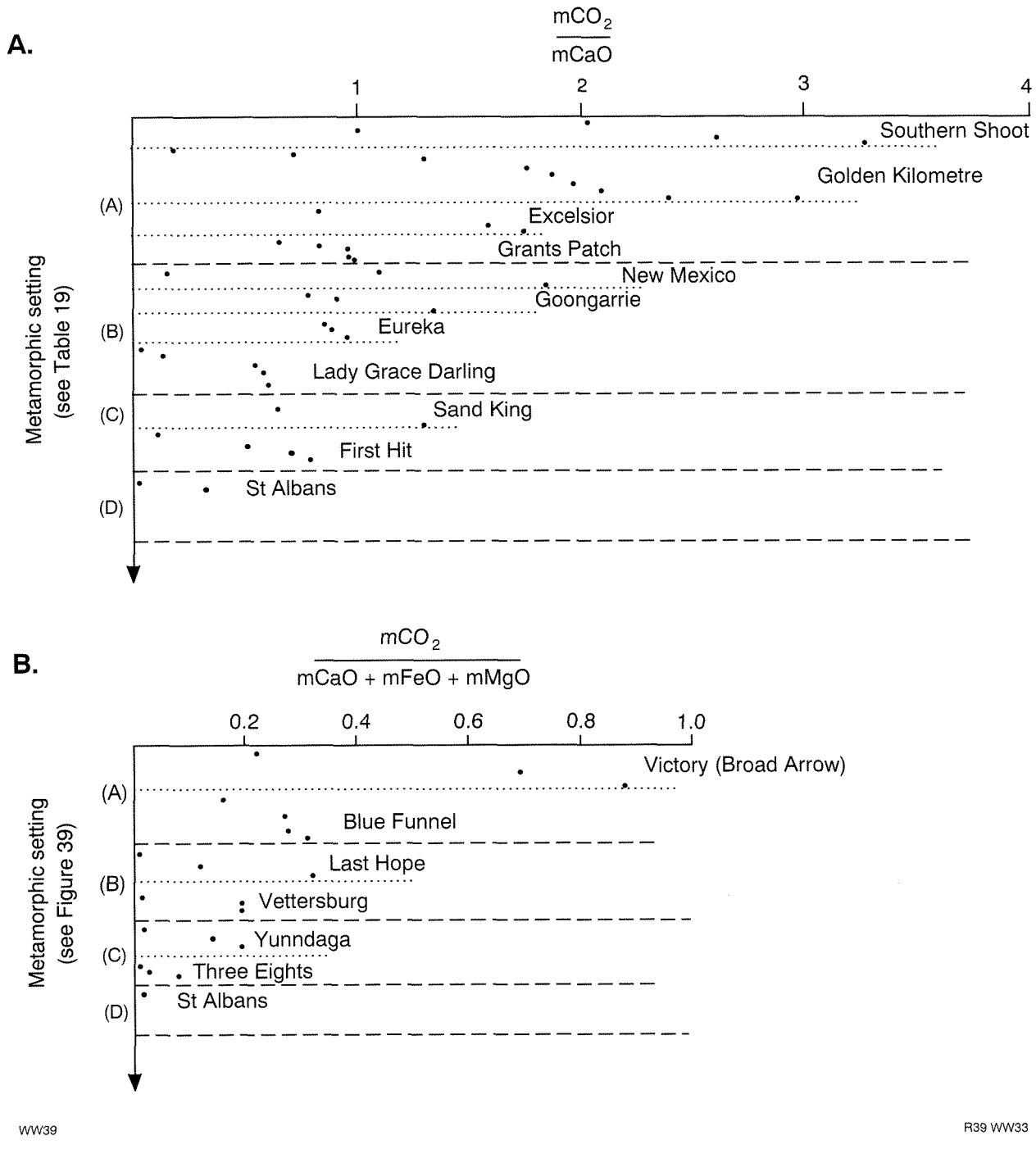

Figure 33. ***Variation in degree of carbonation of altered rocks associated with gold mineralization, with metamorphic grade of host rocks.***

A. — altered mafic rocks; degree of carbonation measured by $mCO_2/mCaO$;
B. — altered ultramafic rocks; degree of carbonation measured by $mCO_2/(mCaO+mMgO+mFeO)$

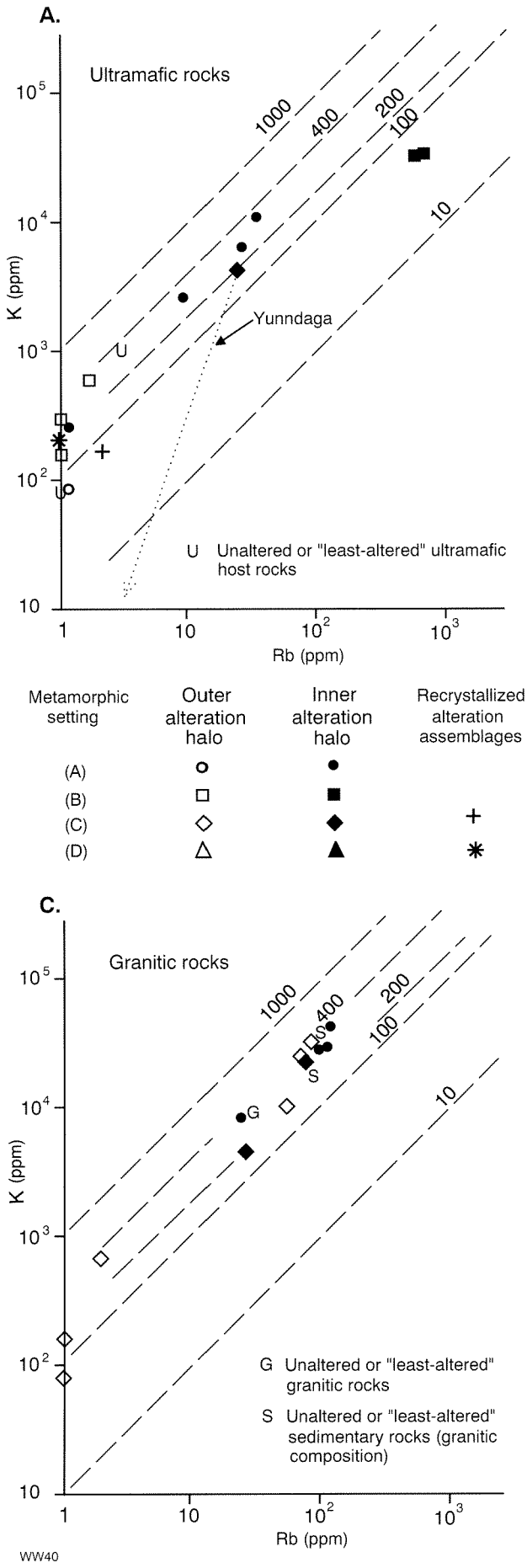
A.
Ultramafic rocks
1000
400
200
100
10
Yunndaga
U
U Unaltered or "least-altered" ultramafic host rocks
K (ppm)
Rb (ppm)
Metamorphic setting
Outer alteration halo
Inner alteration halo
Recrystallized alteration assemblages
(A)
(B)
(C)
(D)
C.
Granitic rocks
G
S
G Unaltered or "least-altered" granitic rocks
S Unaltered or "least-altered" sedimentary rocks (granitic composition)
WW40

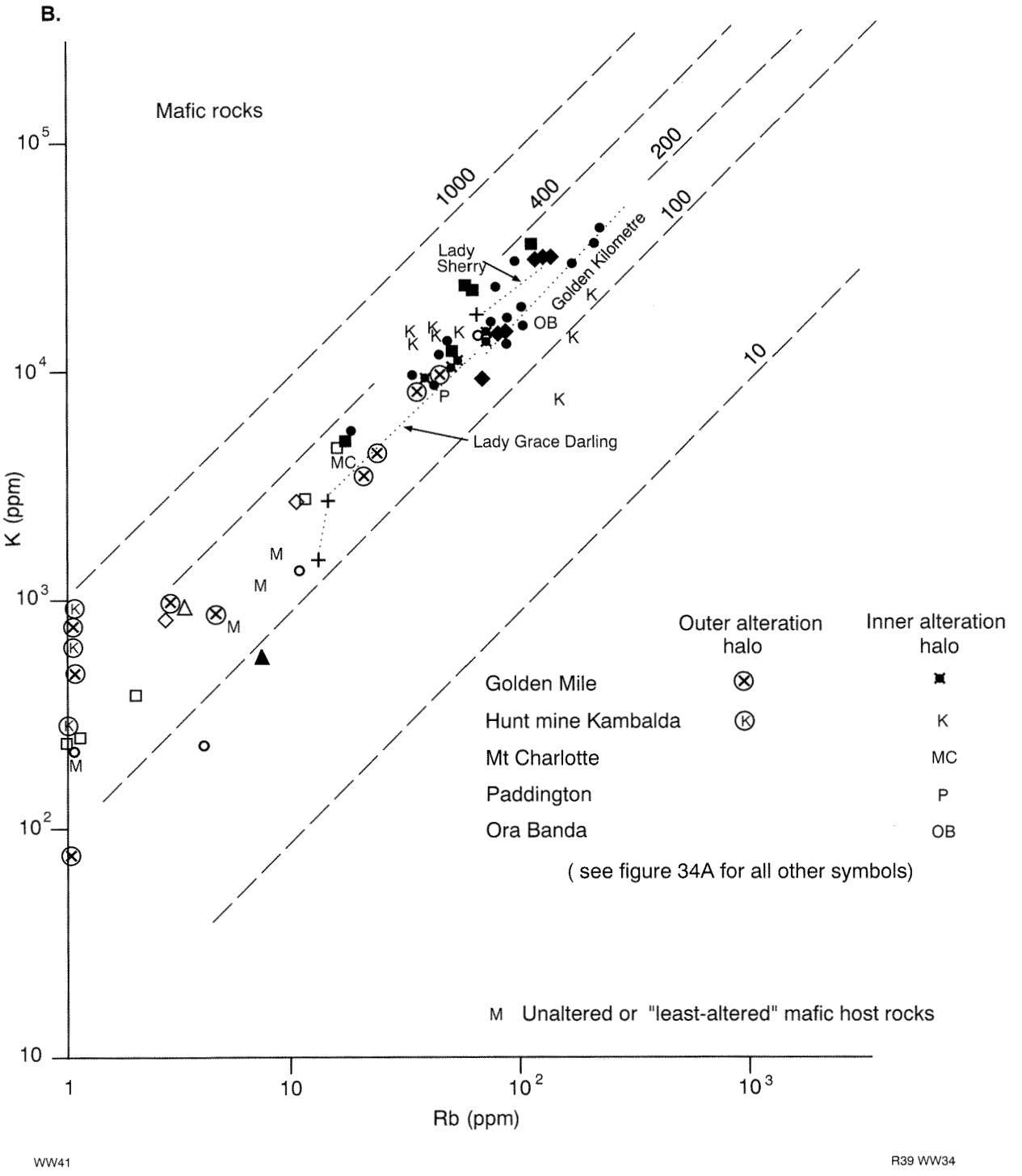

Figure 34. K versus Rb for altered rocks associated with gold mineralization:

A. — ultramafic rocks;
B. — mafic rocks — Golden Mile data from Phillips (1986); Kambalda data from McNaughton, de Laeter et al. (1988); Mt Charlotte, Paddington, Ora Banda data from Perring and Barley (1990);
C. — granitic rocks

Broken tie lines join samples from the same deposit. Recrystallized alteration assemblage from Yunndaga plots off the diagram

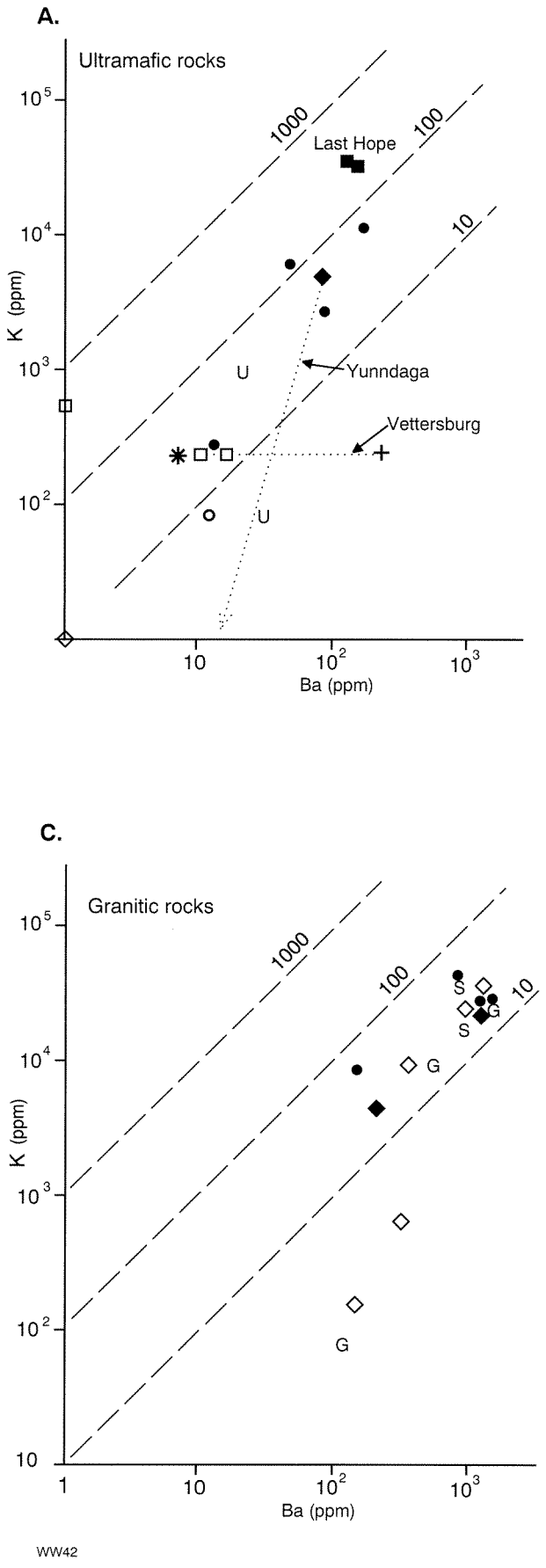
A.
Ultramafic rocks
1000
100
10
Last Hope
Yunndaga
Vettersburg
U
U
K (ppm)
Ba (ppm)
C.
Granitic rocks
S
S
G
G
G
K (ppm)
Ba (ppm)
WW42

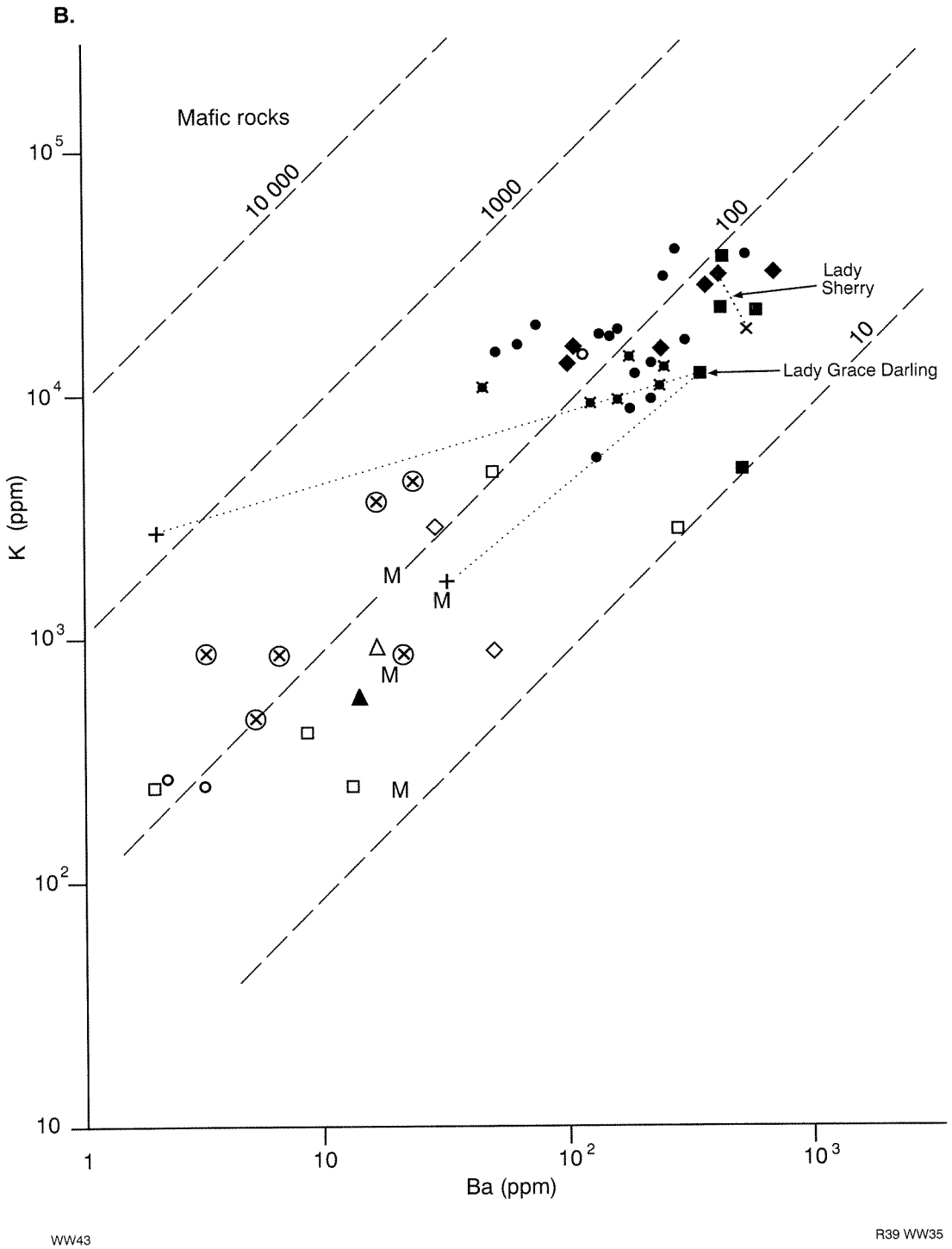

Figure 35. K versus Ba for altered rocks associated with gold mineralization:

A. — ultramafic rocks;
B. — mafic rocks;
C. — granitic rocks

Symbols and data sources as for Figure 34

Table 26. Major and trace element whole-rock chemistry for altered and unaltered ultramafic rocks in gold mines from the Menzies–Kambalda belt

	Victory (Broad Arrow)			*Blue Funnel*				*Excel-sior*	*Vettersburg*			*Last Hope*			*Three Eights*			*Yunndaga*			*St Albans*
	1	*2*	*3*	*4*	*5*	*6*	*7*	*8*	*9*	*10*	*11*	*12*	*13*	*14*	*15*	*16*	*17*	*18*	*19*	*20*	*21*
													Percentage								
SiO_2	38.7	50.6	37.0	38.1	38.2	37.0	38.4	37.4	40.2	53.6	58.0	40.9	29.5	46.3	44.6	45.0	87.3	38.6	70.2	39.8	47.4
TiO_2	0.21	0.11	0.17	0.29	0.29	0.14	0.34	0.25	0.20	0.21	0.17	0.33	0.23	0.30	0.41	0.25	0.02	0.23	0.11	0.33	0.33
Al_2O_3	5.29	3.08	4.10	8.05	7.40	3.31	7.95	5.41	5.06	4.88	4.17	6.70	5.06	6.39	7.91	4.52	1.20	5.34	2.79	6.72	9.29
Fe_2O_3	0.60	0.65	0.93	0.84	0.64	0.64	1.00	0.88	0.95	1.95	1.98	5.59	7.47	8.70	2.05	2.69	0.44	2.17	3.34	1.26	1.21
FeO	7.75	3.60	4.66	8.44	8.20	6.18	8.41	7.71	7.33	4.27	6.83	6.45	4.02	3.52	7.80	5.24	2.00	7.01	3.77	8.27	8.48
MnO	0.20	0.27	0.34	0.19	0.17	0.12	0.14	0.19	0.16	0.15	0.35	0.10	0.51	0.08	0.17	0.21	0.06	0.19	0.16	0.21	0.19
MgO	22.0	7.84	6.67	18.6	20.4	29.8	23.2	21.5	25.1	18.2	14.3	22.4	19.5	21.5	21.7	21.7	4.05	24.2	8.00	21.8	19.7
CaO	7.43	12.3	22.0	6.76	6.66	2.22	4.56	7.78	5.61	4.60	8.01	3.43	8.61	0.02	7.07	10.4	2.65	5.95	4.59	8.72	6.37
Na_2O	0.25	1.09	0.28	0.51	0.65	0.24	0.24	0.25	0.28	2.90	3.04	0.44	0.35	0.48	0.61	0.41	0.88	0.26	0.32	0.24	0.65
K_2O	0.73	0.32	0.05	0.12	0.00	0.01	1.40	<0.05	<0.05	<0.05	<0.05	0.07	3.93	4.15	0.01	0.01	0.00	0.00	0.54	0.00	0.03
P_2O_5	<0.05	<0.05	<0.05	0.05	0.03	0.03	0.04	<0.05	<0.05	<0.05	<0.05	0.05	0.04	0.04	0.05	0.04	0.03	0.04	0.03	0.05	0.05
CO_2	7.99	17.8	19.1	8.75	8.91	12.0	5.72	10.1	7.20	5.15	0.22	3.67	10.6	0.08	0.12	3.12	0.24	6.85	0.35	5.12	0.21
S	0.06	0.14	0.14	0.05	0.05	0.07	0.06	0.15	0.03	0.01	0.07	0.01	5.18	0.02	0.02	0.02	0.01	0.07	1.12	0.90	0.02
LOI	15.7	19.6	23.8	15.7	15.5	18.8	12.7	16.9	14.2	8.44	1.86	11.5	19.2	6.05	6.11	8.10	0.83	14.0	3.81	10.8	5.31
													Parts per million								
Ag	1	1	2	0	0	1	1	<1	<1	<1	1	1	43	1	1	0	1	0	1	0	0
As	776	1 101	<6	587	654	953	746	909	134	35	653	7	270	214	0	4	0	6	22 516	1 116	0
Au	0.03	0.06	0.02	0.06	0.01	0.13	0.25	0.08	0.04	0.13	0.16	<0.01	1.44	8.11	0.01	0.01	16.9	0.07	3.64	0.02	0.05
Ba	48	90	12	25	13	12	174	10	11	16	219	1	152	136	28	3	4	1	85	8	8
Bi	<6	<6	<6	0	1	0	0	<6	<6	<6	<6	2	3	4	1	2	0	1	0	1	1
Co	57	38	75	n.d.	52	67	n.d.	58	85	52	62	86	77	n.d.	55	54	11	n.d.	n.d.	n.d.	n.d.
Cr	2 104	999	1 527	2 885	2 486	1 749	2 562	2 453	2 102	1 867	1 494	2 304	2 599	2 844	2 607	2 088	136	2 279	926	2 754	2 006
Cu	10	40	52	24	22	43	41	27	13	149	7	64	178	1 996	67	174	7	29	11	122	34
F	194	<40	294	99	52	24	10 800	600	<40	<40	<40	583	8 040	55	67	79	18	48	120	402	196
Li	39	15	43	21	17	10	30	13	11	12	<6	32	91	107	14	5	<2	2	8	6	151
Mo	<2	<2	<2	<2	<2	<2	<2	<2	<2	<2	2	<2	<2	<2	<2	<2	4	<2	4	<2	<2
Nb	<2	<2	2	1	2	2	0	<2	<2	2	<2	1	2	1	2	1	1	1	1	1	0
Ni	799	258	760	687	844	1 898	800	829	1 457	793	875	821	743	678	433	752	105	1 393	418	1 031	753
Pb	3	18	4	1	2	2	2	<3	<3	<3	3	1	19	182	3	5	0	3	38	3	2
Rb	25	9	<2	3	0	1	35	<2	<2	<2	2	2	616	694	1	0	1	0	24	2	1
Sb	4	3	<3	6	7	13	5	4	4	<3	5	2	11	2	2	2	1	2	2	4	1
Sc	15	8	12	23	22	11	23	19	16	14	11	20	14	170	26	16	5	17	9	19	28
Sn	<4	<4	<4	0	0	0	0	<4	<4	<4	<4	1	0	0	0	1	1	0	0	0	0
Sr	89	136	68	99	51	34	121	197	38	24	10	9	30	12	10	36	8	107	24	108	8
Th	<3	<3	<3	0	0	0	1	<3	<3	<3	<3	0	0	0	0	0	0	1	9	0	2
U	<2	<2	<2	1	0	1	2	2	<2	2	3	0	8	1	1	1	1	2	2	3	1
V	127	65	90	171	158	75	167	134	116	89	97	145	228	230	195	128	18	119	58	131	180
W	3	11	6	n.d.	6	6	n.d.	18	5	31	432	4	29	n.d.	4	6	5	n.d.	n.d.	n.d.	n.d.
Y	6	4	6	7	7	4	7	5	4	6	6	7	12	2	10	9	2	5	3	7	7
Zn	48	24	41	63	55	32	51	151	77	190	238	147	410	560	135	114	84	59	87	109	59
Zr	12	5	10	20	15	9	18	13	10	11	7	18	12	13	23	13	2	13	7	32	19

Table 26. (*continued*)

	Victory (Broad Arrow)			*Blue Funnel*				*Excel-sior*	*Vettersburg*			*Last Hope*			*Three Eights*			*Yunndaga*			*St Albans*
	1	*2*	*3*	*4*	*5*	*6*	*7*	*8*	*9*	*10*	*11*	*12*	*13*	*14*	*15*	*16*	*17*	*18*	*19*	*20*	*21*
S.G.	2.86	2.79	2.78	2.83	2.71	2.90	2.86	2.79	2.82	2.72	2.93	2.72	2.87	2.70	2.85	2.75	2.71	2.91	2.82	2.89	2.93
MCO_2	0.23	0.89	0.69	0.28	0.27	0.31	0.17	0.29	0.20	0.20	0.01	0.12	0.35	0.00	0.00	0.09	0.03	0.19	0.02	0.14	0.01

1. Carbonated ultramafic schist, Victory (Broad Arrow); BA–8, 110.3 m; GSWA 97011
2. Mineralized ultramafic schist, Victory (Broad Arrow); BA–8, 115.3 m; GSWA 97012
3. Brecciated mineralized shear in ultramafic rock, Victory (Broad Arrow); BA–8, 179.5 m; GSWA 97016
4. 'Least-altered' komatiite, Blue Funnel; DDH 3001, 72.3 m; GSWA 100868
5. Carbonated ultramafic schist, Blue Funnel; DDH 3001, 145.2 m; GSWA 100871
6. Carbonated ultramafic schist, Blue Funnel; DDH 3001, 117.2 m; GSWA 100870
7. Mineralized ultramafic schist, Blue Funnel; DDH 3001, 98.0 m; GSWA 100869
8. Carbonated ultramafic schist, Excelsior mine (Bardoc); DXL–182, 132 m; GSWA 97724
9. Carbonated ultramafic schist, Vettersburg; mine dump; GSWA 97080A
10. Talc–albite(–tremolite) schist after ultramafic rock, Vettersburg; mine dump; GSWA 97080
11. Quartz–amphibole shear in ultramafic rock, Vettersburg; mine dump; GSWA 97081
12. Carbonated ultramafic schist, Last Hope; mine dump; GSWA 97769
13. Biotite–pyrite–talc–carbonate schist, Last Hope; mine dump; GSWA 97772
14. Pyritic talc–carbonate schist, Last Hope; mine dump; GSWA 97770
15. Talc–chlorite schist after ultramafic rock, Three Eights; mine dump; GSWA 98173A
16. Recrystallized carbonated ultramafic rock, Three Eights; mine dump; GSWA 98173
17. Quartz–tremolite shear in ultramafic rock, Three Eights; mine dump; GSWA 98173B
18. Carbonated ultramafic schist, Yunndaga; 320-D1, 140.9 m; GSWA 98290
19. Siliceous shear zone in ultramafic rock, Yunndaga; 320-D1, 118.8 m; GSWA 98288
20. Recrystallized carbonated ultramafic schist, Yunndaga, 320-D1, 119.1 m; GSWA 98289
21. Tremolite–chlorite schist, St Albans; mine dump; GSWA 98220

Table 27. Major and trace element whole rock chemistry of altered and unaltered mafic rocks from gold mines in the Menzies–Kambalda belt

	Golden Kilometre mine, Mount Pleasant									*Southern Shoot, Mount Pleasant*				*Excelsior mine (Bardoc)*		
	1	*2*	*3*	*4*	*5*	*6*	*7*	*8*	*9*	*10*	*11*	*12*	*13*	*14*	*15*	*16*
									Percentage							
SiO_2	54.5	44.9	46.7	46.1	50.4	45.1	43.5	45.9	48.3	46.6	42.3	49.5	52.4	47.8	46.2	40.6
TiO_2	1.51	1.98	1.38	1.53	1.16	1.27	1.18	1.76	0.12	1.79	1.32	1.25	0.93	0.66	0.62	0.37
Al_2O_3	12.1	12.6	10.7	10.7	10.9	10.9	12.3	12.9	3.04	11.5	11.6	10.9	5.85	12.6	11.5	10.4
Fe_2O_3	5.73	5.80	2.87	2.55	2.48	17.0	13.2	1.76	4.67	4.82	1.52	0.70	10.1	1.89	1.38	1.47
FeO	11.1	15.0	12.1	12.7	12.1	1.61	4.04	15.7	4.75	13.2	13.1	14.9	3.61	7.29	7.02	6.31
MnO	0.30	0.35	0.22	0.27	0.25	0.28	0.20	0.33	0.75	0.27	0.28	0.23	0.27	0.21	0.26	0.27
MgO	2.28	4.43	1.48	1.72	1.65	3.18	1.39	2.32	4.94	2.09	2.06	1.35	2.40	5.80	4.52	4.48
CaO	6.48	4.88	7.57	6.83	5.02	4.84	4.59	0.74	11.5	7.14	7.48	3.72	6.47	10.1	9.42	12.6
Na_2O	2.33	1.27	1.28	1.93	0.57	0.86	0.35	0.21	0.22	2.97	3.63	2.87	0.25	2.44	3.07	1.62
K_2O	0.17	<0.05	2.02	1.86	3.80	2.39	4.66	4.90	1.12	0.18	2.09	2.24	2.18	<0.05	0.69	1.23
P_2O_5	0.22	0.17	0.19	0.16	0.24	0.25	0.29	0.22	<0.05	0.15	0.23	0.33	0.05	0.10	0.09	0.06
CO_2	0.91	2.71	10.5	10.6	8.26	11.3	4.95	10.1	16.9	5.56	11.7	9.42	11.5	6.51	11.8	17.8
S	0.28	0.29	0.08	0.09	4.58	0.31	10.5	0.81	3.54	0.04	3.56	2.27	7.23	0.10	0.45	0.94
LOI	2.48	7.45	12.1	12.7	10.8	13.1	14.2	10.8	20.3	8.09	12.3	10.1	14.9	10.9	14.7	20.0
									Parts per million							
Ag	1	<1	<1	1	1	<1	1	<1	2	0	0	1	1	1	<1	1
As	7	<6	20	24	<6	23	336	28	562	0	3	2	1 418	6	100	799
Au	n.d.	n.d.	n.d.	n.d.	n.d.	n.d.	n.d.	n.d.	n.d.	<0.01	0.02	3.50	14.7	<0.02	0.62	1.5
Ba	28	<4	58	48	241	71	524	263	168	0	303	146	129	19	128	217
Bi	<6	<6	<6	<6	<6	<6	<6	<6	<6	1	0	1	0	<6	<6	<6
Co	n.d.	n.d.	n.d.	n.d.	n.d.	n.d.	n.d.	n.d.	n.d.	n.d.	n.d.	n.d.	n.d.	40	29	76
Cr	<1	<1	<1	<1	<1	<1	<1	<1	<1	0	0	0	0	91	92	1 226
Cu	38	21	11	13	225	9	72	31	12	8	125	45	34	41	62	48
F	352	380	570	496	2 090	1 010	3 040	2 970	918	358	835	955	1 117	225	130	161
Li	<6	11	6	<6	18	7	24	26	7	5	12	6	13	28	16	11
Mo	<2	<2	<2	<2	<2	<2	<2	<2	2	<2	<2	<2	50	<2	<2	<2
Nb	8	7	7	7	9	8	9	10	<2	6	6	9	7	4	3	3
Ni	5	4	7	8	7	5	9	6	8	8	6	4	11	55	49	365
Pb	4	<3	<3	4	7	4	29	15	40	2	1	3	74	8	19	4
Rb	7	4	85	81	158	101	192	200	42	11	75	83	86	<2	18	30
Sb	<3	<3	<3	3	<3	<3	<3	3	5	2	0	2	24	7	<3	3
Sc	23	26	21	20	17	18	19	22	8	27	24	20	17	25	26	24
Sn	<4	<4	<4	<4	<4	<4	<4	<4	<4	0	1	0	0	<4	<4	<4
Sr	116	52	86	96	98	76	72	15	202	114	154	73	82	143	137	145
Th	<3	<3	<3	<3	<3	<3	<3	<3	<3	0	1	2	2	<3	3	<3
U	3	<2	<2	<2	2	<2	3	2	<2	3	1	2	0	2	3	2
V	41	67	19	32	<1	7	<1	<1	37	78	61	0	80	209	193	168
W	n.d.	n.d.	n.d.	n.d.	n.d.	n.d.	n.d.	n.d.	n.d.	n.d.	n.d.	n.d.	n.d.	5	9	10
Y	47	39	40	38	48	48	57	53	14	33	42	50	16	17	15	10
Zn	95	140	88	96	99	124	76	99	52	122	25	70	26	90	46	70
Zr	160	129	130	134	173	159	197	189	14	108	150	172	40	77	68	28

Table 27. (*continued*)

	Golden Kilometre mine, Mount Pleasant									*Southern Shoot, Mount Pleasant*				*Excelsior mine (Bardoc)*		
	1	*2*	*3*	*4*	*5*	*6*	*7*	*8*	*9*	*10*	*11*	*12*	*13*	*14*	*15*	*16*
S.G.	3.08	3.01	2.88	3.01	3.03	3.00	3.16	3.12	2.93	2.90	2.95	2.93	2.91	2.80	2.81	2.83
MCO_2	0.18	0.71	1.76	1.97	2.09	2.97	1.37	2.41	1.87	0.99	1.99	3.22	2.62	0.82	1.59	1.80

1. Unaltered quartz gabbro, Golden Kilometre (Mt Pleasant); WD–152, 116.8 m; GSWA 89936
2. Chlorite–carbonate alteration after quartz gabbro, Golden Kilometre (Mt Pleasant); WD–152, 116.8 m; GSWA 89937
3. Chlorite–carbonate, transitional to carbonate–sericite alteration, Golden Kilometre (Mt Pleasant); WD–152, 126.0 m; GSWA 89938
4. Carbonate–sericite alteration, Golden Kilometre (Mt Pleasant); WD–152, 126.0 m; GSWA 89939
5. Carbonate–sericite alteration, Golden Kilometre (MtPleasant); WD–152, 126.75 m; GSWA 89942
6. Carbonate–sericite, transitional to sericite–pyrite alteration, Golden Kilometre (Mt Pleasant); WD–152, 126.75 m; GSWA 89941
7. Sericite–pyrite alteration, Golden Kilometre (Mt Pleasant); WD–152, 126.75 m; GSWA 89943
8. Sericite–carbonate(–biotite) alteration, Golden Kilometre (Mt Pleasant); WD–152, 131.7 m; GSWA 89944
9. Siliceous shear zone in quartz gabbro, Golden Kilometre (Mt Pleasant); WD–152, 128.9 m; GSWA 89940
10. Chlorite–carbonate alteration after quartz gabbro, Southern shoot (Mt Pleasant);WD–153, 156.4m; GSWA 89920
11. Quartz–carbonate–albite alteration after quartz gabbro, Southern shoot (Mt Pleasant); WD–153, 139.8 m; GSWA89919
12. Sericite–carbonate alteration, Southern shoot (Mt Pleasant); WD–153, 173.5 m; GSWA 89924
13. Siliceous shear in quartz gabbro, Southern shoot (Mt Pleasant); WD–153, 169.4 m; GSWA 89923
    NOTE: 10–12 represent alteration around 45° N-dipping quartz veins; 13 represents alteration around bounding shear
14. 'Least-altered' basalt, Excelsior (Bardoc); DXL–182, 215.3 m; GSWA 97727
15. Chlorite–carbonate, transitional to sericite–pyrite alteration, Excelsior (Bardoc); DXL–182, 203.1 m; GSWA97726
16. Sericite (fuchsite)–pyrite alteration, Excelsior (Bardoc); DXL–182, 180.4 m; GSWA 97725

Table 27. (*continued*)

	Grants Patch					*Lady Grace Darling*					*Eureka*			*Goongarrie*		
	17	*18*	*19*	*20*	*21*	*22*	*23*	*24*	*25*	*26*	*27*	*28*	*29*	*30*	*31*	*32*
								Percentage								
SiO_2	43.9	45.1	56.5	44.5	49.3	51.9	48.6	42.4	45.6	37.6	43.1	42.4	43.7	48.5	37.4	36.0
TiO_2	1.11	1.15	0.76	1.18	0.99	0.92	0.89	0.81	0.51	0.72	0.69	0.77	0.61	1.44	1.33	1.47
Al_2O_3	13.9	14.4	10.6	15.2	12.9	14.7	13.7	12.6	8.54	11.0	13.0	13.2	13.4	14.3	14.2	15.8
Fe_2O_3	3.02	2.02	2.02	2.21	3.92	2.61	1.79	1.97	11.0	4.32	1.79	1.96	1.98	2.27	5.58	6.39
FeO	9.73	8.73	4.25	7.76	4.43	7.55	8.61	6.13	14.9	6.78	8.61	8.26	8.70	8.79	6.22	8.92
MnO	0.22	0.19	0.16	0.25	0.23	0.24	0.27	0.18	0.15	0.46	0.21	0.19	0.20	0.24	0.20	0.14
MgO	5.53	4.19	1.92	3.23	2.83	6.52	6.60	5.67	2.65	6.75	7.09	6.96	7.09	3.83	4.97	4.98
CaO	9.38	9.08	9.24	10.2	9.18	10.8	9.49	14.7	5.29	18.9	10.0	10.7	8.80	7.87	9.59	6.73
Na_2O	1.99	1.40	1.19	1.30	0.85	1.75	0.89	2.19	1.37	0.21	2.01	2.59	2.10	3.15	2.40	3.56
K_2O	<0.05	1.50	1.69	1.77	2.18	0.10	<0.05	1.52	0.34	0.20	0.35	<0.05	0.62	0.61	2.84	2.80
P_2O_5	0.12	0.12	0.09	0.13	0.11	0.09	0.09	0.06	0.10	0.16	0.08	0.08	0.08	0.17	0.19	0.20
CO_2	4.72	6.99	7.21	6.91	7.12	0.53	4.35	7.10	1.65	8.25	6.60	7.49	6.73	4.87	6.92	7.15
S	0.14	0.77	1.00	0.21	2.80	0.17	0.83	0.61	7.11	0.01	0.19	0.27	0.40	0.58	3.22	4.10
LOI	10.4	10.7	9.56	11.6	12.3	2.52	8.58	11.4	7.84	12.4	12.5	12.1	11.0	7.94	11.2	12.6
								Parts per million								
Ag	<1	4	58	<1	3	<1	<1	<1	18	1	1	1	1	1	<1	<1
As	51	1 527	396	49	961	20	7	52	120	12	9	<6	<6	33	17 550	412
Au	0.06	13.9	154	0.05	66.3	0.12	n.d.	0.08	3.9	n.d.	n.d.	n.d.	n.d.	n.d.	n.d.	n.d.
Ba	<4	177	209	107	131	19	<4	356	<4	29	275	13	501	48	415	583
Bi	<6	<6	<6	<6	<6	<6	<6	<6	6	<6	<6	<6	<6	<6	<6	11
Co	40	35	22	36	32	57	47	41	245	n.d.	48	49	47	43	40	49
Cr	121	100	64	100	84	316	297	197	240	152	247	214	199	189	182	187
Cu	98	113	482	83	108	91	133	124	14 800	412	58	106	91	110	113	158
F	183	188	84	210	219	131	216	350	75	n.d.	106	110	101	161	180	118
Li	16	18	8	16	13	10	31	27	10	19	14	13	12	12	15	14
Mo	<2	<2	<2	<2	<2	<2	<2	<2	6	4	<2	<2	<2	<2	<2	<2
Nb	4	4	4	4	4	3	3	2	6	3	4	2	3	6	7	6
Ni	74	46	29	53	37	156	138	123	371	102	134	123	131	93	75	80
Pb	11	98	3 662	11	158	6	13	4	7	14	<3	3	3	9	<3	8
Rb	<2	40	44	66	81	4	<2	49	14	13	11	<2	17	15	61	58
Sb	<3	4	16	5	3	20	11	<3	6	8	<3	3	3	3	6	<3
Sc	29	28	18	27	24	35	33	28	20	31	27	30	28	28	28	28
Sn	<4	<4	<4	<4	<4	<4	16	4	17	17	<4	<4	<4	<4	<4	<4
Sr	81	49	40	57	53	114	135	149	118	140	46	90	56	126	102	105
Th	<3	<3	<3	<3	<3	<3	<3	<3	<3	<3	<3	<3	<3	<3	8	<3
U	2	3	<2	<2	<2	2	<2	<2	2	<2	<2	<2	<2	3	3	<2
V	281	304	193	288	247	308	282	232	162	184	231	240	248	289	309	365
W	3	54	31	7	20	5	4	6	5	n.d.	5	4	49	14	35	47
Y	23	24	17	26	16	20	18	15	13	28	15	16	15	28	28	31
Zn	114	260	1 859	161	139	114	234	333	1 224	541	84	80	91	104	37	58
Zr	79	76	60	81	67	57	50	46	69	41	43	39	43	115	108	123

Table 27. (*continued*)

	Grants Patch					*Lady Grace Darling*					*Eureka*			*Goongarrie*		
	17	*18*	*19*	*20*	*21*	*22*	*23*	*24*	*25*	*26*	*27*	*28*	*29*	*30*	*31*	*32*
S.G.	2.90	2.79	2.82	2.80	2.80	2.99	2.93	3.17	3.18	2.67	2.81	2.81	2.79	2.82	2.93	2.87
MCO_2	0.64	0.98	0.99	0.86	0.99	0.06	0.58	0.61	0.14	0.55	0.84	0.89	0.97	0.79	0.92	1.35

17. Chlorite–carbonate alteration after basalt, Prince of Wales mine (Grants Patch); E–W lode, 5-level; GSWA 93975
18. Silicified basalt, Prince of Wales mine (Grants Patch); E–W lode, 7-level; GSWA 93972
19. Silicified lode centre, Prince of Wales mine (Grants Patch);E–W lode, 5-level; GSWA 93974
20. Chlorite–carbonate alteration after basalt, Prince of Wales mine (Grants Patch); N–S shear, 3-level; GSWA 93976
21. Sericite–pyrite alteration after basalt, Prince of Wales mine (Grants Patch); N–S shear, 3-level; GSWA 93973
22. 'Least-altered' sheared basalt, Lady Grace Darling; GDD14, 113.2 m; GSWA 97710
23. Chloritized basalt, Lady Grace Darling; GDD14, 113.2 m; GSWA 97712
24. Biotite–chlorite alteration after basalt, Lancashire Hero; mine dump; GSWA 97086
25. Recrystallized biotite–chlorite alteration after basalt, Lady Grace Darling; GDD 14, 124.6 m; GSWA97714
26. Calc-silicate alteration after basalt, Lady Grace Darling; GDD14, 130.1 m; GSWA 97715
27. Chlorite–carbonate alteration after basalt, Eureka; DEK–23, 191.0 m; GSWA 93941
28. Chlorite–carbonate alteration with sulfides, Eureka; DEK–23, 233.6 m; GSWA 93943
29. Chlorite–carbonate alteration with biotite, Eureka; DEK–23, 211.2 m; GSWA 93956
30. Carbonate–chlorite schist after basalt, New Boddington mine (Goongarrie); NBD–5, 163.0 m; GSWA 93928
31. Carbonate–biotite schist after basalt, New Boddington mine (Goongarrie); NBD–5, 141.0 m; GSWA 93922
32. Brecciated carbonate–biotite shear after basalt, New Boddington mine (Goongarrie); NBD–5, 139.1 m; GSWA 93921

Table 27. ***(continued)***

	New Mexico			*First Hit*				*Sand King*		*Lady Sherry*				*St Albans*	
	33	*34*	*35*	*36*	*37*	*38*	*39*	*40*	*41*	*42*	*43*	*44*	*45*	*46*	*47*
								Percentage							
SiO_2	32.1	44.9	54.9	49.4	47.5	39.9	43.7	47.4	34.9	51.1	78.5	43.7	48.8	44.3	48.9
TiO_2	0.33	0.29	0.47	0.96	0.93	0.81	0.85	1.38	1.53	0.88	0.32	0.97	0.99	0.88	0.81
Al_2O_3	9.40	8.93	13.1	14.4	13.7	11.8	12.8	13.3	14.3	14.7	6.25	14.1	15.1	12.5	12.7
Fe_2O_3	4.53	1.68	5.61	2.01	2.41	2.19	6.87	2.54	3.98	6.48	2.65	1.57	2.69	1.86	3.09
FeO	5.36	8.11	1.96	9.13	7.23	6.50	4.66	10.4	10.8	4.00	2.72	8.03	8.14	7.05	6.58
MnO	0.22	0.20	0.09	0.21	0.21	0.27	0.19	0.24	0.30	0.25	0.13	0.23	0.21	0.26	0.32
MgO	11.3	19.4	3.90	7.47	4.57	4.06	3.88	3.28	4.79	3.62	1.45	4.56	4.92	4.18	4.50
CaO	15.7	7.69	4.92	11.3	12.8	17.3	10.0	8.23	10.9	16.2	5.64	12.2	11.3	21.3	20.8
Na_2O	0.22	0.33	0.62	1.95	1.15	1.26	1.58	2.17	2.43	0.46	0.37	0.93	0.83	1.52	0.76
K_2O	0.05	0.00	4.44	0.21	1.66	1.92	1.89	3.76	3.97	0.11	0.35	4.02	2.27	0.11	0.07
P_2O_5	0.04	0.05	0.03	0.10	0.09	0.08	0.09	0.16	0.14	0.10	0.06	0.09	0.11	0.08	0.10
CO_2	13.2	0.98	7.12	1.05	5.17	11.0	5.52	4.28	10.9	0.18	0.30	6.39	2.99	5.68	0.75
S	2.95	0.03	4.06	0.06	0.86	1.75	4.24	0.60	3.88	0.02	0.13	2.09	0.20	0.10	0.26
LOI	19.8	6.65	8.86	1.85	6.95	13.1	12.6	6.03	9.75	2.16	1.37	9.19	4.19	6.50	1.48
								Parts per million							
Ag	0	1	2	0	2	1	2	0	1	1	0	1	0	0	0
As	35	1	146	9	6	5	16	2	0	39	1	45	40	0	0
Au	0.04	<0.01	0.22	0.02	0.90	2.52	2.19	0.29	3.87	0.01	0.49	0.76	0.23	0.01	0.06
Ba	8	9	410	17	94	101	222	361	682	48	27	405	528	16	14
Bi	1	0	0	1	0	1	1	2	0	2	2	0	2	1	4
Co	55	78	41	n.d.	n.d.	37	n.d.	n.d.	n.d.	40	21	30	40	39	45
Cr	1 185	2 158	1 663	289	276	248	276	89	93	267	92	299	300	260	255
Cu	62	23	28	151	156	120	399	121	160	27	675	148	125	94	152
F	1 710	223	214	82	164	147	172	410	628	276	69	199	229	94	761
Li	22	12	15	11	35	44	76	31	37	4	6	65	48	67	73
Mo	<2	<2	<2	<2	<2	<2	<2	<2	<2	4	8	<2	<2	<2	<2
Nb	1	2	2	3	2	3	3	3	4	2	2	4	3	3	3
Ni	361	713	711	159	129	106	160	74	75	153	60	129	162	125	147
Pb	3	1	11	2	11	12	28	10	19	65	131	41	10	3	5
Rb	2	1	109	8	66	76	74	113	120	3	10	135	63	3	7
Sb	4	4	2	0	4	6	3	2	0	0	2	2	6	0	0
Sc	32	24	28	31	30	28	28	33	35	28	11	31	33	29	29
Sn	0	0	0	0	1	0	0	0	0	0	0	0	0	0	1
Sr	39	6	31	173	96	86	69	102	185	89	57	83	63	99	98
Th	0	0	0	1	0	1	0	1	2	0	0	0	1	1	3
U	0	0	3	3	1	2	0	6	1	2	1	3	1	2	1
V	169	143	218	273	269	235	286	334	385	250	91	285	299	229	230
W	15	5	17	n.d.	n.d.	12	n.d.	n.d.	n.d.	8	6	41	9	5	117
Y	6	5	15	19	19	20	18	31	33	16	7	18	20	16	17
Zn	65	64	21	80	84	81	135	136	146	111	487	142	95	69	86
Zr	21	18	29	55	54	45	52	103	107	54	21	54	56	50	47

Table 27. (*continued*)

	New Mexico			*First Hit*				*Sand King*		*Lady Sherry*				*St Albans*	
	33	*34*	*35*	*36*	*37*	*38*	*39*	*40*	*41*	*42*	*43*	*44*	*45*	*46*	*47*
S.G.	2.77	2.90	2.85	3.01	2.89	2.86	2.75	2.90	2.94	3.15	2.91	2.20	2.93	3.05	3.21
MCO_2	1.07	0.16	1.84	0.12	0.51	0.81	0.70	0.66	1.27	0.01	0.07	0.67	0.34	0.34	0.01

33. Carbonated high-Mg basalt, New Mexico; mine dump; GSWA 98140
34. Recrystallized carbonated high-Mg basalt; New Mexico; mine dump; GSWA 98141
35. Potassic (biotite–carbonate–pyrite overprints quartz–sericite) alteration, New Mexico; mine dump; GSWA 98143
36. 'Least-altered' amphibolite, First Hit; MZD–2, 69.5 m; GSWA 98297
37. Biotite amphibolite, First Hit; MZD–2, 62.3 m; GSWA 98295
38. Biotite amphibolite, transitional to pyritic shear, First Hit; MZD–2, 62.3 m; GSWA 98295A/B
39. Pyritic shear in amphibolite, First Hit; MZD–2, 60.1 m; GSWA 98294
40. Biotite–chlorite alteration after basalt, Sand King; SAD–8, 143.1 m; GSWA 97722
41. Biotite–pyrite alteration after basalt, Sand King; SAD–8, 145.4 m; GSWA 97723
42. Quartz–epidote alteration after amphibolite, Lady Sherry; mine dump; GSWA 98230
43. Quartz–epidote alteration after amphibolite, Lady Sherry; mine dump; GSWA 98226
44. Biotitized amphibolite, Lady Sherry; mine dump; GSWA 98228
45. Recrystallized biotitized amphibolite, Lady Sherry; mine dump; GSWA 98229
46. Diopsidic amphibolite, St Albans; mine dump; GSWA 98220A
47. Garnet–diopside rock, St Albans; mine dump; GSWA 98222

Table 28. Major and trace element contents of unaltered and altered rocks of granitic composition in gold mines of the Menzies–Kambalda region

	Binduli			*Lady Bountiful*			*Bellevue*			*Three Eights*			*Yunndaga*				*Goodenough*		
	1	*2*	*3*	*4*	*5*	*6*	*7*	*8*	*9*	*10*	*11*	*12*	*13*	*14*	*15*	*16*	*17*	*18*	*19*
									Percentage										
SiO_2	64.5	58.1	64.0	66.6	64.8	62.4	63.5	65.0	66.2	66.6	64.7	63.9	67.7	67.3	64.9	65.7	66.7	60.3	67.8
TiO_2	0.27	0.64	0.68	0.46	0.48	0.44	0.40	0.43	0.16	0.32	0.52	0.51	0.32	0.40	0.41	0.37	0.48	0.72	0.13
Al_2O_3	15.3	13.6	14.7	15.0	15.2	15.3	15.5	17.1	6.24	18.4	16.0	15.9	16.5	14.8	15.4	12.6	15.0	14.7	6.86
Fe_2O_3	0.98	2.59	2.52	1.73	2.13	2.15	1.95	2.78	10.6	0.29	1.25	1.74	1.19	1.84	1.98	3.13	1.27	0.37	10.9
FeO	0.85	3.00	1.63	1.47	1.26	1.05	1.92	0.64	2.38	0.63	2.03	1.84	0.59	1.75	1.42	2.32	1.56	1.57	0.75
MnO	0.06	0.16	0.05	0.06	0.07	0.06	0.08	0.05	0.29	0.02	0.05	0.02	0.03	0.06	0.06	0.09	0.05	0.09	0.10
MgO	1.08	2.44	1.42	1.44	1.50	1.38	2.38	1.49	2.35	0.73	2.25	2.10	1.25	1.22	2.02	2.09	1.61	1.17	0.46
CaO	2.26	4.63	2.53	3.03	3.20	3.98	4.43	2.11	0.72	0.83	1.80	2.06	1.56	2.02	2.50	2.26	3.21	9.70	2.64
Na_2O	8.07	2.54	2.59	4.34	4.06	3.58	4.32	0.45	0.73	10.6	9.37	9.40	1.88	3.52	2.34	1.95	4.46	3.94	2.17
K_2O	0.54	3.77	3.91	3.08	3.42	3.55	1.09	5.22	1.07	0.01	0.02	0.08	4.37	3.05	3.86	2.92	2.19	1.26	0.56
P_2O_5	0.17	0.80	0.83	0.30	0.34	0.32	0.14	0.15	0.07	0.19	0.25	0.25	0.12	0.18	0.36	0.30	0.17	0.09	0.06
CO_2	3.73	5.70	2.90	0.50	1.65	3.24	0.17	0.50	6.41	0.44	9.12	0.18	1.29	2.48	0.87	1.60	1.25	4.75	7.13
S	0.59	0.05	0.03	0.07	0.40	0.44	0.04	1.42	7.80	0.02	0.01	0.01	0.94	1.23	0.77	1.63	0.29	0.15	7.46
LOI	3.93	7.54	4.54	1.45	2.91	5.31	1.89	4.18	7.63	0.65	0.74	1.24	3.54	2.82	3.12	4.09	2.26	5.57	7.34
									Parts per million										
Ag	1	1	1	<1	1	1	1	1	2	1	2	1	1	1	3	1	2	0	11
As	2	7	1	<6	66	18	8	120	324	9	5	110	67	82	150	344	11	32	38
Au	1.01	0.02	0.01	n.d.	n.d.	0.22	0.11	n.d.	4.25	0.03	1.84	0.03	0.05	0.01	n.d.	n.d.	0.04	<0.01	4.70
Ba	989	2 124	2 295	1 245	1 206	1 419	539	828	150	127	148	323	803	948	1 295	1 226	891	364	205
Bi	1	1	0	<6	<6	<6	1	0	1	0	7	3	0	0	1	0	0	1	3
Co	3	n.d.	15	13	n.d.	12	n.d.	n.d.	n.d.	n.d.	6	4	n.d.	n.d.	n.d.	n.d.	7	64	26
Cr	5	147	179	15	16	15	87	96	49	17	48	37	177	46	54	61	33	806	35
Cu	107	25	26	24	32	24	62	54	1 122	5	18	79	27	98	50	83	14	65	30
F	483	1 260	1 177	784	1 290	1 080	293	254	74	29	55	105	638	574	445	362	299	306	662
Li	7	30	11	12	17	16	10	26	7	<2	5	9	7	9	10	8	71	35	11
Mo	<2	<2	<2	<2	<2	<2	<2	<2	4	<2	<2	<2	<2	2	2	<2	2	4	4
Nb	10	6	6	6	6	6	3	3	2	2	4	4	6	7	7	6	4	4	3
Ni	8	42	33	17	16	17	48	46	82	9	31	26	60	26	37	38	33	383	80
Pb	435	13	14	60	23	18	7	9	15	18	32	47	36	25	65	73	17	10	27
Rb	12	89	95	71	96	110	25	114	24	1	1	2	96	70	88	74	81	56	27
Sb	3	2	3	<3	3	5	1	2	5	2	0	0	2	1	1	2	1	1	4
Sc	2	16	6	4	5	5	8	8	12	2	6	6	6	6	6	6	5	22	3
Sn	0	0	0	<4	<4	<4	0	0	1	0	3	6	3	1	1	0	0	0	0
Sr	586	475	399	759	584	434	660	94	29	67	143	268	203	341	316	252	568	164	79
Th	18	30	32	14	11	13	4	6	4	10	9	9	11	15	38	29	9	0	5
U	5	8	7	5	5	4	2	5	1	3	2	2	5	4	9	8	4	2	3
V	44	161	141	51	56	66	66	77	41	6	59	55	47	52	68	76	49	218	38
W	25	n.d.	46	4	n.d.	18	n.d.	n.d.	n.d.	n.d.	12	8	n.d.	n.d.	n.d.	n.d.	5	43	13
Y	13	25	21	9	10	9	9	8	8	4	7	7	8	10	15	13	8	10	4
Zn	79	63	34	59	73	50	66	131	139	6	49	31	199	405	203	228	42	58	5
Zr	191	232	241	144	143	130	110	118	50	134	134	132	142	161	218	179	152	48	62

Table 28. (*continued*)

	Binduli			*Lady Bountiful*			*Bellevue*			*Three Eights*			*Yunndaga*				*Goodenough*		
	1	*2*	*3*	*4*	*5*	*6*	*7*	*8*	*9*	*10*	*11*	*12*	*13*	*14*	*15*	*16*	*17*	*18*	*19*
S.G.	2.66	2.81	2.76	2.71	2.75	2.73	2.78	2.86	2.91	2.61	2.67	2.65	2.62	2.68	3.07	2.69	2.71	2.57	2.90

1. Altered porphyry, Binduli; BDH–1, 47.8 m; GSWA 100872
2. Altered hanging-wall sediment, Binduli; BDH–1, 41.9 m; GSWA 100873
3. Altered footwall sediment, Binduli; BDH–1, 67.7 m; GSWA 100874
4. 'Least-altered' granodiorite, Lady Bountiful; LBD-21, 184.4 m; GSWA 89904
5. Transition to sericite–pyrite alteration, Lady Bountiful; LBD–21, 256.2 m; GSWA 89907
6. Sericite–pyrite alteration after granodiorite, Lady Bountiful; LBD–21, 233.9 m; GSWA 89908
7. 'Least-altered' porphyry, Bellevue (Grants Patch); BV–25, 33.4 m; GSWA 97002
8. Sericitic alteration after porphyry, Bellevue (Grants Patch); BV–26, 47.7 m; GSWA 97003
9. Silicified brecciated porphyry, Bellevue (Grants Patch); BV–22, 52.9 m; GSWA 97008
10. Albitic porphyry, Three Eights; mine dump; GSWA 98176
11. Carbonated albitic porphyry, Three Eights; mine dump; GSWA 98178
12. Decarbonated albitic porphyry, Three Eights; mine dump; GSWA 98177
13. Weakly muscovitized sediment, Yunndaga; 320–D1, 94.7 m; GSWA 98285
14. Moderately muscovitized sediment, Yunndaga; 320–D1, 73.7 m; GSWA 98282
15. Sheared muscovitized sediment, Yunndaga; 320–D1, 87.0 m; GSWA 98284A
16. Sheared muscovitized sediment, Yunndaga; 320–D1, 87.0m; GSWA 98284
17. 'Least-altered' sediment, Goodenough; mine dump; GSWA 100848
18. Carbonated fuchsitic sediment, Goodenough; mine dump; GSWA 100849
19. Quartz–pyrite shear in sediment, Goodenough; mine dump; GSWA 100846

Chapter 7

Fluid composition and the transport and deposition of gold

Composition of the hydrothermal fluids

Phillips and Groves (1983) characterized the fluids associated with Archaean epigenetic gold deposits as slightly alkaline, reducing, low-salinity H_2O–CO_2 fluids, based partly on detailed studies at Mt Charlotte and Hunt mine in the Menzies–Kambalda region. The composition of the fluids was determined from a combination of fluid inclusion data and a qualitative assessment of wallrock alteration assemblages. Subsequent studies of fluid inclusions in samples from the Golden Mile deposits and Victory–Defiance, and reconnaissance studies at Ora Banda, Lady Bountiful, Paddington, and Boorara have identified similar low-salinity, H_2O–CO_2 fluids with variable, but mostly minor, methane (Ho, 1987; Ho et al., 1990). Chemical and mineralogical changes associated with wallrock alteration, documented in Chapters 5 and 6, indicate that the fluids also carried significant amounts of K, S, and Au (see also Phillips, 1986; Clark, 1980; Phillips and Groves, 1984). More detailed thermodynamic analysis of wallrock alteration mineralogy at Hunt mine has led to a more extensive estimation of hydrothermal fluid parameters (Neall and Phillips, 1987; Mikucki and Groves, 1990). Results of investigations into fluid composition at Mt Charlotte and Hunt mine are summarized in Tables 29 and 30.

Clark (1980), Kerrich (1986b), Neall and Phillips (1987), and Mikucki and Groves (1990) noted the potential for fluid buffering by the following wallrock reactions:

1. chlorite = albite + muscovite
2. chlorite + calcite = muscovite + ankerite
3. chlorite + albite = biotite + quartz
4. chlorite(1) + quartz = albite + chlorite(2).

These authors used the data of Montoya and Hemley (1975) to predict slightly acid to slightly alkaline pH for the hydrothermal fluids.

Phillips and Groves (1983) and Kerrich (1986b) considered that the Na/K ratios of hydrothermal fluids could be determined where fluids are in equilibrium with albite and muscovite. For example, Na/K ratios of 4–8 were determined for fluids at Mt Charlotte and Hunt. However, such reasoning should be applied with caution since albite and muscovite commonly appear not to be in equilibrium with one another in many alteration assemblages. Although reaction 1 (above) may buffer fluids locally, relatively acid or relatively potassic fluids may react incompletely with albite due to kinetic effects. The stability of albite rather than K-feldspar requires Na > K at the relevant temperatures (Orville, 1963), but the absence of paragonite in alteration assemblages suggests that Na is not orders of magnitude greater than K in the hydrothermal fluids (Fig. 36).

Table 29. Calculated and experimentally determined hydrothermal fluid parameters at Mount Charlotte (Clark, 1980; Ho, 1987; Neall, 1987)

Temperature:	260–360°C (a)
Pressure:	1.5–2.3 kb
Composition:	H_2O–CO_2 fluid, X_{CO_2} = 0.2–0.3
Salinity:	<4 wt% NaCl equiv. (approximately)
Na/K:	4.4
pH:	4.7–6.0
fO_2:	$10^{-27.8}$–$10^{-26.4}$
fS_2	10^{-8}–$10^{-10.5}$
Gold in solution:	10^{-1} to 10^{-4} ppm as $Au(HS)_2^-$
	10^{-7} to 10^{-12} ppm as $AuCl_2^-$
Fluid/rock ratios:	high (b)

(a) Clark (1980) originally estimated a temperature of 400 ± 40°C, but more recent determinations (Ho, 1987; Neall, 1987) support the figures cited
(b) Mikucki and Groves (1990) cited ratios of 5000–10 000

Table 30. Calculated and experimentally determined hydrothermal fluid parameters at Hunt mine, Kambalda (from Neall and Phillips, 1987)

Temperature:	350–400°C
Pressure:	0.8–1.8 kb (a)
Composition:	H_2O–CO_2 fluid; X_{CO_2} = 0.18–0.25
Salinity:	2 equiv. wt% NaCl
Na/K:	8 ± 5 (b)
	89 ± 13 (c)
pH:	6.9
fO_2:	$10^{-29.7}$
fS_2:	$>10^{-0.60}$ to $10^{-0.75}$ (decreases from vein to margin of alteration halo)
Gold in solution:	0.5 ppm as $Au(HS)_2^-$
	10^{-6} ppm as $AuCl_2^-$
Fluid/rock ratios:	10–100

(a) Clark et al. (1988) estimated pressures of 2–3 kb for Victory–Defiance
(b) the preferred value, derived from fluid-inclusion studies (Ho, 1987)
(c) derived from thermodynamic calculations, subject to possible errors

12854—8

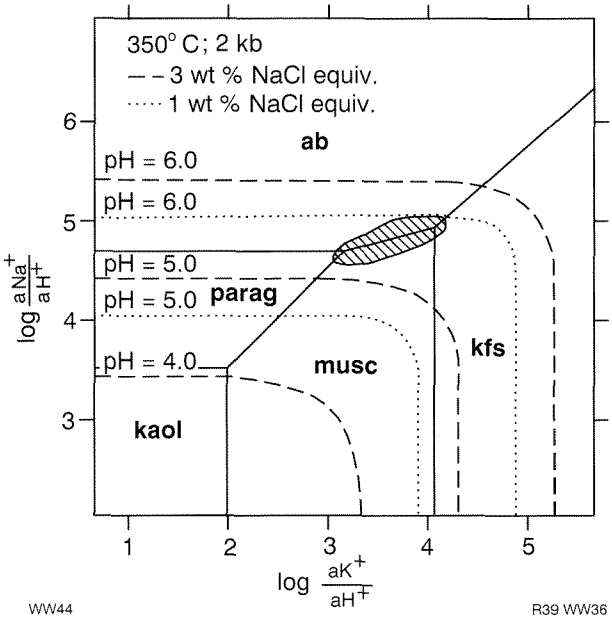

Figure 36. Stability relations in the system K_2O–Na_2O–Al_2O_3–SiO_2–H_2O–HCl at 350°C and 2 kb (from Mikucki and Groves, 1990). The shaded area corresponds to the field of compositions for most ore fluids responsible for gold deposits in sub-amphibolite facies rocks. pH contours are given for 3 wt% NaCl (long-dashed lines) and 1 wt% NaCl (short-dashed lines). Abbreviations: ab = albite; kaol = kaolinite; kfs = K-feldspar; musc = muscovite; parag = paragonite

Oxygen fugacity and sulfur fugacity

Oxygen and sulfur fugacity (fO_2 and fS_2) of the fluids tends to be buffered by reactions between chlorite or magnetite, hematite, pyrrhotite, and pyrite (Fig. 37; Clark, 1980; Neall and Phillips, 1987; Mikucki and Groves, 1990). The reducing nature of the hydrothermal fluids is apparent in the widespread reduction of wallrock Fe^{3+} in silicates (mainly amphiboles) and magnetite to Fe^{2+} in sulfide minerals (Kerrich, 1986b; Colvine et al., 1984). However, chemical data presented in Chapter 6 commonly define a trend towards oxidation of wallrocks, particularly within inner zones of alteration. The presence of green (Fe^{3+}-rich) biotite at several deposits (Hannan South, Mt Martin, Camperdown), and of anhydrite locally in the Golden Mile deposits, constitutes further evidence for relatively oxidizing fluids. Fluctuating fO_2 and fS_2 is suggested at a number of deposits by the presence of secondary magnetite which replaces sulfides, silicate minerals, and/or hematite in some mineralized alteration assemblages (e.g. White Hope, Hannans South, Hampton–Boulder, Binduli). The predominance of pyrrhotite in inner and outer alteration zones in high-grade metamorphic environments (e.g. Menzies, Paris) probably reflects the higher temperatures of these alteration environments rather than lower sulfur fugacities.

At 300–400°C, relatively reducing fluids in mines such as the Golden Mile, Mt Charlotte, and Mt Pleasant control equilibrium between coexisting magnetite, pyrrhotite, and pyrite (Fig. 37). The commonly observed sequence from magnetite in unaltered metamorphic assemblages through an outer pyrrhotite-bearing alteration zone to an inner pyritic zone suggests increasing fS_2 towards the centres of mineralized structures at relatively low fO_2, as has been documented in detail at Hunt mine (Neall and Phillips, 1987). A similar increase in fS_2 towards inner alteration zones in the presence of relatively oxidized fluids is suggested for mines such as Lady Bountiful where a sequence from magnetite in unaltered wallrocks passes through a zone of hematite into an inner pyritic zone (Fig. 37).

Based on observations such as these, Mikucki and Groves (1990) concluded that hydrothermal fluids record oxygen fugacities in the range from 10^{-33} to 10^{-37} (approximately) and that sulfur fugacity generally increases inwards, towards the central, more intensely altered zones, where values of $10^{-0.5}$ to 10^{-2} may be typical. Kerrich (1986b) also recognized a relatively wide range of oxidizing to reducing conditions associated with hydrothermal alteration in Canadian Archaean gold deposits.

Summary

In general, the observations made during this study are consistent with previous descriptions of auriferous hydrothermal fluids responsible for Archaean epigenetic gold mineralization. Such fluids are low-salinity, near-neutral pH, slightly reducing to oxidative H_2O–CO_2 fluids containing significant amounts of K, S, and Au, in addition to NaCl (Phillips and Groves, 1983; Smith et al., 1984; Kerrich, 1986b; Robert and Kelly, 1987; Colvine et al., 1988). Although there is general agreement on the nature of the hydrothermal fluids in all Archaean gold provinces, some outstanding problems remain, at least in the Menzies–Kambalda region. They are:

(a) Conclusions are based on data which are strongly biased towards deposits in lower- to upper-greenschist facies metamorphic domains. There is an urgent need for fluid inclusion, thermodynamic, and isotopic studies to characterize the composition of fluids responsible for deposits in higher grade metamorphic rocks, such as those at Siberia and Menzies.

(b) Albitization in ultramafic to mafic rocks can probably be explained in terms of evolving or fluctuating Na/K ratios (and temperature) of the low-salinity, H_2O–CO_2 hydrothermal fluid. However, the more thorough and pervasive albitization of small felsic porphyry bodies is more difficult to explain in these terms. Kerrich (1986b) suggested sea-floor spilitization due to convecting oxidative seawater to explain sodic porphyries associated with gold mineralization in Canada. However, the late timing of secondary albite, and its close association with the mineralizing event (chapter 5), suggest that albitization of porphyries is caused by the same fluids that produced potassic alteration in mafic rocks, and that host-rock controls such as those proposed by Bohlke (1989) are

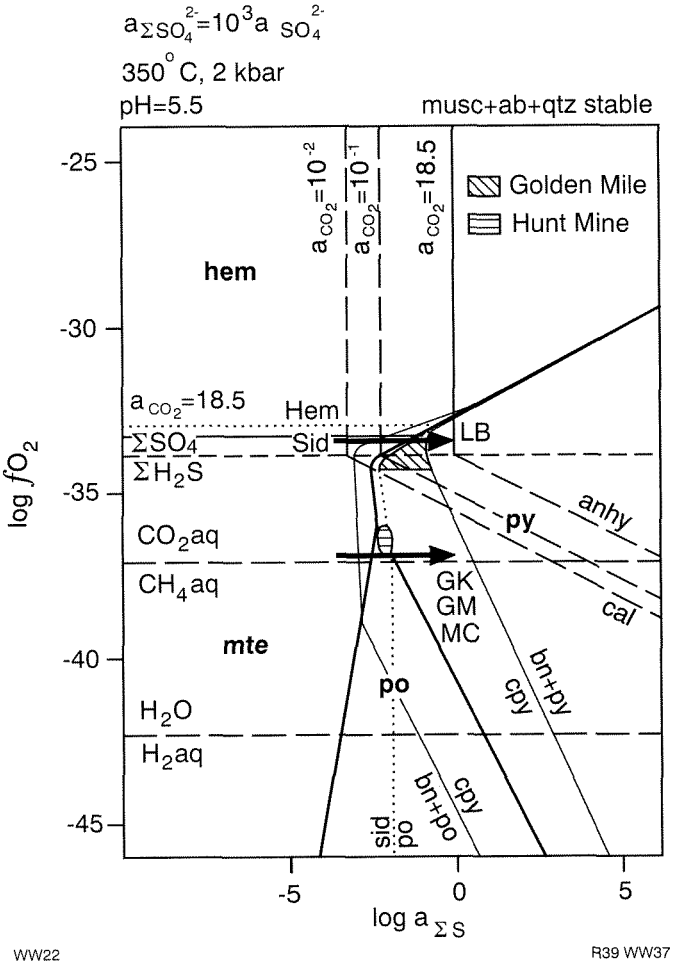

Figure 37. ***Log fO_2–$a_{\Sigma S}$ diagram showing stability fields of alteration minerals in the presence of quartz, albite and muscovite at 350°C, 2 kb and pH = 5.5 (from Mikucki and Groves, 1990). Arrows indicate approximate range of conditions, from metamorphic through outer alteration halo, to inner alteration assemblage at selected deposits.***

LB = Lady Bountiful;
GK = Golden Kilometre;
GM = Golden Mile (main lode system);
MC = Mt Charlotte

The shaded areas are from the original diagram by Mikucki and Groves (1990) and indicate conditions in the inner zone of alteration at Hunt mine, Kambalda (horizontal lines) and in alteration assemblages associated with Oroya-style mineralization, Golden Mile (diagonal lines). Abbreviations: anhy = anhydrite; bn = bornite; cal = calcite; cpy = chalcopyrite; hem = hematite; mte = magnetite; po = pyrrhotite; py = pyrite; sid = siderite

responsible for the stabilization of albite over muscovite (Witt, 1992).

(c) A recent fluid-inclusion study (Bennett, 1989) indicated that low-CO_2 hydrothermal fluids at the Black Flag gold and base metal deposit, Mt Pleasant, were cooler (200–285°C) and more saline (0–11 equiv. wt% NaCl) than the H_2O–CO_2 fluids associated with typical Archaean epigenetic gold deposits.

Transport and deposition of gold

Gold is generally considered to be transported mainly as the $Au(HS)_2^-$ complex in the low-salinity fluids described above (Phillips and Groves, 1983; Colvine et al., 1984; Neall and Phillips, 1987; R.G. Roberts, 1988), based largely on the experimental work of Seward (1973, 1984). The solubility of gold as $Au(HS)_2^-$ with respect to pH and fO_2 is shown in Figure 38.

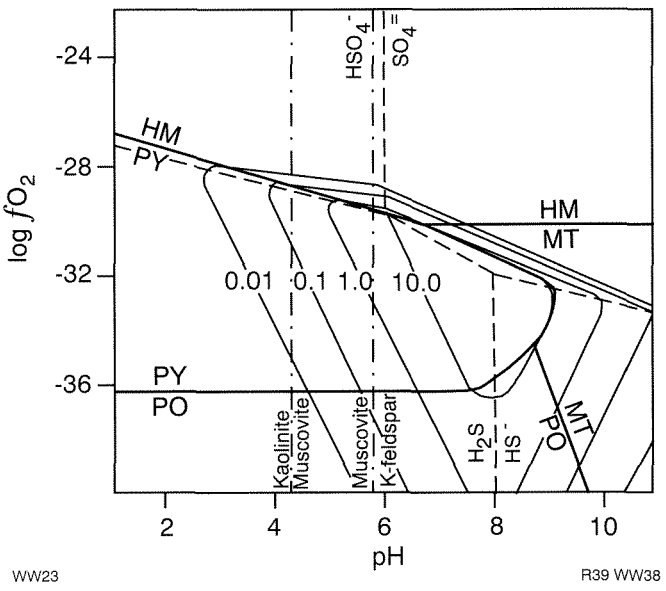

Figure 38. Calculated gold solubilities (as $Au(HS)_2^-$) as a function of pH and log fO_2 (after R.G. Roberts, 1988). Solubility contours are in ppm. Temperature = 300°C and total sulfur = 0.05m. Solubility data from Seward (1973, 1984); equilibrium pH of the K-feldspar–muscovite, and muscovite–kaolinite hydrolysis reactions derived from the thermodynamic data of Helgeson (1969). Abbreviations: HM = hematite; MT = magnetite; PO = pyrrhotite; PY = pyrite

The main depositional mechanism emphasized by Phillips and Groves (1983), Neall (1987), and Neall and Phillips (1987) is the reaction of gold thiosulfide complexes with Fe-rich wallrocks to precipitate iron sulfides and gold. Colvine et al. (1984) emphasized that this is a reductive process that is balanced by oxidation of hydrothermal fluids, a reaction which further promotes the precipitation of gold (Fig. 38). The widespread occurrence of sulfide-rich gold deposits in Fe-rich tholeiitic basalt and doleritic rocks in the Menzies–Kambalda region is consistent with such a mechanism. However, many deposits also occur in granitic and ultramafic rocks which do not contain a large amount of iron, and some of these deposits do not contain large amounts of sulfide minerals. Bohlke (1988) suggested that total Fe contents are less important than high Fe/Mg ratios for deposition of gold in granitic rocks. High Fe/Mg ratios stabilize pyrite, with respect to carbonate minerals, in granitic rocks which equilibrate with auriferous hydrothermal fluids. However, if the degree to which gold is concentrated is proportional to the amount of sulfide deposited, mineralization is limited by the absolute amount of Fe available in the granite, which is low.

Mineralized granitic plutons such as the Liberty Granodiorite display mineralogical evidence, including abundant accessory magnetite, titanite, epidote, and green biotite, that indicates relatively oxidizing late- to post-magmatic conditions (Witt and Swager, 1989b). The metasomatic mineralogy associated with mineralization in some granitic rocks (hematite at Binduli, Lady Bountiful; green biotite at Yunndaga) suggest that alteration occurred under relatively oxidized conditions. Interaction of hydrothermal fluids with the granitic host rock causes reduction of Fe^{3+} in magnetite and mafic minerals (epidote, hornblende, biotite), and oxidation of the fluids. As noted by Colvine et al. (1984), oxidation of hydrothermal fluids will lead to a rapid decrease in the solubility of $Au(HS)_2^-$ (Fig. 38). Oxidation of ore fluids, combined with some pyrite formation in the wallrocks, may be a sufficient mechanism for the deposition of gold in granitic rocks.

Carbonation of wallrocks would cause fluid pH to decrease, decreasing stability of $Au(HS)_2^-$, but the wide spacing of solubility contours (Fig. 38) suggests that this is not an efficient mechanism for concentrating gold. If acidification of the fluid does play a role, it is likely to be most effective in ultramafic rocks which fix large quantities of CO_2 as secondary carbonate minerals. Phase separation occurred in hydrothermal fluids associated with some Archaean epigenetic gold deposits (Ho, 1987; Robert and Kelly, 1987), and could lead to removal of H_2S as well as CO_2, thereby destabilizing gold thiocomplexes and precipitating gold.

Phase separation would be favoured by rapid loss of confining pressure during the hydraulic fracturing of wallrocks, a widespread process in the generation of mineralized structures in the Menzies–Kambalda region. Ultramafic-hosted mineralization in high-strain zones may be dependent upon hydraulic fracture of carbonated wallrocks, rapid pressure release, and consequent boiling

or effervescence of hydrothermal fluids. However, phase separation in the relatively dilute hydrothermal fluids implicated in Archaean gold mineralization is unlikely at T > 400°C, for P = 2 kb (Bowers and Helgeson, 1983).

Another, less efficient mechanism which might be considered is the reduction of fluids by reaction with carbonaceous sediments such as interflow black shales.

Isotopic data

Isotopic data have been widely used to constrain models for the origin of hydrothermal fluids responsible for Archaean epigenetic gold mineralization. In this section, the limited data pertaining to the Menzies–Kambalda region are presented, and compared with similar data from other Archaean gold provinces.

Oxygen and hydrogen isotopes

Oxygen isotope data are available for Mt Charlotte, Golden Mile, Victory–Defiance, Hunt, Lady Bountiful, and Black Flag; and hydrogen isotope data have also been collected from Mt Charlotte and Victory–Defiance. Results published by Golding and Wilson (1987), Golding, Barley et al. (1990), and Bennett (1989) are summarized in Table 31. $\delta^{18}O$ of vein quartz from Canadian gold deposits (Colvine et al., 1988; Kerrich, 1986b; Kerrich et al., 1987) overlap the range of data from the Menzies–Kambalda region (excluding Black Flag) but extend to higher values (+10 to +16‰), a fact which may reflect the broader geographical spread of the more extensive Canadian data. Similarly, the range of calculated $\delta^{18}O$ of ore fluids is somewhat broader for Canadian deposits (+5 to +12‰). The relatively restricted range of $\delta^{18}O$ data (excluding Black Flag), independent of host rock lithology, and consistent over a vertical range of hundreds of metres, has been interpreted to indicate a homogeneous, externally derived ore fluid and high fluid/rock ratios (Kerrich 1986b; Golding and Wilson, 1987; Colvine et al., 1988). The calculated $\delta^{18}O$ fluid values are consistent with either a metamorphic, mantle, or magmatic origin but are incompatible with most fluids of meteoric or marine origin.

The low $\delta^{18}O$ fluid values associated with the Black Flag deposit contrast with most other Archaean gold deposits, and have been interpreted by Bennett (1989) as indicating meteoric water or seawater.

Carbon isotopes

Carbon isotope data from carbonate minerals in mineralized environments at Mt Charlotte, Golden Mile, Victory–Defiance, Hunt, and Lady Bountiful are presented in Table 32. Golding et al. (1987) presented more extensive carbon isotope data, including samples

Table 31. Summary of oxygen and hydrogen isotope data for gold mines in the Menzies–Kambalda region

Deposit	*Quartz* $\delta^{18}O$ (‰)	*Carbonate* $\delta^{18}O$ (‰)	*Chlorite* δD (‰)	*Model temperature*	*Calculated fluid composition* $\delta^{18}O$ (a) (‰)	$\delta^{18}O$ (b) (‰)	δD (‰)
Mt Charlotte							
quartz veins	11.4 ± 5	10.4 ± 1.1		350° ± 50°C	6 ± 2	6 ± 2	
wallrocks		10.4 ± 1.3		350° ± 50°C		6 ± 2	
Golden Mile							
No. 4 lode (centre)	13.4 ± 0.1	13.3 ± 0.7		300° ± 50°C	6.5 ± 2	8 ± 2	
No. 4 lode (wallrocks)		12.4 ± 0.6		300° ± 50°C		7 ± 2	
Hunt							
quartz veins	12.8 ± 0.9						
wallrocks		11.0 ± 0.3					
Victory–Defiance							
quartz veins	12.1 ± 0.5			350° ± 50°C	7 ± 2		
wallrocks		11.1 ± 2.2	–73 ± 10	350° ± 50°C		7 ± 3	–30 ± 12
Lady Bountiful							
quartz veins		13.1 ± 2.0					
Black Flag							
quartz in complex quartz breccia	9.4 ± 1			250°–270°C	–0.1 ± 1		

(a) calculated from silicate data
(b) calculated from carbonate data

Data from Golding and Wilson (1987) — compiled from Golding (1982, 1984); Golding and Wilson (1983); Golding, Barley et al. (1990); Golding, Clark, et al. (1990). Black Flag data from Bennett (1989)

Table 32. Summary of carbon isotope data from gold mines in the Menzies–Kambalda region

Deposit	*No. of samples*	$\delta^{13}C‰$ *Range*	*Mean (± std dev)*	*Median*
Mt Charlotte (excluding outliers)				
Reward orebody	20	−7.6 to −1.6	−5.7 ± 1.8	−6.1
Charlotte orebody	36	−7.9 to −2.8	−5.9 ± 1.3	−6.1
Golden Mile				
No. 4 lode	21	−4.1 to +1.5	−3.3 ± 0.6	−3.5
N. Kalgurli main lode	16	−3.8 to −3.1		−3.3
N. Kalgurli flat lode	4	−6.7 to −0.2		−2.7
Victory–Defiance				
dolerite	5	−7.4 to −4.4	−6.1 ± 1.6	−7.0
porphyries	22	−8.7 to −4.6	−7.1 ± 1.3	−7.3
lamprophyre (diorite)	3	−7.0 to −4.5	−5.7 ± 1.3	−5.6
Hunt mine				
basalt	3	−6.4 to −4.4	−5.3 ± 0.9	−4.7
porphyries	8	−6.6 to −4.7	−5.1 ± 0.6	−5.1
Lady Bountiful	6	−5.8 to −5.1		−5.6

Data from Golding et al. (1987), and McNaughton, Barley et al. (1990)

representing sea-floor alteration, district-scale alteration, and regional carbonation in large-scale shear zones. Only alteration carbonates directly related to gold mineralization are considered here, but the significance of the more extensive carbon isotope data is considered in Chapter 8. Calculated $\delta^{13}C$ for the fluid depositing carbonate minerals at 350 ±50°C in gold-related alteration assemblages is -5 ±3‰, comparable to that calculated for fluids in carbonated regional shear zones (-4.6 ±1‰). Isotopic data for carbonates in gold-related alteration assemblages in the Canadian Abitibi belt (Colvine et al., 1988; Kerrich et al., 1987) are broadly similar to those determined for the Menzies–Kambalda region.

The calculated $\delta^{13}C$ signature of the auriferous hydrothermal fluids is consistent with, and generally interpreted as having, a predominantly mantle derivation. Kerrich et al. (1987) did not rule out a contribution from mantle CO_2, but suggested degassing of CO_2 from the lower crust during regional tectonism as an alternative source. The lower crustal carbon is thought to have been originally derived from the hydrosphere during sea-floor spilitization of mafic volcanics. Groves et al. (1988b) argued that carbon isotope data from gold-related carbonates are incompatible with derivation of carbon from spilitized greenstones, and suggested that the carbon is derived from reworking of mantle-derived carbonate in regional shear zones.

Variation of carbonate C isotopes between different mines (provinciality) is interpreted as resulting from variation in the proportions of oxidized and reduced carbon species in solution (Groves et al., 1988b); variable mixing of seawater-derived and mantle-derived carbon (Groves et al., 1988b; Kerrich et al., 1987); or Raleigh fractionation of isotopes during progressive depletion of CO_2 from the fluid (Fyon, 1986, cited in Colvine et al., 1988).

Sulfur isotopes

Sulfur isotope data from mines at Kalgoorlie and Kambalda are summarized in Table 33 (after Lambert et al., 1984). The data are quite variable. Most Western Australian Archaean gold deposits contain pyrite with $\delta^{34}S$ in the range +1 to +4‰, but pyrite from the Golden Mile displays anomalously light sulfur isotope values. Colvine et al. (1988) recorded a similar range of sulfur isotope data for Canadian Archaean gold deposits. Positive $\delta^{34}S$ in pyrite has been interpreted as indicating derivation of sulfur from the greenstones by reducing fluids (Lambert et al., 1984). The large range of isotopic data is thought to reflect sulfur isotope partitioning between oxidized and reduced sulfur species in the hydrothermal fluid (Cameron and Hattori, 1987; Colvine et al., 1988) rather than diverse sources of sulfur. For example, Lambert et al. (1984) interpreted the negative $\delta^{34}S$ in pyrite from the Golden Mile as recording the oxidation of hydrothermal fluids during extensive and prolonged interaction with the magnetite-bearing, Fe-rich quartz dolerite host rock.

Strontium isotopes

Kerrich et al. (1987) presented Sr isotope data for calcium-bearing metasomatic minerals (tourmaline, scheelite, actinolite, piemontite) from a number of mines in the Abitibi greenstone belt of Ontario, but there is at present very limited information for gold deposits in the Menzies–Kambalda region. Whole-rock Sr isotope data

Table 33. Summary of sulfur isotope data for gold mines in the Menzies–Kambalda region

Deposit	*Sulfide*	*No. of analyses*	$\delta^{34}S$ *Average*	$\delta^{34}S$ *Range*
Mt Charlotte	pyrite	5	+2.5	+1.0 to +4.2
Golden Mile				
Main lode system	pyrite	10	–4.2	–1.6 to –7.0
Telluride ore	pyrite	2	–4.8	–4.5 to –5.2
Hunt mine	pyrite	3	+6.0	+4.4 to +8.0

Data from Lambert et al. (1984)

Table 34. Summary of strontium isotope data for gold mines in the Menzies–Kambalda region

Deposit	*Average of n samples*	*Rb*	*Sr*	*K/Rb*	$^{87}Sr/^{86}Sr \pm 2\sigma$
Hunt mine					
least-altered basalt	4	<1	103	0.08	0.70193 ± 0.00001
K-metasomatized basalt, remote from veins	5	115	233	238	0.71818 ± 0.00002
K-metasomatized basalt, adjacent to veins	4	41	273	379	0.71362 ± 0.00001
Auriferous vein carbonate (a)	3	n.a.	n.a.	n.a.	0.70187 ± 0.00002

n.a. not analyzed
(a) All data from whole-rock samples, except auriferous vein carbonate
Data from McNaughton, de Laeter et al. (1988)

from Hunt mine at Kambalda are summarized in Table 34. McNaughton et al. (1988b) interpreted data from the Hunt mine as being consistent with derivation of Sr and alkalis from the thick underlying basalt sequence, or from lower crustal granulites or greenstones. Kerrich et al. (1987) interpreted the Canadian data to suggest that Sr was derived from a heterogeneous lower crust.

Pb isotopes

McNaughton and Dahl (1987), Dahl et al. (1987), Browning et al. (1987), Bennett (1989), and McNaughton et al. (1990b) presented Pb isotope data for sulfide minerals (galena, pyrite) from several deposits within the Menzies–Kambalda region. Dahl et al. (1987) and Browning et al. (1987) derived maximum model Pb ages of 2750 Ma for this group of mines.

Linear uranogenic Pb isotope arrays at Mt Charlotte, Golden Mile, and Hunt were interpreted as due to mixing of Pb from the host rock and Pb introduced by the mineralizing fluid (Dahl et al., 1987). There is some evidence to suggest that the latter was derived from sialic basement. Mixing lines converged to a common point on the ^{208}Pb–^{206}Pb–^{204}Pb mantle growth curve, suggesting synchronous mineralization at each of the three deposits, a few tens of millions of years after formation of the greenstones. Very young model ages for the Zuleika deposit are not well understood but may be due to resetting of isotopes during minor thermal events and activity on the Zuleika Shear. McNaughton and Cassidy (1990) and McNaughton et al. (1990b) extended the Pb isotope data base to Lady Bountiful, Golden Kilometre, Racetrack (Mt Pleasant), and Victory (Kambalda) and concluded that data are compatible with synchroneity of mineralization at all deposits so far investigated (excluding Black Flag), within the precision of analysis (about 30 Ma). Initial Pb isotope ratios for most deposits at Mt Pleasant, Kalgoorlie, and Kambalda 'cluster' together on a crustal mixing line at c. 2.63 Ga, but deposits near Menzies display relatively radiogenic Pb isotope ratios (McNaughton et al., 1990b).

Galena from the Black Flag deposit is more radiogenic than galena from Lady Bountiful, Golden Kilometre, and Racetrack, and can be modelled to yield a younger age. Assuming an age of 2.63 Ga for the main group of deposits (from the U–Pb rutile age reported at Victory by Clark et al., 1988), a model age of c. 2.54 Ga for the Black

Flag deposit is deduced (Bennett, 1989). Although de Laeter (unpublished data) arrived at a different age using another model, he also concluded that Black Flag mineralization was (about 60 Ma) younger than mineralization at Golden Kilometre.

Chapter 8

Timing relationships between deformation, metamorphism, and mineralization

Timing of gold-related alteration with respect to deformation

All gold deposits documented in this study (excluding some within surficial deposits) are structurally controlled. It is therefore unlikely that alteration predated formation of the ore-controlling structures. Woodall (1979) suggested that the Golden Mile deposits formed by infiltration of mineralizing fluids into pre-existing structures (the concept of 'prepared ground'). This was rejected by Boulter et al. (1987) who argued that strain-induced textural modification of alteration minerals indicated that mineralization occurred during formation of the mineralized structures. The following observations made on a broad spectrum of deposits during this study indicate that gold-related alteration took place during formation of the mineralized structures, or at least while the mineralized structures were still active. Locally and regionally, metasomatic minerals continued to form up to the latest stages of deformation.

(a) Alteration is intimately associated with quartz veining and brecciation in most deposits. The dominant mode of vein formation within low-strain domains and in shear zones, was hydraulic fracture, including crack-seal deformation (see Chapter 4). Textures indicative of open-space deposition in pre-existing fractures are not common — with the exception of the Black Flag deposit near Mt Pleasant. Early-formed veins in mineralized brittle–ductile shears are commonly folded or brecciated by progressive deformation (PLATES III, G; V, E and VI, E) but later-formed veins post-date the shear fabric (PLATES III, B–D).

(b) Metasomatic phyllosilicate minerals (chlorite, talc, muscovite, biotite) display a variety of textures, but are commonly oriented in spaced, anastomosing seams which form a shear fabric of variable intensity (PLATES IX, A–H). Where two or more phyllosilicate minerals occur together, the degree of orientation is commonly variable. For example, biotite and talc are commonly more randomly oriented than chlorite (PLATE IX, G) suggesting that crystallization of those minerals outlasted chlorite growth. Elsewhere, porphyroblasts of undeformed biotite or muscovite overprint earlier phyllosilicate shear fabrics (PLATES IX, C and H). Phyllosilicate alteration minerals are also commonly deposited in the pressure shadows of idioblastic sulfide minerals (PLATE X, E).

(c) Carbonate minerals exhibit varying degrees of deformation (microfaulting, kinking of twins, etc.), pressure solution and recrystallization. Early carbonate veins or schistosity-controlled carbonate bands may be broken up or folded during progressive deformation (PLATE V, E). Later carbonate forms undeformed, rhombohedral porphyroblasts (PLATE XII, D).

(d) Opaque minerals display a variety of textural habits — depending upon their timing with respect to progressive deformation. Metamorphic oxides such as ilmenite become recrystallized in highly strained rocks, ultimately forming trails of fine disseminations in the plane of the foliation (PLATE X, A–B). Where pyrrhotite occurs in highly strained rocks, it commonly exhibits a form similar to that of ilmenite, suggesting its introduction at an early stage during progressive deformation (PLATE X, B, F, G). Recrystallization of pyrrhotite-bearing assemblages in higher grade metamorphic rocks may modify the texture so that pyrrhotite occurs interstitial to neoblastic amphiboles (PLATE X, D). More commonly, trails of disseminated pyrrhotite and ilmenite are preserved within the neoblastic amphibole (PLATE X, C). By contrast, arsenopyrite is almost uniformly idioblastic in form, even in highly strained rocks (PLATE X, G). However, small pressure shadows develop adjacent to idioblastic pyrite and arsenopyrite in many cases (PLATE X, E) suggesting minor movement continued after crystallization of the idioblastic sulfides. Phillips et al. (1988) related pyrite morphology to the degree of recrystallization undergone during progressive deformation. Pyrite forms idioblastic porphyroblasts where unmodified by progressive deformation (e.g. PLATES X, E–F) but tends to form fine-grained trails and disseminations where progressive deformation has caused recrystallization.

The textural features of minerals intimately associated with gold mineralization suggest they were not all present prior to the onset of deformation. Nor were they all introduced into pre-existing structures after deformation had ceased. On the contrary, the wide variety of textural habits displayed by metasomatic minerals indicates that they were introduced progressively during the deformation which produced the ore-bearing structures. Sibson et al. (1975) have shown that seismic pumping during movement on fault zones is a very efficient way of moving large volumes of fluid through the Earth's crust.

It is concluded that auriferous hydrothermal fluids gained access to mineralized structures forming or active during D_3 and D_4 (Chapter 4) and reacted with the host rocks to produce the observed metasomatic assemblages. Furthermore, in many cases high fluid pressure during this deformation actively contributed to the formation of the mineralized structures.

Timing of gold-related alteration with respect to metamorphism

Figure 39 shows the distribution of four idealized alteration assemblages in mafic rocks associated with gold mineralization in the Menzies–Kambalda region (Table 19). Comparison between Figures 39 and 13 demonstrates a reasonable correlation between alteration assemblages and regional metamorphic grade which, as discussed in Chapter 2, is a reflection of several factors, including the stratigraphic depth of crust exposed, and proximity to syntectonic, synmetamorphic granitoids.

North of Kalgoorlie, alteration assemblages are clearly related to distance from syn-D_3 diapirs at Siberia and Menzies where biotite is the dominant form of K in alteration assemblages in high-grade aureoles. Very high-grade alteration assemblages containing microcline occur in middle to upper-amphibolite facies rocks in the immediate aureole of the Jorgenson Monzogranite at Menzies. The importance of syn-D_3 diapirs is also apparent around Coolgardie (Fig. 13) where alteration assemblages are characterized by the presence of biotite.

South of Kalgoorlie, the relationship between higher grade alteration assemblages and syn-D_3 granitoids is less clear. Biotite-bearing assemblages at Celebration and Kambalda probably reflect higher grade metamorphic host rocks, related to the presence of syn-D_3 diapirs east and west of Kambalda (Figs 13 and 39). Highest grade alteration assemblages in the Celebration area are difficult to explain, but may reflect the presence of a syn-D_3 granite at depth. Keats (1987) interpreted aeromagnetic data as suggesting the presence of unexposed granites between Kalgoorlie and Celebration, but there is little aeromagnetic evidence to indicate the presence of granite directly beneath Celebration.

Areas containing gold mines with characteristic alteration assemblages are separated by lines interpreted as metamorphic isograds (Plates 1A, B; Fig. 39). Consideration of mineral phases which become stable or unstable in assemblages which characterize progressively higher grade metamorphic rocks suggest isograds 1, 2, and 3 correspond to reactions 14, 21, and 30 (Table 23), respectively. These reactions may not actually take place but they do control critical assemblages which result from reaction between mafic rocks and the hydrothermal fluids.

Pre- to syn-D_2 granitoid domes and late-tectonic granitoids appear to have little influence on the position of the alteration isograds, consistent with their earlier and later timing, respectively, with respect to peak regional metamorphism and gold mineralization. Note that high P_{CO_2} in the Bardoc Tectonic Zone is apparently responsible for a marked inflection in isograd 1, defined by relatively low-grade assemblages at Excelsior and Zoroastrian, whereas biotite dominates deposits in adjacent, less deformed greenstones (e.g. Wycheproof, Eureka). The biotite-dominant assemblages in upper-greenschist to lower-amphibolite facies rocks east of the Bardoc Tectonic Zone may reflect uplift of the eastern greenstones across this fault.

Many authors have followed the example of Phillips (1986) in interpreting the replacement of metamorphic minerals (especially amphiboles) by metasomatic minerals in the outer margin of the alteration halo at gold deposits as an indication of post-peak metamorphic (retrograde) alteration. However, the work of Clark et al. (1986) and Colvine et al. (1988) has shown that apparent retrograde assemblages can be stabilized under high P_{CO_2} conditions, even where temperatures are not significantly below those recorded by adjacent regional metamorphic assemblages (Fig. 23). Therefore, other evidence such as fluid inclusion, mineralogical, and isotopic data should be sought when attempting to establish timing relationships between regional metamorphism and gold-related metasomatism.

Bavington (1979), Wong (1986), and Roberts and Elias (1990) indicated that lower amphibolite facies metamorphism at Kambalda peaked at 520 ± 20°C and 2.5 ± 1 kb. Fluid-inclusion data indicate temperatures of 196–325°C and pressures of 0.8–3.3 kb during formation of alteration assemblages associated with gold mineralization at Hunt mine (Ho, 1987). Calculated and experimental stability fields of metasomatic minerals associated with gold mineralization at Victory–Defiance suggest hydrothermal conditions of 410 ± 40°C and 2 kb (Clark et al., 1986, 1988). When combined with textural relationships between regional metamorphic minerals and metasomatic minerals, these data indicate that alteration associated with auriferous fluids at Kambalda was retrograde with respect to peak regional metamorphism.

Similarly, at Kalgoorlie, middle to upper-greenschist facies metamorphism (Phillips, 1986) implies regional metamorphic temperatures of 350–450°C at 2–4 kb, if the greenschist/amphibolite facies transition is taken to be 450–500°C at the same pressures (Moody et al., 1983). Temperatures determined from fluid inclusions associated with mineralization at Mt Charlotte and the Golden Mile (Lake View lodes and telluride lodes) fall in the range 196–360°C, at pressures of 1.5–4.0 kb (Ho, 1987). These values are also retrograde with respect to peak regional metamorphism.

In some other areas there is textural and mineralogical evidence for metamorphic recrystallization of alteration assemblages ('prograde' metasomatism). The clearest evidence for metamorphic recrystallization is the presence of late, unoriented amphiboles which grow within and across the predominant schistosity or shear fabric of the altered rock and are interpreted as being the product of decarbonation reactions. Amphiboles with this textural habit occur in both mafic and ultramafic rocks and the composition of the amphiboles reflects the bulk composition of the altered rock. The distribution of late, unoriented amphibole porphyroblasts in altered mafic and

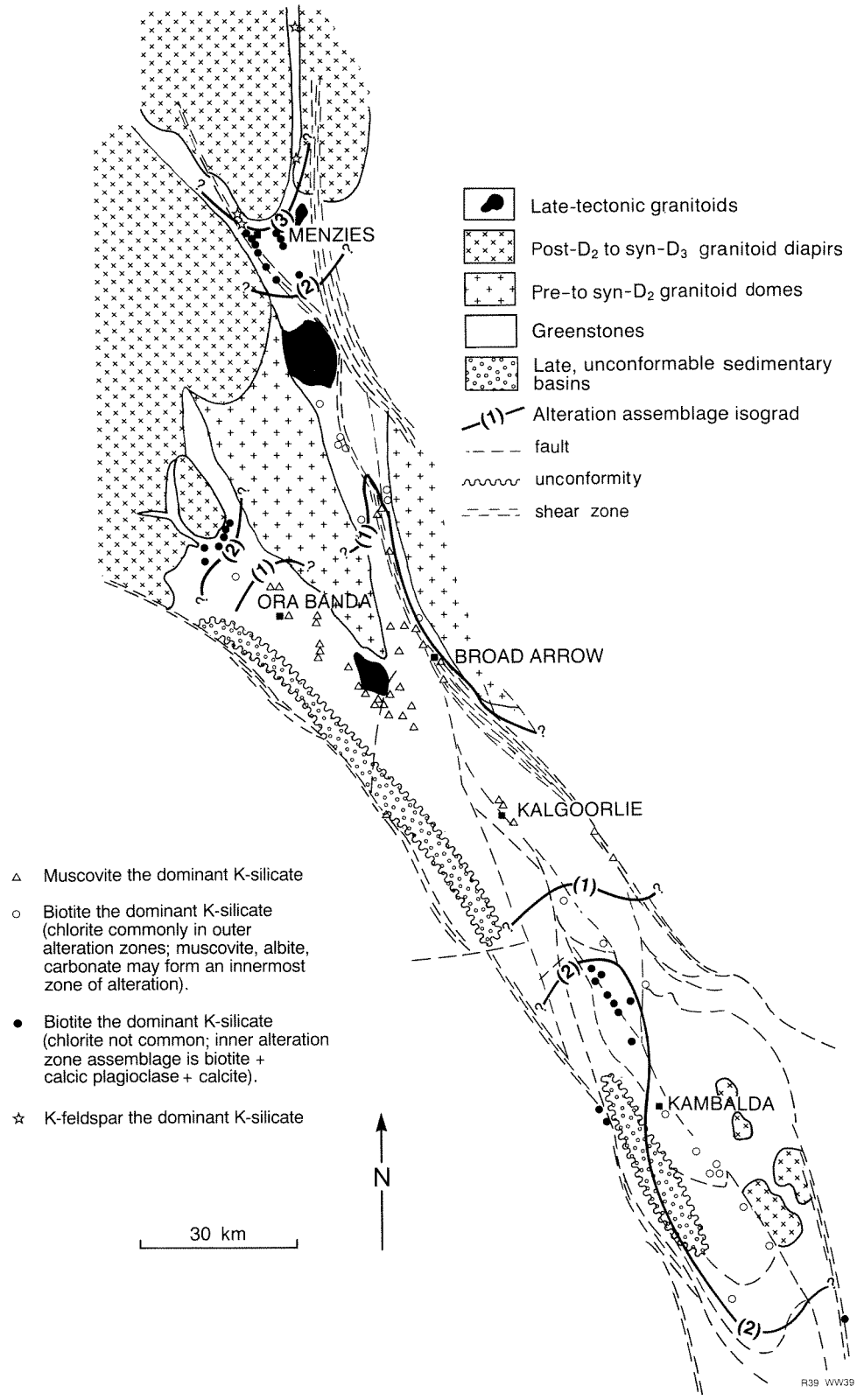

Figure 39. Distribution of alteration assemblages in mineralized mafic rocks in the Menzies–Kambalda region. Isograds (1), (2), and (3) separate alteration assemblages equivalent to or approximating (A), (B), (C), and (D) (Table 19), and represent equilibrium in T–Xco_2 space (at 2–4 kb), probably for the following reactions:

1. **Muscovite + ankerite + quartz + fluid = biotite + calcite + fluid (reaction 14, Table 23);**
2. **Ankerite + chlorite + fluid = anorthite + quartz + fluid (reaction 21, Table 23);**
3. **Biotite + calcite + quartz = microcline + diopside + fluid (reaction 30, Table 23)**

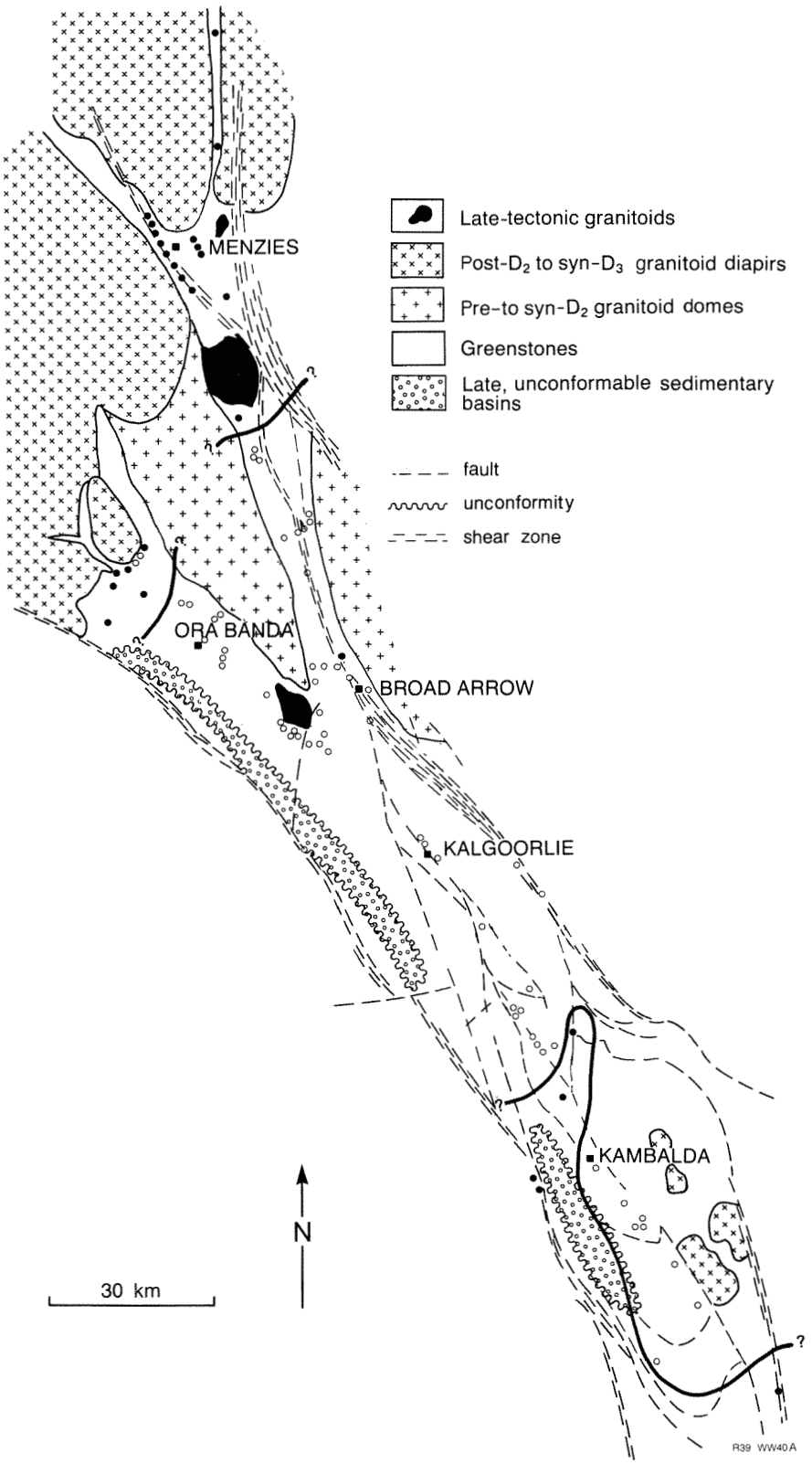

Figure 40. Distribution of metamorphically recrystallized alteration assemblages associated with gold mineralization in the Menzies–Kambalda region. Open circles denote recrystallization textures not observed; closed circles denote recrystallization textures observed.

A. Mafic-hosted gold deposits. Heavy lines show position of isograds interpreted to represent equilibrium in T–Xco_2 space (at 2–4 kb) for one or both of the following reactions:

Anorthite + biotite + quartz + fluid = hornblende + fluid (reaction 27, Table 23);
Chlorite + calcite + quartz = calcic amphibole + anorthite + fluid (reaction 28, Table 23)

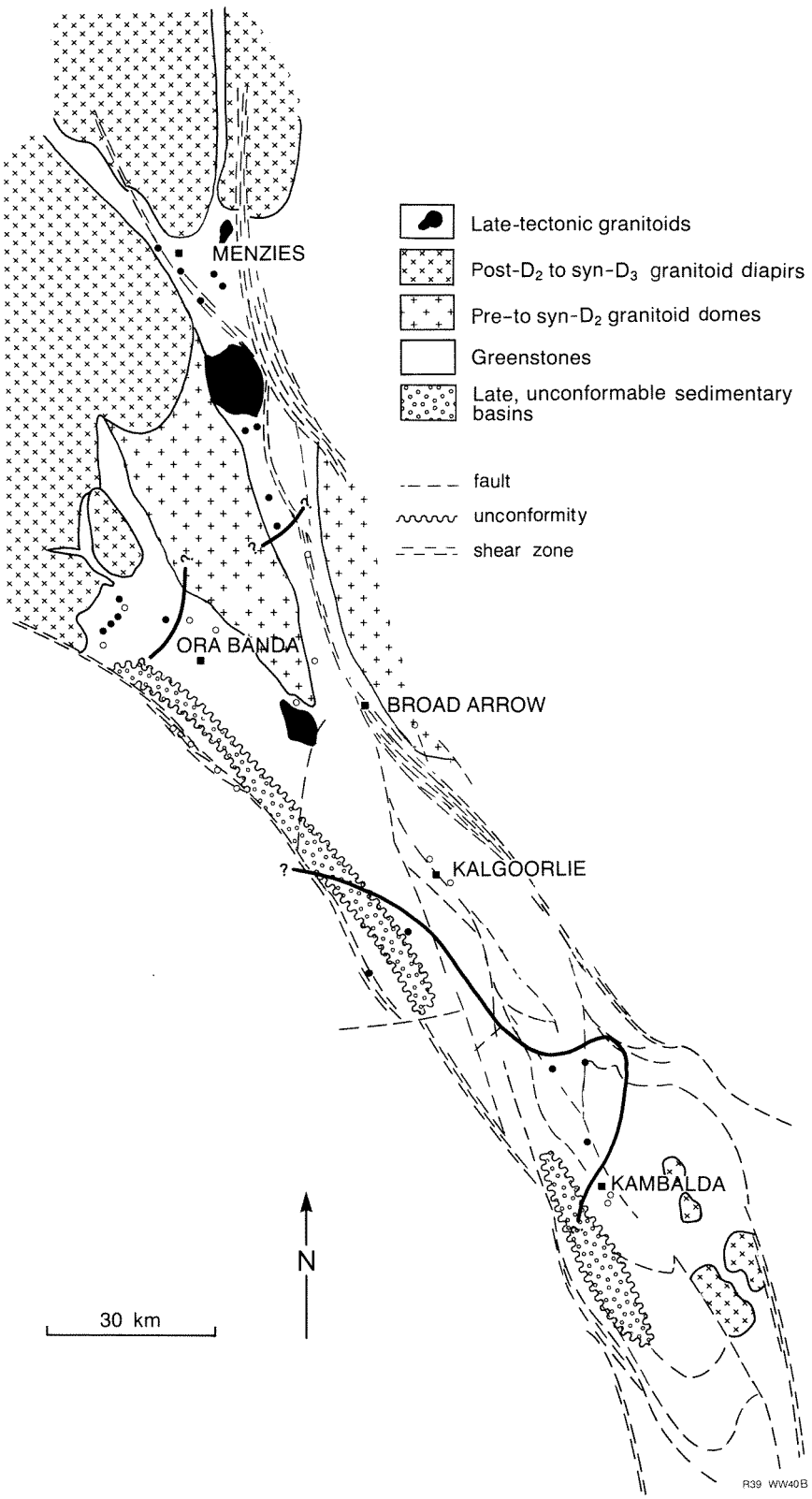

Figure 40B. Ultramafic-hosted gold deposits. Heavy lines show position of isograds interpreted to represent equilibrium in T–Xco_2 space (at 2–4 kb) for one or both of the following reactions:

Talc + calcite + quartz = tremolite + fluid (reaction 1, in reverse, Table 24);
Dolomite + quartz + fluid = tremolite + calcite + fluid (reaction 9, Table 24)

ultramafic rocks is shown in Figure 40. Metamorphic isograds (see Figure captions for suggested reactions) are defined by the distribution of mines which have metamorphically recrystallized alteration assemblages and those that do not. These isograds mimic the alteration assemblage isograds, with metamorphic recrystallization occurring in the high-grade metamorphic aureoles adjacent to syn-D_3 granitoid diapirs. The importance of syn-D_3 diapirs in controlling metamorphic recrystallization is also apparent around Coolgardie, Widgiemooltha, and Dunnsville (Fig. 13), where late, unoriented amphiboles are widespread. The relatively widespread development of tremolite porphyroblasts in altered ultramafic rocks, south of Menzies, suggests that the threshold temperature (at constant Xco_2) for metamorphic recrystallization is lower than for mafic rocks.

Large areas north and south of Kalgoorlie appear to lack late amphibole porphyroblasts, and their presence in the remaining areas of prograde metasomatism is somewhat erratic. For example, in drillhole 320–D1 at Yunndaga (Witt, 1993a, fig. 10), late amphiboles occur in an ultramafic-hosted, mineralized shear zone beneath an arkosic sedimentary unit, but are absent in deeper unmineralized shears in the same ultramafic rocks. Late amphiboles were noted in some ultramafic schists on some of the mine dumps and exploration trenches near the Dawns Hope mine, but not in others. The sporadic development of late amphibole porphyroblasts presumably reflects variable T or Pco_2 of fluids at a specific locality (Fig. 24). Since temperature is likely to be controlled by ambient metamorphic conditions, variable Pco_2 is probably implicated.

The distribution of amphibole porphyroblasts is also irregular within individual structures. For example, in mafic-hosted shears, hornblende porphyroblasts are best developed in the outer alteration zones suggesting that continued activity and high Pco_2 inhibited decarbonation reactions in the shear centres. Conversely, late tremolite is commonly most abundant towards the centres of ultramafic-hosted shears. This distribution may be related to the intense silicification and albitization observed in many ultramafic-hosted shear centres. These styles of alteration may tend to 'weld' the shear centres, which cease to be active, with a consequent fall in Pco_2. Strain would then be partitioned into the phyllosilicate-rich shear margins where high Pco_2 would tend to inhibit formation of amphiboles.

The systematic relationship between mineralization-related alteration assemblages and regional metamorphic grade suggests a fundamental metamorphic control on the origin of the gold mineralization. Since textural observations described earlier in this chapter indicate alteration assemblages are not the products of static metamorphic recrystallization, the regional metamorphic gradients must have been in place during mineralization-related metasomatism. Furthermore, relations among alteration assemblages, regional metamorphic grade, and syn-metamorphic granitoids suggest mineralization was a single event involving a greenstone belt-scale hydrothermal system, centred on synmetamorphic granitic diapirs.

The following points further suggest deposition of gold was a single event, relatively restricted in time, in relation to an extended and complex regional metamorphic history:

(a) As discussed in the previous chapter, the composition of the fluids — as indicated by fluid inclusion data — and the chemistry and mineralogy of the altered wallrocks are relatively uniform, arguing against multiple fluid sources, and multiple mineralization events (excepting Black Flag, and the surficial deposits).

(b) Gold-bearing structures can generally be related to D_3 and D_4 periods of deformation, and textural evidence suggests that the introduction of auriferous hydrothermal fluids occurred during these latest stages in the tectonic evolution of the granite–greenstone terrain.

(c) A single, synchronous gold mineralization event (within 30 Ma) is also indicated by Pb isotope data (Dahl et al., 1987; McNaughton and Cassidy, 1990; and Chapter 7) from the Hunt mine and Victory–Defiance (Kambalda); Golden Mile and Mt Charlotte (Kalgoorlie); and Golden Kilometre and Lady Bountiful (Mt Pleasant). Pb isotope data further indicate craton-wide synchroneity of gold mineralization in the Yilgarn Craton (Browning et al., 1987; McNaughton et al., 1990b). Similarly, U–Pb zircon dating indicates broadly synchronous gold mineralization in different greenstone belts of the geologically similar Superior Province in Canada (Colvine et al., 1988).

The presence of deposits with retrograde alteration assemblages, and others in which alteration assemblages are metamorphically recrystallized, may seem inconsistent with a single mineralizing event. However, there are two possible explanations for these apparently contradictory observations, either or both of which may be relevant to the Menzies–Kambalda region (Fig. 41).

(a) Although broadly coincident with D_3 deformation, peak regional metamorphism may not have been strictly coeval throughout the Menzies–Kambalda region. Regional metamorphic grade was at least partly controlled by proximity to syn-D_3 granitoid intrusions, which were unlikely to have been emplaced at exactly the same time. For example, mineralization at Kambalda may have been retrograde with respect to peak metamorphic temperatures imposed by syn-D_3 granitoids north and south of Widgiemooltha. However, alteration assemblages related to contemporaneous mineralization at Siberia would be recrystallized if nearby granitoids were emplaced later than those at Widgiemooltha. This explanation is represented schematically by pathway A in Figure 24.

(b) Alternatively, mineralization may have been retrograde with respect to peak regional metamorphism throughout the Menzies–Kambalda region, but metamorphic recrystallization was made possible by higher initial temperatures of alteration in thermal aureoles adjacent to syn-D_3 granitoids. For example,

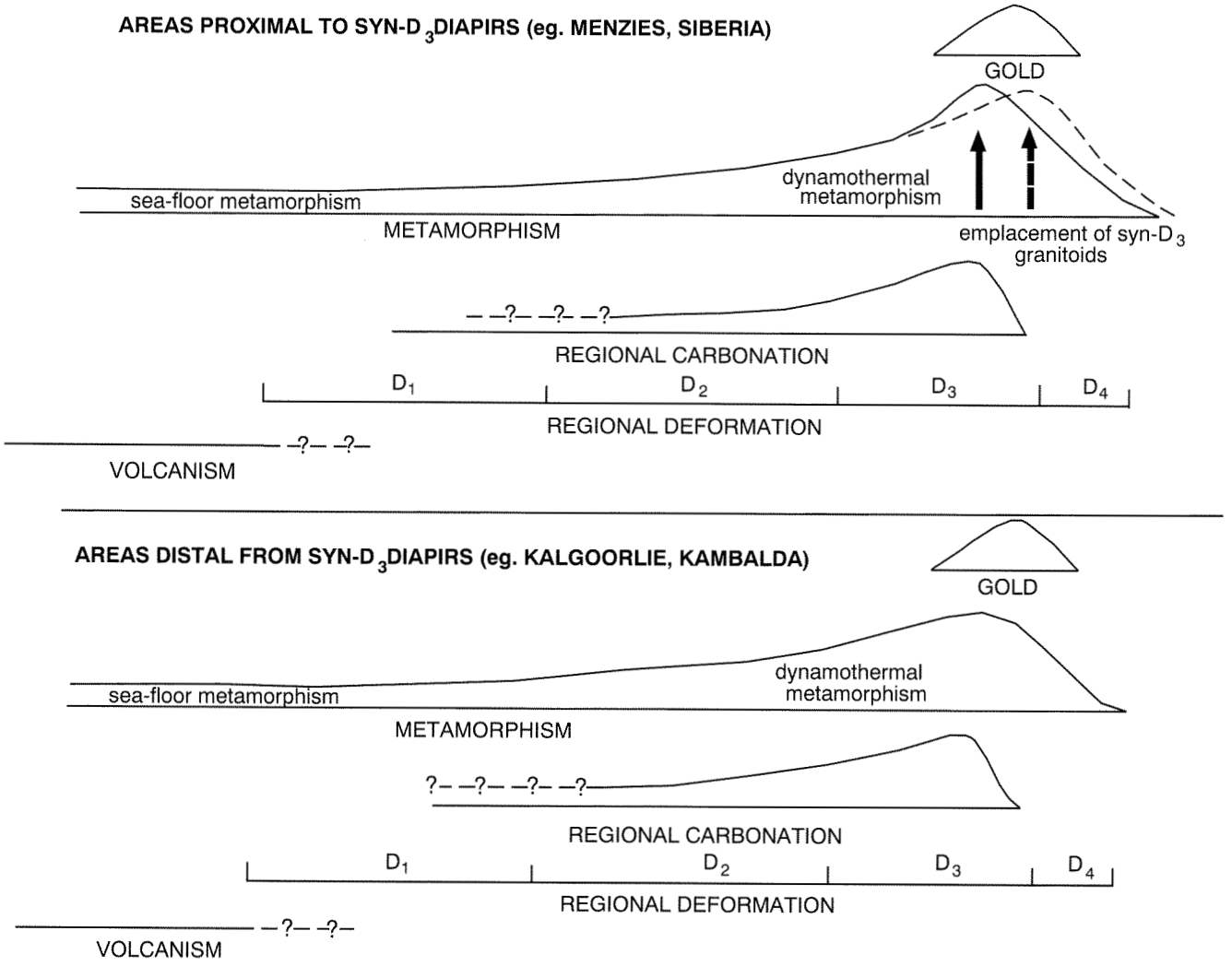

Figure 41. Relative timing of regional events in areas of contrasting metamorphic grade in the Menzies–Kambalda region. Note that the horizontal (time) scale is not uniform. The full and broken lines for metamorphism in areas proximal to syn-D_3 diapirs represent alternative evolutions of metamorphic grade, depending on exact timing of emplacement of the diapirs with respect to gold mineralization

mineral assemblages suggest alteration took place at approximately 500°C at Siberia, and at approximately 400°C at Kambalda. If P_{CO_2} falls as regional metamorphic temperatures decline, consider what may occur at 100°C below initial alteration temperatures. At Siberia, a relatively small decrease in P_{CO_2} at 400°C would be sufficient to promote recrystallization of alteration assemblages (according to pathway B in Fig. 24). At Kambalda, the same small decrease in P_{CO_2} at 300°C would not shift the alteration system into the amphibole stability field, and recrystallization would not occur.

The alteration assemblages and their relationship to syntectonic granitoids, particularly north of Kalgoorlie, are very similar to those described for regionally metamorphosed impure limestones in Maine (Ferry, 1976a). Ferry (1980) also noted irregularities in isograds where they crossed relatively permeable zones of deformation, similar to that which occurs across the Bardoc Tectonic Zone. Ferry's (1980) interpretation of these patterns suggested that the granitic plutons were foci of high heat flow and fluid fluxes during metamorphism. Similarly, it is suggested that syn-D_3 granitoids in the Menzies–Kambalda region were a source of heat (and possibly H_2O-rich fluids) during regional metamorphism and gold-related hydrothermal alteration. The difference is that pervasive introduction of CO_2-rich fluids from a deep source maintained high fCO_2 during metamorphism in zones of deformation in the Menzies–Kambalda region, whereas metamorphism of pre-existing carbonate-rich rocks occurred in Maine.

Summary

This chapter documents relationships between the timing of hydrothermal alteration related to gold mineralization, movement on predominantly D_3 and D_4 structures which control the mineralization, and regional metamorphism. Textural observations indicate that alteration occurred as fluids were introduced into D_3 and D_4 structures as they formed or were reactivated. The mineralogical composition of the alteration assemblages varies systematically with regional metamorphic grade suggesting broad contemporaneity between mineralization and metamorphism. Regional relationships between alteration assemblages, regional metamorphism, and synmetamorphic (syn-D_3) granitoids suggest that all primary deposits (excepting Black Flag) formed during a single mineralizing event which took the form of a greenstone belt-scale hydrothermal system, centred on the syn-metamorphic intrusions. Pb isotope data (McNaughton and Cassidy, 1990) constrain the duration of this system to less than 30 Ma.

Figure 41 summarizes possible timing relationships in areas of prograde (Menzies/Siberia) and retrograde (Kalgoorlie/Kambalda) hydrothermal alteration related to gold mineralization.

Chapter 9

Origin of the hydrothermal fluids and a model for the genesis of epigenetic gold mineralization

Gold mineralization in the Menzies–Kambalda region occurred during the final stages of the tectonothermal evolution of the granite–greenstone terrain. It was broadly coeval with D_3 and D_4 deformation, peak regional metamorphism, and emplacement of syn-D_3 diapirs and late-tectonic granitoid intrusions. Gold mineralization also occurred towards the end of a regional carbonation event which caused pervasive carbonation in regional shear zones and more restricted haloes which envelop mineralized structures in low-strain domains. Gold mineralization in mafic rocks is most closely associated with more restricted zones of potassic alteration and sulfidization which are enveloped by the carbonation haloes. Less strongly mineralized ultramafic rocks are intensely carbonated but display relatively subtle enrichment of potassium and sulfur. Mineralized granitic rocks display similar qualitative trends in alteration geochemistry but quantitative enrichments and depletions are relatively small (Chapter 6) suggesting hydrothermal fluids were close to being chemically equilibrated with granitic rocks. Furthermore, Pb and Sr isotopic data also suggest that hydrothermal fluids equilibrated with granitic crust (McNaughton et al., 1990b).

Isotopic and regional studies indicate that auriferous fluids were part of a large-scale, craton-wide hydrothermal event in which fluids were externally, rather than locally, derived. These conclusions are similar to those reported by Groves et al. (1988a) for the Yilgarn Craton as a whole, and by Colvine (1988) for the Superior Province in Canada.

There is still controversy regarding the source of the hydrothermal fluids responsible for Archaean epigenetic gold mineralization. Recent reviews of possible fluid sources are given by Perring et al. (1987), Groves et al. (1988a) and Colvine et al. (1988). The three main alternatives are assessed below, particularly in terms of the degree to which they are consistent with observations and data from the Menzies–Kambalda region.

Magmatic fluids

Magmatic fluids, derived from late granitoid or porphyry intrusions spatially associated with gold mineralization, have been proposed by Mason and Melnik (1986); Burrows et al. (1986); and Cameron and Hattori (1987).

Porphyry intrusions are intimately associated, i.e. exposed in mine workings, with about 35% of the gold deposits in the Menzies–Kambalda region — significantly less than the 80% reported by Perring et al. (1987) for Western Australia as a whole, and less than the proportion reported by Hodgson and McGeehan (1982) for Canada. Even fewer deposits (about 10%) in the study area are associated with granitic intrusions. Although there are clusters of deposits around some late-tectonic granitoids, mineralization is much more widespread and there is no gradient in size and grade of deposits or metal ratios away from the intrusions. Mineralization shows a much more consistent association with mafic rocks (almost 60% of the deposits).

Cameron and Hattori (1987) noted an association of alteration minerals indicative of oxidized hydrothermal fluids with granitoids which crystallized from relatively oxidized, hydrous and CO_2-rich magmas. They suggested that unmixing of a magmatically-derived fluid produced low-salinity, H_2O–CO_2 auriferous fluids. However, this model overlooks the variable fO_2 of auriferous fluids, which are commonly regarded as reducing (Phillips and Groves, 1983; Kerrich, 1986b; Colvine et al., 1988).

The composition of late-tectonic granitoids with spatially associated gold mineralization varies from leucocratic syenogranite (Fair Adelaide Syenogranite), through biotite–hornblende granodiorite (Liberty Granodiorite) to trondjhemite (Kambalda Granodiorite), but mineralization is consistently related to low-salinity, H_2O–CO_2 fluids. The porphyry intrusives are similarly variable in composition, and furthermore are volumetrically small. It is inconceivable that such small volumes of melt could yield the large volumes of fluid implicated in the mineralizing hydrothermal system. Furthermore, late-tectonic granitoids display little evidence — in the form of internal pegmatoid bodies or pervasive hydrothermal activity — to suggest separation of a significant volatile-rich component.

The solubility of CO_2 in felsic melts is low, and decreases rapidly below 5 kb (Eggler and Burnham, 1973; Eggler, 1974; Holloway, 1976). Although CO_2 could be concentrated from initially low levels by phase separation, evidence for phase separation is commonly lacking in some well-documented deposits. If mineralizing fluids were derived from late-tectonic granitoids, the separation must have occurred at deeper crustal levels than presently exposed, thus implying a model very different from the classical magmatic–hydrothermal models.

Finally, although C and O isotopic data are consistent with a magmatic origin for the fluids, Perring et al. (1987) have pointed out that Pb isotope data from Hunt mine is incompatible with derivation from the nearby Kambalda Granodiorite.

Metamorphic fluids

A metamorphic origin for mineralizing fluids, produced by devolatilization of greenstones below the amphibolite–greenschist facies boundary, has been advocated by Kerrich and Fryer (1979); Kerrich and Fyfe (1981); and Groves et al. (1984, 1987). A high geothermal gradient, indicated by low-pressure metamorphism in the Menzies–Kambalda region, is required to promote devolatilization and prevent melting of deep crustal rocks. More recent models published by Groves et al. (1988a) have modified the original metamorphic model to allow for a possible contribution from deeper seated fluids derived from the lower crust and/or mantle.

Low-salinity, CO_2–H_2O fluids are common in some metamorphic rocks, particularly at higher metamorphic grades (Hollister and Burruss, 1976; Crawford, 1981; Touret, 1981). The craton-wide gold mineralization, the apparent focussing of fluids through deep crustal structures (regional shear zones), and O isotope data are compatible with a metamorphic origin for the fluids. The main problems with the original metamorphic model include the following:

(a) The occurrence of large gold deposits — Big Bell (Chown et al., 1984; Phillips and DeNooy, 1988) and Hemlo (Cameron and Hattori, 1985), and smaller examples (Twin Hills, St Albans) in the Menzies–Kambalda region — in middle to upper-amphibolite facies metamorphic rocks is not predicted by the metamorphic model. Groves et al., (1987, 1988a) invoked progressive prograde metamorphism to explain these deposits. However, prograde metamorphism does not explain why gold is not remobilized during high-grade metamorphism and redeposited in greenschist facies rocks. Furthermore, textural features of biotite, sulfides, and carbonates indicate that alteration assemblages in middle to upper-amphibolite facies rocks in the Menzies–Kambalda region are not the products of static metamorphic recrystallization. Where these alteration assemblages have undergone partial recrystallization, amphibole porphyroblasts are produced, not the higher temperature K-feldspar–diopside–garnet assemblage.

(b) Although gold mineralization is broadly synchronous with peak regional metamorphism, the retrograde nature of alteration at Kambalda and Kalgoorlie, and the occurrence of mineralization in unmetamorphosed, late-tectonic granitoids such as the Liberty Granodiorite, is incompatible with a single pass metamorphic-fluid flow regime.

(c) Groves et al. (1988b) pointed out that C isotope data are incompatible with a source for CO_2 in syn-metamorphic auriferous fluids from devolatilization of sea-water carbonate in spilitized greenstones during amphibolite-grade metamorphism. Furthermore, seafloor alteration of exposed greenstones is volumetrically minor and is unlikely to have yielded the large amounts of CO_2 deposited by mineralizing fluids. Groves et al. (1988b) proposed a two-stage process to account for CO_2 in the hydrothermal fluids. They contrasted metamorphic recrystallization of talc–carbonate schist in regional shear zones in the Widgiemooltha area (indicated by late amphibole overgrowths) with mineralized lodes in which metasomatic carbonate minerals replace metamorphic assemblages. Carbon isotope data were interpreted as being consistent with derivation of C in mineralized lode carbonates by dissolution of mantle-derived carbonate in regional shear zones during regional metamorphism. However, the conclusion that there were two carbonation events, separated by peak regional metamorphism, is inconsistent with the observation, made during this study, that late metamorphic amphiboles occur in alteration assemblages associated with gold deposits as well as in unmineralized but carbonated regional shear zones. On the other hand, late amphiboles are absent in some parts of regional shear zones such as the Bardoc Tectonic Zone. In both cases, the presence of late amphiboles appears related to relatively high metamorphic temperatures in the thermal aureoles of syn-D_3 granitoids.

Mantle degassing

A contribution from mantle-derived volatiles has been stressed by Colvine et al. (1988); Fyon et al. (1988); Rock et al. (1988b); and Cameron (1989a,b), who postulated that a CO_2-rich fluid could be transferred from the mantle to the lower crust, and thence to upper crustal levels, either directly or dissolved in mantle-derived melts. Fyon et al. (1988), and Colvine (1988) related this process to the final stages of cratonization of the Archaean Superior Province in Canada. Models deriving CO_2–H_2O fluids from the mantle or lower crust are consistent with craton-wide regional carbonation and gold mineralization events, and the focussing of fluids through deeply penetrating regional shear zones. The presence of spatially associated, contemporaneous lamprophyre intrusions at some deposits (McNeil and Kerrich, 1986; Rock et al., 1988a,b) constitutes further evidence of mantle processes in the origin of gold mineralization.

Carbon isotope data are generally interpreted to indicate a mantle origin for carbonate in pervasively carbonated regional shear zones, and a juvenile component of C in mineralized alteration assemblages (Golding et al., 1987; Groves et al., 1988b; Colvine et al., 1988). Oxygen isotope data are also compatible with a mantle origin for mineralizing solutions (Golding and Wilson, 1987; Colvine et al., 1988).

Archibald et al. (1981) reported regional gravity and deep seismic data which suggest the presence of granulites at the base of the crust below the Yilgarn Craton. Streaming of CO_2-rich fluids could have caused granulitization of the lower crust (Newton et al., 1980;

Fyon et al., 1988; Cameron, 1989a) with consequent loss of H_2O, K, Rb, Ba, Th, Li, and B to the fluids. These elements correspond closely to those that are concentrated in alteration envelopes surrounding mineralized structures (Phillips and Groves, 1984; Phillips, 1986; Kerrich, 1986a; Colvine et al., 1988). However, Kerrich (1989c) noted that K/Rb and K/Ba ratios in altered, mineralized rocks in Canada do not complement changes in the ratios of these elements predicted to occur in the lower crust during granulitization. Alternatively or additionally, introduction of volatiles, or volatile-rich melts from the mantle into the lower crust may have induced melting to yield syn-D_3 granitic diapirs and late-tectonic granitoids. Volatiles and melts would subsequently move towards upper crustal levels independently.

Toward a model for epigenetic gold mineralization in the Menzies–Kambalda region

Hydrothermal alteration of greenstones in the Menzies–Kambalda region commenced with sea-floor alteration during, or soon after, volcanism (Barley and Groves, 1987). Sea-floor alteration involved only minor carbonation compared to the very large amounts of mantle-derived carbon which was fixed as carbonate minerals in regional shear zones during D_3 deformation. D_3 deformation coincided with peak regional metamorphism, and emplacement of diapiric granitoids into the greenstones. Diapiric granitoid emplacement uplifted deeper, hotter levels of the crust represented by middle to upper-amphibolite facies greenstones. Heat generated by crystallization of the granitoids produced a thermal aureole around the intrusions, which was superimposed on the regional metamorphic gradient.

During D_3, large quantities of CO_2-bearing fluid migrated from the mantle, into the upper crust, via active, deeply penetrating regional shear zones, and an array of smaller structures. These fluids may have combined with dilute aqueous fluids generated by metamorphic devolatilization in the lower crust. Internal pegmatite bodies are widespread in syn-D_3 granitoids, suggesting volatile saturation occurred during crystallization. Thus, the granitoid melts may have introduced a low-salinity aqueous magmatic fluid into the dominantly mantle/lower crustal-derived hydrothermal system.

Hydrothermal fluids with a mantle-derived CO_2 component were responsible for a regional carbonation event which caused massive addition of carbonate to mafic and ultramafic rocks in regional shear zones, and more restricted haloes around smaller structures in low-strain domains. Alteration assemblages resulting from regional carbonation are identical to those found in the outer alteration haloes which envelop mineralized potassic alteration assemblages in greenschist to lower-amphibolite facies rocks, providing a link between regional carbonation and mineralization. Despite the large volumes of fluid, and high Pco_2, implied by intense, pervasive carbonation in regional shear zones, potassic alteration and mineralization are not correspondingly widespread in these structures, suggesting a degree of temporal separation between the two events. Textural observations on mineralized samples indicate potassic alteration is accompanied by carbonation but superimposed on non-potassic carbonate alteration. However, the close and consistent spatial association of potassic alteration with regional carbonation implies an evolutionary trend within a single hydrothermal event rather than two distinct events.

Spatial relationships between syn-D_3 granitoids and the metamorphic and alteration assemblage isograds, described in Chapter 8, suggest the intrusions were probably foci of heat and fluid flow during metamorphism. Similar relationships are described by Ferry (1976a,b). The granitoids, therefore, provided an ideal heat engine to drive the hydrothermal system (Fig. 42). Etheridge et al. (1983) have suggested that large volumes of fluid can convect through the crust at depths of 6–9 km if a suitable, impermeable capping exists. Suitable horizons in the Menzies–Kambalda region might include the contact between mafic/ultramafic volcanic rocks and the dominantly sedimentary Black Flag Formation; the contact between ultramafic rocks and underlying basalt; and numerous interflow-sediment horizons.

Deeply convecting fluids would deposit CO_2 in mafic and ultramafic rocks in regional shear zones and, over time, equilibrate with regionally abundant granitic rocks which probably form a more or less continuous layer beneath the greenstones. During this process, the fluids would evolve toward a more potassic composition, equilibrate with radiogenic Pb and Sr, and possibly leach sulfur from the granitic rocks.

As regional metamorphic temperatures fell from peak values, and the volume of fluids circulating through the system decreased, K, CO_2, S, and Au became fixed in predominantly mafic rocks, within pre-existing carbonation haloes. Local gradients of Pco_2 increasing toward centres of fluid pathways still existed at this time, but only the central parts of the alteration envelopes were enriched in potassium and related components. The modal compositions of the potassic alteration assemblages were controlled by ambient metamorphic temperatures. The regional distribution of different potassic alteration assemblages reflects metamorphic gradients which were still in place during potassic alteration and mineralization, though absolute temperatures were below their peak value.

Outwardly migrating isotherms following emplacement of syn-D_3 diapirs caused local increases in temperature toward the outer margin of the thermal aureole during potassic alteration. These temperature variations resulted in a temporal evolution from sericitic to biotite-bearing assemblages at individual deposits (e.g. mines between New Mexico and Lady Bountiful). The late, biotite-bearing phase of potassic alteration was, however, volumetrically minor at these 'distal' deposits. Biotite-dominant assemblages in more 'proximal' deposits probably formed directly from relatively high-temperature metamorphic precursors.

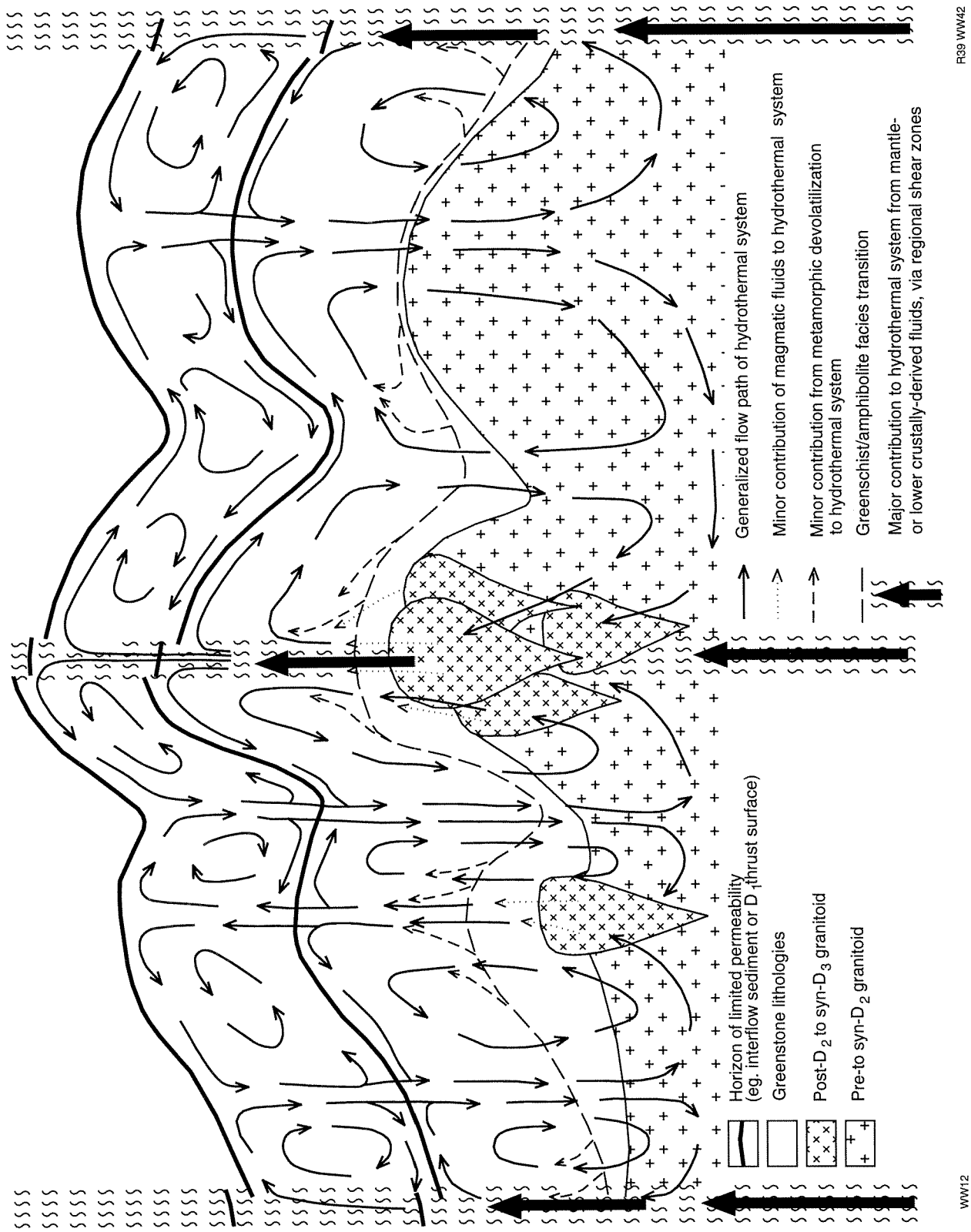

Figure 42. Schematic diagram depicting the hydrothermal convection model for the generation of epigenetic gold mineralization in the Menzies–Kambalda region

As regional metamorphic temperatures continued to fall, the convecting hydrothermal system contracted and Pco_2 decreased. Metamorphic recrystallization of alteration assemblages accompanied the drop in Pco_2 within relatively high-temperature thermal aureoles. District- and outcrop-scale variations in Pco_2 determined whether or not recrystallization occurred at any given temperature, with relatively high Pco_2 maintaining the stability of carbonate assemblages in those structures which remained active. Metamorphic recrystallization did not take place in deposits outside the thermal aureoles because Pco_2 did not fall far enough or fast enough to stabilize amphiboles at the lower temperatures.

The duration of the proposed convecting hydrothermal system is difficult to quantify. Pb isotope data constrain the timing of the gold mineralizing event to within 30 Ma of peak regional metamorphism. Although data are limited, the latter is generally held to be c. 2660 Ma, the age of the Kambalda Granodiorite (Barley and Groves, 1987; Hill and Campbell, 1989). Thus, metasomatic rutile associated with mineralization at Victory–Defiance (Kambalda), dated at c. 2627 Ma (Clark et al., 1989), may have formed during the final stages of the hydrothermal system. Fluid circulation must have ceased relatively rapidly after peak metamorphism in order to preserve the high-temperature alteration assemblages from retrograde alteration.

The synmetamorphic hydrothermal convection model explains a number of observations made in the Menzies–Kambalda region:

(a) the systematic variation in alteration assemblages associated with gold mineralization in metamorphic rocks which range from low- to middle-greenschist facies to upper-amphibolite facies;

(b) regional zonation of metamorphic grade and alteration assemblages with respect to syn-D_3 granitoid intrusions;

(c) spatial and temporal relationships between regional carbonation assemblages and potassic alteration assemblages associated with gold mineralization;

(d) the retrograde nature of gold mineralization and alteration with respect to peak regional metamorphism;

(e) widespread, but not ubiquitous, metamorphic recrystallization of alteration assemblages in the thermal aureoles;

(f) textural and timing relationships between sericite and biotite in alteration haloes at mines toward the outer margins of thermal aureoles associated with syn-D_3 granitoids;

(g) localization of gold mineralization in structures which formed or were active during D_3 and D_4;

(h) the apparent absence of a complementary relationship between K/Rb ratios in alteration haloes and those in granulite terrains (Kerrich 1989c) may be explained by modification of deep crustal fluids during interaction with granitic rocks in the middle to upper crust.

Although the model satisfies many observations, there is controversy regarding the ability of large volumes of fluid to convect through the crust at the depths proposed (Wood and Walther, 1986). The model does not identify a source for the gold, though several possibilities can be identified. Gold may have been transported from the mantle in mantle-derived melts (Rock et al., 1988b), leached from the zone of granulitization at the base of the crust (Cameron, 1989a), or derived from greenstones in the upper crust (Groves et al., 1987; Phillips et al., 1987) during early, carbonating (high pH) stages of the hydrothermal system. According to the present model, the transition from a gold-leaching hydrothermal system to a gold-depositing system is associated with a change from early, relatively alkaline fluids to lower pH, as the fluids equilibrate with granitic crust.

Woodall (1979) drew attention to the large amount of gold produced from the Archaean compared to younger rocks. The period 2500–3000 m.y. ago was the most favourable for the concentration of gold, with major contemporaneous gold-producing provinces in Western Australia, Southern Africa, Canada, and South America. The Witwatersrand deposits, hosted by sedimentary rock, were probably derived from Archaean granite–greenstone terrains (Minter, 1979). Any model for Archaean epigenetic gold mineralization should attempt to explain this temporal association. Lambert (1981) concluded that the late Archaean was a period of maximum heat flow and crustal growth in the Earth's history. Heat could be transferred from the mantle to the crust by volatile degassing, igneous activity, or both, with consequent concentration of gold in the upper crust, as described above. The bias towards gold concentration in the late Archaean is thus more readily explained by a mantle-degassing model than by conventional magmatic, or strictly metamorphic, models since magmatism and metamorphism are widespread processes in younger geological terrains.

Some recent publications (Nesbitt et al., 1986; Barley et al., 1989), though not challenging the importance of Archaean gold mineralization, have identified similar styles of mineralization in younger rocks. These authors noted similarities in geological setting, structural control, alteration mineralogy, and isotopic and fluid inclusion data between Archaean gold deposits and the Mesozoic to Tertiary mesothermal deposits in the western U.S.A. (described by Bohlke and Kistler, 1986; and Weir and Kerrick, 1987). Palaeozoic 'orogenic gold–quartz veins' in the Georgetown and Charters Towers areas of North Queensland (Peters and Golding, 1987; Morrison, 1988) also display many similarities to the Archaean epigenetic gold deposits described in this study.

Summary

The main alternatives proposed for the origin of hydrothermal fluids responsible for craton-scale Archaean epigenetic gold mineralization are 1) magmatic;

2) metamorphic; and 3) mantle degassing. While most isotopic data are consistent with a magmatic origin for the fluids, there is no consistent association between mineralization and distinctive contemporaneous intrusions which display evidence of having yielded a separate volatile-rich fluid phase. Granitic and porphyry intrusions display a wide range of compositions whereas mineralizing fluids are quite uniform by comparison. Syn-D_3 diapirs which appear to have been centres of heat and fluid flow during the metamorphic/mineralization event probably crystallized from crustally derived melts (cf. Archibald et al., 1981), whereas C in carbonate minerals associated with mineralized alteration assemblages is derived from the mantle. Many observations are consistent with the metamorphic model, but the occurrence of deposits in amphibolite-grade domains precludes the generation of metamorphic fluids at the amphibolite–greenschist transition, as originally proposed.

Gold mineralization occurred toward the end of, and is an integral part of, a regional carbonation event, for which carbon isotope data indicate a mantle origin. Other isotopic data suggest a mixed origin for the mineralizing fluids, with some crustally derived components. Although a mantle degassing model (cf. Colvine et al., 1988; Cameron, 1989a — in which mantle-derived CO_2-rich fluids initiate granulitization and partial melting in the lower crust — appears to explain most of the observed relationships and data, Kerrich (1989c) presented data which suggest that the mantle CO_2/granulitization model requires further refinement. A model suggested in this report involves modification of fluids from several sources (mantle, lower crust, syn-D_3 granitoid intrusions) by extensive interaction with regionally abundant granitic rocks as a result of large-scale convection driven by synmetamorphic intrusions. A broader data base, particularly incorporating data from higher grade metamorphic terrains, backed up by a sound knowledge of relationships at a greenstone-belt scale, will contribute to a better understanding of Archaean epigenetic gold deposits.

Bennett (1989) interpreted the Black Flag deposit as a mixed orebody in which gold was deposited as part of the craton-scale mineralization event, but in which base metals (Pb–Zn–Cu–Ag) were deposited at least 100 m.y. later, from meteoric or sea water, in an epithermal convection system driven by an unexposed granitic intrusion.

References

AHMAT, A. L., 1986, Metamorphic patterns in the greenstone belts of the Southern Cross Province, Western Australia: Western Australia Geological Survey, Report 19, p. 1–21.

AHMAT, A. L., in prep., Kanowna W.A.: Western Australia Geological Survey, 1:100 000 Geological Series map.

ANDREWS, A., HUGON, H., DUROCHER, M., CORFU, F., and LAVIGNE, M. J., 1986, The anatomy of a gold-bearing greenstone belt: Red Lake, northwestern Ontario, *in* Gold '86 *edited by* A. J. MacDONALD: Toronto, International symposium on the geology of gold, Proceedings, 1986, p. 3–22.

ANHAEUSSER, C. R., 1965, Wrench faulting and its relationship to gold mineralization in the Barberton Mountain Land: University of Witwatersrand, Economic Geology Research Unit, Information Circular 24.

ARCHIBALD, N. J., and BETTENAY, L. F., 1977, Indirect evidence for tectonic reactivation of a pre-greenstone sialic basement in Western Australia: Earth and Planetary Science Letters, v. 33, p. 270–278.

ARCHIBALD, N. J., BETTENAY, L. F., BICKLE, M. J., GROVES, D. I., 1981, Evolution of Archaean crust in the Eastern Goldfields Province of the Yilgarn Block, Western Australia, *in* Archaean Geology *edited by* J. E. GLOVER and D. I. GROVES: International Archaean Symposium, 2nd, Perth, W.A., 1980, Proceedings: Geological Society of Australia, Special Publication no. 7, p. 491–504.

ARCHIBALD, N. J., BETTENAY, L. F., BINNS, R. A., GROVES, D. I., and GUNTHORPE, R. J., 1978, The evolution of Archaean greenstone terrains, Eastern Goldfields Province, Western Australia: Precambrian Research, v. 6, p. 101–131.

ARNDT, N. T., 1977, Thick, layered peridotite-gabbro lava flows in Munro Township: Canadian Journal of Earth Sciences, v. 14, p. 2620–2637.

ARNDT, N. T., and NISBET, E. G., 1982, What is a komatiite?, *in* Komatiites *edited by* N. T. ARNDT and E. G. NISBET: London, George Allen and Unwin.

ARNDT, N. T., and JENNER, G. A., 1986, Crustally contaminated komatiites and basalts from Kambalda, Western Australia: Chemical Geology, v. 56, p. 229–255.

ARNDT, N. T., NALDRETT, A. J., and PYKE, D. R., 1977, Komatiitic and iron-rich tholeiitic lavas of Munro Township, northeast Ontario: Journal of Petrology, v. 18, p. 319–369.

ARNDT, N. T., FRANCIS, D., and HYNES, A. J., 1979, The field characteristics and petrology of Archean and Proterozoic komatiites: Canadian Mineralogist, v. 17, p. 147–163.

ASHLEY, P. M., and MARTYN, J., 1987, Chromium-bearing minerals from a metamorphosed hydrothermal alteration zone in the Archaean of Western Australia: Neues Jahrbuch fur Mineralogie, Abh. 157, p. 81–111.

BARLEY, M. E., 1986, Incompatible-element enrichment in Archean basalts: A consequence of contamination by older sialic crust rather than mantle heterogeneity: Geology, v. 14, p. 947–950.

BARLEY, M. E., and GROVES, D. I., 1987, Hydrothermal alteration of Archaean supracrustal sequences in the central Norseman–Wiluna belt, Western Australia: a brief review, *in* Recent advances in understanding Precambrian gold deposits *edited by* S. E. HO and D. I GROVES: University of Western Australia, Department of Geology and Extension Service, Publication no. 11, p. 51–66.

BARLEY, M. E., and GROVES, D. I., 1988, Geological setting of gold mineralization in the Norseman–Wiluna Belt, Eastern Goldfields Province, Western Australia, *in* Western Australian gold deposits, Bicentennial Gold 88 Excursion Guide Book *edited by* D. I. GROVES, M. E. BARLEY, S. E. HO, and G. M. F. HOPKINS: University of Western Australia, Department of Geology and Extension Service, Publication no. 14, p 17–46.

BARLEY, M. E., and GROVES, D. I., 1989, Exploration significance of regional and local scale hydrothermal alteration patterns in greenstone belts: Minerals and Energy Research Institute of Western Australia (MERIWA), Report no. 43.

BARLEY, M. E., EISENLOHR, B. N., GROVES, D. I., PERRING, C. S., and VEARNCOMBE, J. R., 1989, Late Archean convergent margin tectonics and gold mineralization: a new look at the Norseman–Wiluna belt: Geology, v. 17, p. 826–829.

BARTRAM, G. D., and McCALL, G. J. H., 1971, Wall-rock alteration associated with auriferous lodes in the Golden Mile, Kalgoorlie: Geological Society of Australia, Special Publication no. 3, p. 191–199.

BARTSCH, R. D., 1990, Lady Bountiful gold mine, *in* Geology of the mineral deposits of Australia and Papua New Guinea *edited by* F. HUGHES: Australasian Institute of Mining and Metallurgy, Monograph 14, p. 401–404.

BAVINGTON, O., 1979, Interflow sedimentary rocks from the Kambalda ultramafic sequence: their geochemistry, metamorphism and genesis: Australian National University, Canberra, Ph.D. thesis (unpublished).

BENNETT, J., 1989, Comparison of Archaean Pb–Zn–(Au) mineralization at Black Flag and Au mineralization at Lady Bountiful, Mt Pleasant area, Western Australia: University of Western Australia, Crawley, B.Sc. (Hons) thesis (unpublished).

BETTENAY, L. F., 1988, The nature and origin of batholithic granitoids in the Yilgarn Block, Western Australia, and their significance to gold mineralization, *in* Advances in understanding Precambrian gold deposits, Volume 2 *edited by* S. E. HO and D. I. GROVES: University of Western Australia, Department of Geology and Extension Service, Publication no. 12, p. 227–237.

BICKLE, M. J., and ARCHIBALD, N. J., 1984, Chloritoid and staurolite stability: implications for metamorphism in the Archaean Yilgarn Block in Western Australia: Journal of Metamorphic Petrology, v. 2, p. 179–203.

BINNS, R. A., GUNTHORPE, R. J., and GROVES, D. I., 1976, Metamorphic patterns and development of greenstone belts in the eastern Yilgarn Block, *in* The early history of the Earth *edited by* B. F.WINDLEY: New York, John Wiley and Sons, p. 303–316.

BLOCH, J., 1988, A petrographic study of the Paddington 1 mafic sequence: W.A. School of Mines, Kalgoorlie, Western Australia, B. Eng. (Mineral Exploration and Mining Geology) thesis (unpublished).

BOHLKE, J. K., 1988, Carbonate–sulphide equilibria and 'stratabound' disseminated epigenetic gold mineralization: a proposal based on examples from Alleghany, California, U.S.A.: Journal of Applied Geochemistry, v. 3, p 499–516.

BOHLKE, J. K., 1989, Comparison of metasomatic reactions between a common CO_2-rich vein fluid and diverse wall rocks: intensive variables, mass transfers and Au mineralization at Alleghany, California: Economic Geology, v. 84, p. 291–327.

BOHLKE, J. K., and KISTLER, R. W., 1986, Rb–Sr, K–Ar and stable isotope evidence for the ages and sources of fluid components of gold-bearing quartz veins in the northern Sierra Nevada foothills metamorphic belt, California: Economic Geology, v. 81, p. 296–322.

BOOTH, G. W., CURRIE, D. A., GOVETT, G. J. S., COHEN, D. R., AMOS, Q. G., ROBERTSON, I. G., LOWDER, G. G., and HANCOCK, M. C., 1988, Selected aspects — geology and geochemistry — The Paddington gold deposit, Broad Arrow, Western Australia, *in* Bicentennial Gold 88, Extended Abstracts Poster Programme, volumes 1 and 2 *compiled by* A. D. T. GOODE, E. L. SMYTH, W. D. BIRCH, and L. I. BOSMA: Geological Society of Australia, Abstracts Series no. 23, p 425–427.

BOTTOMER, L. R., and BRABHAM, G. R., 1987, Geology of Excelsior and Zoroastrian gold mines, Bardoc, W.A., *in* The Second Eastern Goldfields Geological Field Conference, Abstracts and Excursion Guide, 1987 *edited by* W. K WITT and C. P. SWAGER: Geological Society of Australia (Western Australian Division), p. 84–87.

BOTTOMER, L. R., and ROBINSON, C., 1988, Geology of the Bardoc Gold Pty. Ltd. deposits, Bardoc–Davyhurst area, Eastern Goldfields, W.A., *in* Bicentennial Gold 88, Extended Abstracts Poster Programme, volumes 1 and 2 *compiled by* A. D. T. GOODE, E. L. SMYTH, W. D. BIRCH, and L. I. BOSMA: Geological Society of Australia, Abstracts Series no. 23, p 54–56.

BOTTOMER, L. R., and ROBINSON, C., 1990, The Bardoc gold deposits *in* Geology of the mineral deposits of Australia and Papua New Guinea *edited by* F. HUGHES: Australasian Institute of Mining and Metallurgy, Monograph 14, p. 385–388.

BOULTER, C. A., and PHILLIPS, G. N., 1985, Gold mineralization at Kalgoorlie, Western Australia: a review, *in* Metallogeny of basic and ultrabasic rocks *edited by* M. J. GALLAGHER, R. A. IXER, C. R. NEARY, and H. M. PRICHARD: London, Institution of Mining and Metallurgy, Edinburgh Conference Proceedings, p. 109–120.

BOULTER, C. A., FOTIOS, M. G., and PHILLIPS, G. N., 1987, The Golden Mile, Kalgoorlie: a giant gold deposit localised in ductile shear zones by structurally induced infiltration of an auriferous metamorphic fluid: Economic Geology, v. 82, p. 1661–1678.

BOWERS, T. S., and HELGESON, H. C., 1983, Calculations of the thermodynamic and geochemical consequences of non-ideal mixing in the system H_2O–CO_2–NaCl on phase relations in geologic systems: equation of state for H_2O–CO_2–NaCl fluids at high pressures and temperatures: Geochimica et Cosmochimica Acta, v. 47, p. 1247–1275.

BROWNING, P., GROVES, D. I., BLOCKLEY, J. G., and ROSMAN, K. J. R., 1987, Lead isotope constraints on the age and source of gold mineralization in the Archean Yilgarn Block, Western Australia: Economic Geology, v. 82, p. 971–986.

BURROWS, D. R., and JEMIELITA, R. A., 1989, Lithophile element systematics of Archean greenstone belt Au–Ag vein deposits: implications for source processes: Discussion: Canadian Journal of Earth Sciences, v. 26, p. 2741–2743.

BURROWS, D. R., WOOD, P. C., and SPOONER, E. T. C., 1986, Carbon isotope evidence for a magmatic origin for Archaean gold–quartz vein ore deposits: Nature, v. 321, p. 851–854.

BUTT, C. R. M., 1987, Lateritic and supergene gold deposits in the Yilgarn Block: genesis and geochemistry, *in* The Second Eastern Goldfields Geological Field Conference, Abstracts and Excursion Guide, 1987 edited by W. K WITT and C. P. SWAGER: Geological Society of Australia (Western Australian Division), p. 8–10.

BUTT, C. R. M., 1988, Genesis of lateritic and supergene deposits in the Yilgarn Block, Western Australia, *in* Bicentennial Gold 88, Extended Abstracts Oral Programme, *compiled by* A. D. T. GOODE and L. I. BOSMA: Geological Society of Australia, Abstracts Series no. 22, p. 359–364.

BUTT, C. R. M., 1989, Genesis of supergene gold deposits in the lateritic regolith of the Yilgarn Block, Western Australia, *in* The geology of gold deposits: the perspective in 1988 *edited by* R. R. KEAYS, W. R. H. RAMSAY, and D. I. GROVES: Economic Geology Monograph 6, p. 460–470.

CAMERON, E. M., 1989a, Derivation of gold by oxidative metamorphism of a deep ductile shear zone: Part 1. Conceptual model: Journal of Geochemical Exploration, v. 31, p. 135–147.

CAMERON, E. M., 1989b, Derivation of gold by oxidative metamorphism of a deep ductile shear zone: Part 2. Evidence from the Bamble Belt, south Norway: Journal of Geochemical Exploration, v. 31, 149–169.

CAMERON, E. M., and HATTORI, K., 1985, The Hemlo gold deposit, Ontario: a geochemical and isotopic study: Geochimica et Cosmochimica Acta, v. 49, p. 2041–2050.

CAMERON, E. M., and HATTORI, K., 1987, Archean gold mineralization and oxidised hydrothermal fluids: Economic Geology, v. 82, p. 1177–1191.

CAMPBELL, I. H., and HILL, R. I., 1988, A two-stage model for the formation of the granite–greenstone terrains of the Kalgoorlie–Norseman area, Western Australia: Earth and Planetary Science Letters, v. 90, p. 11–25.

CASSIDY, K. F., 1988, Petrology and alteration of an Archaean granitoid-hosted gold deposit, Lawlers, Western Australia, *in* Advances in understanding Precambrian gold deposits, Volume 2 *edited by* S. E. HO and D. I. GROVES: University of Western Australia, Department of Geology and Extension Service, Publication no. 12, p. 165–184.

CHANTER, S. C., 1987, Hydrothermal alteration and gold mineralization in the Devon Consols Basalt, Kalgoorlie, Western Australia: University of Western Australia, B.Sc. (Hons) thesis (unpublished).

CHAPMAN, D. M., 1987, Mount Pleasant gold project — Golden Kilometre mine, *in* The Second Eastern Goldfields Geological Field Conference, Abstracts and Excursion Guide, 1987 *edited by* W. K. WITT and C. P. SWAGER: Geological Society of Australia (Western Australian Division), p. 86–91.

CHAPPELL, B. W., and WHITE, A. J. R., 1974, Two contrasting granite types: Pacific Geology, v. 8, p. 173–174.

CHAUVEL, C., DUPRE, B., and JENNER, G. A., 1985, The Sm–Nd age of Kambalda volcanics is 500 Ma too old!: Earth and Planetary Science Letters, v. 74, p. 315–324.

CHOWN, E. H., HICKS, J., PHILLIPS, G. N., and TOWNSEND, R., 1984, The disseminated Archean Big Bell gold deposit, Murchison Province, Western Australia: an example of pre-metamorphic hydrothermal alteration, *in* Gold '82 — The geology, geochemistry and genesis of gold deposits *edited by* R. P. FOSTER: Rotterdam, A. A. Balkema Publishers, Geological Society of Zimbabwe, Special Publication no. 1, p. 305–324.

CHRISTIE, D., 1975, Scotia nickel sulphide deposit, *in* Economic geology of Australia and Papua New Guinea, I. Metals *edited by* C. L. KNIGHT: Australasian Institute of Mining and Metallurgy, Monograph 5, p. 121–124.

CLAOUÉ-LONG, J. C., COMPSTON, W., and COWDEN, A., 1988, The age of the Kambalda greenstones resolved by ion-microprobe: implications for Archaean dating methods: Earth and Planetary Science Letters, v. 89, p. 239–259.

CLARK, M. E., 1980, Localisation of gold, Mt Charlotte, Kalgoorlie, Western Australia: University of Western Australia, B.Sc. (Hons) thesis (unpublished).

CLARK, M. E., ARCHIBALD, N. J., and HODGSON, C. J., 1986, The structural and metamorphic setting of the Victory gold mine, Kambalda, Western Australia, *in* Proceedings of Gold '86, an International Symposium on the geology of gold *edited by* A. J. MacDONALD: Toronto, 1986, p 243–254.

CLARK, M. E., CARMICHAEL, D. M., and HODGSON, C. J., 1988, Metasomatic processes and T–XCO_2 conditions of wall rock alteration, Victory gold mine, Kambalda, Western Australia, *in* Bicentennial Gold 88, Extended Abstracts Oral Programme, *compiled by* A. D. T. GOODE and L. I. BOSMA: Geological Society of Australia Abstracts Series no. 22, p. 230–234.

CLARK, M. E., CARMICHAEL, D. M., HODGSON, C. J., and FU, M., 1989, Wall-rock alteration, Victory gold mine, Kambalda, Western Australia: processes and P–T–X_{CO_2} conditions of metasomatism, *in* The geology of gold desposits: the perspective in 1988 *edited by* R. R. KEAYS, W. R. H. RAMSAY, and D. I. GROVES: Economic Geology Monograph 6, p. 445–459.

CLARKE, E. de C., 1925, The geology of a portion of the East Coolgardie and North-East Coolgardie Goldfields, including the mining centres of Monger and St Ives: Western Australia Geological Survey, Bulletin 90.

CLOUT, J. M. F., CLEGHORN, J. H., and EATON, P. C., 1990, Geology of the Kalgoorlie gold field, *in* Geology of the mineral deposits of Australia and Papua New Guinea *edited by* F. HUGHES: Australasian Institute of Mining and Metallurgy, Monograph 14, p. 411–431.

CLOUT, J. M. F., CLEGHORN, J. H., and WATT, R. D., 1988, Geology of Kalgoorlie Mining Associated leases, Kalgoorlie, *in* Western Australian gold deposits, Bicentennial Gold 88 Excursion Guide Book *edited by* D. I. GROVES, M. E. BARLEY, S. E. HO, and G. M. F. HOPKINS: University of Western Australia, Department of Geology and Extension Service, Publication no. 14, p. 70–77.

COLVILLE, R. G., KELLY, D., and FISH, B. L., 1990, Goongarrie gold deposits, *in* Geology of the mineral deposits of Australia and Papua New Guinea *edited by* F. HUGHES: Australasian Institute of Mining and Metallurgy, Monograph 14, p. 363–366.

COLVINE, A. C., 1988, Gold mineralization in the Superior Province, Canada: a product of terminal Archaean cratonisation, *in* Bicentennial Gold 88, Extended Abstracts Oral Programme *compiled by* A. D. T. GOODE and L. I. BOSMA: Geological Society of Australia, Abstracts Series no. 22, p. 36–44.

COLVINE, A. C., et al., 1984, An integrated model for the origin of Archean lode gold deposits: Ontario Geological Survey, Open File Report 5524.

COLVINE, A. C., FYON, J. A., HEATHER, K. B., MARMONT, S., SMITH, P. M., and TROOP, D. G., 1988, Archean lode gold deposits in Ontario: Ontario Geological Survey, Miscellaneous Paper 139.

COMPSTON, W., WILLIAMS, I. S., CAMPBELL, I. H., and GRESHAM, J. J., 1986, Zircon xenocrysts from the Kambalda volcanics: age constraints and direct evidence for older continental crust below the Kambalda–Norseman greenstone belt: Earth and Planetary Science Letters, v. 76, p. 299–311.

COWDEN, A., 1988, The Cave Rocks gold deposit, *in* Bicentennial Gold 88, Extended Abstracts Poster Programme, volumes 1 and 2 *compiled by* A. D. T. GOODE, E. L. SMYTH, W. D. BIRCH, and L. I. BOSMA: Geological Society of Australia, Abstracts Series no. 23, p 68–70.

COWDEN, A., and ARCHIBALD, N. J., (in prep.), Stratigraphy of the Kambalda–Kalgoorlie Archaean greenstone terrain, Western Australia: Australian Journal of Earth Sciences.

CRAWFORD, M. L., 1981, Fluid inclusions in metamorphic rocks — low and medium grade, *in* Short Course in fluid inclusions: applications to petrology *edited by* L. S. HOLLISTER and M. L. CRAWFORD: Mineralogical Association of Canada, Short Course Handbook, no. 6, p. 157–181.

CULLEN, I., and NORRIS, N., 1988, Gold deposits of the New Celebration gold mine, *in* Western Australian gold deposits, Bicentennial Gold 88 Excursion Guide Book *edited by* D. I. GROVES, M. E. BARLEY, S. E. HO, and G. M. F. HOPKINS: University of Western Australia, Department of Geology and Extension Service, Publication no. 14, p. 87–90.

DAHL, N., McNAUGHTON, N. J., and GROVES, D. I., 1987, A lead-isotope study of sulphides associated with gold mineralization in selected deposits from the Archaean of Western Australia, *in* Recent advances in understanding Precambrian gold deposits *edited by* S. E. HO and D. I GROVES: University of Western Australia, Department of Geology and Extension Service, Publication no. 11, p. 189–201.

DAVIES, J. F., WHITEHEAD, R. E., HUANG, J., and NAWARATNE, S., 1990, A comparison of progressive hydrothermal carbonate alteration in Archean metabasalts and metaperidotites: Mineralium Deposita, v. 25, p. 65–72.

DENN, S., 1987, Summary of the Victory and Talbot mines at Broad Arrow, *in* The Second Eastern Goldfields Geological Field Conference, Abstracts and Excursion Guide, 1987 *edited by* W. K. WITT and C. P. SWAGER: Geological Society of Australia (Western Australian Division), p. 68–72.

DEVLIN, S. P., and CRIMEEN, J. D., 1990, Lady Bountiful Extended gold deposit, *in* Geology of the mineral deposits of Australia and Papua New Guinea *edited by* F. HUGHES: Australasian Institute of Mining and Metallurgy, Monograph 14, p. 405–410.

DOEPEL, J. J. G., 1973, Norseman, W.A.: Western Australia Geological Survey, 1:250 000 Geological Series Explanatory Notes.

DONALDSON, M. J., 1983, Progressive alteration of barren and weakly mineralized Archaean dunites from Western Australia: University of Western Australia, Crawley, Ph.D. thesis (unpublished).

DONALDSON, M. J., LESHER, C. M., GROVES, D. I., and GRESHAM, J. J., 1986, Comparison of Archaean dunites and komatiites associated with nickel mineralization in Western Australia: implications for dunite genesis: Mineralium Deposita v. 21, p. 296–305.

DOWLING, K., and MORRISON, G. W., 1989, Application of quartz textures to the classification of gold deposits using North Queensland examples, *in* The geology of gold deposits: the perspective in 1988 *edited by* R. R. KEAYES, W. R. H. RAMSAY, and D. I. GROVES: Economic Geology Monograph 6, p. 342–355.

EGGLER, D. H., 1974, Application of a portion of the system $CaAl_2Si_2O_8$–$NaAlSi_3O_8$–SiO_2–MgO–Fe–O_2–H_2O–CO_2 to the genesis of the calc-alkaline suite: American Journal of Science, v. 274, p. 297–315.

EGGLER, D. H., and BURNHAM, C. W., 1973, Crystallisation and fractionation trends in the system andesite–H_2O–CO_2–O_2 at pressures to 10 kb: Geological Society America Bulletin, v. 84, p. 2517–2532.

EINAUDI, M. T., MEINERT, L. D., and NEWBERRY, R. J., 1981, Skarn deposits: Economic Geology 75th Anniversary Volume, p. 317–191.

EISENLOHR, B., 1987, Structural geology of the Kathleen Valley–Lawlers region, Western Australia, and some implications for Archaean gold mineralization, *in* Recent advances in understanding Precambrian gold deposits *edited by* S. E. HO and D. I GROVES: University of Western Australia, Department of Geology and Extension Service, Publication no. 11, p. 85–96.

ETHERIDGE, M. A., WALL, V. J., and VERNON, R. H., 1983, The role of the fluid phase during regional metamorphism and deformation: Journal of Metamorphic Geology, v. 1, p. 205–226.

FERRY, J. M., 1976a, P, T, fCO_2, and fH_2O during metamorphism of calcareous sediments in the Waterville–Vassalboro area, South-Central Maine: Contributions to Mineralogy and Petrology, v. 57, p. 119–143.

FERRY, J. M., 1976b, Metamorphism of calcareous sediments in the Waterville–Vassalboro area, South-Central Maine: mineral reactions and graphical analysis: American Journal of Science, v. 276, p. 841–882.

FERRY, J. M., 1980, A case study of the amount and distribution of heat and fluid during metamorphism: Contributions to Mineralogy and Petrology, v. 71, p. 373–385.

FINUCANE, K. J., 1965, Ore distribution and lode structures in the Kalgoorlie Goldfield, *in* Geology of Australian ore deposits (2nd edition) *edited by* J. McANDREW: Commonwealth Mining and Metallurgical Congress, 8th, Australia and New Zealand, 1965, Publications v.1 p. 80–86.

FORMAN, F. G., 1937, The Ora Banda Amalgamated gold mine, Grants Patch, Broad Arrow Goldfield: Western Australia Geological Survey, Annual Report 1936, p. 5–8.

FOSTER, R. P., and WILSON, J. F., 1984, Geological setting of Archaean gold deposits in Zimbabwe, *in* Gold '82 — The geology, geochemistry and genesis of gold deposits *edited by* R. P. FOSTER: Rotterdam, A. A. Balkema Publishers, Geological Society of Zimbabwe, Special Publication, no. 1, p. 521–552.

FROST, B. R., 1979, Mineral equilibria involving mixed volatiles in a C–O–H fluid phase: the stabilities of graphite and siderite: American Journal of Science, v. 279, p. 1033–1059.

FYFE, W. S., and KERRICH, R., 1984, Gold: natural concentration processes, *in* Gold '82 — The geology, geochemistry and genesis of gold deposits *edited by* R. P. FOSTER: Rotterdam, A. A. Balkema Publishers, Geological Society of Zimbabwe, Special Publication, no. 1, p. 99–128.

FYON, J. A., 1986, Field and stable isotope characteristics of carbonate alteration zones, Timmins area: McMaster University, Hamilton, Ontario, Ph.D. thesis (unpublished).

FYON, J. A., McDONALD, A. J., MARMONT, S., and TROOP, G., 1988, Shield-wide introduction of gold into Archaean crust, Superior Province, Ontario: coupling between mantle-initiated magmatism and lower crustal maturation, *in* Bicentennial Gold 88, Extended Abstracts Oral Programme, *compiled by* A. D. T. GOODE and L. I. BOSMA: Geological Society of Australia, Abstracts Series no. 22, p. 313–318.

GEE, R. D., 1979, Structure and tectonic style of the Western Australian Shield: Tectonophysics, v. 58, p. 327–369.

GEE, R. D., BAXTER, J. L., WILDE, S. A., and WILLIAMS, I. R., 1981, Crustal development in the Yilgarn Block, Western Australia, *in* Archaean geology *edited by* J. E. GLOVER and D. I. GROVES: International Archaean Symposium, 2nd, Perth, W.A., 1980, Proceedings: Geological Society of Australia, Special Publication no. 7, p. 43–56.

GEMUTS, I., and THERON, A. C., 1975, The Archaean between Coolgardie and Norseman — stratigraphy and mineralisation, *in* Economic geology of Australia and Papua New Guinea, I. Metals *edited by* C. L. KNIGHT: Australasian Institute of Mining and Metallurgy, Monograph 5, p. 65–74.

GEOLOGICAL SURVEY OF WESTERN AUSTRALIA, 1989, Reported resources of Western Australian gold deposits as at May, 1989: Western Australia Geological Survey, Record 1989/11.

GOLDING, L. Y., 1978, Mineralogy, geochemistry and origin of the Kalgoorlie gold deposits, Western Australia: University of Melbourne, Ph.D. thesis (unpublished).

GOLDING, L. Y., 1985, The nature of the Golden Mile Dolerite southeast of Kalgoorlie: Australian Journal of Earth Sciences, v. 32, p. 55–64.

GOLDING, S. D., 1982, An isotopic and geochemical study of gold mineralization in the Kalgoorlie–Norseman region, Western Australia: University of Queensland, Brisbane, Ph.D. thesis (unpublished).

GOLDING, S. D., 1984, Stable isotope and geochemical studies of porphyry-related gold mineralization, Kambalda: Western Mining Corporation Ltd., internal company report (unpublished).

GOLDING, S. D., and WILSON, A. F., 1982, Geochemical and stable isotopic studies of the Crown and Mararoa reefs, Norseman, Western Australia: Revista Brasileira de geosciencias, v. 12, p. 445–456.

GOLDING, S. D., and WILSON, A. F., 1983, Geochemical and stable isotopic studies of the No. 4 lode, Kalgoorlie, Western Australia: Economic Geology, v. 78, p. 438–450.

GOLDING, S. D., and WILSON, A. F., 1987, Oxygen and hydrogen isotope relations in Archaean gold deposits of the Eastern Goldfields Province, Western Australia: constraints on the source of Archaean gold-bearing fluids, *in* Recent advances in understanding Precambrian gold deposits *edited by* S. E. HO and D. I GROVES: University of Western Australia, Department of Geology and Extension Service, Publication no. 11, p. 203–214.

GOLDING, S. D., GROVES, D. I., McNAUGHTON, N. J., BARLEY, M. E., and ROCK, N. M. S., 1987, Carbon isotopic composition of carbonates from contrasting alteration styles in supracrustal rocks of the Norseman–Wiluna Belt, Yilgarn Block, Western Australia: their significance to the source of Archaean auriferous fluids *in* Recent advances in understanding Precambrian gold deposits *edited by* S. E. HO and D. I GROVES: University of Western Australia, Department of Geology and Extension Service, Publication no. 11, p. 215–238.

GOLDING, S. D., BARLEY, M. E., CASSIDY, K. F., GROVES, D. I., HO, S. E., HRONSKY, J. M. A., McNAUGHTON, N. J., SANG, J. H., and TURNER, J. V., 1990, Oxygen and hydrogen isotope studies, *in* Gold deposits of the Archaean Yilgarn Block, Western Australia: nature, genesis and exploration guides *edited by* S. E. HO, D. I. GROVES, and J. M. BENNETT: University of Western Australia, Department of Geology and University Extension Service, Publication 20, p. 252–258.

GOLDING, S. D., CLARK, M. E., KEELE, R. A., WILSON, A. F., and KEAYES, R. R., 1990, Geochemistry of Archaean epigenetic gold deposits in the Eastern Goldfields Province, Western Australia, *in* Stable isotopes and fluid processes in mineralization *edited by* H. K. HERBERT, and S. E. HO: University of Western Australia, Department of Geology and University Extension Service, Publication 23, p. 141–176.

GOODE, A. D. T., and BOSMA, L. I., (compilers), 1988, Bicentennial Gold 88, Extended Abstracts Oral Programme: Geological Society of Australia, Abstracts Series no. 22.

GOODE, A. D. T., SMYTH, E. L., BIRCH, W. D., and BOSMA, L. I., (eds), 1988, Bicentennial Gold 88, Extended Abstracts Poster Programme, Vols 1 and 2: Geological Society of Australia, Abstracts Series no. 23.

GOODE, A. H., 1987, The Lady Bountiful mine, *in* The Second Eastern Goldfields Geological Field Conference, Abstracts and Excursion Guide, 1987 *edited by* W. K. WITT and C. P. SWAGER: Geological Society of Australia (Western Australian Division), p. 73–77.

GORMAN, B. E., KERRICH, R., and FYFE, W. S., 1981, Geochemistry and field relations of lode gold deposits in felsic igneous intrusions–porphyries of the Timmins District: Ontario Geological Survey, Miscellaneous Paper 98, p. 108–124.

GRESENS, R. L., 1967, Composition–volume relationships of metasomatism: Chemical Geology, v. 2, p. 47–65.

GRESHAM, J. J., and LOFTUS-HILLS, G. D., 1981, The geology of the Kambalda nickel field, Western Australia: Economic Geology, v. 76, p. 1373–1416.

GRIFFIN, T. J., 1988a, Lake Lefroy, W.A.: Western Australia Geological Survey, 1:100 000 Geological Series map.

GRIFFIN, T. J., 1988b, Cowan, W.A.: Western Australia Geological Survey, 1:100 000 Geological Series map.

GRIFFIN, T. J., 1990a, Eastern Goldfields Province, in Geology and mineral resources of Western Australia: Western Australia Geological Survey, Memoir 3, p. 77–119.

GRIFFIN, T. J., 1990b, Geology of the granite–greenstone terrain of the Lake Lefroy and Cowan 1:100 000 sheets, Western Australia: Western Australia Geological Survey, Report 32.

GRIFFIN, T. J., HUNTER, W. M., and KEATS, W., 1983a, Geology of the Kalgoorlie–Widgiemooltha district, *in* Eastern Goldfields Geological Field Conference, Abstracts and Excursion Guide *edited by* P.C. MUHLING: Eastern Goldfields Geological Discussion Group, p. 7–8.

GRIFFIN, T. J., HUNTER, W. M., and KEATS, W., 1983b, Mount Hunt–Kurrawang Traverse, *in* Eastern Goldfields Geological Field Conference, Abstracts and Excursion Guide *edited by* P. C. MUHLING: Eastern Goldfields Geological Discussion Group, p 33–39.

GROVES, D. I., 1988, Gold mineralization in the Yilgarn Block, Western Australia, *in* Bicentennial Gold 88, Extended Abstracts Oral Programme, *compiled by* A. D. T. GOODE and L. I. BOSMA: Geological Society of Australia, Abstracts Series no. 22, p. 13–18.

GROVES, D. I., and BARLEY, M. E., 1988, Gold mineralization in the Norseman–Wiluna belt, Eastern Goldfields Province, Western Australia, *in* Western Australian gold deposits, Bicentennial Gold 88 Excursion Guide Book *edited by* D. I. GROVES, M. E. BARLEY, S. E. HO, and G. M. F. HOPKINS: University of Western Australia, Department of Geology and Extension Service, Publication no. 14, p. 47–66.

GROVES, D. I., and BATT, W. D., 1984, Spatial and temporal variations of Archaean metallogenic associations in terms of evolution of granitoid–greenstone terrains with particular emphasis on Western Australia, *in* Archaean Geochemistry *edited by* A. KRONER, G. N. HANSON, and A. M. GOODWIN: Berlin, Springer-Verlag, p. 73–98.

GROVES, D. I., and LESHER, C. M., (editors) 1982, Regional geology and nickel sulphide deposits of the Norseman–Wiluna belt: IGCP Projects 91 and 161: Nickel Sulphide Field Conference III, Western Australia, 1982, Excursion Guide.

GROVES, D. I., ARCHIBALD, N. J., BETTENAY, L. F., and BINNS, R. A., 1978, Greenstone belts as ancient marginal basins or ensialic rift zones: Nature, v. 273, p. 460–461.

GROVES, D. I., PHILLIPS, G. N., HO, S. E., HENDERSON, C. A., CLARK, M. E., and WOAD, G. M., 1984, Controls on distribution of Archaean hydrothermal gold deposits in Western Australia, *in* Gold '82 — The geology, geochemistry and genesis of gold deposits *edited by* R. P. FOSTER: Rotterdam, A. A. Balkema Publishers, Geological Society of Zimbabwe, Special Publication, no. 1, p. 689–712.

GROVES, D. I., PHILLIPS, G. N., HO, S. E., HOUSTON, S. M., and STANDING, C. A., 1987, Craton-scale distribution of Archaean greenstone gold deposits: predictive capacity of the metamorphic model: Economic Geology, v. 82, p. 2045–2058.

GROVES, D. I., HO, S. E., McNAUGHTON, N. J., MUELLER, A. G., PERRING, C. S., ROCK, N. M. S., and SKWARNECKI, M. S., 1988a, Genetic models for Archaean lode-gold deposits in Western Australia, *in* Advances in understanding Precambrian gold deposits, Volume 2 *edited by* S. E. HO and D. I. GROVES: University of Western Australia, Department of Geology and Extension Service, Publication no. 12, p. 1–22.

GROVES, D. I., GOLDING, S. D., ROCK, N. M. S., BARLEY, M. E., and McNAUGHTON, N. J., 1988b, Archaean carbon reservoirs and their relevance to the fluid source for gold deposits: Nature, v. 331, p. 254–257.

GROVES, D. I., BARLEY, M. E., and HO, S. E., 1989, The nature, genesis and tectonic setting of mesothermal gold mineralization in the Yilgarn Block, Western Australia, *in* The geology of gold deposits: the perspective in 1988 *edited by* R. R. KEAYES, W. R. H. RAMSAY, and D. I. GROVES: Economic Geology Monograph 6, p. 71–85.

GUHA, J., ARCHAMBAULT, G., and LEROY, J., 1983, A correlation between the evolution of mineralizing fluids and the geomechanical development of a shear zone as illustrated by the Henderson Z mine, Quebec: Economic Geology, v. 78, p. 1605–1618.

GUSTAFSON, J. K., and MILLER, F. S., 1937, Kalgoorlie geology reinterpreted: Australasian Institute of Mining and Metallurgy, Proceedings, v. 106, p. 93–125.

HALLBERG, J. A., 1972, Geochemistry of Archaean volcanic belts in the Eastern Goldfields region of Western Australia: Journal of Petrology, v. 13, p. 45–56.

HALLBERG, J. A., 1985, Geology and mineral deposits of the Leonora–Laverton area, north-eastern Yilgarn Block, Western Australia: Perth, Hesperian Press.

HALLBERG, J. A., 1986, Archaean basin development and crustal extension in the north-eastern Yilgarn Block, Western Australia: Precambrian Research, v. 31, p. 133–156.

HALLBERG, J. A., 1988, A reconnaissance view of the internal granitoids of the Norseman–Wiluna belt: characteristics, lithological and structural associations, and relationships to gold mineralization, *in* Advances in understanding Precambrian gold deposits, Volume 2 *edited by* S. E. HO and D. I. GROVES: University of Western Australia, Department of Geology and Extension Service, Publication no. 12, p. 239–244.

HALLBERG, J. A., and GILES, C. W., 1986, Archaean felsic volcanism in the northeastern Yilgarn Block, Western Australia: Australian Journal of Earth Sciences, v. 33, p. 413–428.

HANCOCK, M. C., ROBERTSON, I. G., and BOOTH, G. W., 1990, Paddington gold deposits, *in* Geology of the mineral deposits of Australia and Papua New Guinea *edited by* F. HUGHES: Australasian Institute of Mining and Metallurgy, Monograph 14, p. 395–400.

HARRIS, L. B., 1987, A tectonic framework for the Western Australian Shield and its significance to gold mineralization: a personal view, *in* Recent advances in understanding Precambrian gold deposits *edited by* S. E. HO and D. I. GROVES: University of Western Australia, Department of Geology and Extension Service, Publication no. 11, p. 1–28.

HARRISON, N., BAILEY, A., SHAW, J. D., PETERSON, G. N., and ALLEN, C. A., 1990, Ora Banda gold deposits, *in* Geology of the mineral deposits of Australia and Papua New Guinea *edited by* F. HUGHES: Australasian Institute of Mining and Metallurgy, Monograph 14, p. 389–394.

HAYCRAFT, J. A., 1965, Ore bodies in the Mt Charlotte – Hannans North area, Kalgoorlie: Australasian Institute of Mining and Metallurgy, Proceedings, v. 213, p. 49–64.

HELGESON, H. C., 1969, Thermodynamics of hydrothermal systems at elevated temperatures and pressures: American Journal of Science, v. 267, p. 729–804.

HILL, B. D., and BIRD, P., 1990, Sand King gold deposit, *in* Geology of the mineral deposits of Australia and Papua New Guinea *edited by* F. HUGHES: Australasian Institute of Mining and Metallurgy, Monograph 14, p. 377–382.

HILL, R. E. T., GOLE, M. J., and BARNES, S. J., 1987, Physical volcanology of komatiites: a field guide to komatiites between Kalgoorlie and Wiluna, Eastern Goldfields Province, Yilgarn Block, Western Australia: Geological Society of Australia (Western Australian Division), Excursion Guide no. 1.

HILL, R. I., and COMPSTON, W., 1987, Age of granite emplacement, southeastern Yilgarn Block, Western Australia: Australian National University, Canberra, Research School of Earth Sciences, Annual Report 1986, p. 70–71.

HILL, R. I., and CAMPBELL, I. H., 1989, A post-metamorphic age for gold mineralization at Lady Bountiful, Yilgarn Block, Western Australia: Australian Journal of Earth Sciences, v. 36, p. 313–316.

HILL, R. I., CAMPBELL, I. H., and COMPSTON, W., 1989, Age and origin of granitic rocks in the Kalgoorlie–Norseman region of Western Australia: implications for the origin of the Archaean crust: Geochimica et Cosmochimica Acta, v. 53, p. 1259–1275.

HO, S. E., 1987, Fluid inclusions: their potential as an exploration tool for Archaean gold deposits, *in* Recent advances in understanding Precambrian gold deposits *edited by* S. E. HO and D. I. GROVES: University of Western Australia, Department of Geology and Extension Service, Publication no. 11, p. 239–264.

HO, S. E., BENNETT, J. M., CASSIDY, K. F., HRONSKY, J. M. A., MIKUCKI, E. J., and SANG, J. H., 1990, Fluid inclusion studies, *in* Gold deposits of the Archaean Yilgarn Block, Western Australia: nature, genesis and exploration guides *edited by* S. E. HO, D. I. GROVES, and J. M. BENNETT: University of Western Australia, Department of Geology and University Extension Service, Publication no. 20, p. 198–211.

HODGSON, C. J., and McGEEHAN, P. J., 1982, A review of the geological characteristics of 'gold only' deposits in the Superior Province of the Canadian Shield, *in* Geology of Canadian gold deposits *edited by* R. W. HODDER and W. PETRUK: Canadian Institute of Mining, Special Volume no. 24, p. 211–228.

HOLDAWAY, M. J., 1971, Stability of andalusite and the aluminium silicate phase diagram: American Journal of Science, v. 271, p. 97–131.

HOLLISTER, L. S., and BURRUSS, R. C., 1976, Phase equilibria in fluid inclusions from the Khtada Lake metamorphic complex: Geochimica et Cosmochimica Acta, v. 40, p. 163–175.

HOLLOWAY, J. R., 1976, Fluids in the evolution of granitic magmas: consequences of finite CO_2 solubility: Geological Society of America Bulletin, v. 87, p. 1513–1518.

HONMAN, C. S., 1916, The geology of the country to the south of Kalgoorlie: Western Australia Geological Survey, Bulletin 66.

HOSCHEK, G., 1973, Die reaktion Phlogopit + calcit + quartz = tremolit + H_2O + CO_2: Contributions to Mineralogy and Petrology, v. 39, p. 231–237.

HUNTER, W. M., 1988a, Yilmia, W.A.: Western Australia Geological Survey, 1:100 000 Geological Series map.

HUNTER, W. M., 1988b, Kalgoorlie, W.A.: Western Australia Geological Survey, 1:100 000 Geological Series map.

HUNTER, W. M., 1993, Geology of the Kalgoorlie and Yilmia 1:100 000 sheets: Western Australia Geological Survey, Report 35.

IVEY, M. E., 1987, The geology of the Hannan South gold mine, Kalgoorlie, *in* The Second Eastern Goldfields Geological Field Conference, Abstracts and Excursion Guide, 1987 *edited by* W. K. WITT and C. P. SWAGER: Geological Society of Australia (Western Australian Division), p. 118–120.

IVEY, M. E., and COOPER, A. R., 1988, The geology of the Hannan South gold mine, Kalgoorlie, W.A., *in* Bicentennial Gold 88, Extended Abstracts Poster Programme, volumes 1 and 2 *compiled by* A. D. T. GOODE, E. L. SMYTH, W. D. BIRCH, and L. I. BOSMA: Geological Society of Australia, Abstracts series no. 23, p. 76–80.

JAQUES, A. L., 1976, An Archaean tholeiitic layered sill from Mt Kilkenny, Western Australia: Journal of the Geological Society of Australia, v. 23, p. 159–168.

JOHNSTON, S. F., SAUTER, P. C. C., HYLAND, S. J., and BRADLEY, T., 1990, Mount Percy gold deposits, *in* Geology of the mineral deposits of Australia and Papua New Guinea *edited by* F. HUGHES: Australasian Institute of Mining and Metallurgy, Monograph 14, p. 433–438.

JOLLY, W. T., 1978, Metamorphic history of the Archean Abitibi belt, *in* Metamorphism in the Canadian Shield *edited by* J. A. FRASER and W. W. HEYWOOD: Canada Geological Survey, Paper 78–10, p. 63–78.

JOLLY, W. T., and HALLBERG, J. A., 1990, Role of crustal contamination in heterogeneous Archean volcanics from the Leonora region, Western Australia: Precambrian Research, v. 48, p. 75–98.

JONES, D. A., 1987, The Paddington gold mine, Broad Arrow, *in* The Second Eastern Goldfields Geological Field Conference, Abstracts and Excursion Guide, 1987 *edited by* W. K. WITT and C. P. SWAGER: Geological Society of Australia (Western Australian Division), p. 92–96.

JUTSON, J. T., 1914, The Mining geology of Ora Banda, Broad Arrow Goldfield: Western Australia Geological Survey, Bulletin 54.

JUTSON, J. T., 1921, The mining geology of Comet Vale and Goongarrie, North Coolgardie Goldfield: Western Australia Geological Survey, Bulletin 79.

KEATS, W., 1987, Regional geology of the Kalgoorlie Boulder gold mining district: Western Australia Geological Survey, Report 21.

KEATS, W., 1991, Geology and gold mines of the Bullfinch – Parker Range region, Southern Cross Province, Western Australia: Western Australia Geological Survey, Report 28.

KEAYS, R. R., 1984, Archaean gold deposits and their source rocks: the upper mantle connection *in* Gold '82 — The geology, geochemistry and genesis of gold deposits *edited by* R. P. FOSTER: Rotterdam, A. A. Balkema Publishers, Geological Society of Zimbabwe, Special Publication, no. 1, p. 17–52.

KERRICH, R., 1986a, Archaean lode gold deposits of Canada: Part I, A synthesis of geochemical data from selected mining camps, with emphasis on pattern of alteration: University of Witwatersrand, Johannesburg, Economic Geology Research Unit, Information Circular 182.

KERRICH, R., 1986b, Archaean lode gold deposits of Canada: Part II, Characteristics of the hydrothermal systems, and models of origin: University of Witwatersrand, Johannesburg, Economic Geology Research Unit, Information Circular 183.

KERRICH, R., 1989a, Source processes for Archean Au–Ag vein deposits: evidence from the lithophile element systematics of the Hollinger–McIntyre and Buffalo–Ankerite deposits, Timmins: Canadian Journal of Earth Sciences, v. 26, p. 755–781.

KERRICH, R. 1989b, Lithophile element systematics for gold vein deposits in Archean greenstone belts: implications for source processes, *in* The geology of gold deposits: The perspective in 1988 *edited by* R. R. KEAYES, W. R. H. RAMSAY, and D. I. GROVES: Economic Geology Monograph 6, p. 508–519.

KERRICH, R., 1989c, Archaean gold: relation to granulite formation or felsic intrusions?: Geology, v. 17, p. 1011–1015.

KERRICH, R., and ALLISON, I., 1978, Vein geometry and hydrostatics during Yellowknife mineralization: Canadian Journal of Earth Sciences, v. 15, p. 1653–1660.

KERRICH, R., and FRYER, B. J., 1979, Archean precious-metal hydrothermal systems, Dome mine, Abitibi greenstone belt, II. REE and oxygen isotope relations: Canadian Journal of Earth Sciences, v. 16, p. 440–458.

KERRICH, R., and FRYER, B. J., 1988, Lithophile-element systematics of Archean greenstone belt Au–Ag vein deposits: implications for source processes: Canadian Journal of Earth Sciences, v. 25, p. 945–953.

KERRICH, R., and FRYER, B. J., 1989, Lithophile-element systematics of Archean greenstone belt Au–Ag vein deposits: implications for source processes — a reply: Canadian Journal of Earth Sciences, v. 26, p. 2744–2748.

KERRICH, R., and FYFE, W.S., 1981, The gold–carbonate association: source of CO_2 fixation reactions in Archean lode deposits: Chemical Geology, v. 33, p. 265–294.

KERRICH, R., FRYER, B. J., KING, R. W., WILMORE, L. M., and van HEES, E., 1987, Crustal outgassing and LILE enrichment in major lithosphere structures, Archean Abitibi greenstone belt: evidence on the source reservoir from strontium and carbon isotope tracers: Contributions to Mineralogy and Petrology, v. 97, p. 156–168.

KERRICK, D. M., 1974, Review of metamorphic mixed-volatile (H_2O–CO_2) equilibria: American Mineralogist, v. 59, p. 729–762.

KISHIDA, A., and KERRICH, R., 1987, Hydrothermal alteration zoning and gold concentration at the Kerr-Adison Archean lode gold deposit, Kirkland Lake, Ontario: Economic Geology, v. 82, p. 649–690.

KWAK, T. A. P., 1986, W–Sn skarn deposits and related metamorphic skarns and granitoids: Amsterdam, Elsevier.

LAMBERT, I. B., PHILLIPS, G. N., and GROVES, D. I., 1984, Sulfur isotope compositions and genesis of Archaean gold mineralization, Australia and Zimbabwe, *in* Gold '82 — The geology, geochemistry and genesis of gold deposits *edited by* R. P. FOSTER: Rotterdam, A. A. Balkema Publishers, Geological Society of Zimbabwe, Special Publication, no. 1, p. 373–388.

LAMBERT, R. St J., 1981, Earth tectonics and thermal history: review and a hot-spot model for the Archaean, *in* Precambrian Plate Tectonics *edited by* A. KRONER: Amsterdam, Elsevier, p. 453–467.

LANGSFORD, N., 1989, The stratigraphy of Locations 48 and 50, *in* The 1989 Kalgoorlie gold workshops (field volume) *edited by* I. M. GLACKEN: Australasian Institute of Mining and Metallurgy and Eastern Goldfields Geological Discussion Group, Kalgoorlie, Western Australia, p. B1–B8.

LAWRENCE. L. M., 1988, The morphology and geochemistry of supergene gold at Hannan South gold mine, Western Australia, *in* Bicentennial Gold 88, Extended Abstracts Poster Programme, volumes 1 and 2 *compiled by* A. D. T. GOODE, E. L. SMYTH, W. D. BIRCH, and L. I. BOSMA: Geological Society of Australia, Abstracts Series no. 23, p 360–364.

LIOU, J. G., 1971, Synthesis and stability relations of prehnite, $Ca_3Al_2Si_3O_{10}(OH)_2$: American Mineralogist, v. 56, p. 507–531.

LIOU, J.G., 1973, Synthesis and stability relations of epidote, $Ca_2Al_2FeSi_3O_{12}(OH)$: Journal of Petrology, v. 14, p. 381–413.

MAITLAND, A. G., 1919, The gold deposits of Western Australia: Western Australia Geological Survey, Memoir 1 (reprinted 1984, Perth, Hesperian Press).

MANN, A. W., 1984, Mobility of gold and silver in lateritic weathering profiles: some observations from Western Australia: Economic Geology, v. 79, p. 38–49.

MARMONT, S., 1986, The geological setting of the Detour Lake gold mine, Ontario, Canada, *in* Proceedings of Gold '86, an international symposium on the geology of gold *edited by* A. J. MacDONALD: Toronto, 1986, p. 81–96.

MARSTON, R. J., 1979, Copper mineralization in Western Australia: Western Australia Geological Survey, Mineral Resources Bulletin 13.

MARSTON, R. J., 1984, Nickel mineralization in Western Australia: Western Australia Geological Survey, Mineral Resources Bulletin 14.

MARTYN, J. E., and JOHNSON, G. I., 1986, Geological setting and origin of fuchsite-bearing rocks near Menzies, Western Australia: Australian Journal of Earth Sciences, v. 33, p. 1–18.

MASON, R., and MELNIK, N., 1986, The anatomy of an Archean gold system — the McIntyre-Hoolinger Complex at Timmins, Canada, *in* Proceedings of Gold '86, an international symposium on the geology of gold *edited by* A. J. MacDONALD: Toronto, 1986, p. 40–55.

MAZZUCHELLI, R. H., 1962, The geology of Mount Pleasant, Broad Arrow Goldfield, Western Australia: University of Western Australia, Crawley, B.Sc. (Hons) thesis (unpublished).

McNAUGHTON, N. J., and CASSIDY, K. F., 1990, A reassessment of the age of the Liberty Granodiorite: implications for a model of synchronous mesothermal gold mineralization within the Norseman–Wiluna Belt, Western Australia: Australian Journal of Earth Sciences, v. 37, p. 373–376.

McNAUGHTON, N. J., and DAHL, N., 1987, A geochronological framework for gold mineralization in the Yilgarn Block, Western Australia, *in* Recent advances in understanding Precambrian gold deposits *edited by* S. E. HO and D. I GROVES: University of Western Australia, Department of Geology and Extension Service, Publication no. 11, p. 29–50.

McNAUGHTON, N. J., TURNER, J. V., GOLDING, S. D., and GROVES, D. I., 1988a, Carbon in carbonated ultramafic rocks of the Norseman–Wiluna belt: further implications for the source of carbon in Archaean mesothermal gold deposits, *in* Advances in understanding Precambrian gold deposits, Volume 2 *edited by* S. E. HO and D. I. GROVES: University of Western Australia, Department of Geology and Extension Service, Publication no. 12, p. 195–208.

McNAUGHTON, N. J., de LAETER, J. R., and GROVES, D. I., 1988b, Constraints on the source of strontium and alkalis in auriferous alteration zones at Hunt mine, Kambalda, Norseman–Wiluna belt, *in* Advances in understanding Precambrian gold deposits, Volume 2 *edited by* S. E. HO and D. I. GROVES: University of Western Australia, Department of Geology and Extension Service, Publication no. 12, p. 209–216.

McNAUGHTON, N. J., BARLEY, M. E., CASSIDY, K. F., GOLDING, S. D., GROVES, D. I., HO, S. E., HRONSKY, J. M. A., SANG, J. H., and TURNER, J. V., 1990a, Carbon isotope studies, *in* Gold deposits of the Archaean Yilgarn Block, Western Australia: Nature, genesis and exploration guides *edited by* S. E. HO, D. I. GROVES, and J. M. BENNETT: University of Western Australia, Department of Geology and University Extension Service, Publication no. 20, p. 246–251.

McNAUGHTON, N. J., CASSIDY, K. F., DAHL, N., GROVES, D. I., PERRING, C. S., and SANG, J. H., 1990b, Lead isotope studies, *in* Gold deposits of the Archaean Yilgarn Block, Western Australia: Nature, genesis and exploration guides *edited by* S. E. HO, D. I. GROVES, and J. M. BENNETT: University of Western Australia, Department of Geology and University Extension Service, Publication no. 20, p. 226–236.

McNEIL, A. M., and KERRICH, R., 1986, Archean lamprophyre dykes and gold mineralization, Matheson, Ontario: the conjunction of LILE-enriched mafic magmas, deep crustal structures, and gold concentration: Canadian Journal of Earth Sciences, v. 23, p. 324–343.

McQUEEN, K. G., 1981, Volcanic-associated nickel deposits from around the Widgiemooltha Dome, Western Australia: Economic Geology, v. 76, p. 1417–1443.

MIKUCKI, E. J., and GROVES, D. I., 1990, Mineralogical constraints, *in* Gold deposits of the Archaean Yilgarn Block, Western Australia: Nature, genesis and exploration guides *edited by* S. E. HO, D. I. GROVES, and J. M. BENNETT: University of Western Australia, Department of Geology and University Extension Service, Publication no. 20, p. 212–220.

MINTER, W. E. L., 1979, A review of gold mineralization in Southern Africa, *in* Gold mineralization *edited by* J. E GLOVER and D. I. GROVES: University of Western Australia, Department of Geology and University Extension Service, Publication no. 3, p. 35–44.

MONTGOMERY, A., 1904, Western Australia Geological Survey, Annual Report 1903.

MONTGOMERY, A., 1909, Report on the Waverley or Siberia District: Western Australia, Department of Mines.

MONTOYA, J. W., and HEMLEY, J. J., 1975, Activity relations and stabilities in alkali feldspar and mica alteration reactions: Economic Geology, v. 70, p. 577–583.

MOODY, J. B., MEYER, D., and JENKINS, J. E., 1983, Experimental characterisation of the greenschist/amphibolite boundary in mafic systems: American Journal of Science, v. 283, p. 48–92.

MORRIS, P. A., in press. Physical volcanology and geochemistry of Archean mafic and ultramafic volcanic rocks between Menzies and Norseman, eastern Yilgarn Craton: Western Australia Geological Survey, Report 36.

MORRISON, G. W., 1988, Classification of North Queensland gold deposits based on deposit style and genetic associations, *in* Styles of gold mineralization in North Queensland, Eastern Goldfields Geological Discussion Group, Kalgoorlie, Workshop Handbook.

MUELLER, A. G., 1988, Archaean gold–silver deposits with prominent calc-silicate alteration in the Southern Cross greenstone belt, Western Australia: analogues of Phanerozoic skarn deposits *in* Advances in understanding Precambrian gold deposits, Volume 2 *edited by* S. E. HO and D. I. GROVES: University of Western Australia, Department of Geology and Extension Service, Publication no. 12, p. 141–164.

MUELLER, A. G., HARRIS, L. B., and LUNGAN, A., 1988, Structural control of greenstone-hosted gold mineralization by transcurrent shearing: a new interpretation of the Kalgoorlie mining district, Western Australia: Ore Geology Reviews, v. 3, p. 359–387.

NASH, B. M., and HEATH, A., 1987, Reported reserves and grades of Western Autralian gold deposits: Western Australia Geological Survey, Record 1987/7.

NEALL, F.B., 1987, Sulphidation of iron-rich rocks as a precipitation mechanism for large Archaean gold deposits in Western Australia: thermodynamic confirmation, *in* Recent advances in understanding Precambrian gold deposits *edited by* S. E. HO and D. I GROVES: University of Western Australia, Department of Geology and Extension Service, Publication no. 11, p. 265–269.

NEALL, F. B., and PHILLIPS, G. N., 1987, Fluid–wall rock interaction in an Archaean hydrothermal gold deposit: a thermodynamic model for the Hunt mine, Kambalda: Economic Geology, v. 82, p. 1679–1694.

NESBITT, B. E., MUROCHICK, J. B., and MUEHLENBACHS, K., 1986, Dual origins of lode gold deposits in the Canadian Cordillera: Geology, v. 14, p. 506–509.

NESBITT, R. W., and SUN, S. S., 1976, Geochemistry of Archaean spinifex-textured peridotites and magnesian and low-magnesian tholeiites: Earth and Planetary Science Letters, v. 31, p. 433–453.

NESBITT, R. W., SUN, S. S., and PURVIS, A. C., 1979, Komatiites: geochemistry and genesis: Canadian Mineralogist, v. 17, p. 165–186.

NEWTON, R. C., SMITH, J. V., and WINDLEY, B. F., 1980, Carbonic metamorphism, granulites and crustal growth: Nature, v. 288, p. 45–50.

NICKEL, E. H., 1977, Mineralogy of the 'green leader' gold ore at Kalgoorlie, Western Australia: Australasian Institute of Mining and Metallurgy, Proceedings, v. 263, p. 9–13.

NORRIS, N., 1987, The Hampton Boulder gold deposit, *in* The Second Eastern Goldfields Geological Field Conference, Abstracts and Excursion Guide, 1987 *edited by* W. K. WITT and C. P. SWAGER: Geological Society of Australia (Western Australian Division), p. 115–117.

NORRIS, N. D., 1990, New Celebration gold deposits, *in* Geology of the mineral deposits of Australia and Papua New Guinea *edited by* F. HUGHES: Australasian Institute of Mining and Metallurgy, Monograph 14, p. 449–454.

ORVILLE, P. M., 1963, Alkali ion exchange between vapour and feldspar phases: American Journal of Science, v. 261, p. 201–237.

OVERSBY, V. M., 1975, Lead isotope systematics and ages of Archaean acid intrusives in the Kalgoorlie–Norseman area, Western Australia: Geochimica et Cosmochimica Acta, v. 39, p. 1107–1125.

PAGE, M. L., and SCHMULIAN, M. L., 1981, The proximal volcanic environment of the Scotia nickel deposit: Economic Geology, v. 76, p. 1469–1479.

PERRIAM, R., 1985, The tectonic evolution of the Mount Martin – Carnilya Hill district of the eastern Goldfields, Western Australia: University of Western Australia, Crawley, M.Sc. thesis (unpublished).

PERRING, C. S., 1988, Petrogenesis of the lamprophyre 'porphyry' suite from Kambalda, Western Australia, *in* Advances in understanding Precambrian gold deposits, Volume 2 *edited by* S. E. HO and D. I. GROVES: University of Western Australia, Department of Geology and Extension Service, Publication no. 12, p. 277–294.

PERRING, C. S., and BARLEY, M. E., 1990, K/Rb ratios, *in* Gold deposits of the Archaean Yilgarn Block, Western Australia: nature, genesis and exploration guides *edited by* S. E. HO, D. I. GROVES, and J. M. BENNETT: University of Western Australia, Department of Geology and University Extension Service, Publication no. 20, p. 263–267.

PERRING, C. S., GROVES, D. I., and HO, S. E., 1987, Constraints on the source of auriferous fluids for Archaean gold deposits, *in* Recent advances in understanding Precambrian gold deposits *edited by* S. E. HO and D. I GROVES: University of Western Australia, Department of Geology and Extension Service, Publication no. 11, p. 287–306.

PERRING, C. S., GROVES, D. I., and SHELLABEAR, J. N., 1990, Ore geochemistry, *in* Gold deposits of the Archaean Yilgarn Block, Western Australia: nature, genesis and exploration guides *edited by* S. E. HO, D. I. GROVES, and J. M. BENNETT: University of Western Australia, Department of Geology and University Extension Service, Publication no. 20, p. 93–101.

PERRING, C. S., BARLEY, M. E., CASSIDY, K. F., GROVES, D. I., McNAUGHTON, N. J., ROCK, N. M. S., BETTENAY, L. F., GOLDING, S. D., and HALLBERG, J. A., 1988, The association of linear orogenic belts, mantle–crustal magmatism and Archaean gold mineralization in the Archaean Yilgarn Block of Western Australia, *in* Bicentennial Gold 88, Extended Abstracts Oral Programme, *compiled by* A. D. T. GOODE and L. I. BOSMA: Geological Society of Australia, Abstracts Series no. 22, p. 296–301.

PERRING, C. S., ROCK, N. M. S., GOLDING, S. D., and ROBERTS, D. E., 1989, Criteria for the recognition of metamorphosed or altered lamprophyres: a case study from the Archaean of Kambalda, Western Australia: Precambrian Research, v. 43, p. 215–237.

PETERS, S. G., and GOLDING, S. D., 1987, Relationship of gold quartz mineralization to granodioritic phases and mylonites at Charters Towers Goldfield, Northeastern Queensland, *in* Proceedings, Pacific Rim Congress 87: Australasian Institute of Mining and Metallurgy, Gold Coast, Queensland, 1987, p. 363–367.

PETERSEN, G., 1987, Gold mineralization at Gimlet South, Ora Banda, W.A., *in* The Second Eastern Goldfields Geological Field Conference, Abstracts and Excursion Guide, 1987 *edited by* W. K. WITT and C. P. SWAGER: Geological Society of Australia (Western Australian Division), p. 78–85.

PHILLIPS, G. N., 1986, Geology and alteration in the Golden Mile, Kalgoorlie: Economic Geology, v. 81, p. 779–808.

PHILLIPS, G. N., and BROWN, I. J., 1987, Host rock control on carbonate assemblages in the Golden Mile Dolerite, Kalgoorlie gold deposit, Australia: Canadian Mineralogist, v. 25, p. 265–273.

PHILLIPS, G. N., and DeNOOY, D., 1988, High-grade metamorphic processes which influence Archean gold deposits, with particular reference to Big Bell, Australia: Journal of Metamorphic Geology, v. 6, p. 95–114.

PHILLIPS, G. N., and GROVES, D. I., 1983, The nature of Archaean gold-bearing fluids as deduced from the gold deposits of Western Australia: Australian Journal of Earth Sciences, v. 30, p. 25–39.

PHILLIPS, G. N., and GROVES, D. I., 1984, Fluid access and fluid–wallrock interaction in the genesis of the Archaean gold–quartz vein deposit at Hunt mine, Kambalda, Western Australia, *in* Gold '82 — The geology, geochemistry and genesis of gold deposits *edited by* R. P. FOSTER: Rotterdam, A. A. Balkema Publishers, Geological Society of Zimbabwe, Special Publication, no. 1, p. 389–416.

PHILLIPS, G. N., GROVES, D. I., and BROWN, I. J., 1987, Source requirements for the Golden Mile, Kalgoorlie: significance to the metamorphic replacement model for Archean gold deposits: Canadian Journal of Earth Sciences, v. 24, p. 1643–1651.

PHILLIPS, G. N., GROVES, D. I., AMARO, D., HALLBAUER, D. K., and FOTIOS, M. G., 1988, Morphology and trace element compositions of pyrites from Kalgoorlie gold deposits: sensitive indicators of syndeformational fluid regimes and depositional processes, *in* Advances in understanding Precambrian gold deposits, Volume 2 *edited by* S. E. HO and D. I. GROVES: University of Western Australia, Department of Geology and Extension Service, Publication no. 12, p. 217–226.

PHILLIPS, W. J., 1972, Hydraulic fracturing and mineralization: Journal of the Geological Society, v. 128, p. 337–359.

PIDGEON, R. T., 1986, The correlation of acid volcanics in the Archaean of Western Australia: Western Australian Mining and Petroleum Research Institute (now MERIWA), Report 27.

PLATT, J. P., ALLCHURCH, P. D., and RUTLAND, R. W., 1978, Archaean tectonics in the Agnew supracrustal belt, Western Australia: Precambrian Research, v. 7, p. 3–30.

PURVIS, A. C., 1984, Metamorphosed altered komatiites at Mt Martin, Western Australia — Archaean weathering products metamorphosed at the alumino-silicate triple point: Australian Journal of Earth Sciences, v. 31, p. 96–106.

RAMSAY, J. G., and GRAHAM, R. H., 1970, Strain variations in shear zones: Canadian Journal of Earth Sciences, v. 7, p. 786–813.

RAMSAY, J. G., and HUBER, M. I., 1987, The techniques of modern structural geology, volume 2: folds and fractures: London, Academic Press.

RANSTED, T. W., 1990a, Eureka gold deposit, *in* Geology of the mineral deposits of Australia and Papua New Guinea *edited by* F. HUGHES: Australasian Institute of Mining and Metallurgy, Monograph 14, p. 383–384.

RANSTED, T. W., 1990b, Grants Patch gold deposits, *in* Geology of the mineral deposits of Australia and Papua New Guinea *edited by* F. HUGHES: Australasian Institute of Mining and Metallurgy, Monograph 14, p. 373–376.

RAO, B. B., and JOHANNES, W., 1979, Further data on the stability of staurolite + quartz and related assemblages: Neues Jahrbuch fur Mineralogie, Mh 1979, p. 437–447.

REDMAN, B. A., and KEAYES, R. R., 1985, Archaean basic volcanism in the Eastern Goldfields Province, Yilgarn Block, Western Australia: Precambrian Research, v. 30, p. 113–152.

ROBERT, F., and BROWN, A. C., 1986a, Archean gold-bearing quartz veins at the Sigma mine, Abitibi Belt, Quebec, Part I: geological relations and formation of the vein system: Economic Geology, v. 81, p. 578–592.

ROBERT, F., and BROWN, A. C., 1986b, Archean gold-bearing quartz veins at the Sigma mine, Abitibi Belt, Quebec, Part II: vein paragenesis and hydrothermal alteration: Economic Geology, v. 81, p. 593–616.

ROBERT, F., and KELLY, W. C., 1987, Ore-forming fluids in Archean gold-bearing quartz veins at the Sigma mine, Abitibi greenstone belt, Quebec, Canada: Economic Geology, v. 82, p. 1464–1482.

ROBERT, F., BROWN, A. C., and AUDET, A. J., 1983, Structural control of gold mineralization at the Sigma mine, Val D'Or, Quebec: CIM Bulletin, v. 76 (no. 850), p. 72–80.

ROBERTS, D. E., 1988, Kambalda – St Ives area and the Victory–Defiance Complex, *in* Western Australian gold deposits, Bicentennial Gold 88 Excursion Guide Book *edited by* D. I. GROVES, M. E. BARLEY, S. E. HO, and G. M. F. HOPKINS: University of Western Australia, Department of Geology and Extension Service, Publication no. 14, p. 109–113.

ROBERTS, D. E., and ELIAS, M., 1990, Gold deposits of the Kambalda – St Ives region, *in* Geology of the mineral deposits of Australia and Papua New Guinea *edited by* F. HUGHES: Australasian Institute of Mining and Metallurgy, Monograph 14, p. 479–492.

ROBERTS, D. E., CLARK, M. E., ELIAS, M., GLACKEN, I. M., PERRING, C., WARREN, H., and WOOLARD, C. A., 1989, The geology and mining operations of the Kambalda region, *in* The 1989 Kalgoorlie gold workshops (field volume) *edited by* I. M. GLACKEN: Australasian Institute of Mining and Metallurgy and Eastern Goldfields Geological Discussion Group, Kalgoorlie, Western Australia, p. C1–C34.

ROBERTS, R. G., 1988, Ore deposit models, No.11: Archean lode gold deposits: Geoscience Canada, v. 14, p. 37–52.

ROBERTSON, I. G., JONES, D. A., SMITH, B. E., and BLOCH, J., 1988, The Paddington gold mine, *in* Western Australian gold deposits, Bicentennial Gold 88 Excursion Guide Book *edited by* D. I. GROVES, M. E. BARLEY, S. E. HO, and G. M. F. HOPKINS: University of Western Australia, Department of Geology and Extension Service, Publication no. 14, p. 91–99.

ROCK, N. M. S., HALLBERG, J. A., GROVES, D. I., and MATHER, P. J., 1988a, Archaean lamprophyres in the goldfields of the Yilgarn Block, Western Australia: new indications of their widespread distribution and significance, *in* Advances in understanding Precambrian gold deposits, Volume 2 *edited by* S. E. HO and D. I. GROVES: University of Western Australia, Department of Geology and Extension Service, Publication no. 12, p. 245–276.

ROCK, N. M. S., GROVES, D. I., and PERRING, C. S., 1988b, Gold, porphyries and lamprophyres: a new genetic model, *in* Bicentennial Gold 88, Extended Abstracts Oral Programme, *compiled by* A. D. T. GOODE and L. I. BOSMA: Geological Society of Australia, Abstracts Series no. 22, p. 307–312.

SCHILLER, J. C., and IVEY, M. E., 1990, Hannan South gold deposit, *in* Geology of the mineral deposits of Australia and Papua New Guinea *edited by* F. HUGHES: Australasian Institute of Mining and Metallurgy, Monograph 14, p. 443–448.

SEWARD, T. M., 1973, Thio complexes of gold in hydrothermal ore solutions: Geochimica et Cosmochimica Acta, v. 37, p. 379–399.

SEWARD, T. M., 1984, The transport and deposition of gold in hydrothermal systems, *in* Gold '82 — The geology, geochemistry and genesis of gold deposits *edited by* R. P. FOSTER: Rotterdam, A. A. Balkema Publishers, Geological Society of Zimbabwe, Special Publication, no. 1, p. 165–182.

SHAW, J., 1988, Gimlet South mine, Ora Banda, Western Australia, *in* Bicentennial Gold 88, Core Shed Guidebook *edited by* M. S. BLOOM and P. J. PARRINGTON: Monash University, Melbourne, Office Services and Printing, p. 14.

SHELTON, S., 1989, Paddington gold mine, *in* The 1989 Kalgoorlie gold workshops (field volume) *edited by* I. M. GLACKEN: Australasian Institute of Mining and Metallurgy and Eastern Goldfields Geological Discussion Group, Kalgoorlie, Western Australia, p. A8–A13.

SIBSON, R. H., 1977, Faults and fault rock mechanisms: Journal of the Geological Society, v. 133, p. 191–213.

SIBSON, R. H., 1983, Continental fault structures and the shallow earthquake source: Journal of the Geological Society, v. 140, p. 741–767.

SIBSON, R. H., MOORE, M. J., and RANKIN, A. H., 1975, Seismic pumping — a hydrothermal transport mechanism: Journal of the Geological Society, v. 131, p. 653–659.

SIGGS, B., 1988, Maitland Mining exploration areas, Mt Pleasant, W.A., *in* Excursion Guide Book — Boddington and Eastern Goldfields, Western Australia, The Second International Conference on Prospecting in Arid Terrain *edited by* B. H. SMITH, C. A. STOKES, A. L. GOVEY, and C. J. OATES: University of Western Australia, Department of Geology and Extension Service, Publication no. 18, p. 27–32.

SKWARNECKI, M. S., 1987, Controls on Archaean gold mineralization in the Leonora district, Western Australia, *in* Recent advances in understanding Precambrian gold deposits *edited by* S. E. HO and D. I GROVES: University of Western Australia, Department of Geology and Extension Service, Publication no. 11, p. 109–136.

SKWARNECKI, M. S., 1988, Alteration and deformation in a shear zone hosting gold mineralization at Harbour Lights, Leonora, Western Australia, *in* Advances in understanding Precambrian gold deposits, Volume 2 *edited by* S. E. HO and D. I. GROVES: University of Western Australia, Department of Geology and Extension Service, Publication no. 12, p. 111–130.

SLAUGHTER, J., KERRICK, D. M., and WALL, V. J., 1975, Experimental and thermodynamic study of equilibria in the system $CaO–MgO–SiO_2–H_2O–CO_2$: American Journal of Science, v. 275, p. 143–162.

SMITH, B. H., and KEELE, R. A., 1984, Some observations on the geochemistry of gold mineralization in the weathered zone at Norseman, Western Australia: Journal of Geochemical Exploration, v. 22, p. 1–20.

SMITH, T. J., CLOKE, P. L., and KESLER, S. E., 1984, Geochemistry of fluid inclusions from the McIntyre Hollinger gold deposit, Timmins, Ontario, Canada: Economic Geology, v. 79, p. 1265–1285.

SPRAY, J. G., 1985, Dynamothermal transition zone between Archaean greenstone and granitoid gneiss at Lake Dundas, Western Australia: Journal of Structural Geology, v. 7, p. 187–203.

STILLWELL, F. L., 1931, The occurrence of telluride minerals at Kalgoorlie: Australasian Institute of Mining and Metallurgy, Proceedings, v. 84, p. 115–190.

STILLWELL, F. L., 1953, Tellurides in Western Australia, *in* Geology of Australian ore deposits, (a symposium arranged by Australasian Institute of Mining and Metallurgy) *edited by* A. B. EDWARDS: Empire Mining and Metallurgical Congress, 5th, Australia and New Zealand, 1953, p. 119–127.

STOLZ, G. W., and NESBITT, R. W., 1981, The komatiite nickel sulphide association at Scotia: a petrochemical investigation of the ore environment: Economic Geology, v. 76, p. 1480–1502.

STOTT, G. M., and SMITH, P. M., 1988, Development of gold-bearing structures in the Archean: the role of granitic plutonism, *in* Bicentennial Gold 88, Extended Abstracts Poster Programme, volumes 1 and 2 *compiled by* A. D. T. GOODE, E. L. SMYTH, W. D. BIRCH, and L. I. BOSMA: Geological Society of Australia, Abstracts Series no. 23, p 48–50.

SUN, S. S., and NESBITT, R. W., 1978, Petrogenesis of Archaean ultrabasic and basic volcanics: evidence from rare earth elements: Contributions to Mineralogy and Petrology, v. 65, p. 301–325.

SUN, S. S., NESBITT, R. W., and McCULLOCH, M. T., 1989, Geochemistry and petrogenesis of Archaean and early Proterozoic siliceous high magnesian basalts, *in* Boninites and related rocks *edited by* A. J. CRAWFORD: Allen and Unwin, p. 148–173.

SUND, J. O., SCHWABE, M. R., HAMLYN, D. A., and BONSALL, E. M., 1984, Gold mineralization at the north end of the Kalgoorlie field, Mount Percy – Kalgoorlie, Western Australia: Australasian Institute of Mining and Metallurgy, regional conference on gold mining, metallurgy and geology, Kalgoorlie, W.A., October, 1984, p. 1–8.

SWAGER, C. P., 1989a, Structure of the Kalgoorlie greenstones — regional deformation history and implications for the structural setting of gold deposits within the Golden Mile: Western Australia Geological Survey, Report 25, p. 59–84.

SWAGER, C. P. 1989b, Dunnsville, W.A.: Western Australia Geological Survey, 1:100 000 Geological Series map.

SWAGER, C. P., 1991, Geology of the Menzies 1:100 000 sheet and adjacent Ghost Rocks area on the Riverina 1:100 000 sheet, Western Australia: Western Australia Geological Survey, Record 1990/4.

SWAGER, C. P., and GRIFFIN, T. J., 1990, An early thrust duplex in the Kalgoorlie–Kambalda greenstone belt, Eastern Goldfields Province, Western Australia: Precambrian Research, v. 48, p. 63–73.

SWAGER, C. P., and WITT, W. K., 1990, Menzies, W.A.: Western Australia Geological Survey, 1:100 000 Geological Series map.

SWAGER, C. P., WITT, W. K., GRIFFIN, T. J., AHMAT, A. L., HUNTER, M., McGOLDRICK, P. J., MORRIS, P. A., and WYCHE, S., 1990, Geology of the late Archaean Kalgoorlie granite–greenstone terrane, *in* Third International Archaean Symposium, Perth, 1990, Excursion Guidebook *edited by* S. E. HO, J. E. GLOVER, J. S MYERS, and J. R MUHLING: University of Western Australia, Department of Geology and University Extension Service, Publication no. 21, p. 203–304.

SYLVESTER, A. G., 1988, Strike-slip faults: Geological Society of America Bulletin, v. 100, p. 1666–1703.

TAKAHASHI, E., and SCARFE, C. M., 1985, Melting of peridotite to 14 GPa and the genesis of komatiite: Nature, v. 315, p. 566–568.

TCHALENKO, J. S., 1970, Similarities between shear zones of different magnitudes: Geological Society of America Bulletin, v. 81, p. 1625–1640.

TOMICH, S. A., 1974, A new look at Kalgoorlie Golden Mile geology: Australasian Institute of Mining and Metallurgy, Proceedings, v. 251, p. 27–35.

TOMICH, S. A., 1976, Further thoughts on the application of the volcanogenic theory to the Golden Mile ores at Kalgoorlie: Australasian Institute of Mining and Metallurgy, Proceedings, v. 258, p. 19–29.

TOURET, J., 1981, Fluid inclusions in high grade metamorphic rocks, *in* Short Course in fluid inclusions: applications to petrology *edited by* L. S. HOLLISTER and M. L. CRAWFORD: Mineralogical Association of Canada, Short Course Handbook, no. 6, p. 182–208.

TRAVIS, G. A., WOODALL, R., and BARTRAM, G. D., 1971, The geology of the Kalgoorlie goldfield, *in* Symposium on Archaean rocks *edited by* J.E. GLOVER: Geological Society of Australia, Special Publication no. 3, p. 175–190.

TUREK, A., and COMPSTON, W., 1971, Rubidium–strontium geochronology in the Kalgoorlie region, *in* Symposium on Archaean rocks *edited by* J. E. GLOVER: Geological Society of Australia, Special Publication 3, p.72–73.

WASHAUSEN, G. F., 1990, Mount Martin gold deposit, *in* Geology of the mineral deposits of Australia and Papua New Guinea *edited by* F. HUGHES: Australasian Institute of Mining and Metallurgy, Monograph 14, p. 439–442.

WATKINS, K. P., and HICKMAN, A. H., 1990, Geological evolution and mineralization of the Murchison Province, Western Australia: Western Australia Geological Survey, Bulletin 137.

WEBSTER, J. G., and MANN, A. W., 1984, The influence of climate, geomorphology and primary geology on the supergene migration of gold and silver: Journal of Geochemical Exploration, v. 22, p. 21–42.

WEIR, R. H. Jr, and KERRICK, D. M., 1987, Mineralogic, fluid inclusion, and stable isotope studies of several gold mines in the Mother Lode, Tuolumne and Mariposa Counties, California: Economic Geology, v. 82, p. 328–344.

WILLIAMS, D. A. C., 1972, Archaean ultramafic, mafic and associated rocks, Mt Monger, Western Australia: Journal of the Geological Society of Australia, v. 19, p. 163–188.

WILLIAMS, D. A. C., and HALLBERG, J. A., 1973, Archaean layered intrusions of the Eastern Goldfields region, Western Australia: Contributions to Mineralogy and Petrology, v. 38, p. 45–70.

WILLIAMS, I. R., 1969, Structural layering in the Archaean of the Kurnalpi 1:250 000 sheet area, Kalgoorlie region: Western Australia Geological Survey, Annual Report 1968, p. 40–41.

WILLIAMS, I. R., 1974, Structural subdivision of the Eastern Goldfields Province, Yilgarn Block: Western Australia Geological Survey, Annual Report 1973, p. 53–59.

WILLIAMS, I. R., GOWER, C. F., and THOM, R., 1976, Edjudina, W.A.: Western Australia Geological Survey, 1:250 000 Geological Series Explanatory Notes.

WILLIAMS, P. R., NISBET, B. W., and ETHERIDGE, M. A., 1989, Shear zones, gold mineralization and structural history in the Leonora district, Eastern Goldfields Province, Western Australia: Australian Journal of Earth Sciences, v. 36, p. 383–403.

WITT, W.K., 1987, Stratigraphy and layered mafic/ultramafic intrusions of the Ora Banda sequence, Bardoc 1:100 000 sheet, Eastern Goldfields: an excursion guide, *in* The Second Eastern Goldfields Geological Field Conference, Abstracts and Excursion Guide, 1987 *edited by* W. K. WITT and C. P. SWAGER: Geological Society of Australia (Western Australian Division), p. 49–63.

WITT, W. K., 1990, Geology of the Bardoc 1:100 000 Sheet: Western Australia Geological Survey, Record 1990/14.

WITT, W. K., 1992, Porphyry intrusions in the Bardoc–Kalgoorlie area, and their role in Archean epigenetic gold mineralization: Canadian Journal of Earth Sciences, v. 29, no. 8, p. 1609–1622.

WITT, W. K., 1993a, Gold deposits of the Menzies and Broad Arrow areas, Western Australia — Part 1 of a systematic study of the gold mines of the Menzies–Kambalda region: Western Australia Geological Survey, Record 1992/13.

WITT, W. K., 1993b, Gold deposits of the Mount Pleasant – Ora Banda areas, Western Australia — Part 2 of a systematic study of the gold mines of the Menzies–Kambalda region: Western Australia Geological Survey, Record 1992/14.

WITT, W. K., 1993c, Gold deposits of the Kalgoorlie–Kambalda – St Ives areas, Western Australia — Part 3 of a systematic study of the gold mines of the Menzies–Kambalda region: Western Australia Geological Survey, Record 1992/15.

WITT, W. K., 1993d, Melita, W.A.: Western Australia Geological Survey, 1:100 000 Geological Series map.

WITT, W. K., and HARRISON, N., 1989, Volcanic rocks and bounding shear zones of the Ora Banda greenstone sequence, *in* The 1989 Kalgoorlie gold workshops (field volume) *edited by* I. M. GLACKEN: Australasian Institute of Mining and Metallurgy and Eastern Goldfields Geological Discussion Group, Kalgoorlie, Western Australia, p. A2–A7.

WITT, W. K., and SWAGER, C. P., 1989a, Bardoc, W.A.: Western Australia Geological Survey, 1:100 000 Geological Series map.

WITT, W. K., and SWAGER, C. P., 1989b, Structural setting and geochemistry of Archaean I–type granites in the Bardoc–Coolgardie area of the Norseman–Wiluna belt, Western Australia: Precambrian Research, v. 44, p. 323–351.

WITT, W. K., CHAPMAN, D. M., and FISH, B. L., 1988, The role of layered mafic/ultramafic intrusions as hosts to gold mineralization in the Eastern Goldfields, Western Australia, with particular reference to the Mount Pleasant Sill, *in* Bicentennial Gold 88, Extended Abstracts Poster Programme, volumes 1 and 2 *compiled by* A. D. T. GOODE, E. L. SMYTH, W. D. BIRCH, and L. I. BOSMA: Geological Society of Australia, Abstracts Series no. 23, p 51–53.

WITT, W. K., DAVY, R., and CHAPMAN, D. M., 1991, The Mount Pleasant Sill, Eastern Goldfields, Western Australia — iron-rich granophyre in a layered high-Mg intrusion: Western Australia Geological Survey, Report 30, p. 73–92.

WITT, W. K., SWAGER, C. P., WILLIAMS, P. R., and ETHERIDGE, M. A., 1989, Accretionary tectonics in the Eastern Goldfields Province?, *in* Geoscience mapping towards the 21st century: Canberra, 1989, BMR Research Symposium.

WONG, T., 1986, Metamorphic patterns in the Kambalda area and their significance to Archaean greenstone belts of the Kambalda–Widgiemooltha area: University of Western Australia, Crawley, B.Sc. (Hons) thesis (unpublished).

WOOD, B. J., and WALTHER, J. V., 1986, Fluid flow during metamorphism and its implication for fluid-rock ratios, *in* Fluid-rock interactions during metamorphism *edited by* J. V. WALTHER and B. J. WOOD: Berlin, Springer-Verlag, p. 89–108.

WOODALL, R. W., 1965, Structure of the Kalgoorlie Goldfield, *in* Geology of Australian ore deposits (2nd edition) *edited by* J. McANDREW: Commonwealth Mining and Metallurgical Congress, 8th, Australia and New Zealand, 1965, Publications v.1 p. 71–79.

WOODALL, R. W., 1979, Gold — Australia and the world, *in* Gold mineralization *edited by* J. E. GLOVER and D. I. GROVES: University of Western Australia, Department of Geology and University Extension Service, Publication no. 3, p. 1–34.

WOODWARD, H. P., 1906, Auriferous deposits and mines, North Coolgardie Goldfield: Western Australia Geological Survey, Bulletin 22.

WYCHE, S., and WITT, W. K., 1992, Geology of the Davyhurst 1:100 000 Sheet, Western Australia: Western Australia Geological Survey, Record 1991/3.

PHOTOGRAPHIC PLATES

PLATE I

Macro-scale mineralized structures

A. Simple quartz vein (approximately 0.2 m wide) in Liberty Granodiorite; No. 2 vein, Lady Bountiful mine.

B. Quartz vein (approximately 10 cm wide) with narrow (1–2 cm) zone of deformed (foliated) wallrock; 45° N-dipping vein, Southern Shoot, Mt Pleasant.

C. Shallow ENE-dipping quartz veins, <10 cm wide (arrowed), in quartz dolerite; Paddington No. 1 pit.

PLATE I

A

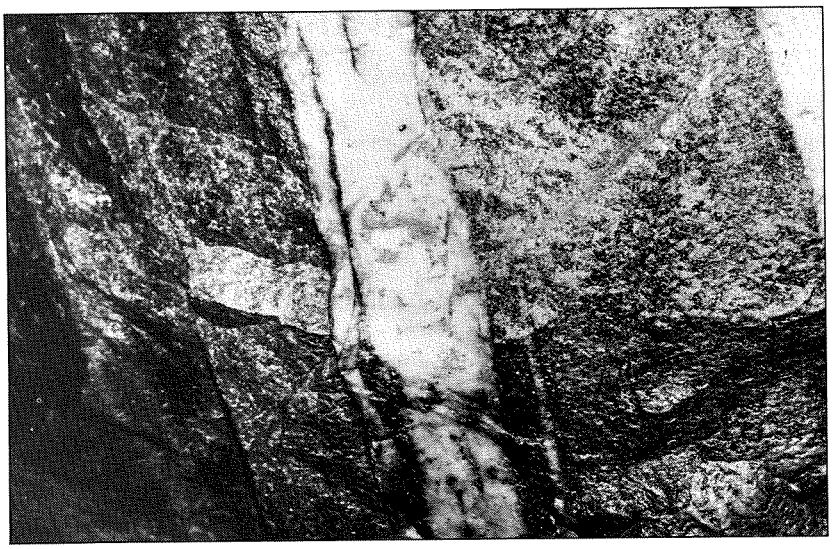

B

C

PLATE II

Macro-scale mineralized structures (continued)

A. Subvertical veined brittle–ductile shear, approximately 50 cm wide (arrowed); a bounding shear to the mineralized, flat-lying vein set in the Paddington No. 1 pit. The shear is localized along a narrow black-shale unit which separates quartz dolerite to the left (west) from ultramafic rocks to the right (east).

B. Veined brittle–ductile shear (approximately 1 m wide) in gabbroic rocks; No. 1 vein, Lady Bountiful mine.

C. Tabular vein/breccia system in tholeiitic basalt; Sand King mine, Siberia.

A

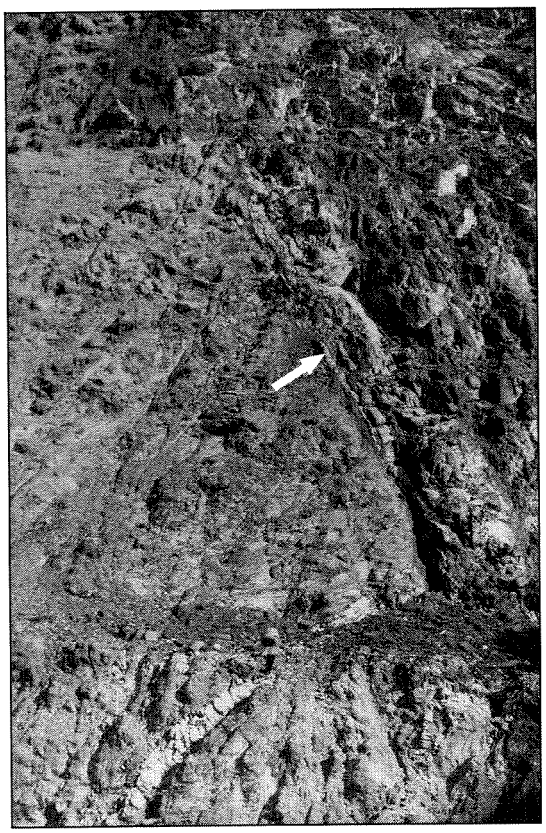

B

C

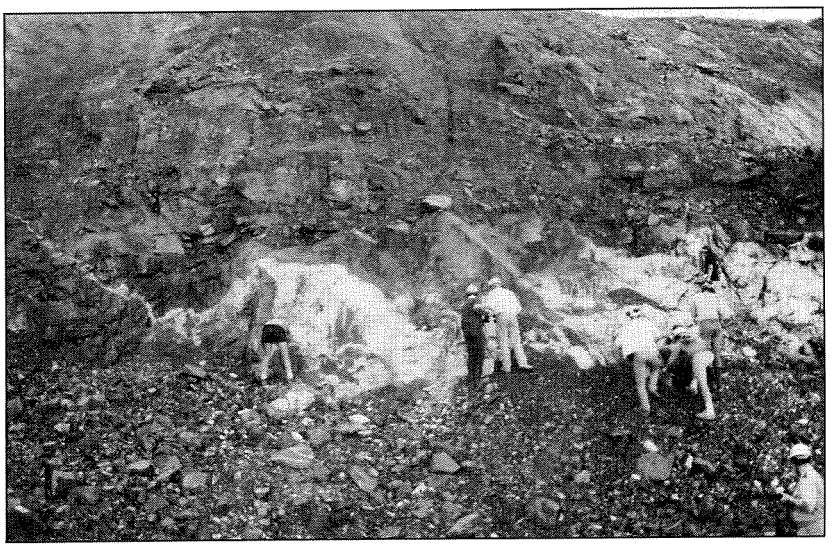

PLATE III

Meso-scale mineralized structures

A. Complex breccia incorporating angular fragments of basalt (dark); Black Flag mine, Mt Pleasant. Note the euhedrally terminated, cockade-textured quartz (C, arrowed) and the late, cross-cutting quartz(– fluorite) veinlets (V).

B – E. Cross-cutting vein/schistosity relationships in veined brittle–ductile shear zones and tabular vein/breccia systems.

B. Mafic-hosted, veined brittle–ductile shear zone; Vesuvio mine, near Broad Arrow. Shear fabric direction indicated by arrow.

C. Mafic-hosted, veined brittle–ductile shear zone; Golden Arrow mine, Broad Arrow.

D. Ultramafic-hosted, veined brittle–ductile shear zone; Dixie mine, near Mt Pleasant.

E. Mafic-hosted vein/breccia system; Missouri mine, Siberia. Note that vein is slightly oblique to weak shear fabric defined by opaque trails (arrowed).

F. Brecciated ultramafic rock in veined brittle–ductile shear zone; Golden Arrow mine, near Broad Arrow. Medium- to dark-grey clasts are fragments of apple green, altered ultramafic rock (talc–carbonate–fuchsite schist) in a matrix of quartz and carbonate (white to light grey). Thin, dark-grey to black bands are probably biotite- and/or chlorite-rich shear planes.

G. Fuchsitic quartz–carbonate schist after strongly deformed ultramafic rock, from Eastern (Excelsior) shear; Excelsior mine, Bardoc. Note the small, irregular quartz veins subparallel and oblique to foliation; and also the late, idioblastic pyrite (P). GSWA 97725.

H. Fine-scale veining due to hydraulic fracture in silicified high-Mg basalt adjacent to the Eastern (Excelsior) shear, Excelsior mine, Bardoc. GSWA 97727.

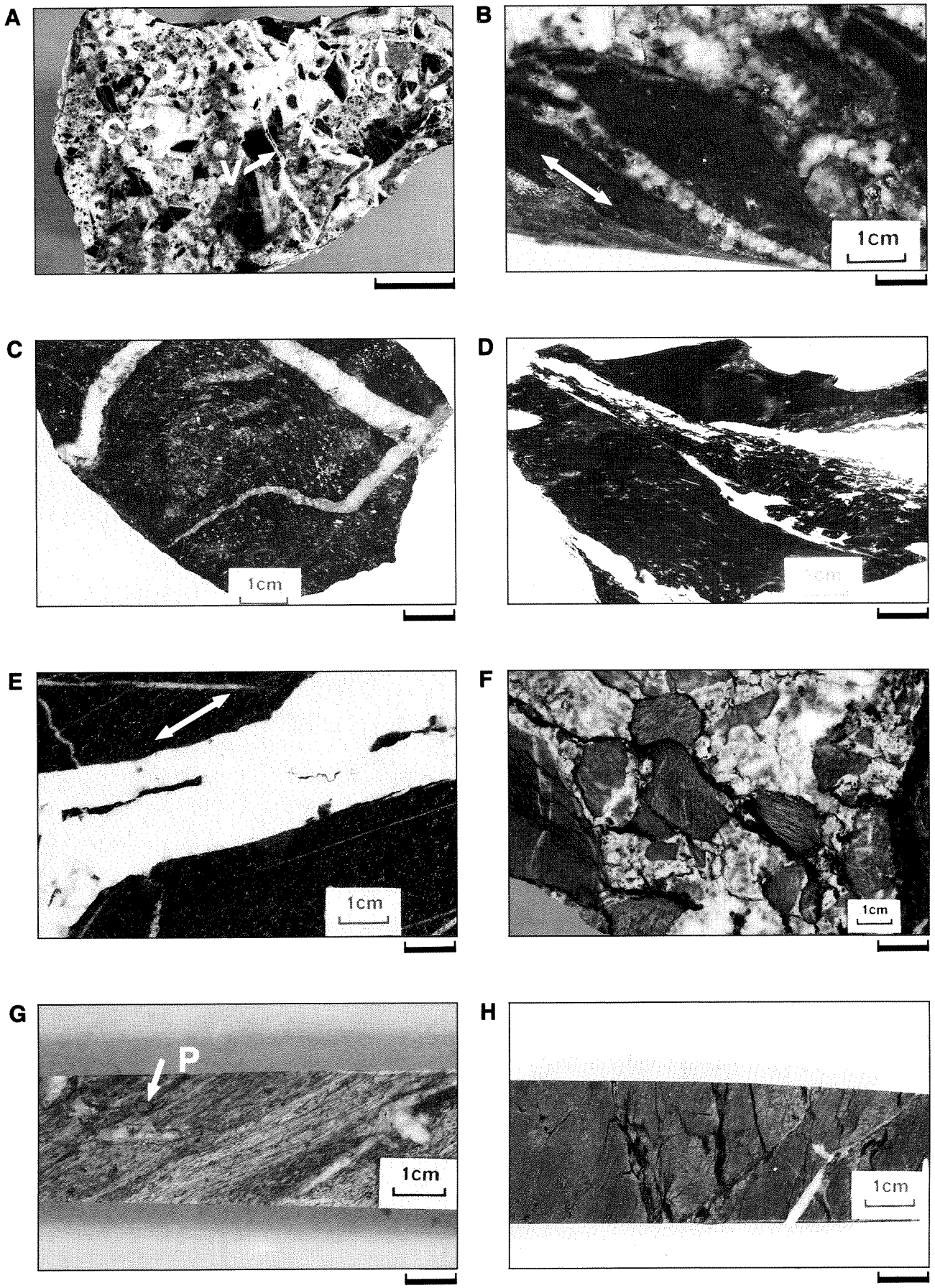
A
C
C
V
B
1cm
C
1cm
D
E
1cm
F
1cm
G
P
1cm
H
1cm

PLATE IV

Meso-scale mineralized structures (continued)

A. Brecciation and quartz veining in a silicified basalt-hosted tabular vein/breccia system; Prince of Wales mine, Grants Patch. GSWA 93950.

B. Brecciated mylonite zone; North Orchin mine, Kambalda. Medium- to dark grey clasts are fragments of biotitized, mylonitic dolerite; they are enclosed in a white to pale grey matrix of quartz, ankerite, albite, and pyrite.

C. Banded brittle–ductile shear zone; Aspacia mine, Menzies. White bands are dominantly quartz; darker bands are biotite–calcic plagioclase schist with minor carbonate, hornblende, and pyrite (fine, white disseminations). GSWA 98244.

D. Banded brittle–ductile shear zone, cut perpendicular to foliation and subparallel to stretching lineation; Warrior mine, Menzies. The mineralogy is similar to that for the Aspacia mine (see above).

E. Banded brittle–ductile shear zone, cut perpendicular to foliation but normal to stretching lineation; same sample as in PLATE IVD, Warrior mine, Menzies.

F. Banded brittle–ductile shear zone; First Hit mine, Menzies. Note the boudinaged and faulted quartz veins which now form discontinuous bands and lenses. The central pale-grey, and marginal white domains in the lenses represent weakly and intensely recrystallized vein quartz, respectively. Dark bands are dominantly biotite, calcic plagioclase and amphibole.

PLATE IV

A

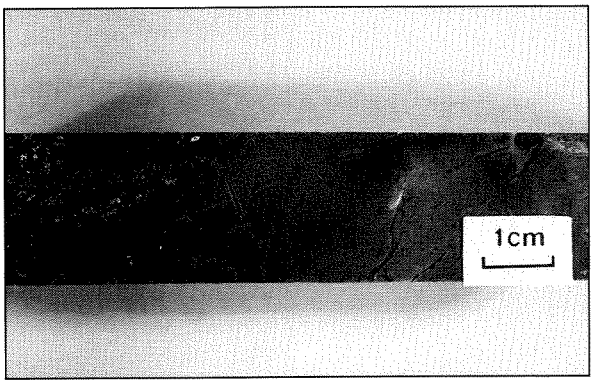

B

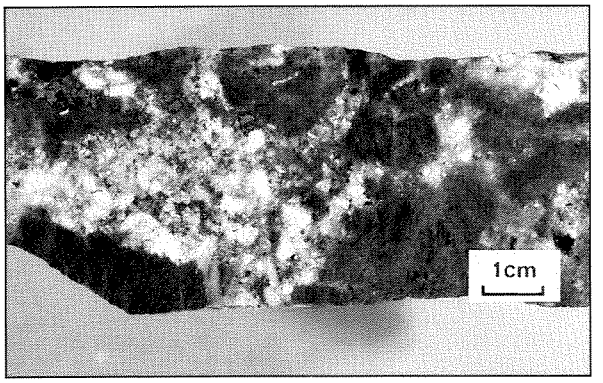

C

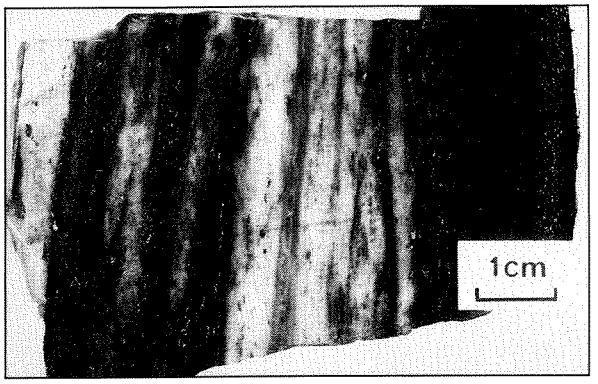

D

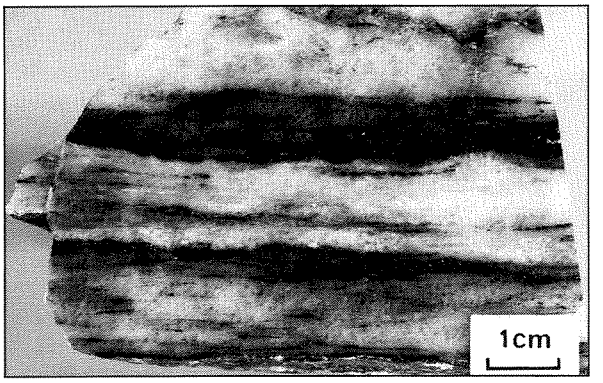

E

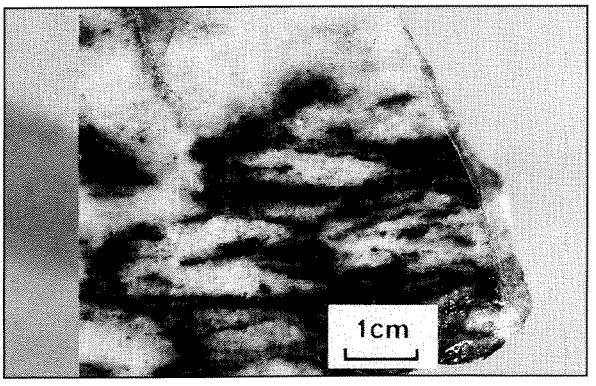

F

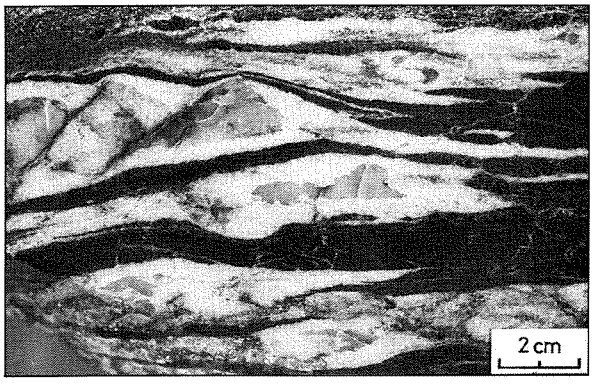

PLATE V

Alteration of mafic rocks, meso-scale

A. Albite–quartz–carbonate alteration (bleached, adjacent to veins) with disseminated ilmenite (black) overprints chlorite–carbonate alteration in quartz gabbro; Golden Kilometre Shoot, Mt Pleasant. Note the fibrous nature of the veins, indicating a crack-seal mode of formation. GSWA 78896.

B. Transition from chlorite–carbonate alteration zone (dark grey) to sericite–carbonate alteration zone (medium- to light-grey) in mineralized quartz gabbro; Golden Kilometre Shoot, Mt Pleasant. Note the apparent absence of a spatial relationship between cross-cutting veins and alteration assemblages. GSWA 78897.

C. Sericite–carbonate alteration zone, mineralized quartz gabbro; Golden Kilometre Shoot, Mt Pleasant. GSWA 78894.

D. Coarse, idioblastic pyrite in sericite–pyrite alteration assemblage adjacent to quartz vein. The vein and related sericite–pyrite alteration cut across chlorite–carbonate alteration in the outer part of the mineralized vein/breccia system in quartz gabbro; Golden Kilometre Shoot, Mt Pleasant. GSWA 78888.

E. Quartz–carbonate vein fragments (arrowed) in silica-rich and fine-grained pyrite-rich breccia, from near the centre of the mineralized vein/breccia system in quartz gabbro; Golden Kilometre Shoot, Mt Pleasant. GSWA 78889.

F. Slight bleaching (about 1 cm either side of the quartz–carbonate vein) represents a carbonate–quartz–albite–pyrite assemblage (indicated by B) which overprints chlorite–carbonate (and minor biotite) alteration of quartz gabbro; Southern Shoot, Mt Pleasant. Note the preservation of an igneous texture. GSWA 89921.

G. Chlorite–carbonate schist after basalt; New Boddington mine, Goongarrie. GSWA 93915. Note the well-developed shear fabric defined by anastomosing chloritic foliae, about 50° to core.

H. Biotite–carbonate schist after basalt; New Boddington mine, Goongarrie. Note the coarse, disseminated pyrite, and the foliation-parallel quartz–carbonate–biotite veins (arrowed). GSWA 93926.

PLATE V

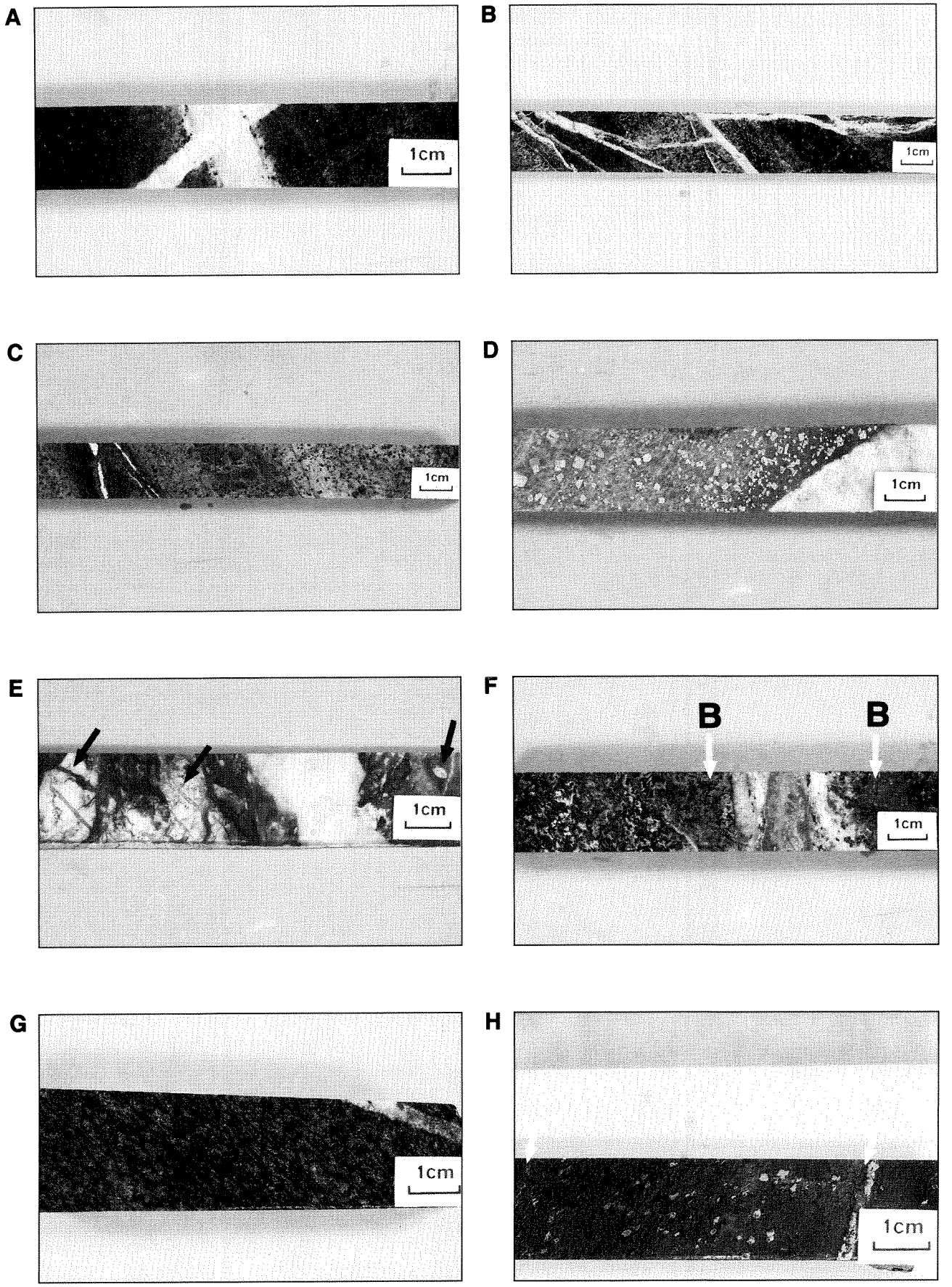

PLATE VI

Alteration of mafic rocks, meso-scale (continued)

A. Coarse, idioblastic arsenopyrite adjacent to chlorite–biotite–carbonate vein in chlorite–biotite–carbonate schist after basalt; New Boddington mine, Goongarrie. Note the bleaching (sericite, albite) adjacent to vein (on right hand side). GSWA 93920.

B. Brecciated biotite–carbonate schist after basalt; New Boddington mine, Goongarrie. GSWA 93921.

C. Variably deformed carbonate(–biotite) veinlets and lenses (dark grey), subparallel to foliation in chlorite–carbonate(–albite) schist after basalt; Eureka mine, Bardoc. GSWA 93954.

D. Hairline fractures (dark) containing quartz and carbonate (with or without minor albite, chlorite, pyrite, and arsenopyrite) cut intensely carbonated basalt; Prince of Wales mine, Grants Patch. GSWA 93952.

E. Abundant variably deformed quartz veins from centre of a mineralized brittle–ductile shear; Eureka mine, Bardoc. Alteration of basalt is predominantly chlorite, carbonate, and pyrite. GSWA 93969.

F. Relict chlorite(–biotite) alteration (dark grey) in quartz–albite–ankerite–sericite mylonite after dolerite; North Orchin mine, Kambalda. Note the disseminated pyrite (white spots) in both alteration assemblages.

G. Relicts (dark grey) of biotite amphibolite alteration assemblage after basalt, in massive to banded epidote-rich rock; Lady Sherry mine, Menzies. GSWA 98830.

H. Banded garnet–diopside rock (indicated) after amphibolite; G (garnet-rich assemblage), D (diopside-rich assemblage). St Albans, Menzies. GSWA 98222.

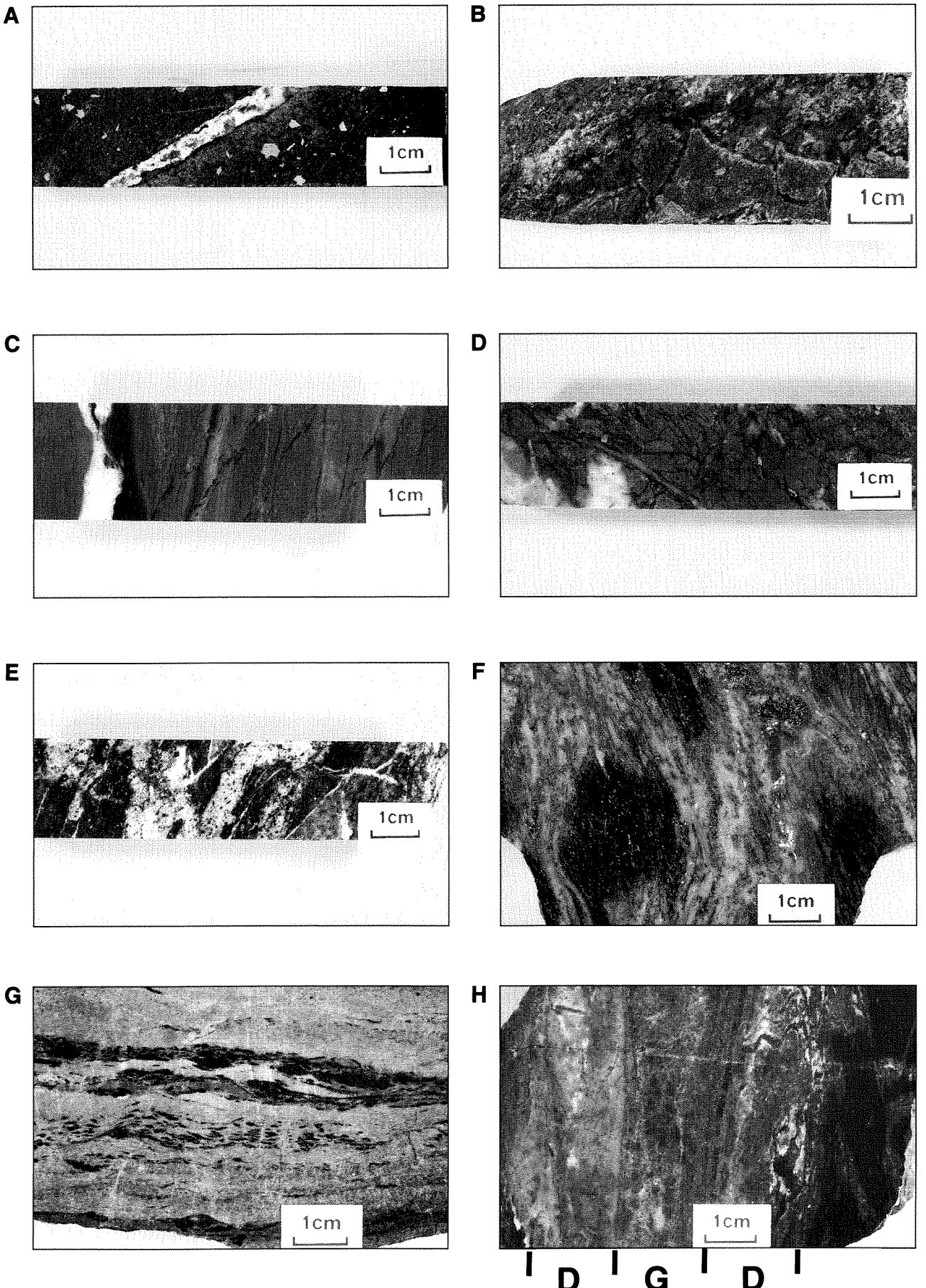
A
1cm
B
1cm
C
1cm
D
1cm
E
1cm
F
1cm
G
1cm
H
1cm
D
G
D

PLATE VII

Alteration of ultramafic rocks, meso-scale

A. Talc–chlorite schist (3) after komatiite, passing inwards through talc–albite (2), to a central zone (1) of albite + amphibole (tremolite and magnesioreibeckite). Note the unoriented amphiboles (dark spots) in the talc–albite assemblage, increasing in abundance towards the shear centre; Vettersburg. GSWA 97080.

B. Late, unoriented amphibole needles in talc-rich assemblage after ultramafic rock; Princess May mine, Yunndaga.

C. Relict patches of quartz (white) in matted mass of unoriented needles and prisms of blue-green tremolite (and magnesioreibeckite); Vettersburg. Note the radiating amphibole sheafs at the margins of quartz domains.

D. Fibrous amphibole veins cut talc–carbonate rock after komatiite; Windanya mine, between Broad Arrow and Bardoc.

PLATE VII

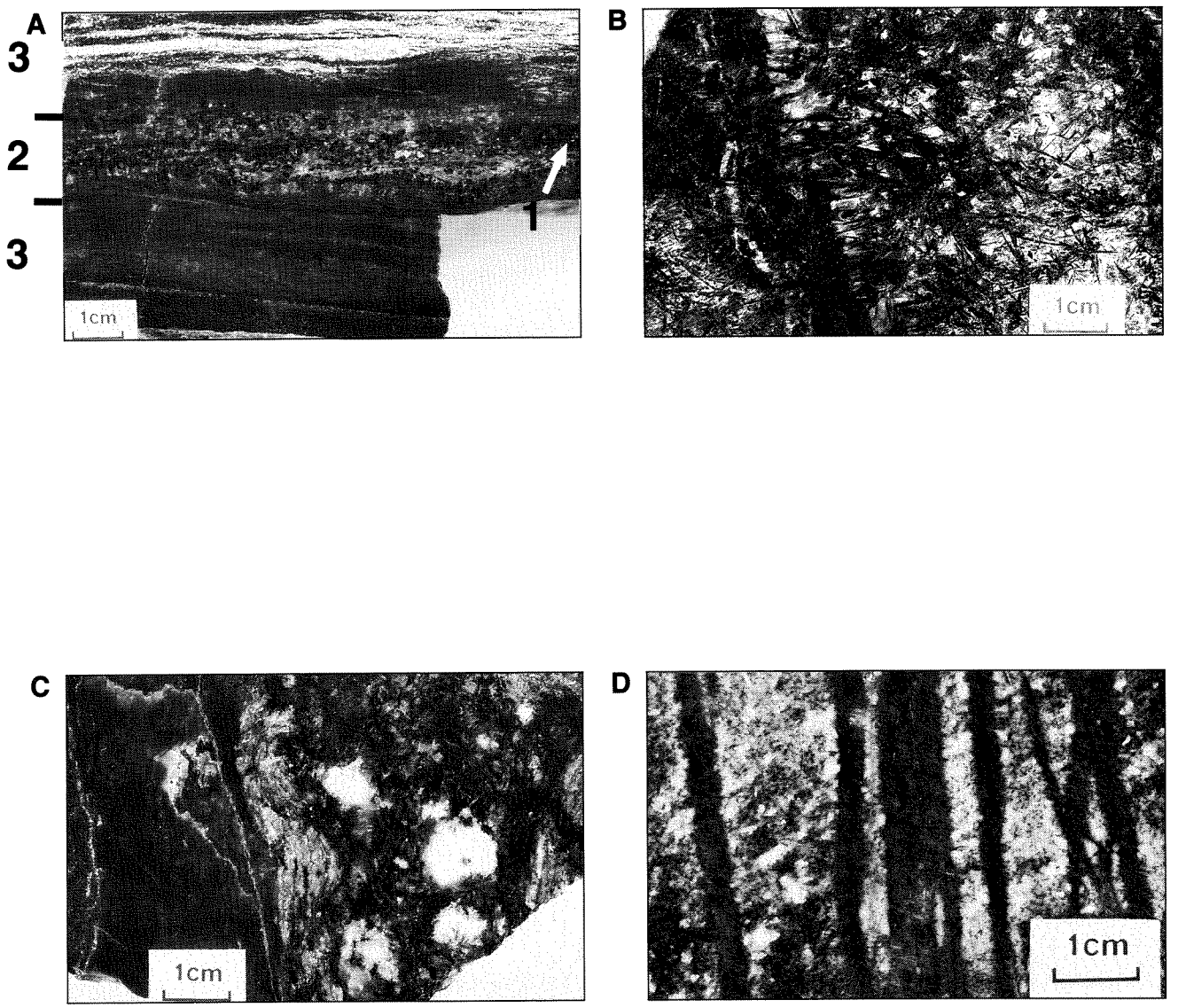

PLATE VIII

Alteration of granitic rocks, and Black Flag breccia, meso-scale

A. Sericite–ankerite–pyrite alteration assemblage (medium grey) adjacent to quartz vein (Q) in Liberty Granodiorite; Lady Bountiful mine, near Mt Pleasant. GSWA 90096.

B. Strongly deformed granodiorite-derived sedimentary rock, host to gold mineralization at Yunndaga and some other mines in the Menzies area; Lady Shenton, Menzies. GSWA 100804. Granodiorite clasts (arrowed) in medium- to coarse-grained arkosic matrix. Deformation has produced a distinct foliation defined by oriented lenses of biotite.

C. Transition from relatively unaltered hornblende–plagioclase porphyry (medium grey) to albitized (white) and biotitized (black spots) porphyry; Hawkins Find mine. GSWA 93966.

D. Transition from albitized porphyry (pale grey) to biotitized and albitized porphyry (mottled). Dark patches comprise biotite–sericite–carbonate–quartz–sulfide (pyrite, pyrrhotite and arsenopyrite) assemblages; Hawkins Find mine. GSWA 93962.

E. Biotite-dominated veinlets and sprays (dark) overprint albitized porphyry; Hawkins Find mine. GSWA 93965.

F. Quartz veins, and veinlets and disseminations of acicular tremolitic amphibole (dark grey) in albitized porphyry; Three Eights mine, Siberia. Pale-grey vein (Q) is quartz.

G. Mineralized quartz breccia; Black Flag mine, Mt Pleasant. Quartz vein at top (white) is bordered by coarse galena (G, medium grey). Darker, angular veins (F, arrowed) are mainly fluorite. GSWA 90075.

H. Complex mineralized quartz breccia; Black Flag mine, Mt Pleasant. Dark- to medium-grey clasts are basalt; veins and interclast material are mainly quartz and fluorite. Disseminated chalcopyrite (C) and sphalerite (S) are indicated. GSWA 90085.

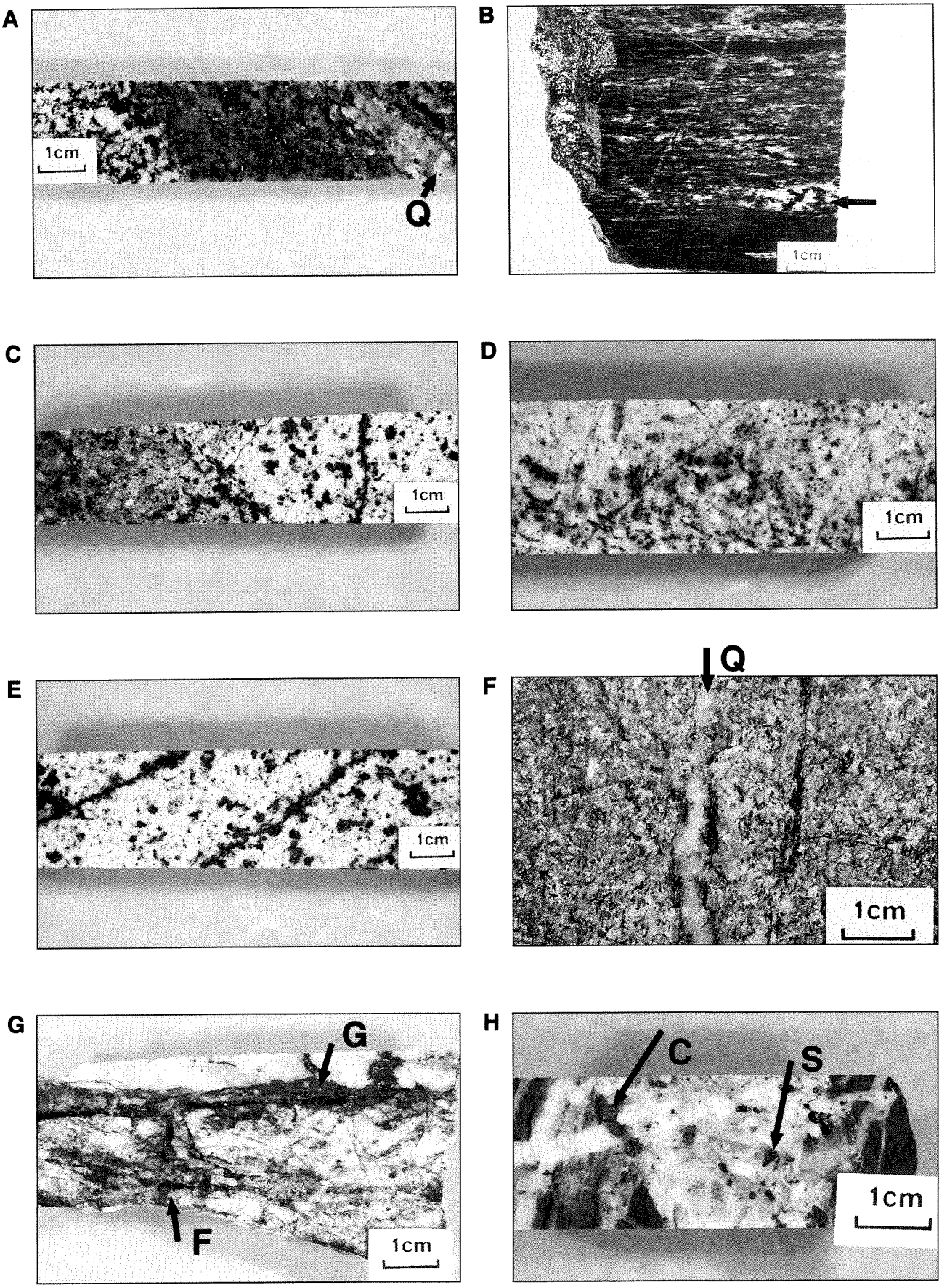
A
1cm
Q
B
1cm
C
1cm
D
1cm
E
1cm
F
Q
1cm
G
G
F
1cm
H
C
S
1cm

PLATE IX

Textural evolution of phyllosilicates (photomicrographs)

A. Chloritized dolerite; New Boddington mine, Goongarrie. Well-oriented chlorite forms irregular microshears which anastomose around less deformed plagioclase (minor carbonation and chloritization); opaque minerals are ilmenite (elongated, recrystallized during deformation) and late, secondary magnetite (cubic, subhedral to euhedral). GSWA 93939, 50X, X-polars. Scale bar is 0.2 mm.

B. Strongly oriented muscovite forms foliation-parallel bands (pale grey, an example, M, is indicated) in altered granodiorite-derived sedimentary rock; Yunndaga. Note the boudinaged quartz vein in centre of photo. Dark-grey seams (B) are predominantly oriented biotite, mottled white to medium-grey bands are quartz(– plagioclase); opaque grains are pyrite. GSWA 98282A, 50X, X-polars. Scale bar is 0.2 mm.

C. Late, unoriented muscovite (white to light grey) porphyroblasts overprint a shear fabric defined by oriented chlorite (dark grey) in altered ultramafic rock; Victory mine, Broad Arrow. GSWA 97014, 50X, X-polars. Scale bar is 0.2 mm

D. Foliation-parallel band (indicated) of biotitized amphibolite in outer margin of a banded brittle–ductile shear; Warrior mine, Menzies. Note the foliation-parallel trails of recrystallized ilmenite (opaque). GSWA 100826, 15X, plane polarized light. Scale bar is 1 mm.

E. Banded biotite–plagioclase(–quartz) assemblage after amphibolite, inner zone of alteration in a banded brittle–ductile shear; Lion mine, Menzies. Note that most biotite grains are oriented subparallel to mineral banding. GSWA 100814, 50X, plane polarized light. Scale bar is 0.2 mm.

F. Oriented biotite (medium grey) in biotite–calcite–calcic plagioclase assemblage after basalt; Lady Sherry mine, Menzies. Opaque mineral is pyrrhotite. GSWA 98228, 50X, plane polarized light. Scale bar is 0.2 mm.

G. Biotite porphyroblasts, oriented at a high angle to the shear fabric, overgrow oriented chlorite in a chlorite–biotite–carbonate schist after basalt; Eureka mine, Bardoc. The opaque mineral is pyrite. GSWA 93956, 50X, plane polarized light. Scale bar is 0.2 mm.

H. Subhedral biotite porphyroblasts overgrow chlorite–carbonate schist after ultramafic rock; Hampton–Boulder deposit, Celebration. A shear fabric is defined by oriented chlorite (medium grey) and discontinuous lenses and bands of carbonate (white to pale grey). Note the preservation of the shear fabric in biotite porphyroblasts as carbonate inclusion trails. GSWA 100898, 50X, plane polarized light. Scale bar is 0.2 mm.

PLATE IX

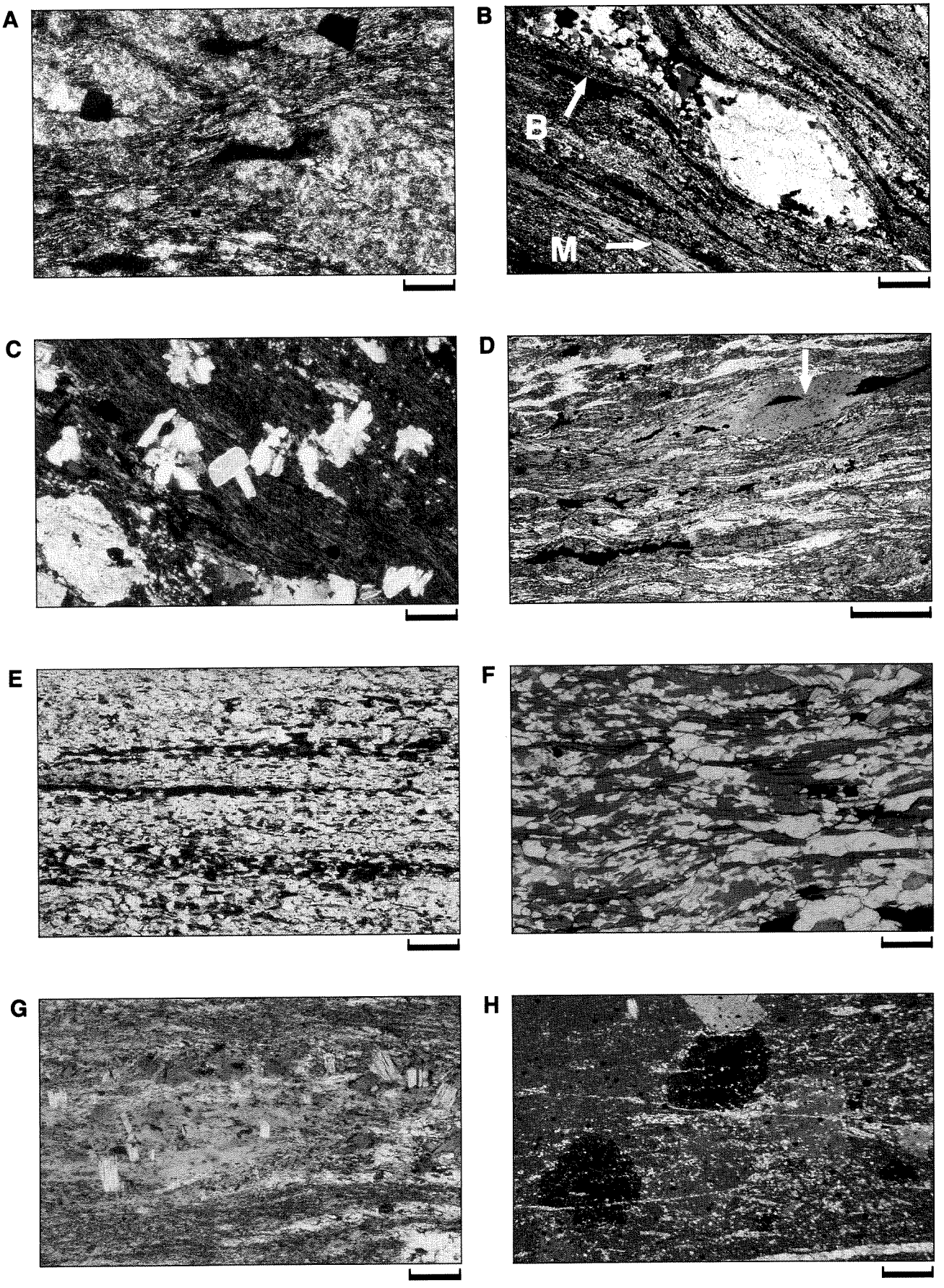

PLATE X

Textural evolution of opaque minerals (photomicrographs)

A. Coarse, skeletal ilmenite in greenschist-facies metamorphic assemblage after quartz gabbro; Southern Shoot, Mt Pleasant. Note the preservation of igneous texture. GSWA 89952, 50X, plane polarized light. Scale bar is 0.2 mm.

B. Foliation-parallel trails of opaque minerals (ilmenite and pyrrhotite) in weakly carbonated amphibolite from the outer margin of a banded brittle–ductile shear zone; Aspacia mine, Menzies. GSWA 98240, 50X, plane polarized light. Scale bar is 0.2 mm.

C. Inclusion trails of ilmenite preserve a relict shear fabric in unoriented, neoblastic hornblende; massive, amphibole-rich band in biotitized amphibolite; Friday mine, Menzies. GSWA 98300, 100X, plane polarized light. Scale bar is 0.1 mm.

D. ?Equilibrium textures between coarse, unoriented, neoblastic amphibole and interstitial, anhedral pyrrhotite (opaque); amphibole-rich band in biotitized amphibolite; Friday mine, Menzies. GSWA 98300, 50X, plane polarized light. Scale bar is 0.2 mm.

E. Well-developed, talcose pressure shadows (pale grey) against idioblastic pyrite (opaque) in talc–biotite–pyrite schist after ultramafic rock; Last Hope mine, Cashmans Shear Zone. GSWA 97770, 15X, plane polarized light. Scale bar is 1 mm.

F. Contrasting habits of pyrrhotite and pyrite in sericite–pyrite alteration zone after quartz gabbro; Golden Kilometre Shoot, Mt Pleasant. Pyrrhotite is fine grained and granular, and forms slightly elongate masses in the plane of the foliation; pyrite is coarse and idioblastic. Note the silicate and carbonate inclusions in the pyrite. GSWA 78888B, 15X, reflected light. Scale bar is 1 mm.

G. Contrasting habits of arsenopyrite and pyrrhotite in altered basalt; New Boddington mine, Goongarrie. Pyrrhotite forms finer grained, granular masses, slightly elongated in the plane of the foliation; arsenopyrite forms coarser grains, tending towards idioblastic. GSWA 93923, 15X, reflected light. Scale bar is 1 mm.

H. Late pyrrhotite (pitted and fractured) replaces pyrite ('clean') in altered quartz gabbro; Golden Kilometre Shoot, Mt Pleasant. GSWA 78888D, 50X, reflected light. Scale bar is 0.2 mm.

PLATE X

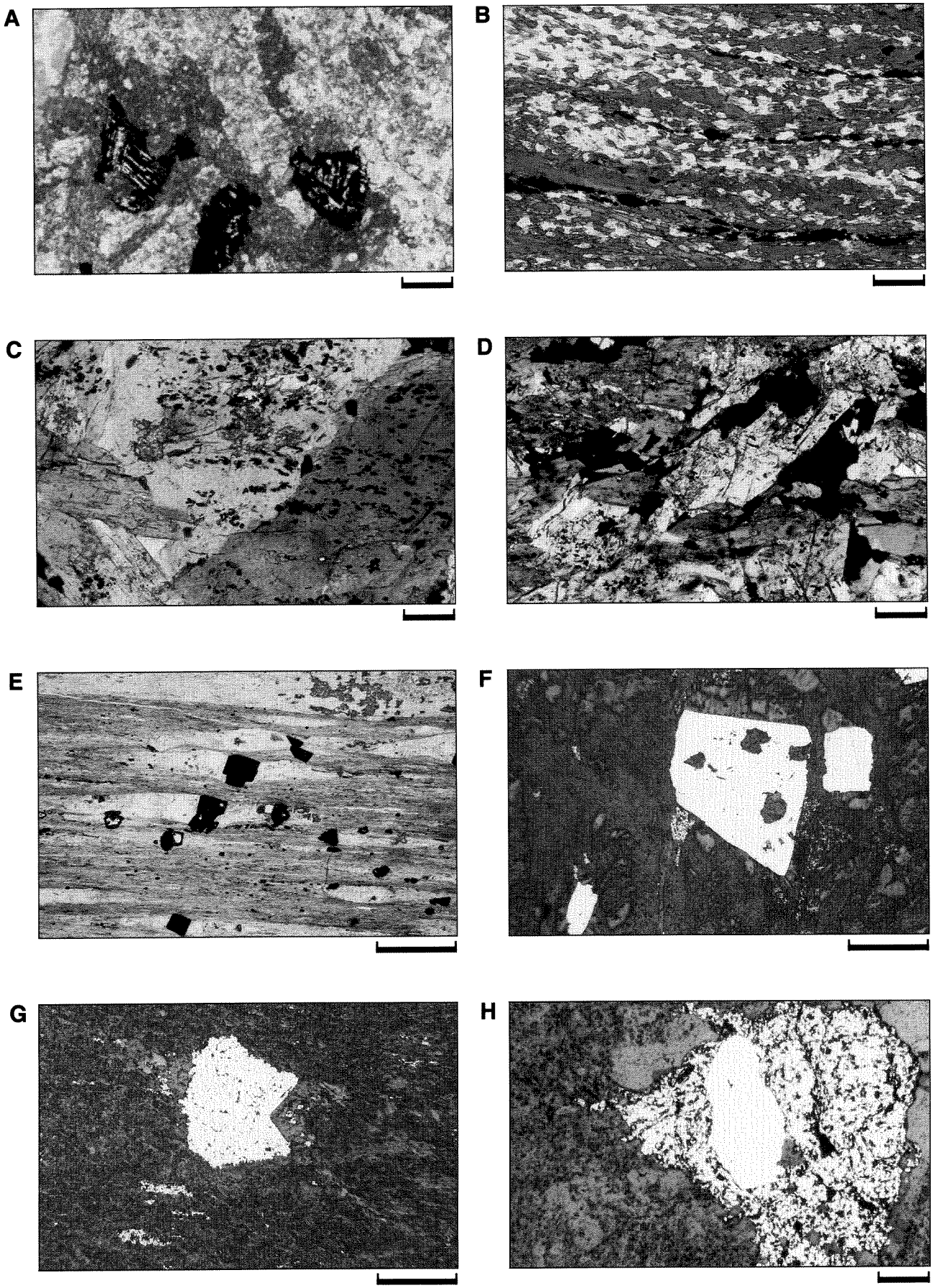

PLATE XI

Late recrystallization of alteration assemblages to produce amphibole porphyroblasts (photomicrographs)

A. Unrecrystallized metamorphic hornblende in mildly carbonated amphibolite; Bonnie Doon mine, Siberia. GSWA 98155, 100X, plane polarized light. Scale bar is 0.1 mm.

B. Recrystallized hornblende in altered and metamorphically recrystallized amphibolite; Camperdown, Siberia. Note the coarser grain size of the neoblastic amphibole compared with amphibole in unaltered amphibolite (PLATE XIA). Note also the inclusion trails of ilmenite and plagioclase in neoblastic amphibole. Minor biotite accompanies plagioclase (white to pale grey). GSWA 98147, 100X, plane polarized light. Scale bar is 0.1 mm.

C. Subhedral amphibole porphyroblast oriented at an angle to the shear fabric in biotite–plagioclase–calcite schist after mafic rock; Sunday Gift mine, Menzies. The shear fabric, defined by oriented biotite and a weak mineral banding, is deflected around the lower end of the porphyroblast. However, inclusion trails of ilmenite, plagioclase, and calcite in the porphyroblast are not rotated with respect to the external foliation. GSWA 100842, 50X, plane polarized light. Scale bar is 0.2 mm.

D. Euhedral hornblende porphyroblast in biotite–plagioclase–calcite schist after mafic rock; Sunday Gift mine, Menzies. Note that the inclusion trails in the porphyroblast are rotated with respect to the external foliation (subparallel to the long axis of the photo, and defined by oriented biotite and a weak mineral banding), suggesting that the prophyroblast initially recrystallized at a high angle to the shear fabric but was subsequently rotated during deformation. GSWA 100842, 50X, plane polarized light. Scale bar is 0.2 mm.

E. Amphibole-rich selvage (S, medium grey) between carbonate-rich band (V, ?vein; pale grey, cleaved) and amphibolite; First Hit mine, Menzies. Note that amphiboles in the amphibole-rich selvage are relatively coarse grained and unoriented with respect to the amphibolite fabric. GSWA 98238, 15X, plane polarized light. Scale bar is 1 mm.

F. Late, unoriented tremolite prisms overgrow the shear fabric, defined by oriented phyllosilicates, in chloritic schist after ultramafic rock; Little Wonder mine, Menzies. GSWA 100819, 100X, X-polars. Scale bar is 0.1 mm.

G. Tremolite–biotite assemblage after ultramafic rock; Yunndaga. Biotite occurs interstitial to unoriented tremolite prisms; disseminated opaques are mainly pyrrhotite. GSWA 98288, 50X, plane polarized light. Scale bar is 0.2 mm.

H. Sprays of unoriented tremolite in a quartz-rich band of a banded quartz–tremolite rock from near the centre of a mineralized brittle–ductile shear; Blowfly mine, Menzies. Note the coarse, prismatic tremolite at the centre of some sprays. GSWA 100856, 50X, X-polars. Scale bar is 0.2 mm.

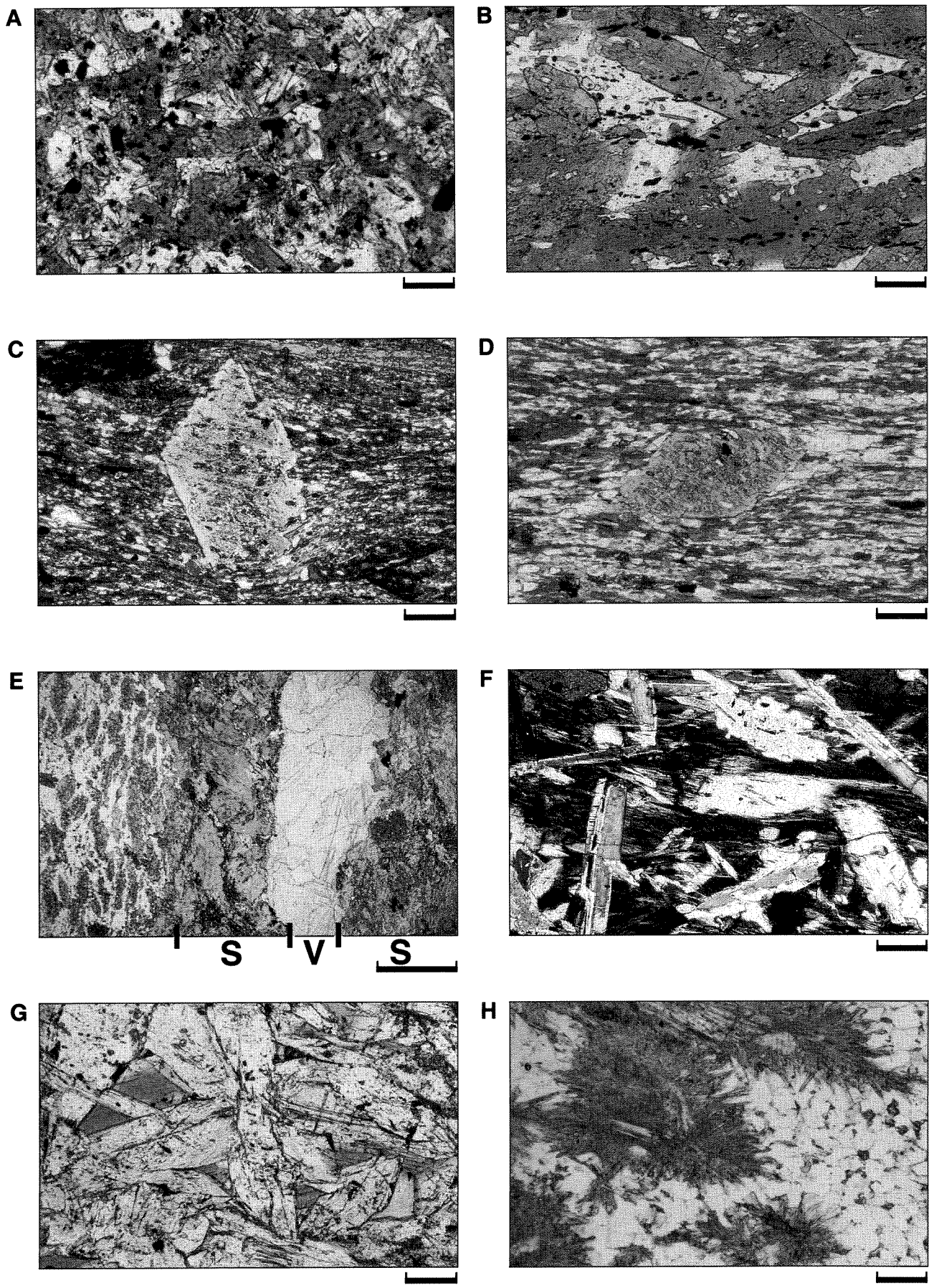
A
B
C
D
E
S
V
S
F
G
H

PLATE XII

Other late porphyroblasts; and high-grade metamorphic alteration assemblages (photomicrographs)

A – D. Other late porphyroblasts formed during late recrystallization of alteration assemblages.

A. Subhedral garnet porphyroblast in altered mafic metasedimentary rock (biotite + plagioclase assemblage); Lady Harriet mine, Menzies. Lozenge-shaped areas of pale grey are plagioclase; medium grey areas are oriented biotite. Note the preservation of the external shear fabric (lower left to upper right of photo, defined by trails of disseminated ilmenite, minor pyrrhotite, and oriented biotite) as inclusion trails in garnet. GSWA 100834, 50X, plane polarized light. Scale bar is 0.2 mm.

B. Subhedral chloritoid porphyroblast in altered mafic metasedimentary rock (plagioclase + biotite assemblage); Lady Harriet mine, Menzies. Note the orientation of the chloritoid prism at an angle to the shear fabric (top left to lower right of the photo, and defined by oriented biotite and trails of disseminated ilmenite), but that inclusion trails of ilmenite preserve the fabric within the porphyroblast. GSWA 100834, 100X, plane polarized light. Scale bar is 0.1 mm.

C. Plagioclase porphyroblasts in chloritic schist after mafic metasedimentary rock; Lady Harriet mine, Menzies. Note the compositional zoning of the plagioclase porphyroblast in the centre of the photo (grey core, white margin). Opaque mineral is ilmenite. GSWA 100835, 100X, X-polars. Scale bar is 0.1 mm.

D. Subhedral to euhedral carbonate porphyroblasts in chlorite–biotite–plagioclase schist after mafic rock; Hampton–Boulder deposit, Celebration. GSWA 100893, 15X, X-polars. Scale bar is 1 mm.

E – H. High-grade metamorphic alteration assemblages

E. Granular diopside (high relief)–microcline (cross-hatched twinning) assemblage after mafic rock; Dublin Castle mine, Menzies. GSWA 98225, 50X, X-polars. Scale bar is 0.2 mm.

F. Granular garnet (isotropic)–diopside assemblage after mafic rock; St Albans mine, Menzies. GSWA 98222, 50X, X-polars. Scale bar is 0.2 mm.

G. Banded microcline (cross-hatched twinning)–tremolitic amphibole (prismatic, light- to medium-grey) rock after amphibolite; Twin Hills mine. GSWA 100861, 100X, X-polars. Scale bar is 0.1 mm.

H. Foliation-controlled replacement band of coarse, granular epidote (high relief, medium- to light-grey) (arrowed) in altered mafic rock; Lady Sherry mine, Menzies. Note the presence of fine-grained epidote in the adjacent bands. GSWA 98226, 50X, plane polarized light. Scale bar is 0.2 mm.

PLATE XII

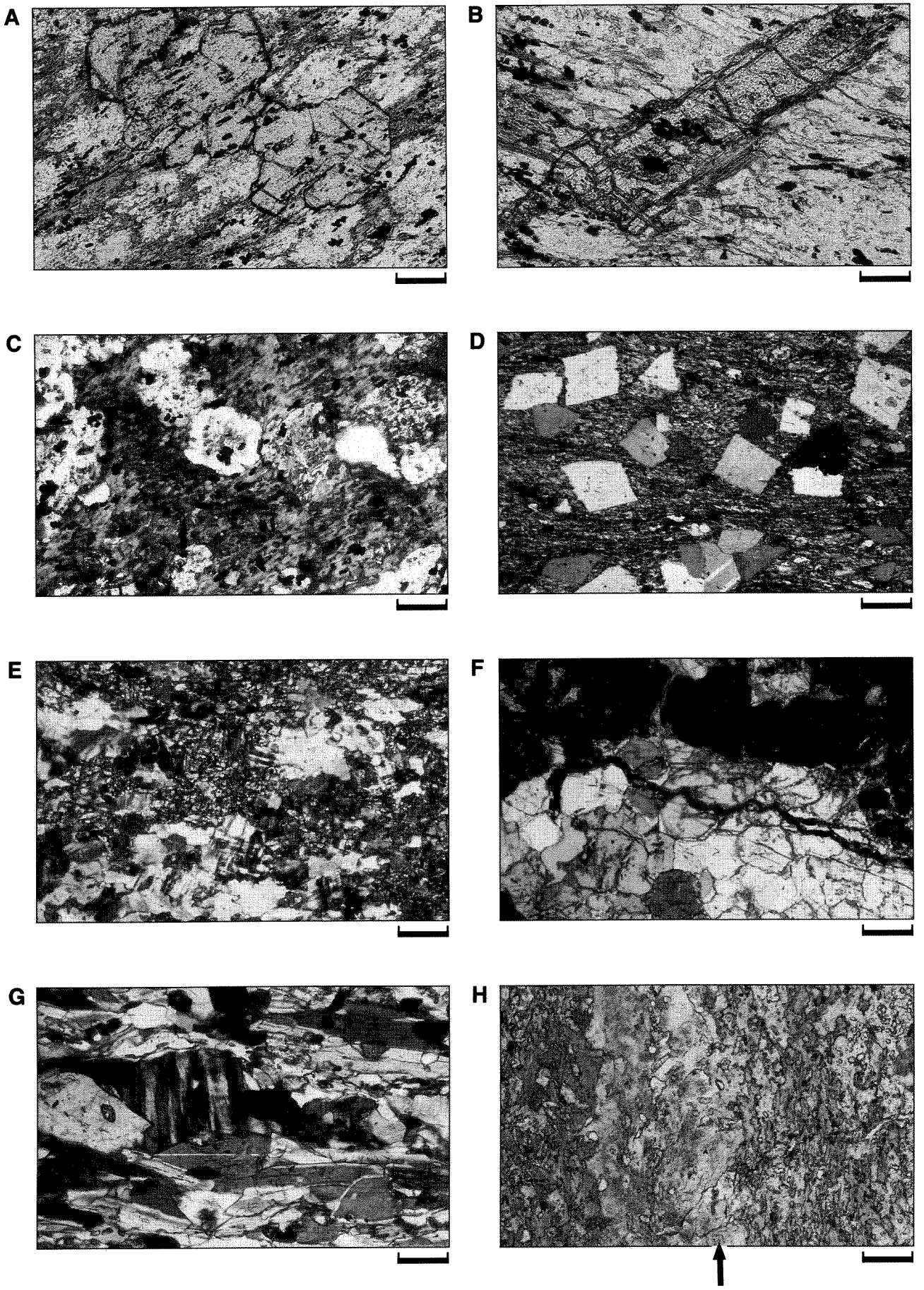

PLATE XIII

Relative timing relationships between carbonation and potassic alteration, and between sericite and biotite in alteration assemblages (photomicrographs)

A. Irregular biotite-rich shear zones cut left to right across a weakly deformed talc–carbonate assemblage, after ultramafic rock; Last Hope mine, Cashmans Shear Zone. GSWA 97772, 15X, plane polarized light. Scale bar is 1 mm.

B. Secondary biotite (dark grey) replaces sericitized plagioclase around grain margins; Lady Bountiful mine, near Mt Pleasant. Note the perfect preservation of igneous texture. GSWA 89909A, 50X, plane polarized light. Scale bar is 0.2 mm.

C. Association of pyrite (opaque) with secondary biotite (dark- to medium-grey) and ankerite (rhombhedral cleavage) in sericitized granodiorite; Lady Bountiful mine, near Mt Pleasant. GSWA 89931A, 50X, plane polarized light. Scale bar is 0.2 mm.

D. Late carbonate–pyrite–biotite (variably altered to chlorite) veins overprint sericite–carbonate alteration assemblage after mafic rock; Prince of Wales mine, Grants Patch. GSWA 93973, 50X, plane polarized light. Scale bar is 0.2 mm.

E. Biotite–pyrite–carbonate(–minor chlorite) vein cuts sericitic alteration of basalt; New Mexico mine. Note the biotite porphyroblasts (dark grey)(indicated) in the sericitic assemblage, adjacent to the vein. GSWA 98143, 15X, plane polarized light. Scale bar is 1 mm.

PLATE XIII

A

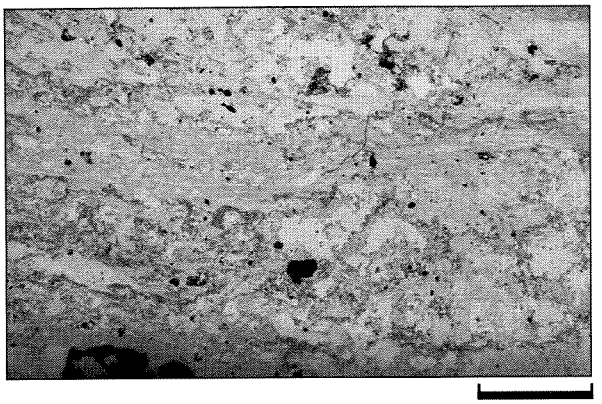

B

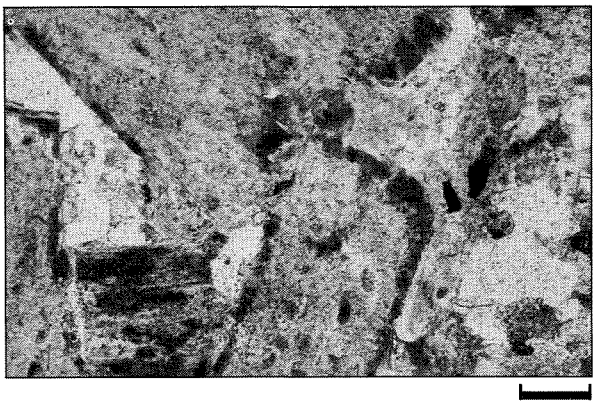

C

D

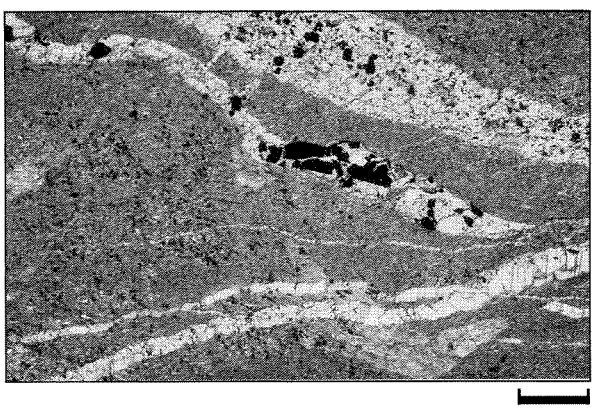

E

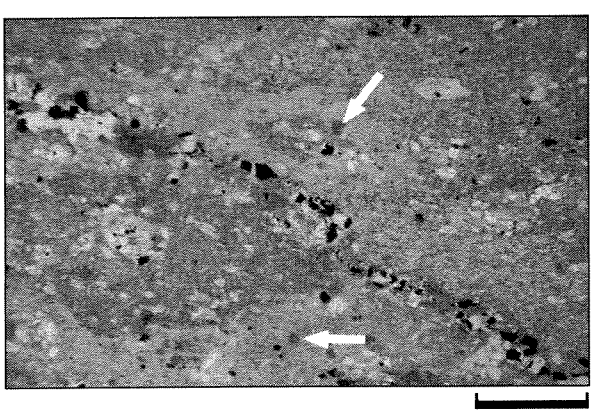

PLATE XIV

Alteration in albitized porphyries (photomicrographs)

A. Variable grain size reflecting variable recrystallization of albite in metasomatic albitite after porphyry; St Albans mine, Menzies. GSWA 98223, 50X, X-polars. Scale bar is 0.2 mm.

B. Late, hydrothermal albite projecting into quartz–carbonate vugh in albitized porphyry; Hawkins Find mine. GSWA 93958, 15X, X-polars. Scale bar is 1 mm.

C. Irregular, anastomosing, spaced chloritic microshears in weakly deformed albitic porphyry; Despatch mine, Vettersburg area. GSWA 97078, 50X, plane polarized light. Scale bar is 0.2 mm.

D. Neoblastic amphibole, in metasomatic albitite after porphyry, increases in abundance towards contact with ultramafic rock (right-hand side of photo); Big Four mine, Vettersburg area. GSWA 15X, X-polars. Scale bar is 1 mm.

E. Detail of the above photomicrograph showing the association of amphibole with chloritic alteration (dark grey) in the albitized porphyry; Big Four mine, Vettersburg area. GSWA 97076, 100X, X-polars. Scale bar is 0.1 mm.

F. Secondary biotite spray in albitized porphyry; Hawkins Find mine. Note the relict amphibole (?tremolite) in the upper part of the spray (R, indicated). The opaque mineral is pyrite. GSWA 93966, 50X, plane polarized light. Scale bar is 1 mm.

G. Disseminated sprays and irregular, discontinuous veinlets of acicular to prismatic tremolitic amphibole in albitized porphyry; Yellow Belle mine, Siberia. GSWA 98181, 15X, plane polarized light. Scale bar is 1 mm.

H. Magnesioreibeckite (darker margins) replaces tremolitic amphibole prisms in albitized porphyry; Three Eights mine, Siberia. GSWA 98177, 200X, plane polarized light. Scale bar is 0.1 mm.

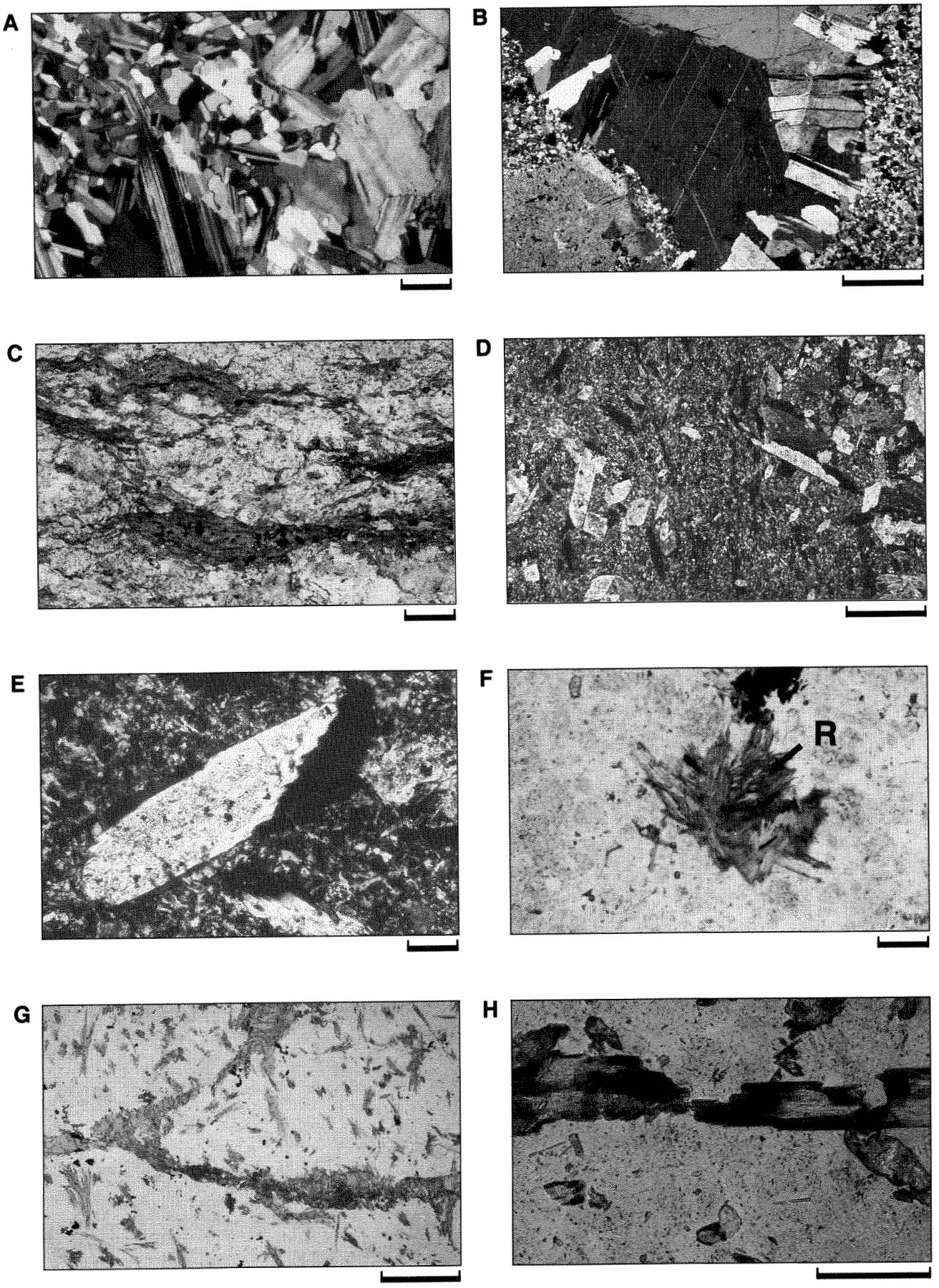
A
B
C
D
E
F
R
G
H

12854/8/93—750—L/6148

DEPARTMENT OF MINERALS AND ENERGY
HON. GEORGE CASH, J.P., M.L.C.
MINISTER FOR MINES
L. C. RANFORD, ACTING DIRECTOR GENERAL

PIETRO GIU
DIRECTOR, GEOLOGICAL SURVEY
OF WESTERN AUSTRALIA

GEOLOGICAL SURVEY OF WESTERN AUSTRALIA
REPORT 39 PLATE 1A

GOLD DEPOSITS
OF THE
MENZIES — KAMBALDA BELT
EASTERN GOLDFIELDS PROVINCE

SCALE 1:100000

1000 Metres 0 1 2 3 4 5 6 7 8 9 10 Kilometres

TRANSVERSE MERCATOR PROJECTION
Grid lines indicate 1000 metre interval of the Australian Map Grid Zone 51

Compiled by W. Witt 1986-90
Geology from 1:100000 series maps (see index maps) and Keats (1987)
Cartography by the Cartographic Services Branch, Surveys and Mapping Division, Department of Minerals and Energy, Western Australia
Compiled and produced using computer-assisted graphic applications
Topographic base from A.U.S.L.I.G., 1983
Published by and available from the Geological Survey of Western Australia, Department of Minerals and Energy, 100 Plain Street, East Perth, Western Australia, 6004
Printed by the State Print, Department of State Services, Western Australia, 1993

INDEX TO 1:100 000 SHEETS

BALLARD 3039	MELITA 3139 Witt (1993d)
INSET PLATE 1A	
RIVERINA 3038	MENZIES 3138 PLATE 1A Swager and Witt (1996)
DAYHURST 3037 Wyche and Witt (1992)	BARDOC 3137 Witt and Swager (1996a)
DUNNSVILLE 3036 Swager (1988c)	KALGOORLIE 3136 PLATE 1B Hunter (1988b) / KANOWNA 3236
	YILMIA 3135 / LAKE LEFROY 3235
CAVE HILL 3134	COWAN 3234

LOCATION DIAGRAM

TWIN HILLS INSET
Scale 1:50000
1000 Metres 0 1 Kilometres

DEPARTMENT OF MINERALS AND ENERGY
HON. GEORGE CASH, J.P., M.L.C.
MINISTER FOR MINES
L. C. RAMFORD, ACTING DIRECTOR GENERAL

PIETRO GLI
DIRECTOR, GEOLOGICAL SURVEY OF WESTERN AUSTRALIA

GEOLOGICAL SURVEY OF WESTERN AUSTRALIA
REPORT 39 PLATE 1B

GOLD DEPOSITS OF THE MENZIES — KAMBALDA BELT EASTERN GOLDFIELDS PROVINCE

SCALE 1:100000

1000 0 1 2 3 4 5 6 7 8 9 10
Metres Kilometres

TRANSVERSE MERCATOR PROJECTION
Grid lines indicate 1000 metre interval of the Australian Map Grid Zone 51

Compiled by M. Witt 1986-90
Geology from 1:100000 series maps (see index maps) and Keats (1987)
Cartography by the Cartographic Services Branch, Surveys and Mapping Division, Department of Minerals and Energy, Western Australia
Compiled and produced using computer-assisted graphic applications
Topographic base from A.U.S.L.I.G., 1983
Published by and available from the Geological Survey of Western Australia, Department of Minerals and Energy, 100 Plain Street, East Perth, Western Australia, 6004
Printed by the State Print, Department of State Services, Western Australia, 1993

INDEX TO 1:100 000 SHEETS

BALLARD 3039 | MELITA 3139
INSET PLATE 1A
PLATE 1A
RIVERINA 3038 | MENZIES 3138
DAVYHURST 3037 | BARDOC 3137
DUNNSVILLE 3036 | KALGOORLIE 3136 Hunter (1988b) | KANOWNA 3236 Keats (1987)
PLATE 1B
YILMIA 3135 Hunter (1988b) | LAKE LEFROY 3235 Griffin (1988b)
CAVE HILL 3134 | COWAN 3234 Griffin (1988b)

LOCATION DIAGRAM

REFERENCE

PROTEROZOIC

- Pdy — Mafic and ultramafic dykes (Widgiemooltha dyke swarm); inferred from aeromagnetic data
- Ax — Shear zone
- Ag — Granitoid rocks (undivided)
- Agx — Syenite
- Agl — Late- to post-tectonic granitoids; massive to weakly deformed
  - Agla Fair Adelaide Syenogranite
  - Aglh Lone Hand Monzogranite
  - Agll Liberty Granodiorite
  - Aglr Red Hill Granitoid Complex
  - Aglx Comet Vale Monzogranite
- Agp — Post-D_2 to syn-D_3 diapiric granitoid; strongly deformed margins, weakly deformed but variably recrystallised in central parts
  - Agpj Jorgemeon Monzogranite
- Agd — Pre- to syn-D_2 domal granitoids; strongly deformed margins, spaced to pervasive NNW foliation
  - Agdg Goongarrie—Mt Pleasant dome
  - Agda Scotia—Kanowna dome
- Ap — Metamorphosed felsic intrusive porphyry
  - Apl Albite-rich porphyry or aplite
  - Apg Granophyre
  - Aph Metamorphosed hornblende-plagioclase porphyry
  - Apq Metamorphosed quartz-feldspar(-biotite) porphyry
  - Apx Xenolithic porphyry
- As — Metamorphosed conglomerate, sandstone, and siltstone
  - Ask Kurrawang Formation
  - Asm Merougil Formation
- Aqf — Quartz-sericite schist, and fine- to coarse-grained sedimentary rocks derived from volcanic or granitic source rocks; includes quartz-kyanite-andalusite rocks (Menzies area)
- Metamorphosed chemical sedimentary rocks
  - Ac Chert
  - Aci Banded iron-formation
- Afv — Metamorphosed volcaniclastic rocks; predominantly fine- to coarse-grained epiclastic sedimentary rock, derived from felsic to intermediate volcanics (includes shale, siltstone, greywacke); locally fine to coarse pyroclastic rocks (tuff, agglomerate)
  - Afvb Black Flag Group
- Amv — Metamorphosed andesite
- Ad — Metamorphosed dolerite and gabbro (includes layered and differentiated mafic—ultramafic sills)
  - Adc Cooee Dolerite
  - Ade Mount Ella Sill
  - Adj Junction Dolerite
  - Adm Golden Mile Dolerite
  - Ado Ora Banda Sill
  - Adp Mount Pleasant Sill
  - Ador Orinda Sill
  - Adt Triumph Gabbro
  - Adw Williamstown Dolerite
  - Ady Pernatty Dolerite
- Ab — Metamorphosed mafic rocks; mainly basalt (low-Mg series and high-Mg series), includes small doleritic and gabbroic bodies
  - Abm Metamorphosed high-Mg series basalt
  - Abo Metamorphosed ocellar, high-Mg series basalt
  - Abg Granite Patch Group
  - Abi Missouri Basalt
  - Abn Lunnon Basalt
  - Abr Paringa Basalt (includes Williamstown Dolerite (Adw) in the Golden Mile—Mt Percy area)
  - Abs Scotia Basalt
  - Abw Wongi Basalt
- Amp — Amphibolite (includes some para-amphibolite)
- Au — Metamorphosed ultramafic rocks (includes minor high-Mg series basalt)
  - Auh Highway Ultramafics
  - Aukk Kambalda Komatiite (includes Devon Consols Basalt)
  - Aukl Lunger and Die Group (includes Big Dick Basalt)

ARCHAEAN

STRATIGRAPHIC CORRELATIONS

STRATIGRAPHIC SUCCESSION	CHARACTERISTIC LITHOLOGIES	ORA BANDA DOMAIN	KAMBALDA DOMAIN	COOLGARDIE DOMAIN	BOORARA DOMAIN
Polymictic conglomerate unit	Polymictic conglomerate, immature sandstone; coarse trough cross beds, graded beds	Kurrawang Formation (Ask)	Merougil Conglomerate (Asm)	absent	absent
Felsic volcanic and sedimentary unit	Felsic volcaniclastic-sedimentary rocks, ranging from coarse clastic sandstone to interbedded sand/siltstone. Rhyolite to dacite, locally andesite; lava, tuff, agglomerate	BLACK FLAG GROUP (Afvb): Pipeline Andesite; Orinda Sill (Ador); Ora Banda Sill (Aoo)	BLACK FLAG GROUP (Afvb): Junction Dolerite (Adj); *Condenser Dolerite; Triumph Gabbro (Adt); Golden Mile Dolerite (Adm)	BLACK FLAG GROUP (Afvb): White Flag Formation; Spargoville Formation; Powder Sill	Felsic unit, volcanic and sedimentary rocks
Upper basalt unit	High-Mg and tholeiitic basalt; massive, pillowed and vesicular lavas	GRANITE/PATCH GROUP (Abg): Victorious Basalt; Bent Tree Basalt; Mt Pleasant Sill (Ado); Mt Ellis Sill (Ade)	KALGOORLIE GROUP: Paringa Basalt (Abr); Defiance Dolerite; Pernatty Dolerite (Ady); Williamstown Dolerite (Adw); Kapai Slate; Devon Consols Basalt (Aukk); Kambalda Komatiite (Aukk); Lunnon Basalt (Abn)	COOLGARDIE GROUP: absent or thin and discontinuous; Hampton Formation; Burbanks Formation; Three Mile Sill	absent or thin and discontinuous; Highway Ultramafics (Auh); Big Blow Chert; Scotia Basalt (Abs)
Komatiite unit	Thin variolitic-textured, high-Mg basalt at top. Thin komatiitic flows with minor interflow sedimentary beds overlying thicker komatiitic flows and/or massive olivine accumulate	LUNGER AND DIE GROUP (Aukl): Big Dick Basalt; Silveria Komatiite; Walter Williams Formation			
Lower basalt unit	Tholeiitic and high-Mg basalt flows, subaqueous	KOLE GROUP (Abw): Missouri Basalt (Abi); Wongi Basalt (Abw)			
References		Witt (1987, 1990)	Woodall (1965), Roberts (1988), Langford (1989), Cowden and Archibald (in prep.)	Hunter (1993)	Christie (1975), Witt (1990)

*Cooee Dolerite (Ado) equivalent

GEOLOGICAL SYMBOLS

- Geological boundary
  - lithological contact
  - interpreted lithological contact from aeromagnetic data
  - unconformable contact
- Faults
  - shear zone and fault, includes strongly deformed granite-greenstone contacts
  - transverse fault; inferred
- Folds
  - D_1 overturned anticline
  - D_1 overturned syncline
  - D_2 overturned anticline
  - D_2 overturned syncline
  - D_3 anticline with plunge direction
  - D_3 syncline with plunge direction
  - D_3 anticline with plunge direction
  - D_3 syncline with plunge direction
  - minor fold; showing plunge and direction
- Bedding
  - strike and dip; vertical
  - younging (way-up) direction
- Foliation
  - strike and dip, with plunge and direction of mineral lineation or slickensides; vertical
- Cleavage
  - subvertical
- Lineation
  - mineral or stretching lineation; plunging, horizontal
- Banding
  - igneous layering, showing dip and strike

MINE STRUCTURE SYMBOLS

- Simple quartz vein showing dip
- Flat-lying to sub-horizontal quartz vein(s)
- Quartz vein with relatively restricted adjacent zone of moderately to strongly foliated wallrock; showing dip; vertical
- Pipe-like breccia system; flat lying
- Quartz vein sets between oblique bounding faults; showing dip of veins and bounding faults
- Quartz vein sets between conformable bounding veined brittle-ductile shears; showing dips of veins and bounding shears; vertical
- Tabular vein/breccia systems; showing dip, vertical
- Veined brittle-ductile shear; showing dip, vertical
- Banded brittle-ductile shear; showing dip, vertical
- Ductile shear zone; showing dip, vertical
- Indicators used with above symbols
  - stretching lineation (H = horizontal; V = vertical)
  - ore shoot
  - stretching lineation and ore shoot
  - relative displacement across mineralized structure (U = up; D = down)

TOPOCADASTRAL SYMBOLS

- Highway with national route marker
- Formed road
- Track
- Railway with siding — Perkerkoon
- Townsite
  - population over 10 000 — KALGOORLIE
  - 1 000 – 10 000 — KAMBALDA
  - under 1 000 — Menzies
- Homestead — Goongarrie
- Locality — Yunndaga
- Building, ruins
- Horizontal control; major, minor
- Microwave tower
- Lake; permanent, ephemeral
- Watercourse, ephemeral
- Pipeline
- Drain
- Tank or dam
- Well or bore with windpump
- Soak, rockhole

PRODUCTION

HISTORICAL — (number in mine circle with > 1000 kg gold production refers to thousands of kg Au produced; question mark in mine circle indicates production unknown but estimated from size of workings and other criterion)

- < 5kg, referred to in Witt (1993a-c)
- 5 kg
- 20 kg
- 50 kg
- 100 kg
- 250 kg
- 500 kg
- 1000 kg — 6.8

MODERN — Post-1990 (number in mine circle with >20 000 kg gold production refers to thousands of kg Au produced and in reserves; question mark in mine circle indicates production unknown but estimated from size of workings and other criterion)

- Up to 000 kg
- 1 000 kg
- 5 000 kg
- 10 000 kg
- 20 000 kg — 103

MINE NAMES

- Mines with historic production only — LADY HARRIET
- Mines with historic and modern production — PADDINGTON
- Mines with little or no historic production — JUNCTION

Note: MT CHARLOTTE (opened in 1964) is included in this group

ASSOCIATED MINOR INTRUSIONS

Exposed in mine workings or immediately adjacent surface exposures

- Associated quartz-feldspar(-biotite) porphyry
- Associated hornblende-plagioclase(-biotite-quartz) porphyry, including lamprophyre
- Associated porphyry, strongly altered; original rock not distinguishable — A

HOST ROCKS

- Surficial deposit (Tertiary to Quaternary host rocks; laterite and alluvial deposits)
- Granitoid rocks
- Porphyry
- Felsic volcanic and sedimentary rocks (including interflow sedimentary beds)
- Gabbro, dolerite
- Low-Mg series basalt
- High-Mg series basalt
- Amphibolite, undifferentiated mafic rocks
- Ultramafic rocks

Note: Low-Mg series basalt and high-Mg series basalt are broadly comparable with tholeiitic and high-Mg or komatiitic basalt, respectively. These are petrographic, not geochemical, terms (after Redman and Keays, 1985).

METAMORPHIC AND METASOMATIC ASSEMBLAGES ASSOCIATED WITH MINERALIZATION IN MAFIC ROCKS IN THE MENZIES—KAMBALDA AREA

1 — Approximate location of isograds for the following reactions:

1. Muscovite + ankerite + quartz + $fluid_1$ ⇌ biotite + calcite + $fluid_2$
2. Ankerite + chlorite + $fluid_1$ ⇌ anorthite + quartz + $fluid_2$
3. Biotite + calcite + quartz ⇌ microcline + diopside + fluid

These isograds separate alteration / assemblages A, B, C and D below

TEMPERATURE °C		Inner alteration zone	Outer alteration zone	Metamorphic assemblage	Example
~ 600	D	MICROCLINE (M or X) ? DIOPSIDE (M or X) ? GARNET (M or X) ? Calcic plagioclase (M) Calcite (M) Pyrrhotite (M) Pyrite (M) Arsenopyrite (M)	HORNBLENDE (R > X) CALCIC PLAGIOCLASE (R > M) BIOTITE (M) Calcite (M) Sphene (M) Pyrrhotite (M)	Hornblende Calcic plagioclase Ilmenite	Twin Hills; St Albans; Dublin Castle — MENZIES
isograd 3					
~ 500	C	QUARTZ (M) BIOTITE (M) ALBITE (M) CALCITE (M) Sphene (-M) Pyrrhotite (M) Pyrite (M) Arsenopyrite (M)	BIOTITE (M) HORNBLENDE (R > X) CALCIC PLAGIOCLASE (R < M) Calcite (M) Garnet (X) Ilmenite (R) Pyrrhotite (M) Pyrite (M)	Hornblende Calcic plagioclase Ilmenite	First Hit; Lady Shenton — MENZIES; Camperdown; Sand King — SIBERIA
isograd 2		QUARTZ (M) ANKERITE (M) ALBITE (M) MUSCOVITE (M) Rutile (M) Pyrite (M)	BIOTITE (M) CHLORITE (R) CALCITE (M) Sphene (M) Epidote (R > M) ? Pyrrhotite (M) Pyrite (M)	Actinolite or hornblende Albite or calcic plagioclase Ilmenite ± Epidote	Wychepoof; New Boddington; Hunt; Defiance — BARDOC; GOONGARRIE; KAMBALDA
~ 400	B				New Mexico — SIBERIA
isograd 1		MUSCOVITE (M) ANKERITE (M) ± SIDERITE (M) Pyrite (M) Pyrrhotite (M) Arsenopyrite (M)	CHLORITE (M) CALCITE (M) or ANKERITE (M) ALBITE (R > M) Epidote (R < M) ? Ilmenite (R) Pyrrhotite (M)	Actinolite Albite Ilmenite ± Epidote	Ora Banda; Granite Patch — ORA BANDA; GK Shoot — MT PLEASANT; The Golden Mile — KALGOORLIE
~ 300	A				

~ 0.2 — Increasing X_{CO_2} — 0

Note: Metasomatic minerals in upper case lettering commonly form >10% of the alteration assemblage; metasomatic minerals in lower case lettering normally form <10% of the alteration assemblage
(R) = Relict metamorphic mineral
(M) = Metasomatic mineral, or relict metamorphic mineral thoroughly recrystallized
(X) = Porphyroblast mineral, formed by recrystallization of metamorphic or metasomatic assemblages

A. BROAD ARROW TO MT EDDY, BARDOC TECTONIC ZONE

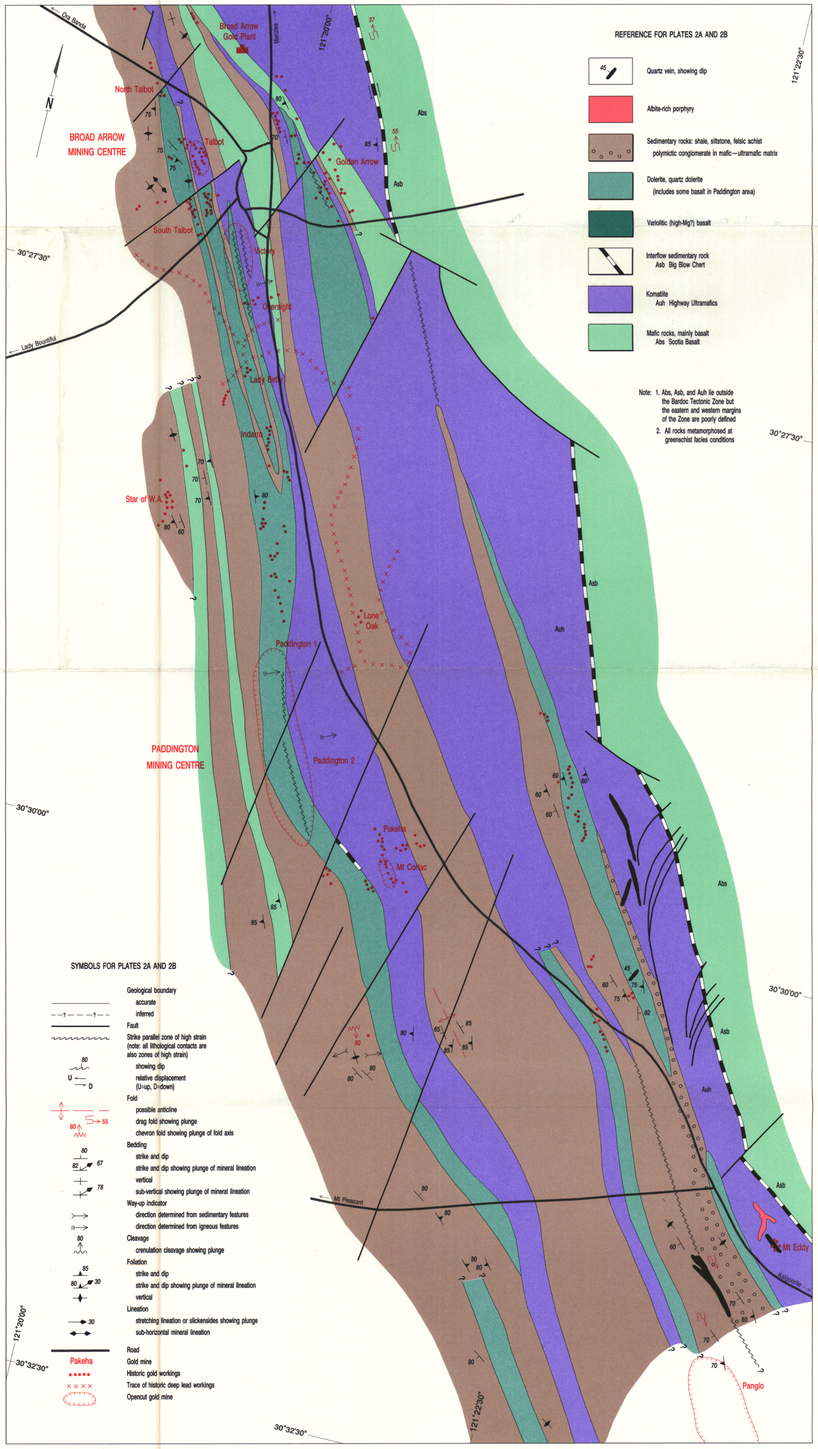

B. BARDOC TO BROAD ARROW, BARDOC TECTONIC ZONE

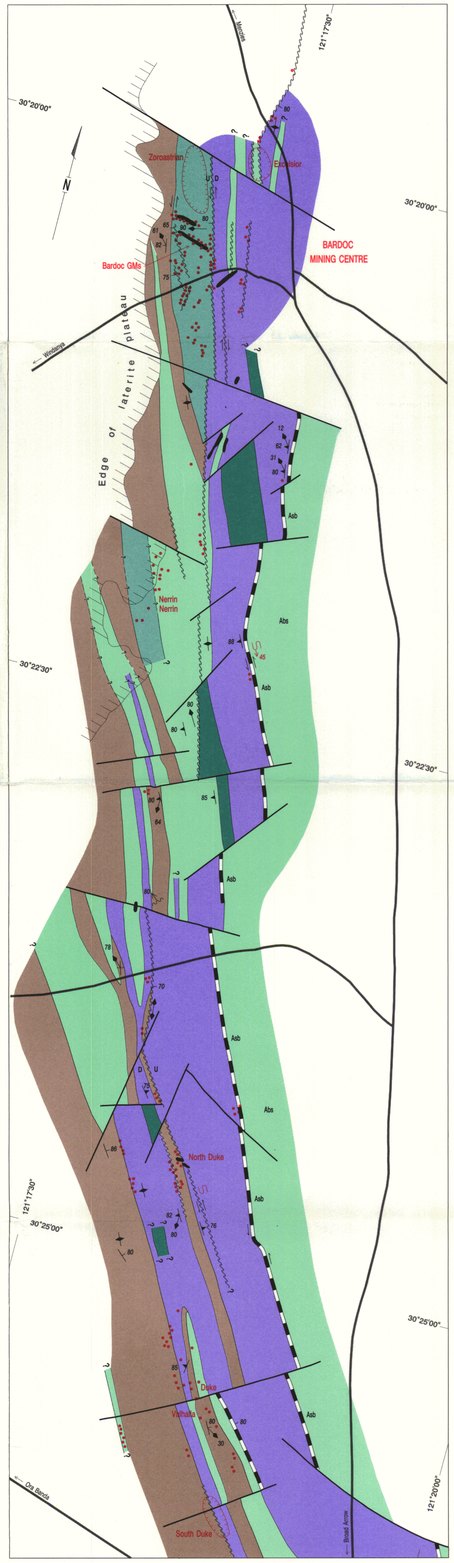

LOCATION OF PLATES 2A, 2B, AND 2C WITHIN PLATE 1A

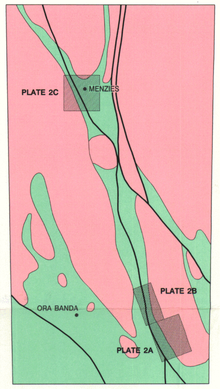

DEPARTMENT OF MINERALS AND ENERGY
HON. GEORGE CASH, J.P., M.L.C.
MINISTER FOR MINES
L. C. RAMFORD, ACTING DIRECTOR GENERAL

PIETRO GIUSTI
DIRECTOR, GEOLOGICAL SURVEY OF WESTERN AUSTRALIA

REPORT 39 PLATE 2

GEOLOGY OF SELECTED PORTIONS OF THE MENZIES — BOORARA SHEAR ZONE

MENZIES — KAMBALDA BELT
EASTERN GOLDFIELDS PROVINCE

SCALE 1:25 000

1000 Metres 0 1 2 Kilometres

Geology by W. Witt 1996-99
Cartography by the Cartographic Services Branch, Surveys and Mapping Division, Department of Minerals and Energy, Western Australia
Compiled and produced using computer-assisted graphic applications
Published by and available from the Geological Survey of Western Australia, Department of Minerals and Energy, 100 Plain Street, East Perth, Western Australia, 6004
Printed by the State Print, Department of State Services, Western Australia, 1983

C. GEOLOGY AND MINERALIZATION IN THE MENZIES SHEAR ZONE, WESTERN MENZIES AREA